PROCEEDINGS OF THE SECOND ANNUAL ADVANCED POLYMER COMPONENTS SYMPOSIUM. VOL. I.

John J. Rusek

PHILLIPS LABORATORY
OLAC PL/RKCP
Edwards AFB CA 93523-5000

DTIC
ELECTE
JAN 2 5 1995
S
G
D

July 1992

Interim Report

19950123 047

DTIC QUALITY INSPECTED 5

PHILLIPS LABORATORY
Propulsion Directorate
AIR FORCE MATERIEL COMMAND
EDWARDS AIR FORCE BASE CA 93524-7001

NOTICE

When U.S. Government drawings, specifications, or other data are used for any purpose other than a definitely related Government procurement operation, the fact that the Government may have formulated, furnished, or in any way supplied the said drawings, specifications, or other data, is not to be regarded by implication or otherwise, or in any way licensing the holder or any other person or corporation, or conveying any rights or permission to manufacture, use or sell any patented invention that may be related thereto.
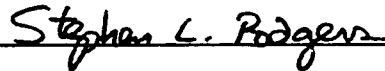
FOREWORD

The work reported in this Phase I Interim report was performed under JON: 573000R9 with the OLAC PL/RKFE Branch at the Phillips Laboratory, Edwards AFB CA 93523−5000. OLAC PL Project Manager was Dr. John J. Rusek.
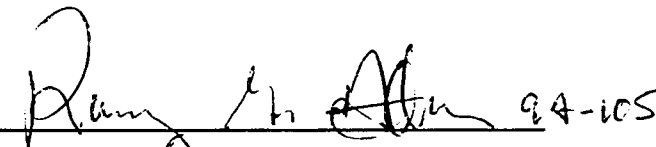
The report has been reviewed and is approved for release and distribution in accordance with the distribution statement on the cover and on the SF Form 298.

DR. JOHN J. RUSEK
Project Manager

STEPHEN L. RODGERS
Chief, Emerging Technologies Branch

RANNEY G. ADAMS
Public Affairs Director

REPORT DOCUMENTATION PAGE

Public reporting burden for this collection of information is estimated to average 1 hour per response, including the time for reviewing instructions searching existing data sources gathering and maintaining the data needed, and completing and reviewing the collection of information. Send comments regarding this burden estimate or any other aspect of this collection of information, including suggestions for reducing this burden to Washington Headquarters Services, Directorate for Information Operations and Reports, 1215 Jefferson Davis Highway, Suite 1204, Arlington, VA 22202-4302, and to the Office of Management and Budget, Paperwork Reduction Project (0740-0188), Washington DC 20503,

1. AGENCY USE ONLY (LEAVE BLANK	2. REPORT DATE July 1992	3. REPORT TYPE AND DATES COVERED Interim

4. TITLE AND SUBTITLE **Proceedings of the Second Annual Advanced Polymer Components Symposium**	5. FUNDING NUMBERS C: PE: 62302F PR: 5730 TA: 00R9
6. AUTHOR(S) John J. Rusek	

7. PERFORMING ORGANIZATION NAME(S) AND ADDRESS(ES) Phillips Laboratory OLAC PL/RKFE Edwards AFB CA 93523-5000	8. PERFORMING ORGANIZATION REPORT NUMBER PL-TR-92-3018
9. SPONSORING/MONITORING AGENCY NAME(S) AND ADDRESS(ES)	10. SPONSORING/MONITORING AGENCY REPORT NUMBER

11. SUPPLEMENTARY NOTES

COSATI CODE(S):21/06; 21/08/01; 21/09/01; 21/08/02; 21/09/02; 07/05; 07/06

12a. DISTRIBUTION/AVAILABILITY STATEMENT Distribution approved for public release; Distribution is unlimited.	12b. DISTRIBUTION CODE A

13. ABSTRACT (MAXIMUM 200 WORDS)

Advanced propulsion concepts rely on advanced propulsion materials. The Phillips Laboratory is aggressively pursuing advanced polymeric materials for use in Solid, Liquid, and Nuclear propulsion component applications. Traditional composite materials have high specific strengths, but suffer from high cost and labor intensive processing. The APC program is currently exploring thermotropic liquid crystal polymers; these materials have high specific strength and can be economically processed by traditional high volume routes such as injection molding and blow molding. Applications envisioned for these materials include rocket nozzles, pressure cases, propellant tanks and conduits, nuclear propulsion containment, fairings, high pressure tanks and orbit-processed habitats for interplanetary voyages. These proceedings contain the papers given at the Second Annual Advanced Polymer Components Symposium, which was held at the United States Air Force Academy at Colorado Springs CO.

14. SUBJECT TERMS Liquid Crystal Polymers; Liquid Propulsion Synchrotron Radiation; Advanced Materials; Solid Propulsion; Neutron Diffraction; Thermotropic Polyester; Nuclear Propulsion; Polyester Synthesis	15. NUMBER OF PAGES
	16. PRICE CODE

17. SECURITY CLASSIFICATION OF REPORT Unclassified	18. SECURITY CLASSIFICATION OF THIS PAGE Unclassified	19. SECURITY CLASSIFICATION OF ABSTRACT Unclassified	20. LIMITATION OF ABSTRACT SAR

TABLE OF CONTENTS
Volumes 1–3

Volume 1

Volume 2

A

Volume 3

Accesion For		
NTIS CRA&I		☒
DTIC TAB		☐
Unannounced		☐
Justification		
By		
Distribution /		
Availability Codes		
Dist	Avail and / or Special	
A-1		

PREFACE

The Advanced Polymer Components Initiative began in December of 1989. The initial purpose of the program was to explore advanced engineering polymers for use in rocket propulsion applications. Three main objectives were established: apply commercially available thermoplastic polymers to solid propulsion needs, apply these materials to liquid propulsion components and establish a design capability for the new processing techniques envisioned to produce parts.

Thermotropic liquid crystal polymers such as VECTRA, XYDAR and others were identified as having the most promise for surviving the rigors identified with rocket propulsion. Within the first year of the program, it became evident that these new materials needed significantly more research before rational component fabrication could be accomplished.

The new, more fundamental focus is detailed in the Proceedings of the First Annual Advanced Polymer Components Symposium, published in July of 1992. The first symposium was so successful that the Second Annual Advanced Polymer Components Symposium was held at the United States Air Force Academy in Colorado Springs from the 14th through the 16th of September, 1993. Thirty-eight researchers were in attendance and twenty-nine papers were presented over the three day span. It was quite clear from the symposium that scientific collaboration works!

The intent of this report is to detail the papers presented at the symposium and indicate the current status of Air Force rocket propulsion research using thermotropic liquid crystal polymers. It is anticipated that a third symposium will be held within the next year.

The United States Air Force is indebted to all of the participants for their goodwill, energy and dedication; these characteristics push the APC program towards the stars.

John J. Rusek
Program Manager
Advanced Polymer Components Initiative

2nd ANNUAL APC SYMPOSIUM
ATTENDANCE LIST

Dr Ismat Abu-Isa   GM NAO R&D Center, 30500 Mound Road
Warren, MI 48090
T(313)986-1240\

Capt Carlo Biagini   SM-ALC/TIEC, 5201 Bailey Loop
McClellan AFB, CA 95652
T(916)643-3810

Dr Kent Blizard   Foster-Miller, 350 Second Avenue
Waltham, MA 02154
T(617)290-0992

Capt Kyle Byard   WL/XPN
Wright-Patterson AFB, OH 45433
T(513)255-0284

Dr Kevin Chaffee   OLAC PL/RKFE, 10 E. Saturn Boulevard
Edwards AFB, CA 93524
T(805)275-5407

Prof Jim Economy   Department of Materials Science, University of Illinois
Urbana, IL 61801
T(217)333-1440

Mr Tom Elkins   412 TW/DOCA, 95 E. North Base Rd.
Edwards AFB, CA 93524
T(805)275-7774

Prof Dave Elliott   Department of Engineering, Arkansas Tech University
Russellville, AR 72801
T(501)968-0338

Mr Jack Etheridge   Organic Technologies, 4654 Kenny Road
Columbus, OH 43220
T(614)459-5000

Mr Chris Frank   SM-ALC/TIEC, 5201 Bailey Loop
McClellan AFB, CA 95652
T(916)643-3810

Mr Allen Gehris   NAWC, Propulsion Systems Division
China Lake, CA 93555
T(619)939-7964

Col Bob Giffen   Department of Astronautics, 2354 Fairchild Drive
USAF Academy, CO 80840
T(719)472-4110

Mr Rich Griffin   OOALC/LARSCA, 7226 Southgate Avenue
Hill AFB, UT 84056
T(801)777-2592

Mr Buck Guest   NAWC, Propulsion Systems Division
China Lake, CA 93555
T(619)939-8897

Dr Ted Helminiak   WL/MLBP, Polymers Branch
Wright-Patterson AFB, OH 45433
T(513)255-9158

Prof Dick Hoffman   Department of Physics, Case Western Reserve University
Cleveland, OH 44106
T(216)368-4012

Mr Paul Jones   OLAC PL/RKFE, 10 E. Saturn Boulevard
Edwards AFB, CA 93524
T(805)275-5414

Prof
Dave Kranbuehl   Department of Chemistry, College of William & Mary
Williamsburg, VA 23187
T(804)221-2542

Capt
Mike Lindauer   4950 TESTW/FFES
Wright-Patterson AFB, OH 45424
T(513)257-4276

Dr Charles Lee   AFOSR/NL, 110 Duncan Avenue
Bolling AFB, DC 20332
T(202)767-4963

Dr Joe Lichtenhan OLAC PL/RKFE, 10 E. Saturn Boulevard
Edwards AFB, CA 93524
T(805)275-5749

Prof Shannon Lieb Chemistry, Butler University
Indianapolis, IN 46208
T(317)283-9410

Capt Mike Lydon Department of Astronautics, 2354 Fairchild Drive
USAF Academy, CO 80840
T(719)472-4204

Prof Jay Mann Department of Chemical Engineering, Case Western Reserve
Cleveland, OH 44106
T(216)368-4181

Dr Pat Mather Department of Materials Science, UC Santa Barbara
Santa Barbara, CA 93106
T(805)893-4282

Mr Hieu Nguyen OLAC PL/RKAM, 4 Draco Drive
Edwards AFB, CA 93524
T(805)275-5629

Prof Charles Noel Department of Textiles, The Ohio State University
Columbus, OH 43210
T(614)292-3515

Prof Phil Oldham Department of Chemistry, Mississippi State University
Mississippi State, MS 39762
T(601)325-3584

Lt John Olson SM-ALC/TIEC, 5201 Bailey Loop
McClellan AFB, CA 95652
T(916)643-3810

Dr Steve Rodgers OLAC PL/RKFE, 10 E. Saturn Boulevard
Edwards AFB, CA 93524
T(805)275-5623

Dr John Rusek   OLAC PL/RKFE, 10 E. Saturn Boulevard
Edwards AFB, CA 93524
T(805)275-5315

Ms Linda Sawyer   Hoechst Celanese, 86 Morris Avenue
Summit, NJ 07901
T(908)522-7795

Ms Debbie Saebo Department of Chemistry, Mississippi State University
Mississippi State, MS 39762
T(601)325-3584

Prof Svein Saebo Department of Chemistry, Mississippi State University
Mississippi State, MS 39762
T(601)325-3584

Mr Dan Schwartz OLAC PL/RKAP, 4 Draco Drive
Edwards AFB, CA 93524
T(805)275-5183

Capt Ron Simmons Department of Astronautics, 2354 Fairchild Drive
USAF Academy, CO 80840
T(719)472-4462

Capt
Scott Wierschke   Department of Chemistry, 2354 Fairchild Drive
USAF Academy, CO 80840
T(719)472-2960

Dr Chris Zorman Department of Physics, Case Western Reserve University
Cleveland, OH 44106
T(216)368-4009

Agenda for the Second Annual Advanced Polymer Components Symposium

Tuesday, September 14

0800 'The Advanced Polymer Components Initiative'
J.J. Rusek; Phillips Laboratory, USAF

0825 'Thermotropic Liquid Crystalline Polymers'
J. Economy; University of Illinois

0920 'Synthesis and Thermal Analysis of Thermotropic Polyesters'
J.J. Rusek; Phillips Laboratory, USAF

0950 Break

1010 'Analytical Studies of Thermotropic Liquid Crystalline Polyesters'
D.B. Saebo, S. Saebo, P.B. Oldham; Mississippi State University

1105 'Thermotropic Polymer Annealing: Theory and Experiment'
S.G. Lieb; Butler University

1200 Lunch at Officer's Club

1300 'A Study of Thermotropic Liquid Crystalline Polymers'
D. Elliott; Arkansas Technical University

1355 'Ion Beam Analysis Techniques Applied to Polymeric Samples'
C. Zorman; Case Western Reserve University

1435 'Experiences with EXAFS'
R.W. Hoffman; Case Western Reserve University

1530 Break

1545 'EXAFS of Halogenated Liquid Crystal Polymers'
K.P. Chaffee; Phillips Laboratory, USAF

1640 'Development and Testing of a Curved Mica X-ray Focusing
Spectrometer for EXAFS Studies'
C. Zorman; Case Western Reserve University

1700 Conclude Day I Papers

1800 Mixer at LeBaron Hotel

Wednesday, September 15

0800 'Characterization, FDEMS Sensing and In Situ Process Monitoring During Cure of High Temperature Liquid Crystal Thermotropes'
D.E. Kranbuehl; College of William and Mary

0855 'Structure-Property Relationships of Vectra Liquid Crystal Polymers'
L. Sawyer; Hoechst Celanese

0950 Break

1010 'Surface Structure and Dynamics of Thermotropic Liquid Crystal Polymers'
J.A. Mann; Case Western Reserve University

1105 'Disclination Formation During the Torsional Shearing Flow of Nematic Liquids'
P.T. Mather; University of California at Santa Barbara

1200 Lunch at Arnold Hall Ball Room

1300 'The United States Air Force Academy Mission'
R.B. Giffen; United States Air Force Academy, USAF

1345 'Hybrid Rocket Research- Project CHIRON'
M. Lydon; United States Air Force Academy, USAF

1430 'Solid Rocket Flight Testing'
R. Simmons; United States Air Force Academy, USAF

1515 Break

1530 'Design of an Air-To-Air Missile Using Liquid Crystal Polymers-Project VIPER'
K.F. Byard; Air Force Institute of Technology, USAF

1615 'Investigation of Annealing Effects on DuPont HX-4000 Liquid Crystal Polymer'
M.L. Lindauer; Air Force Institute of Technology, USAF

1700 Conclude Day II Papers

0800 'Advanced Polymer Processing and Mold Design'
C. Frank; Advanced Composites Program Office, USAF

0850 'Thermoplastic Motor Case for the PREDATOR Missile System'
A.P. Gehris; Naval Air Warfare Center, USN

0940 Break

1010 'Modern Ablatives. The Design, Development and Application of Hybrid Polymers.'
J.D. Lichtenhan; Phillips Laboratory, USAF

1105 'Preliminary Characterization of Graded Interfaces for Solid Rocket Motors'
C.J. Noel; The Ohio State University

1200 Lunch at Arnold Hall Dining Room

1300 'Design and Analysis of AFA Booster Motor Components'
T. Elkins; Phillips Laboratory, USAF

1345 'Design and Performance of AFA Booster Motors'
H. Nguyen; Phillips Laboratory, USAF

1430 Break

1450 Rocket Launching at Jack's Valley on Campus

1700 Conclude APC II Symposium

GLOSSARY

AFM-Atomic Force Microscopy
ANSTO- Australian Nuclear Science and Technology Organisation
AP-Ammonium Perchlorate
APC-Advanced Polymer Components
ASTM-American Society for Testing of Materials
BHQ-Bromohydroquinone
CHQ-Chlorohydroquinone
DESY-Deutsches Elektronen-Synchrotron
EXAFS-Extended X-ray Absorption Fine Structure
FDEMS-Frequency Dependent Electromagnetic Sensing
FEA-Finite Element Analysis
FTIR-Fourier Transform Infrared Spectroscopy
HQ-Hydroquinone
IR-Infrared
LALLS-Low Angle Laser Light Scattering
LCP-Liquid Crystal Polymer
LH2-Liquid Hydrogen
LN2-Liquid Nitrogen
LOX-Liquid Oxygen
MHQ-Methylhydroquinone
MMH-Monomethylhydrazine
NMR-Nuclear Magnetic Resonance
NTO-Nitrogen Tetroxide
OTV-Orbit Transfer Vehicle
PAS-Photoacoustic Spectrospcopy
PEHQ-Phenylethylhydroquinone (See SHQ)
PHQ-Phenylhydroquinone
PICNIC-Propellant Insulation Case Nozzle Integrated Component
PMT-Photomultiplier Tube
QEXAFS-Quick Acquisition EXAFS
RDA-Rheometrics Dynamic Analyzer
RF-Radio Frequency
SHQ-Styrylhydroquinone (See PEHQ)
SANS-Small Angle Neutron Scattering
SAXS-Small Angle X-ray Scattering
TA-Terephthalic Acid or Terephthalate
TGA-Thermogravimetric Analysis
TIRF-Total Internal Reflection Fluorescence
UV-Ultraviolet
VATIRF-Variable Angle TIRF
XRD-X-ray Diffraction

THE ADVANCED POLYMER COMPONENTS INITIATIVE

J.J. Rusek
Phillips Laboratory
United States Air Force
Edwards AFB CA

INTRODUCTION

Thermotropic liquid crystal polymers are the strongest engineering thermoplastic materials available. Their low weight, chemical resistance and ease of processing make them logical candidates for astronautics applications. Their anisotropic behavior present significant challenges to conventional useage, however. Commercially available thermotropes are available with a variety of reinforcements and fillers to reduce the noted anisotropy in macroscopic moldings.

The United States Air Force at the Phillips Laboratory has taken the lead in using these materials in propulsion applications. Initial studies utilized commercial resins and mixtures to assess the viability of thermotropes in solid rocket motor cases and nozzle substructures, liquid and nuclear propulsion tanks and exterior ablative surface components. During this initial development, a phenomena coined polymer physico-chemical annealing was noted. (1)

The annealing phenomena manifested itself as an increased resistance to chemical attack and an dramatic increase or obviation of the traditional polymer melt temperature. Past work has indicated the annealing phenomena to not involve cross-linking or traditional chain-extension as traditionally noted in other polymeric systems. (1) The focus of the Advanced Polymer Components Initiative in its present state is to understand the annealing phenomena, specifically to derive structure and kinetic information of the annealing of main-chain liquid crystal polymers with varying pendant groups.

The primary driver for this initiative is low-cost access to space. Future manned space exploration missions will require the introduction of large launch vehicles that are reliable as well as economical. To meet the needs for these missions, it is hoped that thermotropic liquid crystal polymers will play a major role in solid, liquid, hybrid and nuclear propulsion hardware.

OBJECTIVES

The primary <u>developmental</u> objective of this initiative is to *demonstrate the feasibility of thermotropic liquid crystal polymers as system components for solid, liquid, hybrid and nuclear propulsion.* The manifestations of this objective have

been one pound solid rocket motor cases, two pound flightweight solid motor cases with integrated nozzles, demonstration liquid engine nozzle plugs and hydrostatic burst cases. These articles were fabricated via injection molding and gave critical propulsion data needed to design further components.

The primary research objective of this initiative is to *understand the fundamental mechanisms of liquid crystalline behavior in polymers and predict structure/property relationships to yield fully engineered articles.* A major portion of this objective comprises the understanding of the annealing phenomena discussed earlier.

ACCOMPLISHMENTS

Over eighty significant accomplishments have occurred over the first five years of this program. The following will serve to highlight selected successes.

1800 psi motors fired at one-third steel weight
Rheology of commercial and model LCPs established
Annealing phenomena noted by chemical compatability with rocket fuel
Annealing phenomena observed by thermal analysis
Model LCP's synthesized by solution polymerization
Neat commercial resins injection molded
MOLDFLOW code operational in-house
Relational database developed for propulsion materials
One pound test motor fired
Hybrid propulsion nozzles tested under fire
Low temperature aluminum CVD of LCP's demonstrated
Halogenated LCP's synthesized
Chlorine and bromine EXAFS realized on LCP's
Two pound motor and nozzle injection-molded
Two pound flightweight solid rocket motor fired

METHODOLOGY

The following four questions and associated tasks serve to fulfill the two stated objectives. The tasks range from fundamental to applied as the list progresses.

What is physico-chemical annealing?
> *Structure*
>> <u>X-ray and Synchrotron Studies</u>
>>> X-ray Diffraction
>>> EXAFS
>>> Small Angle X-ray Scattering
>> <u>Nuclear Studies</u>
>>> Neutron Diffraction
>>> Small Angle Neutron Scattering
> *Assembly*
>> Raman Spectroscopy
>> Total Internal Reflectance
> *Kinetics*
>> Molecular Mechanics
>> Micromechanics
>> QEXAFS
>> Neutron Rheology

How is it measured?
> Thermotropic Polyester Synthesis
> Dielectric Spectroscopy
> Thermal Analysis
> Off-Gas FTIR
> Mechanical Analysis
> Rheology
> Chemical Compatibility

How are parts fabricated?
> Materials Database
> Mold Design
> Process Research

What propulsion test articles are important?
> *Heat Transfer Properties*
>> Hybrid Nozzle
>> Flightweight Nozzle
>> Plaques
> *Mass Transfer Properties*
>> One Pound Case
>> Flightweight Case
> *Ablation Rate*
>> Flightweight Nozzle

Plaques
Chemical Compatibility
Discs
Strand Burn Straws
Cryogenic Properties
One Pound Case
Hot Burst Properties
One Pound Case
Impulse Loading
One Pound Case
Flightweight Motor
Transverse G-Loading
Tactical Demonstrator

The vast nature of this program can only be accomplished through effective collaboration. Figure 1 shows the strategic alliance that exists on the Advanced Polymer Components Initiative. Eight universities, five DOD military installations and five commercial industries comprise the domestic collaboration of the initiative. One Australian and one German collaboration exist to complete the strategic alliance. The alliances are defined as true collaborations, wherein each partner contributes to the program and receives the benefits of the entire alliance.
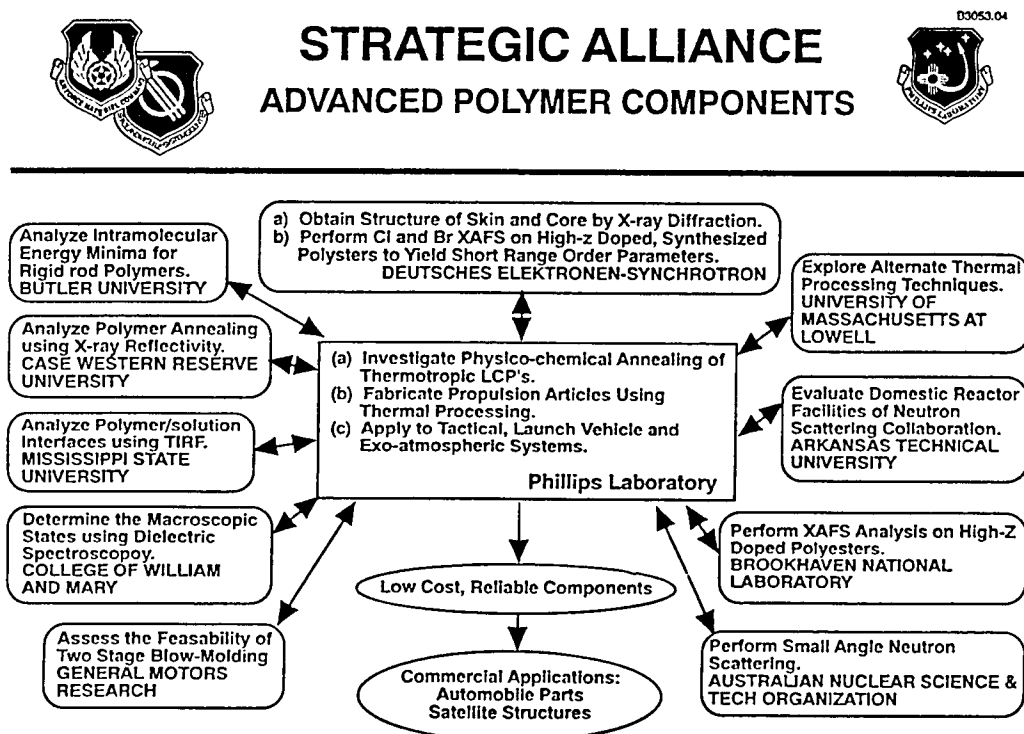

STRATEGIC ALLIANCE
ADVANCED POLYMER COMPONENTS

D3053.04

Analyze Intramolecular Energy Minima for Rigid rod Polymers. BUTLER UNIVERSITY

a) Obtain Structure of Skin and Core by X-ray Diffraction.
b) Perform Cl and Br XAFS on High-z Doped, Synthesized Polysters to Yield Short Range Order Parameters.
DEUTSCHES ELEKTRONEN-SYNCHROTRON

Explore Alternate Thermal Processing Techniques. UNIVERSITY OF MASSACHUSETTS AT LOWELL

Analyze Polymer Annealing using X-ray Reflectivity. CASE WESTERN RESERVE UNIVERSITY

(a) Investigate Physico-chemical Annealing of Thermotropic LCP's.
(b) Fabricate Propulsion Articles Using Thermal Processing.
(c) Apply to Tactical, Launch Vehicle and Exo-atmospheric Systems.
Phillips Laboratory

Evaluate Domestic Reactor Facilities of Neutron Scattering Collaboration. ARKANSAS TECHNICAL UNIVERSITY

Analyze Polymer/solution Interfaces using TIRF. MISSISSIPPI STATE UNIVERSITY

Determine the Macroscopic States using Dielectric Spectroscopoy. COLLEGE OF WILLIAM AND MARY

Perform XAFS Analysis on High-Z Doped Polyesters. BROOKHAVEN NATIONAL LABORATORY

Low Cost, Reliable Components

Assess the Feasability of Two Stage Blow-Molding GENERAL MOTORS RESEARCH

Commercial Applications: Automobile Parts Satellite Structures

Perform Small Angle Neutron Scattering. AUSTRALIAN NUCLEAR SCIENCE & TECH ORGANIZATION

Figure 1. Strategic Alliance within the Advanced Polymer Components Initiative

SUMMARY

This program will have a profound effect on future space missions if the annealing phenomena can be fully understood. The key to working with these highly anisotropic materials is to first understand them and then use or develop the proper thermal processing to accomplish a rationally designed part.

REFERENCES

1 Rusek, J.J., "Proceedings of the First Annual Advanced Polymer Components Symposium," PL-TR-92-3018, Edwards Air Force Base, Ca, July 1992

Liquid Crystalline Copolyesters as High Temperature Adhesives for Aluminum

JAMES ECONOMY*, TANIA GOGEVA and VIJAY HABBU

Department of Materials Science & Engineering, University of Illinois, 1304 W. Green Street, Urbana, IL 61801, U.S.A.

A liquid crystalline copolyester consisting of 4-hydroxybenzoic acid and 6-hydroxy-2-naphthoic acid, with a composition (73:27) was studied as a melt processible, high temperature adhesive. The polymer was used as received without any additional treatment and was applied on an aluminum substrate as a film. The adhesive joints were prepared using different processing conditions and good bonding between the two polymer surfaces was observed under most of these conditions. The reliability of the adhesive bond was estimated by measuring the lap shear strength (1.4–1.6 Ksi) and the crack propagation in the wedge test. Improved adhesion (2 times) over epoxy adhesives, applied on the same substrate, was observed when tested at room temperature and there was no significant decrease in the lap shear strength in the range RT–180°C. The post-failure surfaces were studied with SEM and it was observed that separation occurred within the adhesive.

KEY WORDS adhesive bonding; aluminum; copolyester; 4-hydroxybenzoic acid and 6-hydroxy-2-naphthoic acid; lap shear strength; SEM.

INTRODUCTION

Use of liquid crystalline (LC) aromatic copolyesters as structural adhesives has not been examined to date in any detail. On the other hand, these rod-like polymers are of considerable interest because of their excellent mechanical and thermal properties and high melt flow under shear.[1-6] One such system, a copolyester of p-hydroxybenzoic acid with biphenol terephthalate (Xydar®), has been shown to retain a significant percentage of its mechanical properties up to 350°C.[6] Thus, it would be highly desirable to design LC copolyesters for use as high temperature structural adhesives. Currently there are very few systems available commercially for extended use in the temperature range of 150°–340°C. For intermediate temperatures (up to 200°C) the adhesive systems that are available include unmodified epoxy, epoxy phenolic and nitrile phenolic. Typically their processing conditions are similar to conventional adhesives, *i.e.* curing at ~175°C and moderate pressures (up to 100 psi).[7] Adhesives for higher use temperatures of 200° to 340°C include

---

*To whom all correspondence should be addressed.

polyimide, polyquinoxaline and polybenzimidazoles. These systems require significantly different processing; *e.g.* higher curing temperatures of 343°C, venting or permanent vacuum (to control volatiles) and they should be used with considerable caution.[7] These high temperature adhesives are applied after the substrate is pretreated (most often anodized)[8] and covered with an adhesive primer. They also require corrosion-inhibiting additives and a diluting solvent and display a limited shelf-life.[7]

One possible reason that the LC polyesters have not been evaluated as potential adhesives is the observation that good adhesion between stiff extended chain polymers such as polyimides can only be achieved if the polymer chains penetrate up to several hundred Å across the interface between the coatings.[9] Presumably the rod-like nature of the LC polyesters would further reduce the potential for chain entanglement. On the other hand, in some of our recent work we have shown that the rod-like aromatic copolyesters can undergo very rapid interchain transesterification reactions at elevated temperatures.[4] If such reactions were to occur at the interface between two LC polyester coatings, one would expect to produce a homogeneous composition across the interface between the two coatings. It was, in fact, these observations that led us to pursue the study of the LC polyesters as potential high temperature, structural adhesives.

In this paper, we report on the successful evaluation of an LC copolyester of 73/27 p-hydroxybenzoic acid, 2,6-hydroxynaphthoic acid (HBA/HNA) as a structural adhesive for aluminum.

EXPERIMENTAL

Materials

A copolyester of HBA:HNA = 73:27 (molar %), Vectra A-950®, with a melting temperature at about 280°C, was obtained from Hoechst-Celanese. The polymer was received in the form of granules and was ground before use. A commercial 5-minute curing epoxy adhesive, #10-114 (GC/Thorsen, Rockford, Illinois, U.S.A.), was used as a control. The material used as the adherend (the substrate) was an aluminum alloy 2024 T-3.

Sample Preparation

Specimens were prepared in accordance with ASTM D 1002–83, Strength Properties of Adhesives in Shear by Tension Loading (lap shear joint metal-to-metal) and ASTM D 3762–79, Adhesive-bonded Surface Durability of Aluminum (wedge test). Both types of specimens were made in multiples and then cut into individual test specimens. Sheets of the aluminum substrate were cut to suitable sizes— $17.8 \times 10.2 \times 0.16$ cm ($7 \times 4 \times 0.064$ in) panels (ASTM D 1002) and $15.2 \times 15.2 \times 0.32$ cm ($6 \times 6 \times 0.125$ in) (ASTM D 3762). Prior to the application of the adhesive the surfaces in the overlapping area of each panel were cleaned by the Liquid Honing Process (Vapor Blast Mfg. Co.) using 200 mesh glass beads (soda lime glass) and then dried in a conventional oven (110°C).

The adhesive was applied to an area about 6 mm (0.25 in) longer than the overlap 12.7 mm (0.5 in) as recommended by the test method (ASTM D 1002). The length of the overlap was controlled within ±0.25 mm (0.01 in) using a special fixture— a steel plate with mounted pins (stoppers), forming a framework with the desired dimensions.

The amount of the adhesive used was about 0.016 g/cm^2 (0.1 g/sq. in). It was applied as a film on both substrate surfaces (precoating) or as a powder between the two adherends. The precoating was carried out by heating to 330°C at a pressure of about 100 psi, using polyimide (Kapton®) films as a separating layer and as a spacer to keep the adhesive thickness constant. Cooling was carried out under pressure and a cooling rate at 2°C/min.

With respect to the panels for the wedge test, after applying the adhesive and subsequent processing, a 19 × 152 × 0.025 mm (0.75 × 6 × 0.001 in) separation film was inserted along one of the 152 mm wide edges. The assembled panels were bonded at different temperatures, pressures and durations. All the processing experiments were carried out in an open lab hot press (Carver).

The panels were cut into 25.4 mm (1 in) wide specimens. A wedge was forced into the bondline of the ASTM D 3762–79 specimens and the adhesive system was dipped in water (71°C) for 1 hour. The wedge test was carried out because it is highly reliable in determining and predicting the environmental durability of adherend surface preparation. The method can be correlated with service performance in a manner more reliable than the usual lap shear and peel tests. The substrate was also cut into small pieces 10 × 20 mm and the surfaces were coated and assembled following the above described procedure and boiled in common water until debonding was observed. Cross-sections of the cleaned and precoated aluminum substrate were obtained by fracturing. Metal bars were notch cut, approaching the studied surface, and then separated by pulling apart. Also a plate was prepared for thermal analysis from the copolyester in a stainless steel mold at conditions comparable with those used for the precoating and assembling of the adhesive bond.

Sample Characterization

The thickness of each adhesive layer was measured before testing using a digimatic micrometer (Mitutoyo) with an accuracy ±0.001 mm (0.00005 in).

Some of the lap shear strength measurements were carried out using a screw driven tensile machine (MTS), but most of them were conducted on a servo hydraulic closed loop test system (MTS 880 Series), and with a crosshead speed 1.3 mm (0.05 in)/min in both cases. The length of the specimens gripped in the jaws was constant at 50.8 mm (2 in). The measurements were carried out in the range of room temperature (RT) to 200°C, using a flexible electric heating tape or in an environmental chamber (MTS 880 Series) with control to within 2°C. The specimens were kept at that temperature for 5 min before testing and the temperature was controlled with a thermocouple attached to the joint (in the first case). Other specimens were immersed in boiling water for a period of time and then tested. The crack propagation of the wedged specimens was measured using a magnifier (× 10).

The calorimetric studies were performed on a differential scanning calorimeter (DSC) Shimadzu TA-50 at a scanning rate of 20°/min and a sample weight of about 5–9 mg.

Scanning electron microscopy (SEM) studies were carried out on a Hitachi S-800. Prior to viewing the adhesive surface, specimens were covered with a thin gold-palladium layer in a Polaron sputtering chamber.

RESULTS AND DISCUSSION

Nature of the Liquid Crystalline Copolyesters

The chemical structure of the liquid crystalline polymer used in the present work is given below:
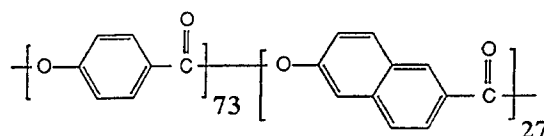
The vendor indicates that this polymer has a Mw in excess of 20,000 and a melting temperature at about 280°C. Figure 1 presents a DSC trace of this material, and like some other authors[4] we observe that it is quite hard to reproduce accurately.
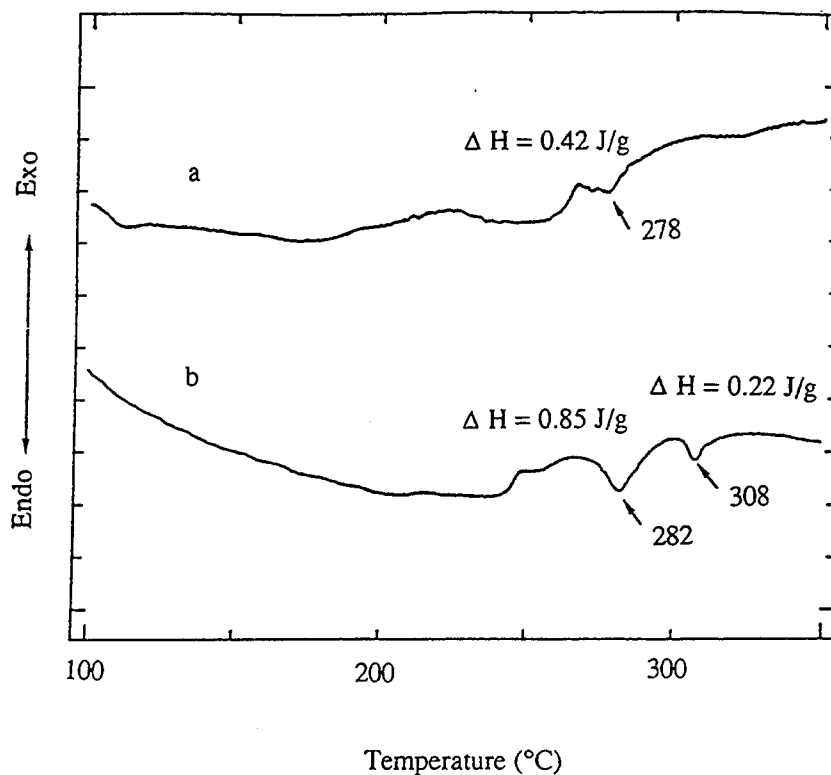
FIGURE 1   DCS scans of (a) the 73/27 composition as received and (b) processed at 300°C, 30 min and 700 psi.

9

The thermal behavior of the as received (curve a) and as processed (curve b) materials shows that the enthalpy values are low and the degree of crystallinity is correspondingly low. This should not be surprising considering that the microstructure of the copolyester is random.

The 73/27 copolyester on melting at its transition temperature at about 280°C converts into a nematic structure. Studies on the rhelogical behavior of this copolymer showed that samples, when kept at temperatures close to the melting point, displayed a significant increase in the complex modulus[5] which appears related to formation of higher melting crystals. Heating at 320°C resulted in a reversion of the more ordered state back to the original system with a m.p. ~278°C. This unusual behavior has recently been interpreted to arise from interchain transesterification reactions.[3] Thus on heating near the crystal nematic transition an ordering of the microstructure within the existing crystallites occurs. On the other hand, heating well above these temperatures results in randomization back to the original microstructure.[4]

Adhesion Studies

The copolyester was applied onto the aluminum surface and heated to a temperature of 330°C (precoating of the substrate). During this step pressure was applied to enhance the flow of the melt. SEM examination of the non-coated and adhesive precoated surfaces (pressure about 100 psi, 330°C) shows that the polymer melt has effectively wet the aluminum surface and formed an even film (Fig. 2).
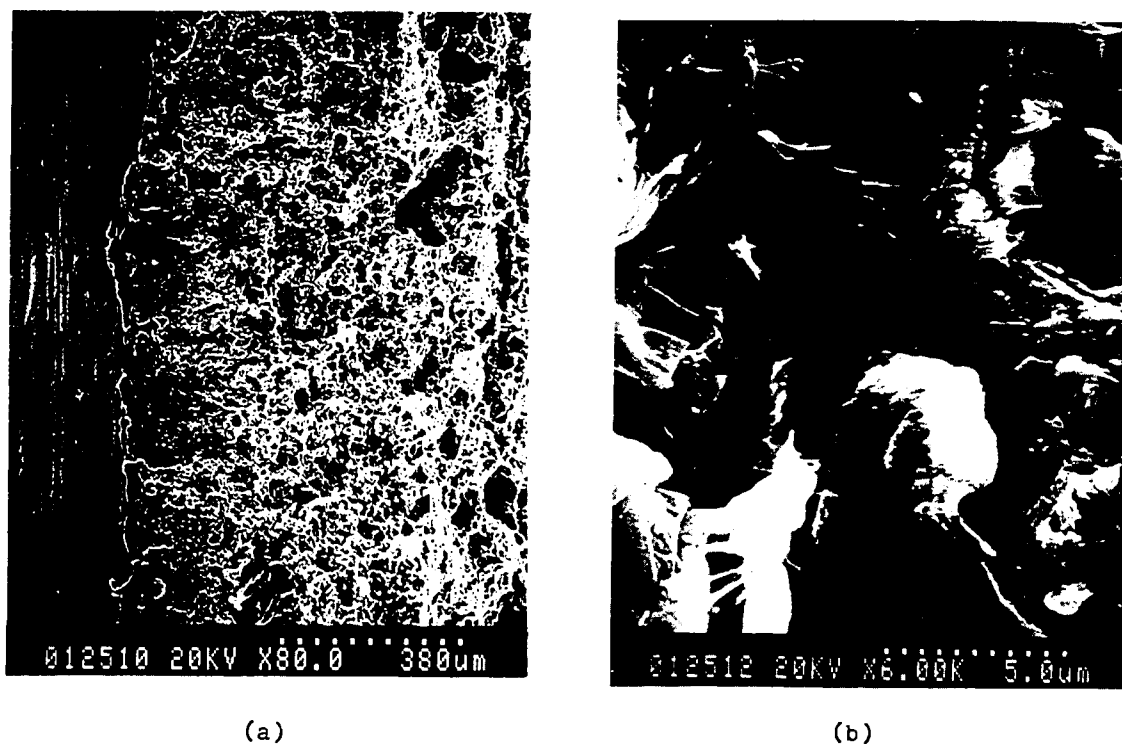

(a)   (b)

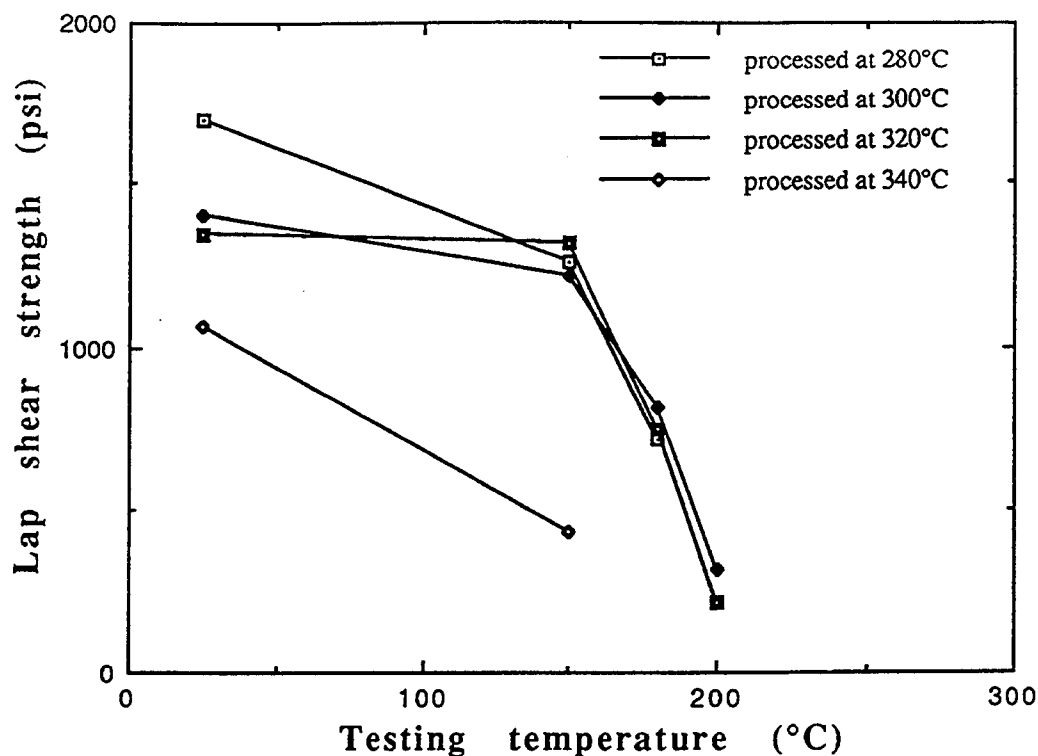FIGURE 2   SEM micrographs of the coated aluminum plates: (a) 80×, (b) 6000×.

FIGURE 3 Effect of the processing temperature on the lap shear strength for specimens tested at different temperatures.

The precoated adherend panels (cooled to RT) were overlapped and processed in a hot press over a temperature range of 250° to 340°C, at pressures of 100, 700 and 1400 psi and durations of 30, 45 and 60 min. Also, samples were prepared from nonprecoated specimens (the polymer was applied as a powder between the adherends). In this latter approach lower mechanical property data was observed, most probably because of the poorer alignment during processing as well as changes in the processing conditions. In this latter case, the adhesive (between the two aluminum plates) was heated to 330°C, kept there for 5 min and then cooled to the processing temperature and kept at this temperature for the designated time (usually 30 min). The lap shear data for samples prepared at different times showed relatively poor bonding after 15 min, very good results for 30 or 45 min and a decrease in the values for 60 min. The latter may be due to decomposition.

The lap shear strength *vs* processing temperature is given in Figure 3, while in Table I these results are summarized along with the wedge test data. Micrographs of representative fracture surfaces are shown in Figure 4 a and b. In Figure 5 the lap shear strength *vs* the processing pressure is illustrated at room temperature and 180°C. The excellent resistance of these adhesive joints to boiling water is shown in Figure 6.

The excellent adhesion of the Vectra A-950® liquid crystalline polymer to aluminum may in part be due to the fact that the polymer at the metal polymer interphase tends to orient on cooling from the melt in such a way as to minimize the mismatch in the coefficient of thermal expension (CTE). Presumably, while cooling in the melt the LC polymer responds to the contraction of the substrate to minimize the stress and thus approximate the CTE of the substrate. This process

TABLE I

Lap shear strength and wedge test data for specimens processed at different temperatures

Nu	Process conditions** T°C	(psi)	Lap shear strength, psi RT	180°C	Wedge test σ (mm)	Δσ (mm)
7*	RT	700	887			
2	280	700	1426	764		
3	300	700	1404	812	70.4	8.9
4	320	700	1346	750		
5	280	100	2025	597	61.7	6.7
6	300	100	2105	578	65.7	9.8
7	320	100	1800	593	60.9	11.3
8***	300	700	1330	750	56.5	23.1

*Epoxy
**30 minutes
***Not precoated

could continue well below the crystal-nematic transition. In addition, the bonding between the aluminum and polymer would be greatly enhanced through the dipolar interactions of the carboxylate ester with the oxide coating on the aluminum.

The good polymer-polymer adhesion observed in this study appears to be primarily a result of rapid ester-ester interchange reactions at the surface with perhaps a minor contribution from chain diffusion processes. The earlier cited work[9] demonstrates convincingly the problem of developing good adhesion between coat-

(a)   (b)
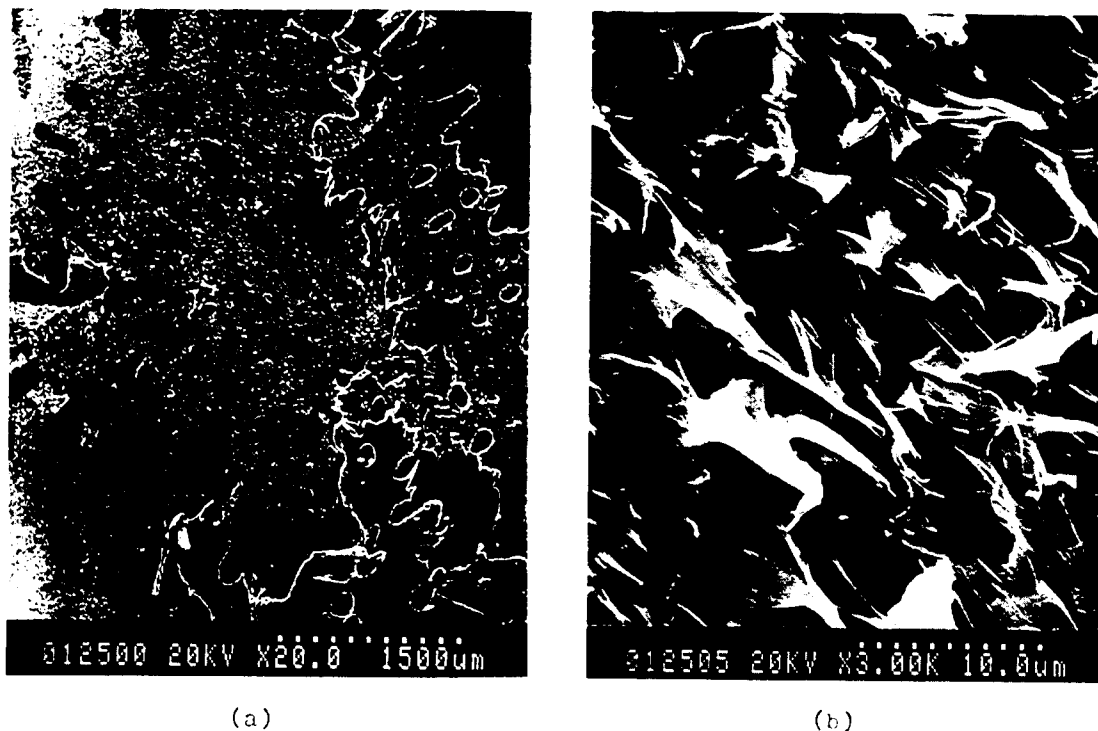
FIGURE 4   SEM micrographs of fracture surfaces: (a) 20×. (b) 3000×.
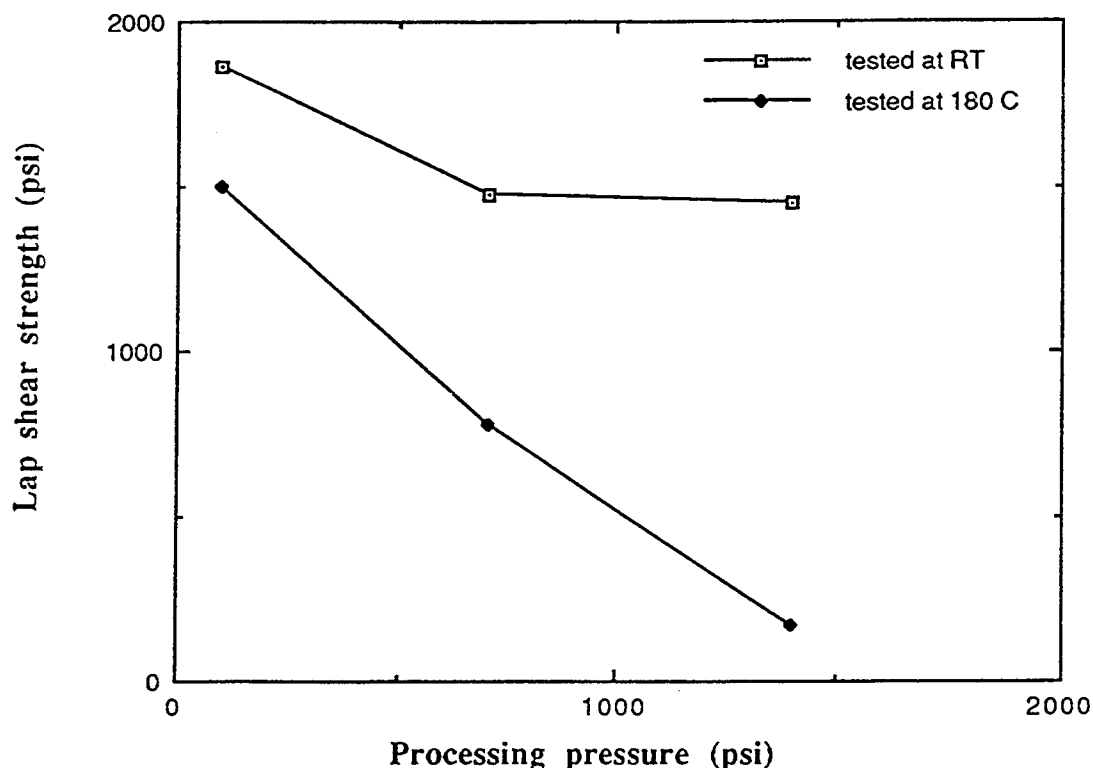
12

FIGURE 5 Effect of the processing pressure *vs* shear strength for specimens heated at room temperature and 180°C.

ings of stiff chain polymers such as polyimide. Additional evidence for interchain transesterification is available from the literature where a mixture of deuterated and undeuterated polyethylene terephthalate was completely randomized on heating at 300°C for one hour.[10] On the other hand, at processing temperatures of 250°C the rate of the ester interchange reaction would be much slower (assuming an Arrhenius process). To summarize, the possibility of rapid interchain transesterification reactions[3] provides a mechanism for forming a good adhesive bond across an interface. The interchain transesterification is most likely catalyzed by the carboxylic acid end group. This kind of reaction is temperature dependent and would appear to require only seconds at 425°–450°C, minutes at 350°–375°C, and hours at 250° to 275°C. Presumably, such a mechanism cannot occur with polyimides.

It is interesting to note that the LC 73/27 copolyester retains good adhesive characteristics well above the polymer glass transition temperature of the LC copolyester ($T_g \sim 110°C$) but well below the crystal nematic transition ($T_m = 278°C$). Presumably, the small amount of crystalline order present in these copolyesters enhances the retention of mechanical properties well above T_g. It should be noted that the potential exists to increase the high temperature mechanical properties further by first annealing at 50–70°C below the T_m and then by heating near the crystalline nematic transition for several hours. The annealing increases the transition enthalpy by a factor of 3–4 while heating near the crystal-nematic transition raises the melting point by 40–60°C.[3] Also by using HBA/HNA compositions with much higher
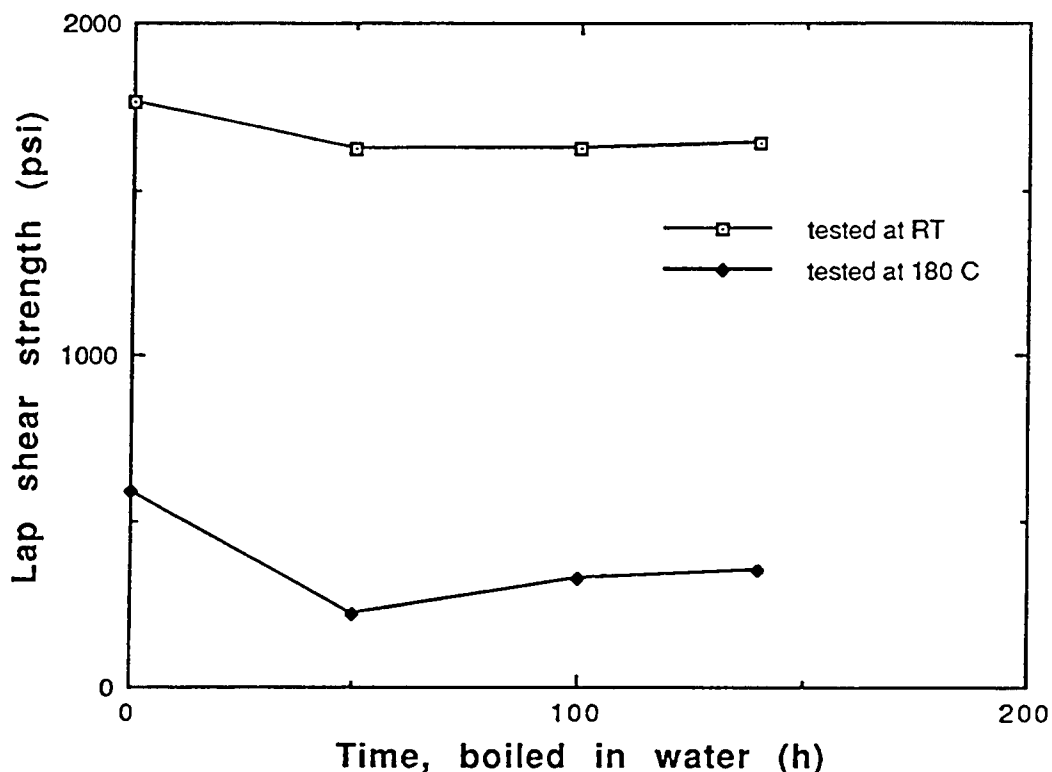
FIGURE 6   Data which demonstrate the outstanding resistance of these adhesive joints to boiling water.

melting points (*e.g.* 350°C), one could obtain an additional enhancement in retention of properties at high temperatures. All these possibilities are now being examined.

CONCLUSIONS

1. The melt processible LC aromatic copolyesters have been shown to function as excellent high temperature adhesives with very good resistance to a corrosive environment.
2. The excellent adhesion to the aluminum substrate appears to be the result of good wetting, and likely the tendency for the polymer to orient at the surface to produce a stress-free interface.
3. Adhesive behavior between the polymer coatings applied to the aluminum arises primarily from chemical processes at the interface of the polymers, *i.e.* interchain transesterification.

References

1. A. Muhlebach, R. D. Johnson, J. Lyerla and J. Economy, *Macromolecules* **21**, 3115 (1988).
2. A. Muhlebach, J. Economy, R. D. Johnson, T. Karis and J. Lyerla, *Macromolecules* **23**, 1803 (1990).

3. J. Kachidza, G. Serpe and J. Economy, Inter. Symp. on Polym. Mat. 10–15 Feb. 1991, Melbourne, Australia, *Makromol. Chem,* in press (1991).
4. A. H. Windle, Ch. Viney, R. Golombok, A. M. Donald and G. R. Mitchell, *Faraday Discuss, Chem. Soc.* **79,** 55 (1985).
5. Y. G. Lin and H. H. Winter, *Macromolecules* **21,** 2439 (1988).
6. J. Economy, *Mol. Cryst. Liq. Cryst.* **169,** 1 (1989).
7. E. C. Millard, in *Adhesive Bonding of Aluminum Alloys,* E. Thrall and R. Shannon, Eds. (Marcel Dekker, Inc., New York, 1985), p. 127.
8. L. Kozma and I. Olefjor, *Mater. Sci. Technol.* **3,** 860 (1987).
9. H. R. Brown, A. C. M. Yang, T. P. Russell, W. Volksen and E. J. Kramer, *Polymer* **29,** 1807 (1988).
10. J. Kugler, J. W. Gilmer, D. W. Wiswe, H. G. Zackmann, K. Hohn, E. W. Fischer, *Macromolecules* **20,** 1116 (1987).

Factors Which Influence the High Temperature Adhesive Characteristics of Liquid Crystalline Copolyesters

J. ECONOMY and A. G. ANDREOPOULOS*

Department of Materials Science and Engineering, University of Illinois at Urbana-Champaign, 1304 W. Green St., Urbana, IL 61801, U.S.A.

Liquid crystalline copolyesters of p-hydroxybenzoic acid and 6-hydroxy-2-naphthoic acid, with compositions 20/80 and 24/76, were studied in order to evaluate the effect of higher melting HBA/HNA copolyesters on the high temperature adhesive properties compared with data for the recently reported 73/27 system. A tetramer of HBA/HNA with a composition of 24/76 was synthesized to examine the effect on adhesion of wetting of the substrate at much lower temperatures. From the results of this study it is now possible to define approaches for achieving very good adhesion characteristics at temperatures well in excess of 250°C.

KEY WORDS high temperature adhesives; liquid crystalline copolyesters; interchain transesterification; chemically induced ordering; glass transition temperature; annealing; processability; lap shear strength; oligomer.

INTRODUCTION

Recently we reported that the 73/27 liquid crystalline copolyester of p-hydroxybenzoic acid (PHBA) and 2,6-hydroxynaphthoic acid (HNA) acted as a good adhesive at temperatures up to 180°C.[1] The unusually good adhesion characteristics were somewhat surprising[2-4] in light of the rod-like nature of the liquid crystalline (LC) chains. Of more technological interest was the fact that this class of polyesters might be able to display good adhesion at even higher temperatures of 200–250°C.

In the present work a study has been made of two higher melting HBA/HNA copolyesters to evaluate the effect of degree of crystallinity and melting point on the high temperature adhesion properties. More specifically, the 20/80 and 24/76 HBA/HNA copolyesters were examined because of their much higher melting points and degrees of crystallinity as compared with the 73/27 copolyester. Other variables that were investigated included the effect of annealing to increase the

---

*Permanent address: Department of Chemical Engineering, NTU of Athens, 9 Iroon Polytechniou Str., 157 80 Zografou, Athens, Greece

transition enthalpy and the possibility to increase further the crystal to nematic transition temperature (T_{CN}) by 40–50°C, by chemical ordering.[5] Also, the role of the glass transition temperature (T_g) on the high temperature properties was examined by determining the T_g of HBA/HNA copolyesters over the compositional range of 20/80 to 73/27. Because of the much higher melting points of these copolyesters compared with the 73/27 system, an oligomer of the 24/76 copolyester was prepared that could more effectively wet the adherend at much lower temperatures and then be further advanced.

EXPERIMENTAL

Materials and Methods

The 20/80 and 24/76 HBA/HNA copolyesters, with a weight average molecular weight of 20000, were supplied by Hoechst-Celanese while the 24/76 oligomer, with a degree of polymerization ~4, was prepared in our laboratory according to the procedure outlined in the section "Preparation of the Oligomer."

The ASTM D 1002-83 test method, Strength Properties of Adhesives in Shear by Tension Loading (lap shear joint metal to metal), was followed for the evaluation of the adhesive bonding. This method was selected among others,[6] as it is specified for adhesion on aluminum substrates.[7]

Characterization of Materials

The polymers used in this study were characterized by Thermal Analysis using a Du Pont 2000 Thermal Analyzer (heating rate 20°C/min). The copolyesters, after being applied on aluminum substrates, were given the following treatments:

a) Annealing at 75°C below their melting points
b) Heating of the annealed samples at 5°C above the melting points of the as received materials.

The annealing took place, under a pressure of 100 psi, in a heated plate hydraulic press, whereas heating was carried out in a Fischer Scientific Isotemp Vacuum Oven, Model 282, under nitrogen.

Preparation of the Oligomer

The 24/76 p-HBA/HNA oligomer was prepared using the acetoxy esters of p-hydroxybenzoic and 6-hydroxy-2-naphthoic acid as starting materials. The acetoxy ester of 6-hydroxy-2-naphthoic acid was prepared by direct acetylation of the sodium salt of the acid as described in detail elsewhere.[8,9] Polymerization was carried out in a heat transfer fluid, Therminol 66 (Monsanto Co). The temperature was raised from 170° to 250°C over a period of 2 hours. The amount of acetic acid evolved was used to approximate the extent of reaction. A degree of polymerization

17

of 4 was assumed at the point that 75% of the total acetic acid was collected. No attempt was made to characterize the compositional distribution, but based on studies of reactivity ratios of the 50/50 HBA/HNA system,[5] it would appear to approximate the composition of the starting material.

Preparation and Testing of Specimens

Specimens were prepared according to ASTM D 1002-83, Strength Properties of Adhesives in Shear by Tension Loading. Sheets of aluminum, alloy 2024T-3, were cut into suitable sizes, *i.e.* $17.78 \times 10.16 \times 0.16$ cm ($7 \times 4 \times 0.064$ inch) panels. Prior to the application of the adhesive, the surfaces in the overlapping area of each panel were cleaned by the Liquid Honing Process (Vapor Blast Mfg. Co.) using 200 mesh glass beads (soda lime glass), rinsed with distilled water and then dried in a conventional oven (110°C).

The adhesive was applied to an area about 6 mm (0.25 in) longer than the overlap 12.7 mm (0.5 in) as recommended by the test method (ASTM D 1002). The length of the overlap was controlled within ± 0.25 mm (0.01 in) using a special fixture, *i.e.* a steel plate with mounted pins as stoppers, forming a framework with the desired dimensions. Consolidation of the framework was carried out at room temperature. The amount of the adhesive used was about 0.016 g/cm^2 (0.1 g/in^2). It was applied as a film on both substrate surfaces so that precoated aluminum sheets were produced. The deposition of the polymer film was carried out by heating above the melting point of the polymer used, at a pressure of about 100 psi, using Kapton polyimide films as a separating layer and as a spacer to keep the adhesive thickness constant. The precoated aluminum specimens were put together and compressed in a heated Carver Hydraulic Press. After trimming the edges, the panels were cut into individual specimens of 2.54 cm (1 in) width.

The lap shear strength measurements were carried out on a servohydraulic closed loop test system (MTS 880 Series) with a grip separation speed 1.3 mm (0.05 in) per min. The length of the specimens gripped in the jaws was constant at 50.8 mm (2 in). The measurements were carried out up to 220°C in an environmental chamber with control to within ± 2°C. The specimens were kept at the testing temperature for 5 min in order to reach equilibrium.

Glass Transition Temperature Measurements

The Glass Transition Temperature (T_g) of the copolyesters used in this study was determined by DSC analysis. The samples were heated, in sealed pans, at temperatures above their melting points for about 15 min and then quenched in liquid nitrogen so that an amorphous product was formed.

DSC experiments were run at a heating rate of 20°C/min, from room temperature up to 400°C, in order to verify whether the samples were completely amorphous. The T_g was calculated from the change in slope shown in the plots of the DSC scans (see Fig. 5). The change in T_g with composition was determined by also characterizing the 30/70, 50/50, 60/40 and 73/27 HBA/HNA copolyesters.

RESULTS AND DISCUSSION

The DSC data for the 20/80 and 24/76 HBA/HNA copolyesters are shown in Table I and compared with the 73/27 system. These data were obtained from DSC curves similar to those presented in Figure 3. The observed differences between DSC's of the oligomer and the copolyesters are consistent with the much lower molecular weight of the oligomer. It is evident, from this Table, that these copolyesters display 40 to 60°C higher melting points compared with the 73/27 system. It therefore seemed reasonable that the above materials would display better high temperature adhesion as compared with the 73/27. On the other hand, the relatively low degree of crystallinity in these copolyesters (5–20%) would suggest that the glass transition temperature (more correctly nematic glass) might also play a significant role.

The data of Table I show that in all three cases the transition enthalpy can be increased by 3 to 4 times upon annealing at temperatures 75°C below the respective melting points. The double endotherm observed on annealing the as-received material can be interpreted either as a broad compositional distribution or a mixture of random and blocky copolymer. It was of interest to determine whether the higher degree of crystallinity would significantly increase the high temperature adhesion characteristics. Although it is difficult to quantify, we estimate from the transition enthalpies that the degree of crystallinity increases from well below 10% to about 25%.

Another variable that was examined in this study was the potential to increase the crystal-nematic transition temperature by 40–50°C by heating the material near its melting point for 20 hours. This kind of increase in the crystal-nematic transition temperature has been observed by various workers, although some confusion exists as to its origin; i.e. is it a physical or a chemical process.[10-11] In some very recent studies[9] we have concluded that it is chemical in nature and proceeds by carboxylic acid end group catalyzed interchain transesterification reactions that occur only within the existing crystalline regions.

It was found that the lap shear strengths at elevated temperatures for both the 20/80 and 24/76 systems showed significant improvement over the results reported with the 73/27 system. Thus, in Figure 1 the 20/80 HBA/HNA copolyester retains

TABLE I
DSC data for the 20/80 and 24/76 HBA/HNA copolyesters
compared with the 73/27 system

Composition	20/80	24/76	73/27
Melting point (°C)			
As received	342	325	281
Annealed[1]	312/349	304/334	243/277
Heated[2]	378	370	332
Endotherms (J/g)			
As received	2.87	2.08	1.02
Annealed[1]	11.16	9.07	5.98
Heated[2]	14.19	8.51	6.90

[1]Annealed at 75°C below the melting point, for 24 hours
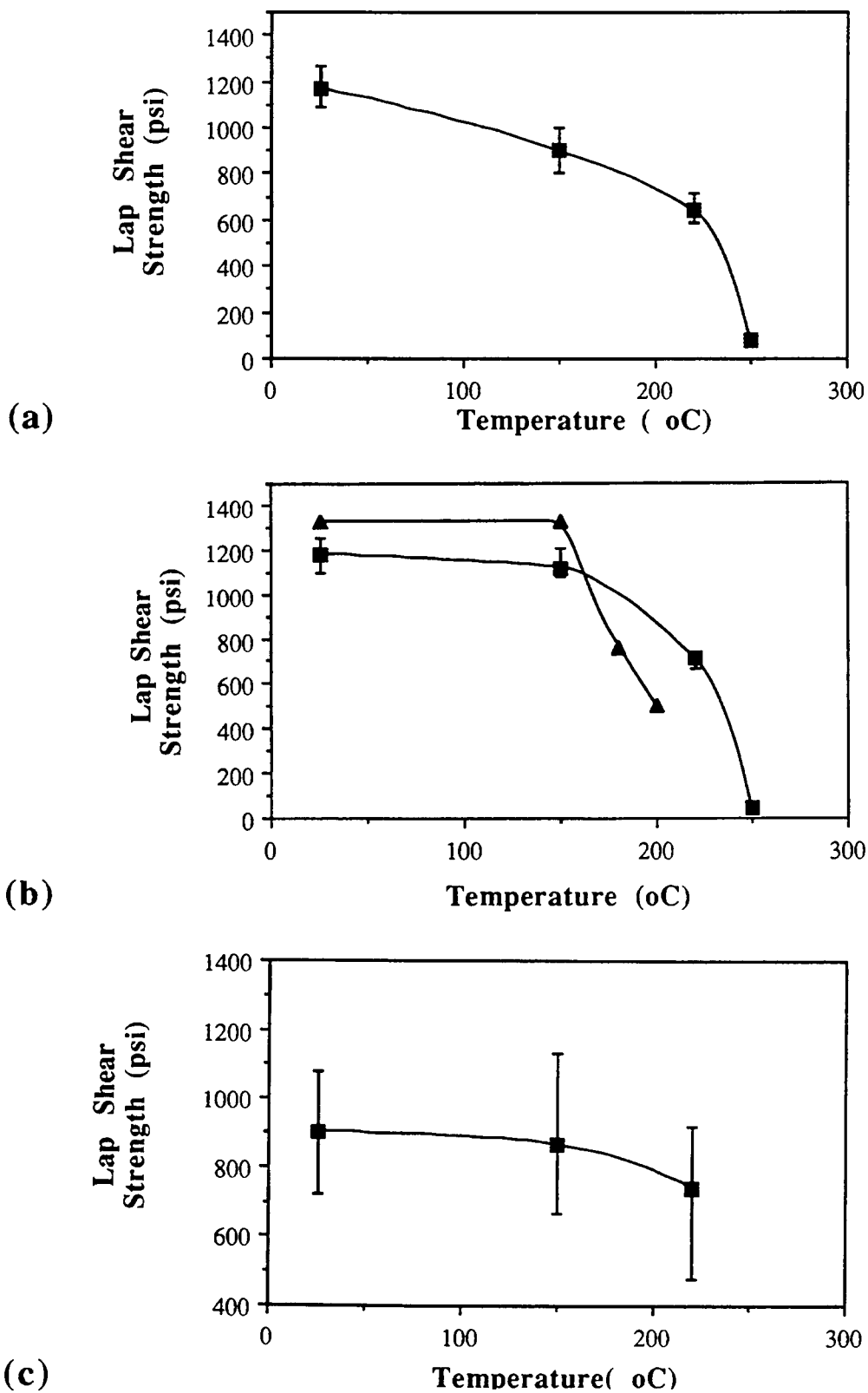[2]Heated at 5°C above the melting point, for 24 hours

FIGURE 1 The lap shear strength for the 20/80 HBA/HNA copolyester: (a) As received, (b) Annealed at 270°C, (c) Heated at 350°C.
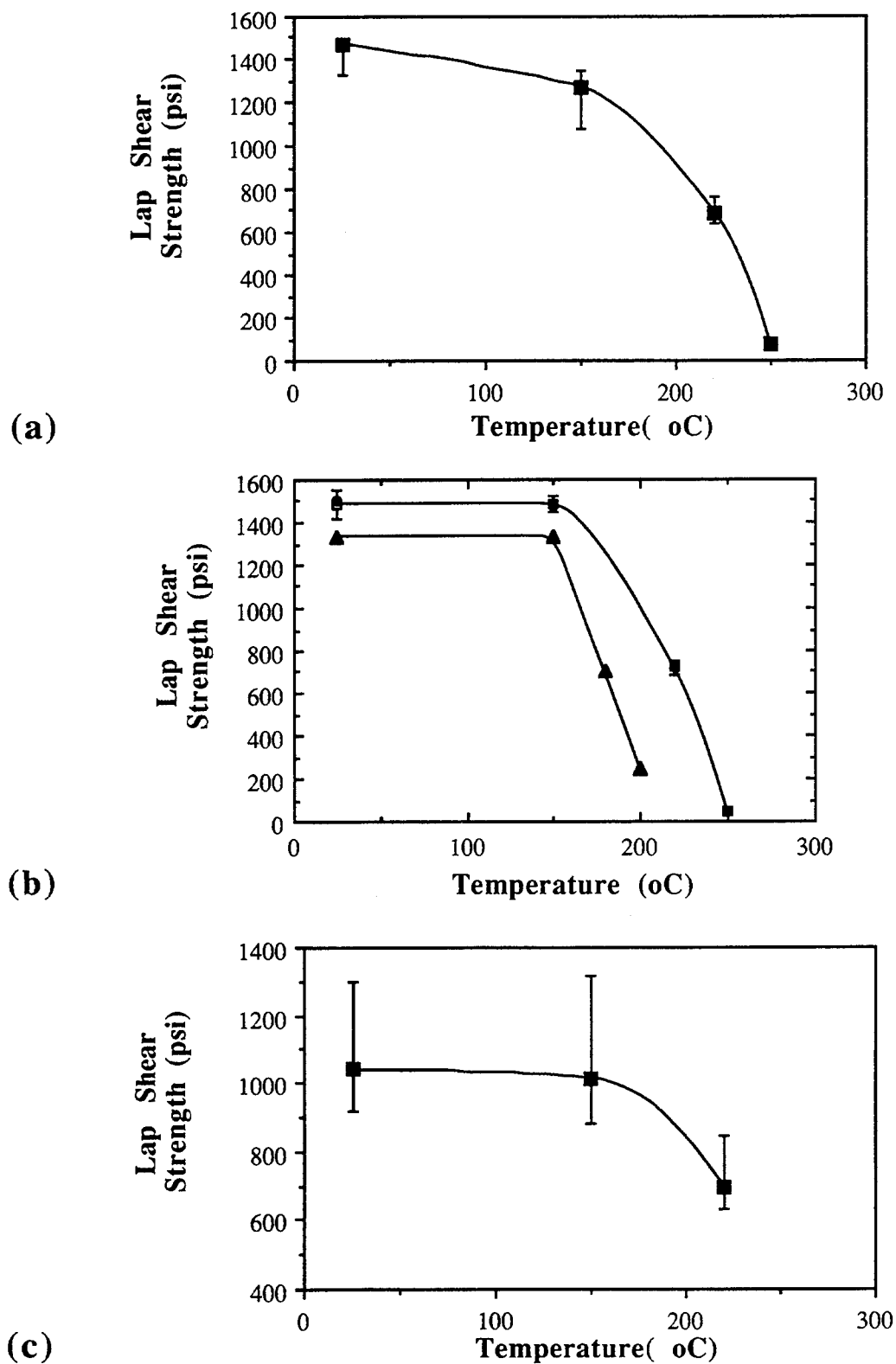
FIGURE 2 The lap shear strength for the 24/76 HBA/HNA copolyester: (a) As received, (b) Annealed at 250°C, (c) Heated at 330°C.

useful lap shear strength to 225°C as compared with the 73/27 which has lost most of its mechanical strength at 200°C. On the other hand, no additional improvement was observed in the 20/80 system either by annealing to increase the degree of crystallinity or by attempting to increase the crystal-nematic transition temperature by heating near the crystal-nematic transition point. The slightly lower lap shear strength at room temperature for the 20/80 *versus* 73/27 copolyester may be a result of having to use a much higher temperature for processing the 20/80 system. In the earlier work on the 73/27 system[1] it was reported that the adhesion dropped dramatically when the test samples were prepared at 340°C.

Moderately improved lap shear strengths were obtained for the 24/76 copolyester compared with the 20/80 system, as shown in Figure 2. This may very well be the result of the use of lower processing temperatures. More pertinent to this study, both the 20/80 and 24/76 copolyesters showed far better retention of properties in the temperature range of 180°–225°C compared with the 73/27 copolyester.

Because of concerns with possible degradation at processing temperatures of 340° and higher, a low molecular weight 24/76 copolyester of HBA/HNA was prepared and evaluated. The DSC scans for the oligomer of about 4 units are shown in Figure 3. The changes in the DSC scans observed here are about the same as those for the 20/80 and 24/76 copolymers and the same interpretation should be applied here also.
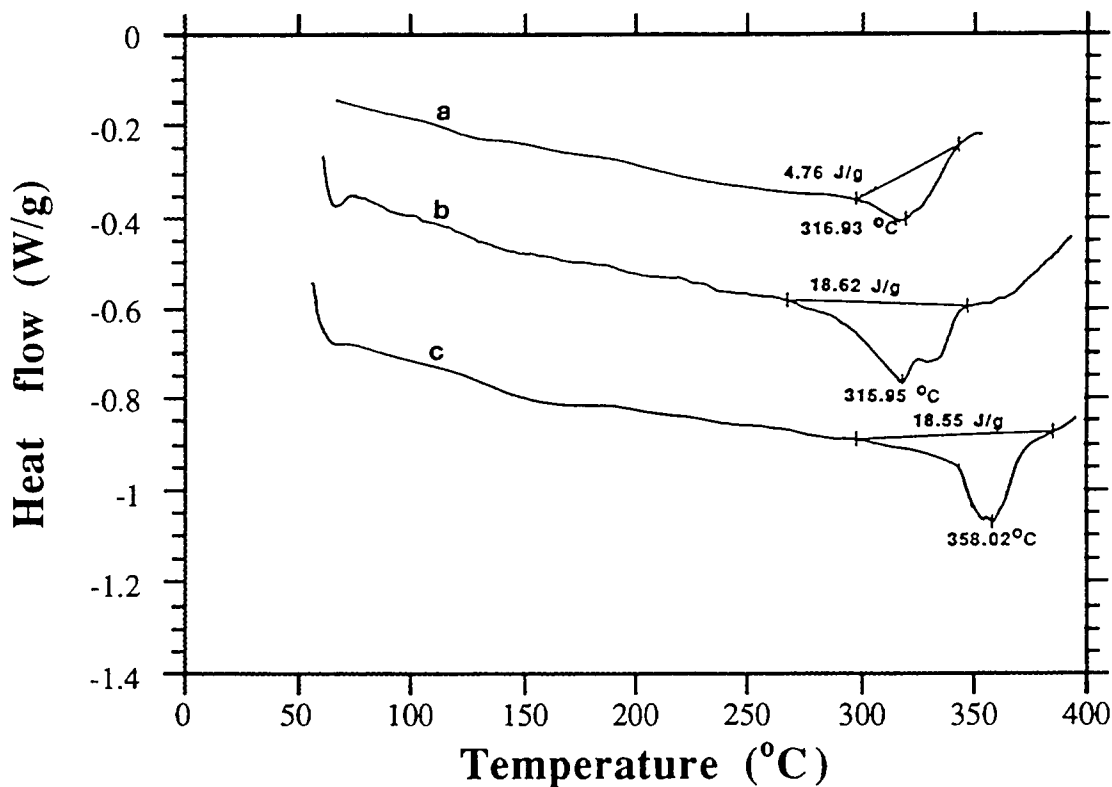
FIGURE 3   DSC scans for the processed 24/76 tetramer (heating rate 10°C/min): (a) As received, (b) Annealed at 240°C, (c) Heated at 310°C.

From the results shown in Figure 4, the 24/76 oligomer does not give higher lap shear strengths, even though better wetting was obtained because of the low viscosity. The oligomer was applied as a precoat at 280°C and then further advanced with elimination of acetic acid. It should be noted that aluminum may undergo undesirable changes during processing at temperatures in excess of 250°C. On the other hand, in all the lap shear tests shown in Figures 1, 2 and 4 failure took place within the adhesive layer, suggesting that the interfacial bonding to the aluminum surface is very strong. The morphology of the break surfaces was not examined in this work, although in Reference 1, Scanning Electron Microscopy (SEM) of specimens fractured at room and elevated temperatures did not reveal any transition from brittle to ductile fracture.

These results indicate that the high temperature adhesion characteristics of the HBA/HNA system can be improved by 40–50°C by using compositions with higher melting points. The fact that no additional improvements were observed by

(a)

(b)
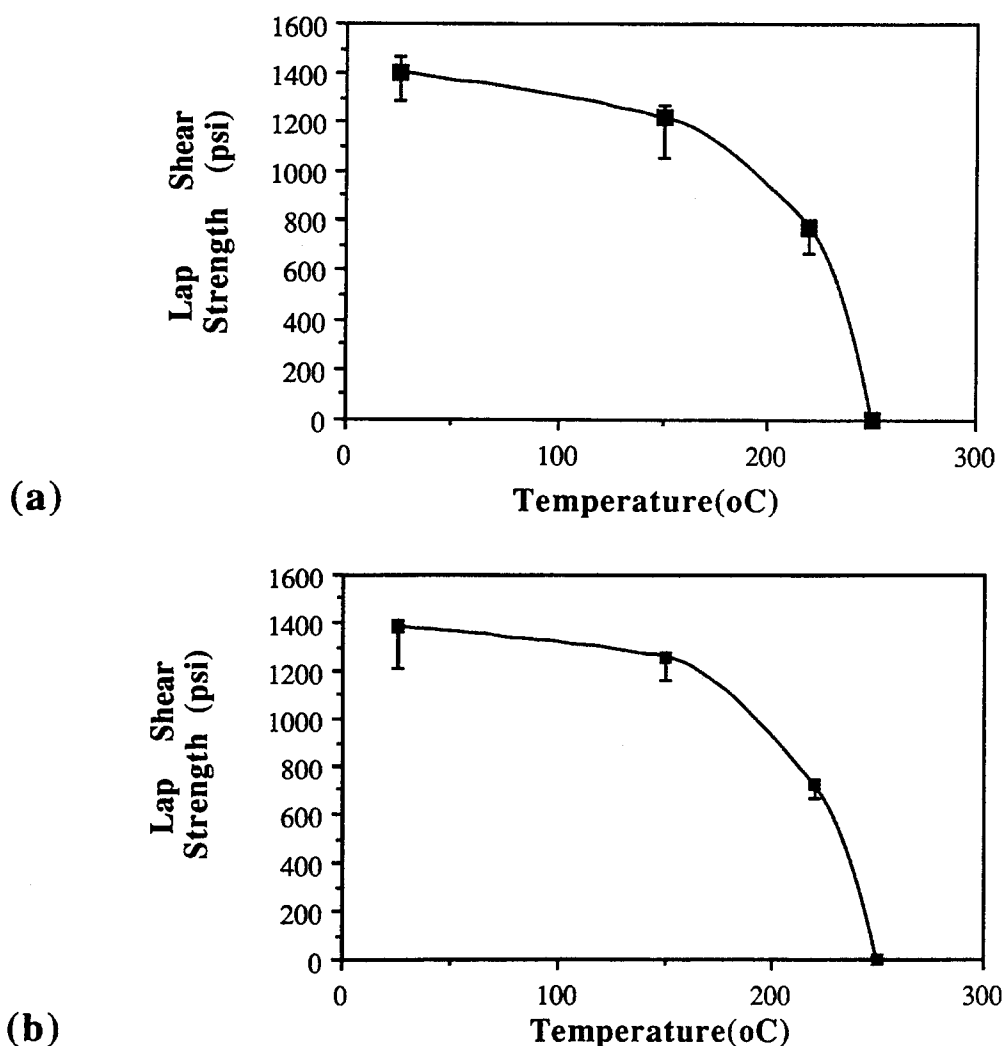
FIGURE 4   The lap shear strength for the 24/76 HBA/HNA tetramer: (a) As processed, (b) Annealed at 250°C.

23

annealing at 75°C below the crystal-nematic transition, or by heating near the crystal-nematic transition point to increase the melting point further by 40–50°C, was surprising. It is certainly possible that within the contained geometries of the aluminum adherends the potential for further crystallization and/or ordering were greatly reduced. Also, the carboxylic acid end groups in the copolyester may have interacted with the aluminum surface, reducing the concentration necessary to catalyze the chemical ordering process. Since the coatings were very thin it was not possible to scrape off the polymers to measure their thermal characteristics.

The glass transition temperature (T_g) was determined for the copolyesters used in this study as well as for the 30/70, 50/50, 60/40 and 73/27 HBA/HNA. The fact that all of these copolyesters display a degree of crystallinity of only 5–20% would suggest that retention of properties at elevated temperatures would be strongly influenced by the T_g. Typical DSC curves for these compositions are shown in Figure 5. The T_g's were calculated based on the changes in deflection of the curves. T_g's are plotted *versus* composition of the copolyesters in Figure 6. It is clear from the curves of Figure 6* that T_g passes through a minimum corresponding to an approximate composition of 45/55 HBA/HNA. Hence, the very modest increase in T_g cannot be used to interpret the 50°C improvement in lap shear strength of the 20/80 and 24/76 systems.
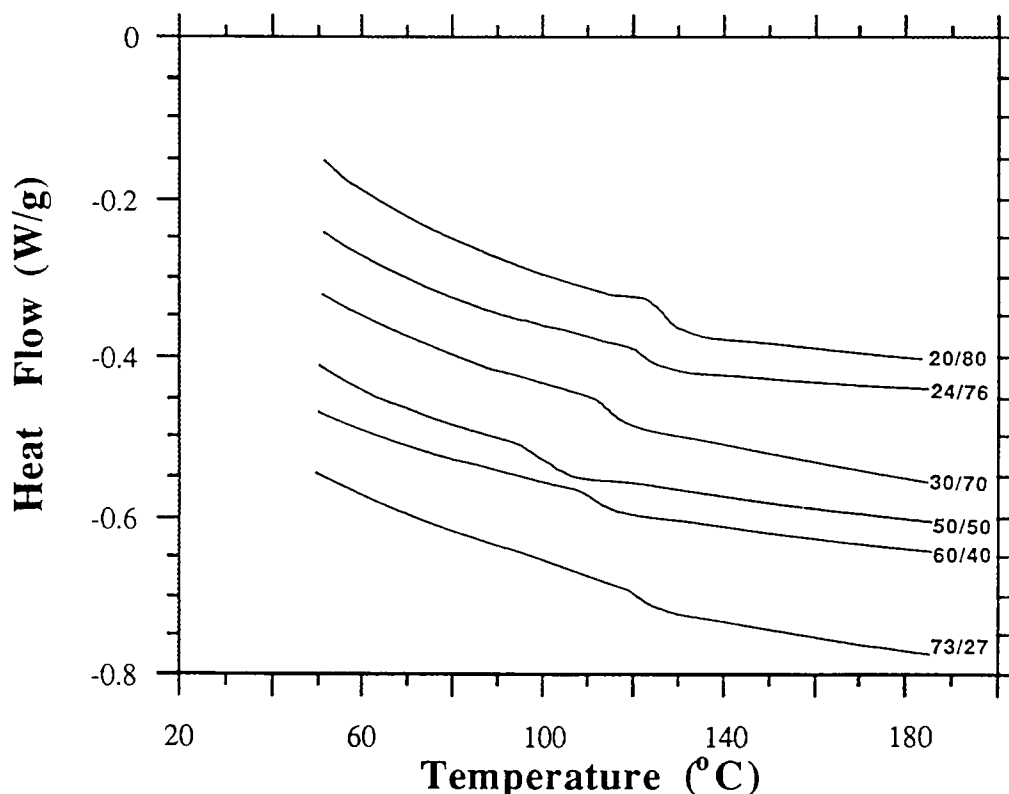
FIGURE 5 Typical DSC curves for quenched HBA/HNA copolyester systems (heating rate 10°C).

---

*A similar curve for the same series of copolyesters was established by other researchers[12] who determined a minimum in T_g values for an HBA content of 50%.
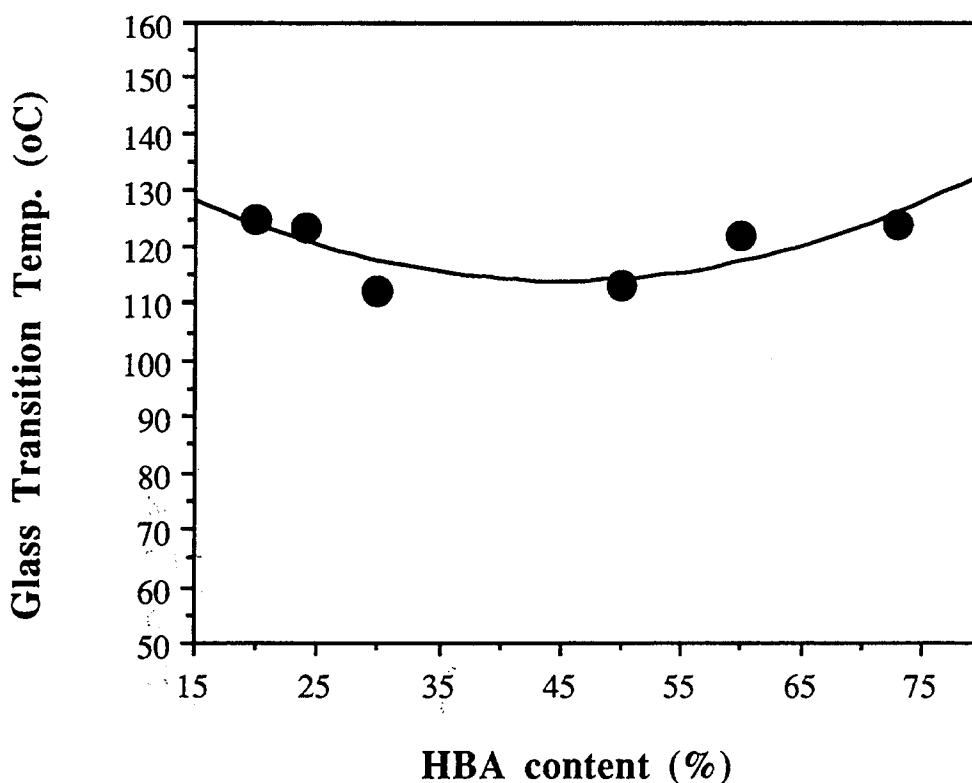
FIGURE 6   The glass transition temperature as a function of composition of HBA/HNA copolyesters.

Some subtle changes in lap shear strength could be detected with specimens annealed at 75°C below T_{CN}. In both the 24/76 and 20/80 systems the lap shear strength remained constant from room temperature to 150°C. In the case where the specimens were annealed slightly above T_{CN} the room temperature lap shear strength was reduced by ~25% suggesting the possibility of high temperature degradation.

CONCLUSIONS

This study shows that:

1. The high temperature adhesive characteristics of the HBA/HNA copolyester system can be significantly improved by using compositions with higher melting points.
2. Attempts to increase the high temperature properties further through annealing and/or chemical ordering were unsuccessful, probably because of interactions of the substrate with the polymer.
3. With all systems studied so far, excellent bonding to the aluminum surface is observed, which suggests potential for further optimization of the cohesive character using fillers.

4. Use of more easily processable oligomeric polyesters has been demonstrated. This permits a far simpler approach to coating and processing of the substrates and also opens the door to processing of even higher melting polyesters.

References

1. J. Economy, T. Gogeva and V. Habbu, *J. Adhesion* **37**, 215–224 (1992).
2. E. C. Millard, in *Adhesive Bonding of Aluminium Alloys*, E. Thrall and R. Shannon, Eds. (Marcel Dekker, Inc., New York, 1985), p. 127.
3. L. Kozma and I. Olefjor, *Mater. Sci. Technol.* **3**, 860 (1987).
4. H. R. Brown, A. C. M. Yang, T. P. Russell, W. Volksen and E. J. Kramer, *Polymer* **29**, 1807 (1988).
5. J. Economy, R. D. Johnson, J. R. Lyerla and A. Muhlebach, ACS Sympos. Series **435**, 129 (1990).
6. P. P. Demetriou, A. G. Andreopoulos and G. L. Polyzois, *Clinical Materials* **3**, 163 (1988).
7. Annual Book of ASTM Standards, Vol. 03.01 (ASTM, Philadelphia, 1989), p. 45.
8. F. D. Chattaway, *J. Chem. Soc., Part III*, 2495 (1939).
9. J. M. Kachidza, MSc Thesis, Dept. of Materials Sci. and Eng., Univ. of Illinois at Urbana, 1991.
10. Y. G. Lin and H. H. Winter, *Macromolecules* **21**, 2439 (1988).
11. S. Z. D. Cheng, *Macromolecules* **21**, 2475 (1988).
12. J. R. Lyerla, IBM Almaden Research Center, CA, 1991, Private Communication.

Cross-linkable High Temperature Copolyesters

J. Economy, D. Frich, K. Goranov, and J.C. Lim

Department of Materials Science and Engineering
University of Illinois at Urbana-Champaign
1304 W. Green St., Urbana, Illinois 61801

INTRODUCTION AND BACKGROUND

During the past 30 years considerable effort has been expended to design easily processible oligomers that could be cross-linked into very thermally stable polymers.[1] A major advantage of epoxy resins is that they can be easily processed as low molecular weight oligomers into a wide variety of forms including adhesives and matrices for composites, and most importantly, without producing volatiles which would create porosity. On the other hand the epoxies cannot be used at temperatures in excess of 180°C and they are particularly susceptible to attack by moisture and corrosive liquids.[2] Some improvement in thermal-oxidative stability has been achieved in going to aromatic oligomers capped with maleimide or acetylene units.[3] However, these end groups form aliphatic or cycloaliphatic links that are susceptible to oxidation at temperatures as low as 200°C. One can conclude from all of this earlier work that it is extremely difficult or perhaps impossible to design a low viscosity oligomer which could be cross-linked into a thermally stable structure without generating volatiles.

Recently, we have reported on a completely new approach for developing an adhesive bond between films of liquid crystalline (LC) aromatic copolyesters, namely, via interchain transesterification reactions (ITR). Thus, LC copolyester coatings on an aluminum substrate when brought together under heat and modest pressure develop to an adhesive with reasonable lap shear properties. Typically such bonds never fail adhesively (i.e. at the polymer metal interface) but always cohesively (within the polymer). It is important to note that these adhesive bonds can be formed above or below the melting point of the LCP, which suggests that the primary mechanism for developing this adhesive bond is through ITR.[4] The possibility to interpret the adhesion process in terms of chain diffusion and chain entanglement is very small considering the rod-like nature of the chains and the relatively short contact time.

In addition, these LCP coatings provide excellent protection for metal substrates against acids, moisture, abrasion, and wear.[5] On the other hand they posses a number of limitations. Thus, the LCP's must be coated at high temperatures, of over 300°C, onto the metal substrate. The strength at high temperature of the LCP adhesive based on HBA/HNA is limited to 200°C due to the relatively low degree of crystallinity.[6] The anisotropic nature of the LCP also appears to provide a limit to the lap shear strength of 1/2 to 2/3 values observed with epoxies.

It would appear that if one could design a cross-linkable copolyester which could first be processed as a low molecular weight oligomeric melt into thin coatings, then subsequent curing would permit the volatile end groups to escape without creating microporosity. Laminating such structures with heat and pressure would lead to adhesion at the interface via ITR (see Figure 1). If such a process could be carried out one would not only have the capability to generate strong adhesive bonds but also to fabricate fiber reinforced composites with very low porosity. Conversely, the potential would also exist to produce rigid structural foams by deliberately working with thicker melts and carrying out the polymerization at higher temperatures where the rate of cross-linking is too rapid, thus trapping the volatile end groups to generate a low density foamed structure. In this paper we describe for the first time successful implementation of the above concepts to prepare adhesives, carbon fiber reinforced composites, and structural foams. In particular, we discuss in each of these three cases specific variations which are designed to illustrate the versatility of this concept. For example, in the case of adhesives and protective coatings the preparation of aliphatic/aromatic oligomers that can be processed at relatively low temperatures is presented. With the carbon fiber reinforced composites not only do we describe the design of cross-linkable oligomers which yield composites that retain all of their mechanical properties to 220°C but also the possibility of a greatly simplified one step fabrication process. Finally, with the structural foams a relatively direct approach is indicated for preparing low density foams with excellent properties over the temperature range 300° to 400°C.

DISCUSSION OF RESULTS

Cross-linkable Polyesters as Readily Processible Adhesives

In this section we describe our program aimed at exploring possibilities of coating, curing, and laminating adhesive bonds at temperatures below 250°C. For this purpose we prepared an aliphatic/aromatic oligomer consisting of an acetoxy terminated copolyester of 1,2,4-triacetoxy benzene, 1,4-diacetoxy benzene and adipic acid with a calculated M_n of 910 and a m.p. of 155°C. A dicarboxylic acid oligomer consisting of adipic acid and 1,4-diacetoxy benzene was also prepared -- (m.p. 214°C) with a calculated M_n of 810. The mixture was heated to 215°C and coated on two aluminum substrates using a glass slide to spread the melt evenly. The coatings were then cross-linked at 240°C for 1 hour, then the cured coatings were bonded at 220°C for 3 hours at 1700 psi. A lap shear strength of 2480 psi was observed with such specimens. This value is over 30% higher than lap shear values observed with our recent published data on LCP's. It is noteworthy that the all aromatic oligomers described in the next section could be processed as adhesives in a manner identical to the above but at significantly higher temperatures.

Design of High Temperature Matrices for Advanced Composites

Turning to the use of these cross-linkable copolyesters as matrices in advanced composites, initially we focused on an all aromatic system that would permit continuous use temperatures of 200-250°C. Thus we designed carboxylic acid terminated oligomers based on trimesic acid, hydroxybenzoic acid (HBA), and hydroquinone (HQ) in combination with the acetoxy terminated oligomers from isophthalic acid, HBA and HQ. The mixture formed a relatively low viscosity melt at 250°C which easily impregnated a carbon fiber lay-up in a few minutes at 290°C. We found that most of the acetic acid could be removed at 290°-310°C on heating for 1 hr. at 250 psi. Surprisingly, high density specimens with thicknesses of up to 1/2 inch could be fabricated with this very simplified process without resorting to the lamination process described in the previous section. We believe a number of factors may contribute to this phenomenon, e.g. the presence of carbon fibers provide a pathway for evolution of the acetic acid. There is reason to believe that in the early stages of cross-linking the primary step is chain extension followed by cross-linking. The use of vacuum facilitates removal of trace amounts of volatiles. Finally, during the final heating some consolidation may occur via interchain transesterification. A stress-strain curve from a three point bend test is shown in Figure 2 indicating good strength and fracture toughness properties. In Figure 3 is shown dynamic mechanical analysis (DMA) spectra indicating the retention of mechanicals at elevated temperatures. In Figure 3 is shown dynamic mechanical analysis (DMA) spectra indicating the retention of mechanicals at elevated temperatures for matrices with different average molecular weights between cross-link points. The three curves show the effect of cross-link density on the flexural modulus at elevated temperatures.

It is interesting to note that the DMA for composition III shows no change from room temperature to 230°C indicating that the cross-link density is a key factor in controlling the high temperature mechanicals. In fact this particular composite retains ~ 60% of its properties up to 350°C. A rising temperature TGA is shown in Figure 4 indicating good stability to over 400°C under inert conditions.

Structural Foams Based on All Aromatic Copolyesters

It would seem fairly obvious that one could prepare structural foams based on these cross-linkable oligomers however to our knowledge no such an experiment has been attempted. By carrying out the cross-linking step at much higher temperatures of 350°C vs. 300°C the acetic acid evolves too rapidly during cross-linking leading to a stable foamed structure. In this manner reasonably uniform foams with densities as low as 0.1g/cc have been obtained. Depending on the degree of cross-linking the foams can range from reasonably tough to modestly brittle. The foams retain their dimensional stability at least to 400°C under inert conditions. In fact foams can be bonded to each other at 400°C under modest pressure via the interchain transesterification reaction. Shown in Figure 5 is thermomechanical analysis (TMA) spectra at 300°C and 350°C indicating some permanent deformation under load at these temperatures.

CONCLUSIONS

Based on the data generated to date we appear to have discovered a completely new approach to design of high temperature adhesives, matrices, and structural foams using cross-linked aromatic copolyesters. The relatively low cost of the starting materials as well as the ease of processing suggest potential for broad commercial use.

REFERENCES

1. P.M. Hergenrother, *J. Macromol. Sci.-Rev. Macromol. Chem.* **C19**, 1 (1980).
2. E.C. Millard in *Adhesive Bonding of Aluminum Alloys*, E. Thrall and R. Shannon, Eds. (Marcel Decker, Inc., New York, 1985), pp. 99-105.
3. P.M. Hergenrother in *Reactive Oligomers*, F.W. Harris and H.J. Spinelli, Eds. (ACS Symposium Series 282, St. Louis, 1985), pp. 1-16.
4. J. Economy, T. Gogeva, V. Habbu, *J. Adhesion* **37**, 215 (1992).
5. D. Frich and J. Economy, *ACS Polymer Preprints* **69**, 438 (1993).
6. J. Economy and A. Andreopoulos, *J. Adhesion* **40**, 115 (1993).
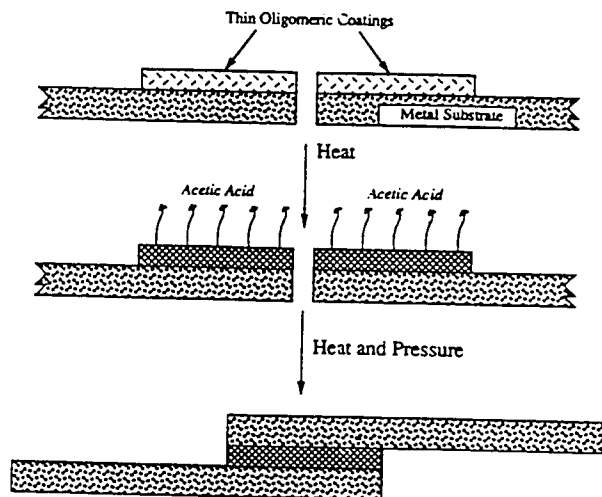
Figure 1. Method of forming adhesive bonds using oligomeric coatings. The substrates are first coated with the copolyester oligomers. The oligomers are advanced through cross-linking, permitting volatile escape. Adhesion between cured coatings is developed by ITR.
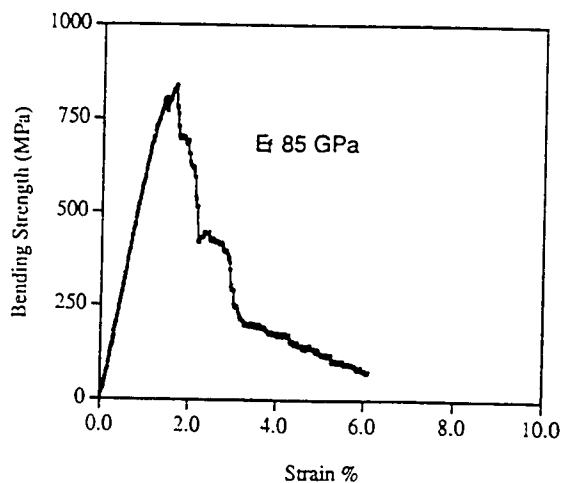
Figure 2. Stress-strain curve from a three point bend test (TPBT) of a carbon fiber composite with a cross-linkable aromatic copolyester matrix.
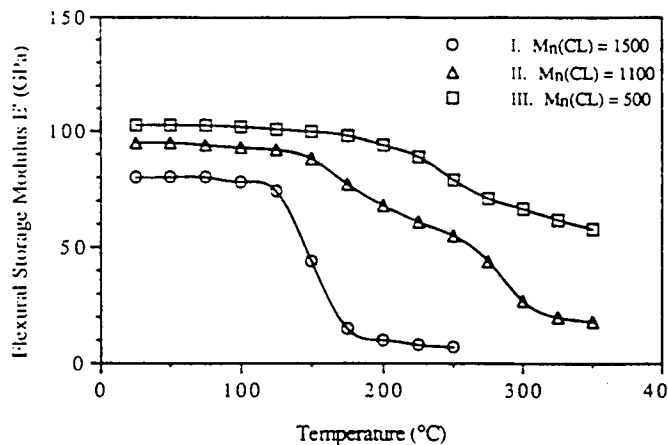
Figure 3. DMA spectra of carbon fiber composites with an aromatic copolyester matrix showing the effect of varying cross-link density. The number average molecular weight between cross-link points for each matrix (I, II, and III) is given as $M_n(CL)$.
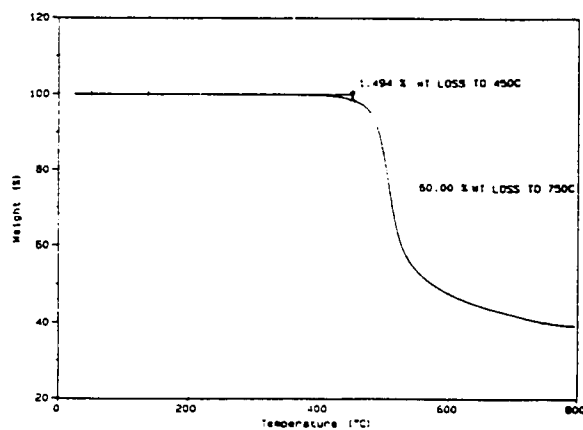
Figure 4. TGA of an all aromatic copolyester resin showing the high thermo-oxidative stability of these materials.
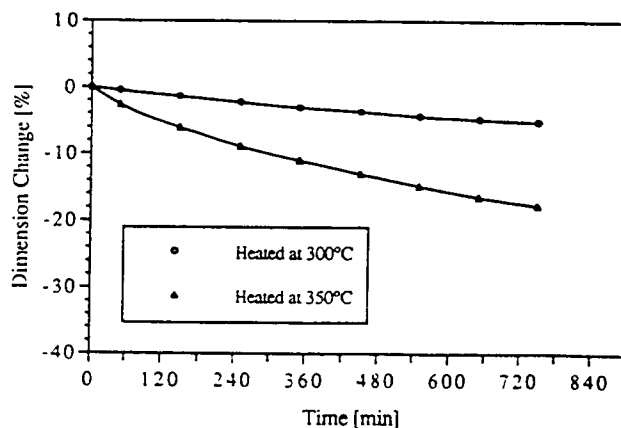
Figure 5. Dimension change of a small porous foam under load held isothermally at elevated temperatures.

SYNTHESIS AND THERMAL ANALYSIS OF THERMOTROPIC POLYESTERS

J.J. Rusek
P.F. Jones
Phillips Laboratory
United States Air Force
Edwards AFB CA

ABSTRACT

This paper will detail the condensation synthetic route for the production of thermotropic liquid crystal polyesters. Thermal analysis, more specifically, Thermogravimetric Analysis (TGA) results will be presented for a variety of synthesized thermotropes. Off-gas Fourier Transform Infrared (FTIR) spectroscopic results will be presented derived from the synthesized polyesters. Data reduction and correlations will be drawn from the previous results. Finally, conclusions will be summarized and future work proposed.

INTRODUCTION

The advent of commercially available thermotropic liquid crystal polymers has led to novel uses of these high strength materials in the astronautics community. The Phillips Laboratory at Edwards Air Force Base has taken the lead in this area by constructing a large in-house initiative to explore these materials for rocket propulsion applications. The investigation of the available materials has led to the discovery of the so-called physico-chemical annealing phenomena inherent to main-chain liquid crystal polymers with defined pendant groups (1). The polymer, when properly annealed, will exhibit a doubling of tensile strength while at least maintaining its modulus value. When an annealable thermotrope is injection molded, the skin region exhibits a partial annealing, while the core remains as-injected. Microscopic studies of this transformation were explored as a function of skin and core regions for various commercial materials (2).

In order to further explore this annealing phenomena, a synthesis program was set up within the Advanced Polymer Components Initiative. The primary purpose of this task was to discover new thermotropic liquid crystalline systems that would exhibit the annealing phenomena so as to finally close the gap on the dependence of annealing with respect to molecular architecture. This task would also supply academic and industrial collaborators with a defined supply of model polymers for analysis. Special needs dependent on type of analysis, for example bromine EXAFS using synchrotron radiation, led to synthesis of further new thermotropic materials (3)

Characterization of the synthesized polymers was accomplished using TGA and combined TGA/FTIR analysis. Polymer decomposition temperatures and weight losses were determined by TGA. Polymer decomposition off-gases were analyzed by FTIR spectroscopy; the TGA was coupled directly to the FTIR for real-time off-gas identification. This paper will focus on the LCP synthesis, TGA and TGA/FTIR results.

SYNTHESIS

The synthesis route is shown in Figure 1. A high purity (>99% w/w) substituted hydroquinone is dissolved in distilled methylene chloride or ethylene dichloride. A stoichiometric amount of purified and dried pyridine is added to effect total dissolution and allow concentrations of 25 % w/w. This base solution is charged into an appropriate reaction kettle or round-bottom flask and purged with dry nitrogen.

ADVANCED POLYMER COMPONENTS

Where R= H
Me
t-Bu
Ph
PhEt
Cl
Br
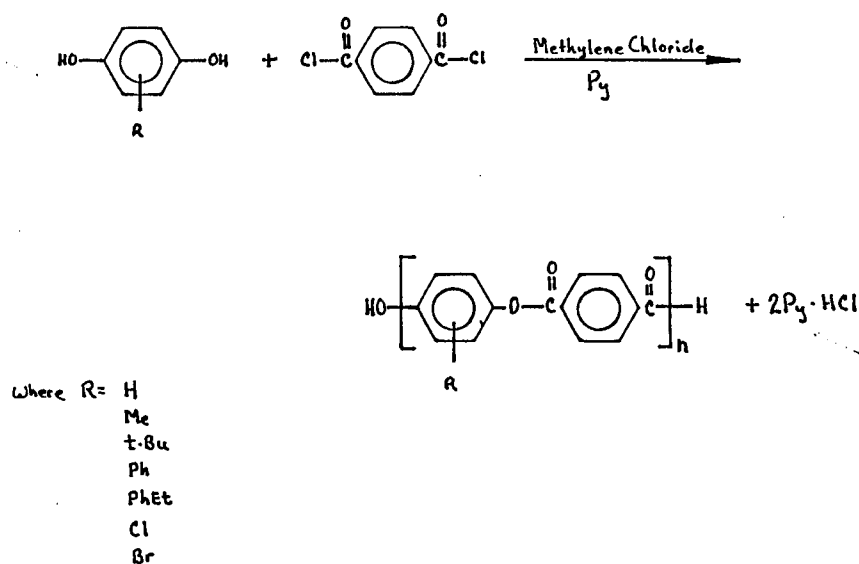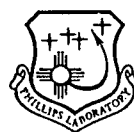
FIGURE 1. Schematic of Synthesis Route for Thermotropic Polyesters

A 25 %w/w solution of distilled terephthaloyl chloride in distilled methylene chloride was procured from Organic Technologies in Columbus, Ohio. This acid solution is charged to an addition funnel and fitted into the base flask. All polymers

were synthesized with a 2 % w/w excess of terephthaloyl chloride to ensure acid end-capping.

The reactor and its contents are cooled to 0 C and the base solution agitated. The acid solution is added at a rate to maintain a maximum temperature of 5 C. This usually yields a volume rate of one-half of the acid solution in twenty minutes and the remainder in ten minutes. The reaction mass is then agitated for one hour at 0-5 C.

The work-up is initiated by charging ten times the predicted polymer weight of distilled water to the flask. The contents are heated to a final temperature of 85 C. During the heating, the methylene chloride is distilled and collected for future synthetic runs. When the slurry reaches 85 C, agitation continues for one hour to extract pyridinium hydrochloride. The slurry is filtered and recharged to an appropriate beaker. This water work-up is repeated once more.

A second work-up, analogous to the above, is performed; acetone is used and the final slurry temperature is 45 C. This work-up is also repeated once. The filter cake is dried in a vacuum oven at 100 C overnight and stored in glass.

Polymers and copolymers have been produced from the following substituted hydroquinones.

HQ	Hydroquinone	poly (p-phenylene terephthalate)
MHQ	Methylhydroquinone	poly (1-methyl-p-phenylene terephthalate)
tBHQ	t-Butylhydroquinone	poly (1-t-butyl-p-phenylene terephthalate)
PHQ	Phenylhydroquinone	poly (1-phenyl-p-phenylene terephthalate)
SHQ	Styrylhydroquinone	poly (1-styryl-p-phenylene terephthalate)
CHQ	Chlorohydroquinone	poly (1-chloro-p-phenylene terephthalate)
BHQ	Bromohydroquinone	poly (1-bromo-p-phenylene terephthalate)

THERMAL ANALYSIS RESULTS

Figure 2 depicts a TGA plot for a bromohydroquinone derived homopolymer. The ordinate is scaled as normalized weight, in percent, while the abscissa is scaled as temperature in degrees C. All data were acquired on a DuPont TA 2000 system using DuPont 951 TGA; a heating rate of 10 C per minute in a dry nitrogen atmosphere was defined as a standard procedure. The onset of weight loss (OWL) is indicated at 275 C while the temperature at maximum initial loss (MIL) is seen as 302 C.


```
Sample:  BRHQ/TA                           TGA      File:  C: TGARUSEK.009
Size:    18.4370 mg                                 Operator:  PAUL JONES
Method:  POLYMERS                                   Run Date:  6-Aug-93   09: 47
Comment: RATE 10°C/MIN, GN2 ATMOSPHERE   50 ML/MIN
```
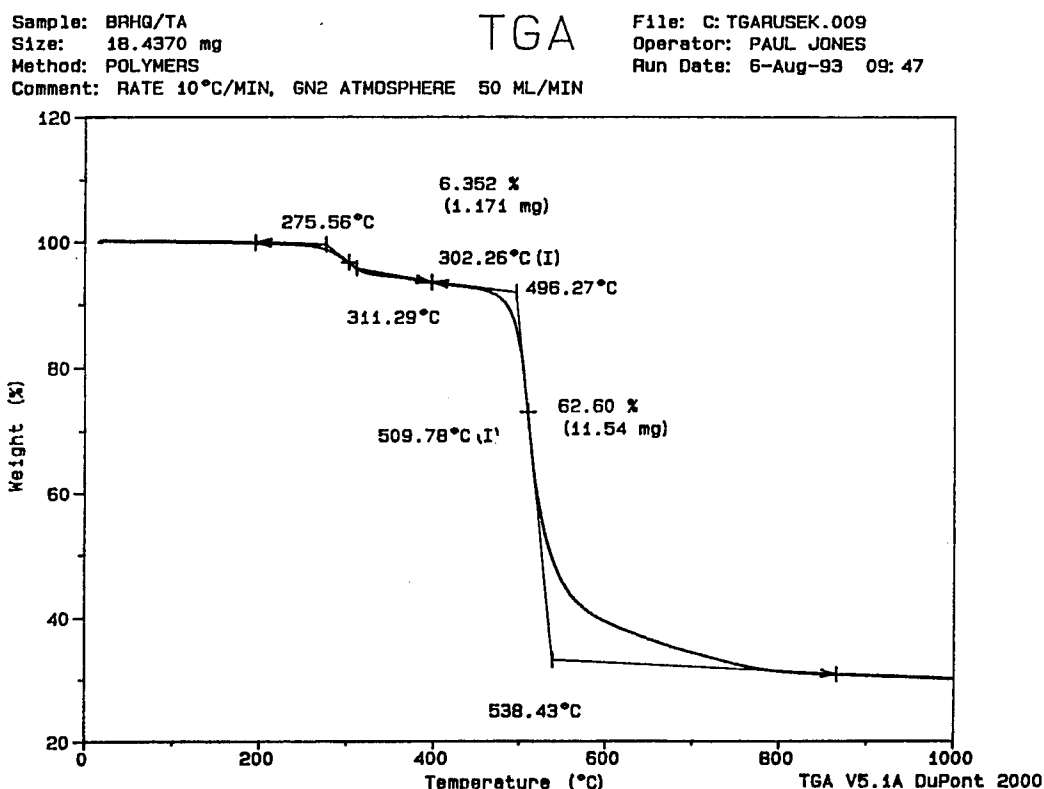
Figure 2. Thermal Analysis Plot for Bromohydroquinone Homopolymer

Figure 3 shows a TGA plot for an annealed bromohydroquinone derived homopolymer. The polymer was annealed at 160 C overnight with a purge of flowing nitrogen at sub-ambient pressure. The onset of weight loss is now at 311 C while the temperature at maximum initial loss is seen to be 337 C. Comparing these data with that shown in Figure 2, it is seen that the onset and maximum initial loss temperatures increase by about 36 C. The polymers are acid end-capped, which inhibits chain extension and there is little probability of cross-linking, hence, this manifestation of annealing appears to be physical in nature. Conditions that would give rise to this annealing are increase in crystallinity or

polymer chain interdigitation. These physical avenues are currently under study under the auspices of the Advanced Polymer Components Initiative. (3)

Sample: ANNEALED BRLCP- RUN 1   TGA   File: C: TGARUSEK.003
Size: 6.0610 mg   Operator: CHARLES NOEL
Method: POLYMERS   Run Date: 4-Aug-93 10: 19
Comment: RATE 10°C/MIN, GN2 ATMOSPHERE   50 ML/MIN
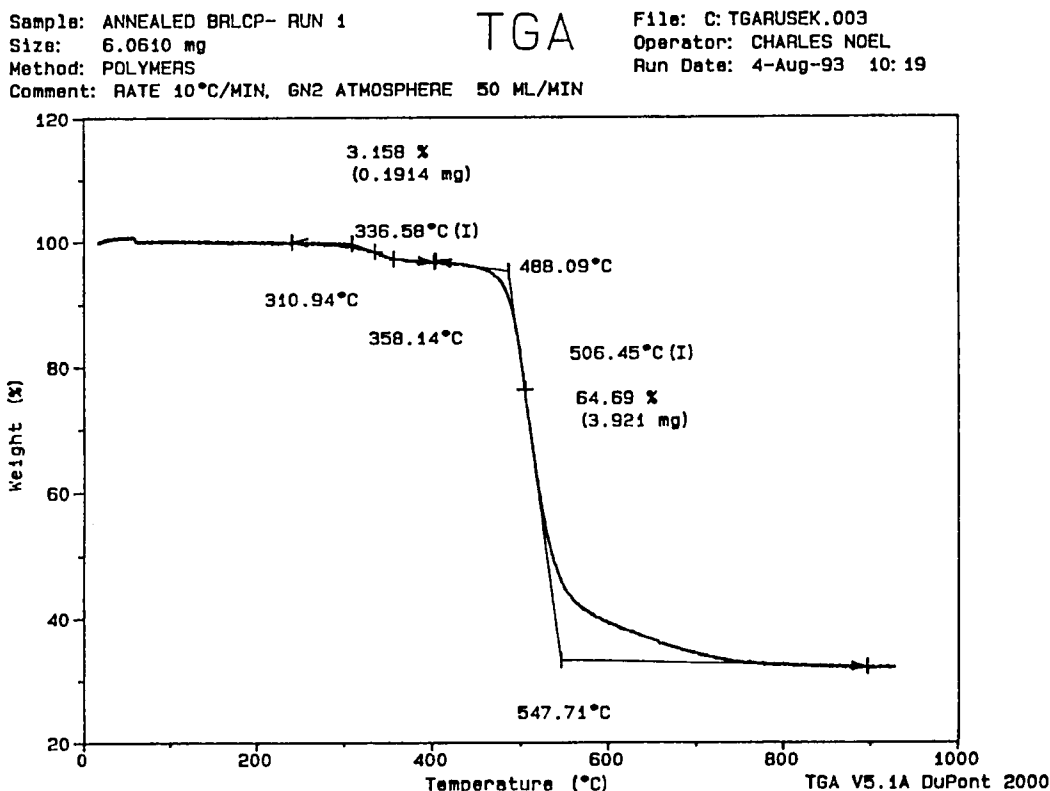
Figure 3. Thermal Analysis Plot for Annealed Bromohydroquinone Homopolymer

Figure 4 depicts a TGA plot of a copolymer derived from styrylhydroquinone and phenyl hydroquinone. Again the characteristic plateaus are in evidence. Figure 5 shows a TGA plot of a commercial variant of this copolymer named GRANLAR obtained from Granmont Corporation. A comparison of the two plots shows the obviation of the initial weight loss (IWL), while the rest of the plots compare quite well. The slight offset in slopes during the secondary weight loss (SWL) is attributable to differences in average molecular weight. The commercial product has gone through a more rigorous work-up which would minimize the low molecular weight fractions extractable by acetone, hence, it is apparent that the first weight loss is predominantly due to low molecular weight material.

Figure 4. Thermal Analysis Plot of Styryl-/Phenylhydroquinone Copolymer
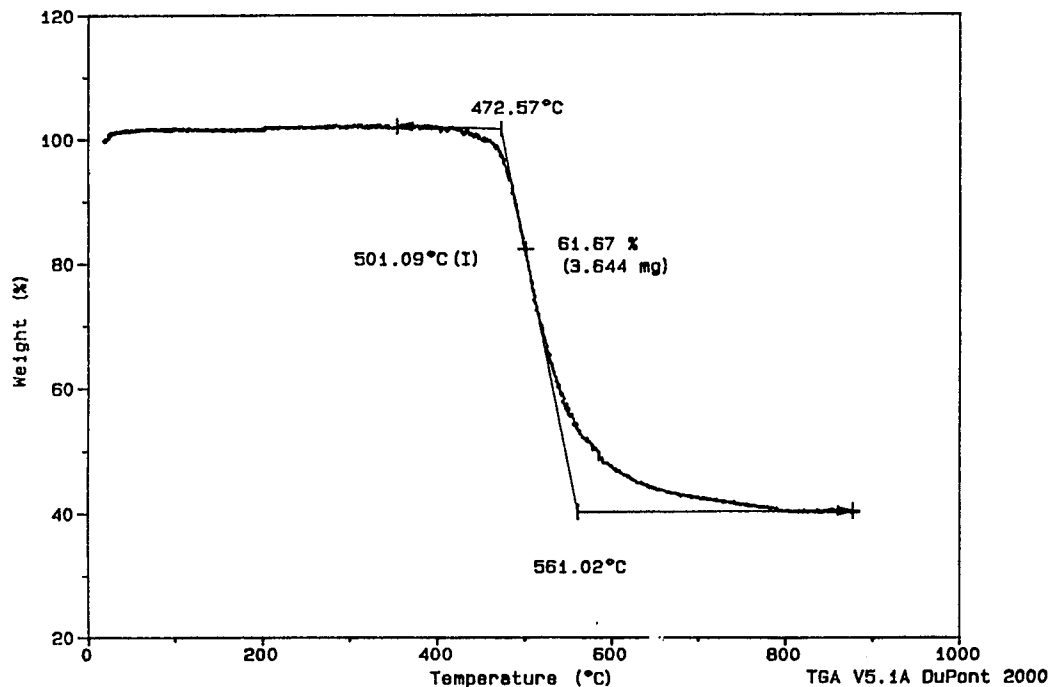
Figure 5. Thermal Analysis Plot of Commercial GRANMONT polyester

45

Figure 6 depicts a TGA plot for a hydroquinone derived homopolymer. Low molecular weight fractions of the polymer give rise to the first downslope at 321 C. The second downslope, or maximum secondary loss (MSL), is attributed to a pure decomposition which essentially stabilizes at 578 C.

Sample: SYN 0 HQ/TA
Size: 9.0950 mg
Method: POLYMERS
Comment: RATE 10°C/MIN, GN2 ATMOSPHERE   50 ML/MIN

TGA

File: C: TGARUSEK.010
Operator: PAUL JONES
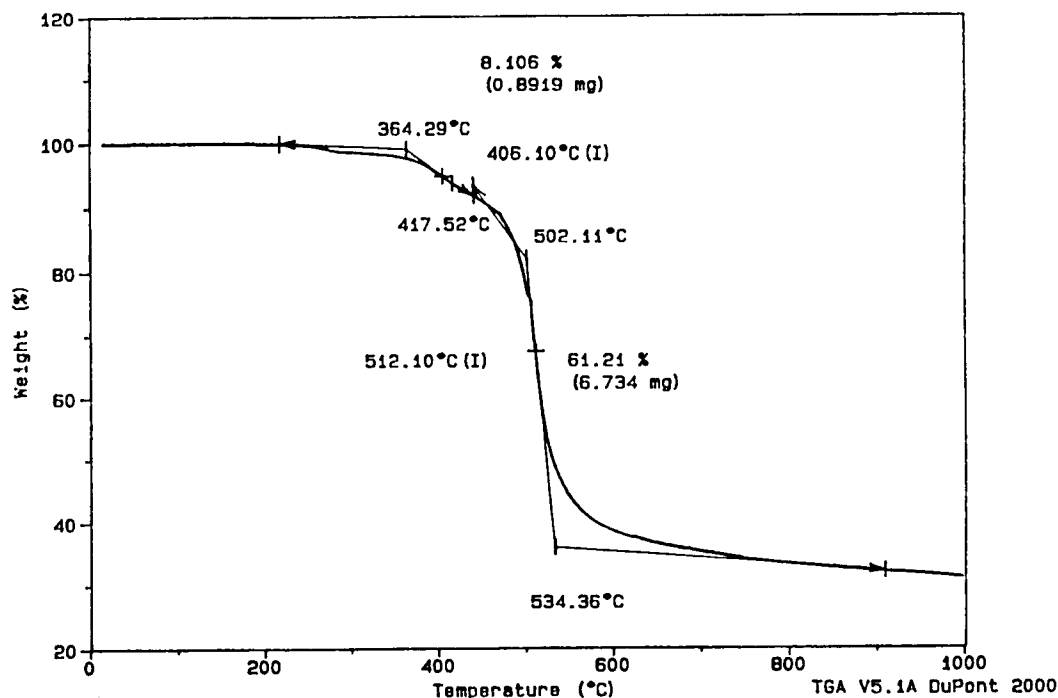Run Date: 6-Aug-93   13: 09

321.67°C

38.68 %
(3.518 mg)

358.84°C (I)

547.60°C

395.29°C

41.47 %
(3.772 mg)

558.85°C (I)

577.75°C

Weight (%)

Temperature (°C)

TGA V5.1A DuPont 2000
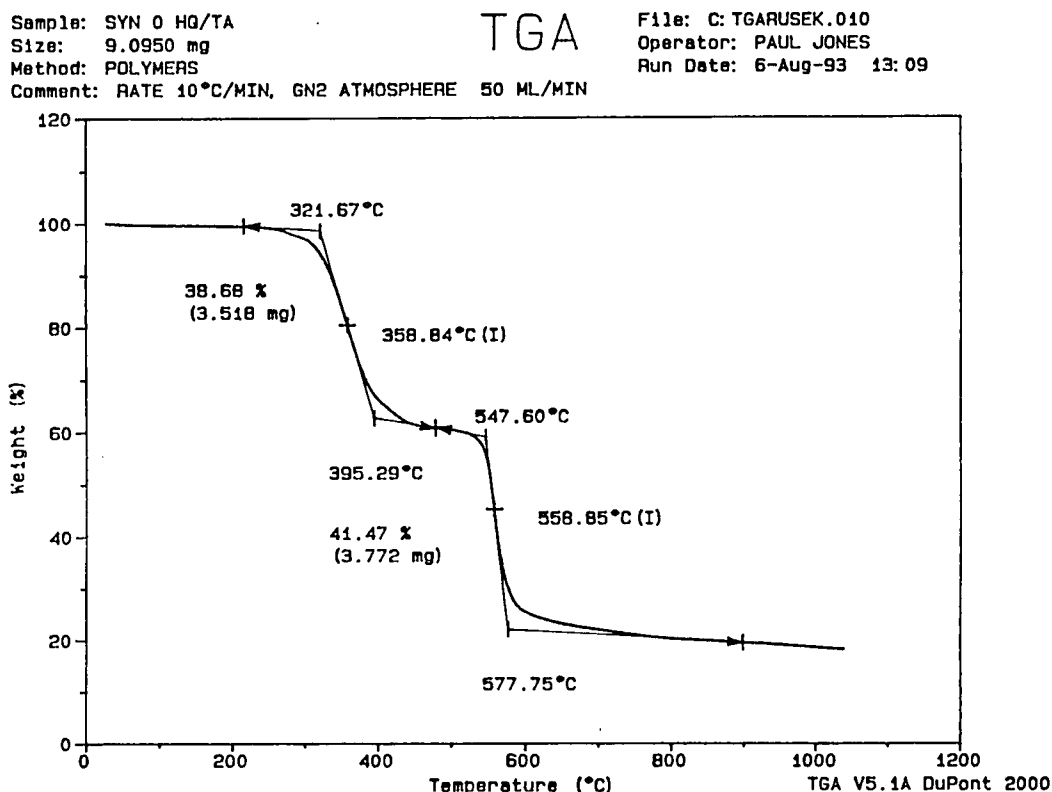
Figure 6. Thermal Analysis Plot of Hydroquinone Homopolymer

The 951 TGA was combined with a Nicolet 710 FTIR spectrometer to identify the off-gas products during polymer decomposition Figure 7 is an FTIR spectrum taken during the hydroquinone homopolymer decomposition. Dominant peaks indicate carbon dioxide (2380, 2330), carbon monoxide (2180, 2110), hydroquinone (3650, 1510 and 1180) and benzoic acid (1760, 1080 and 710). Analysis of the dominant peaks shows that the off-gas vapors are comprised of predominantly hydroquinone, carbon monoxide and benzoic acid, in descending order, with some carbon dioxide present. The sharp line at 668 wavenumber is the symmetric 1,4 aromatic mode, characteristic of all of the synthesized polymers. The FTIR results imply that chain depolymerization is the predominant mechanism of decomposition for this homopolymer.
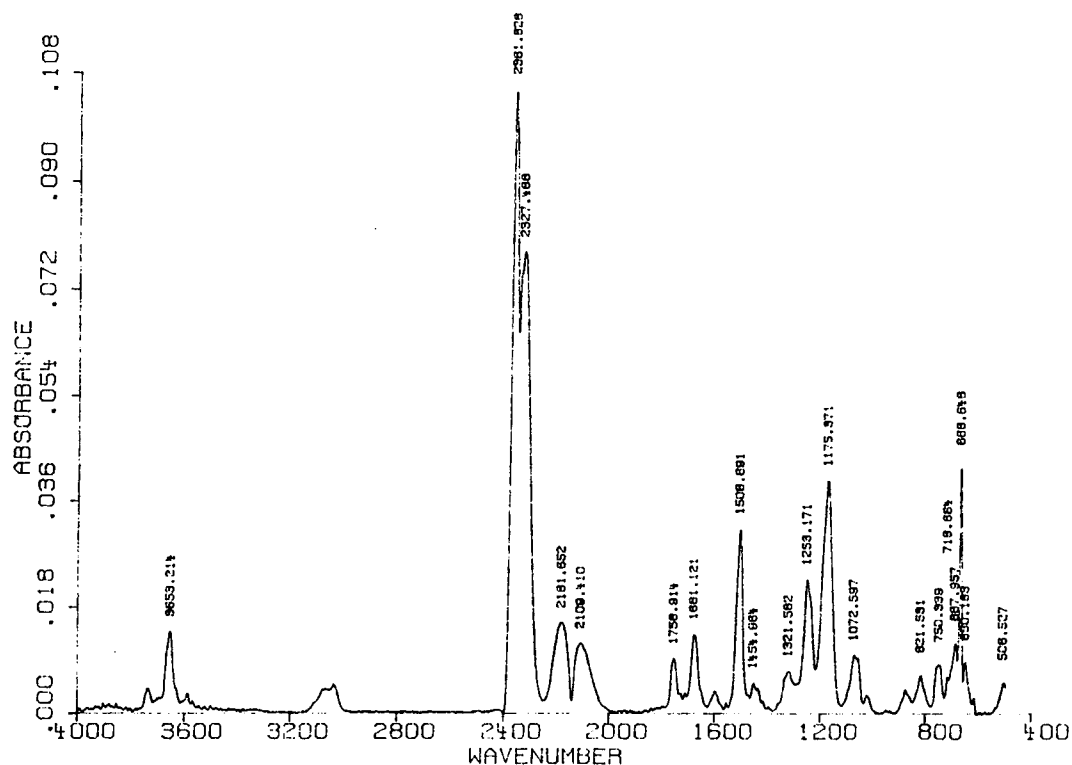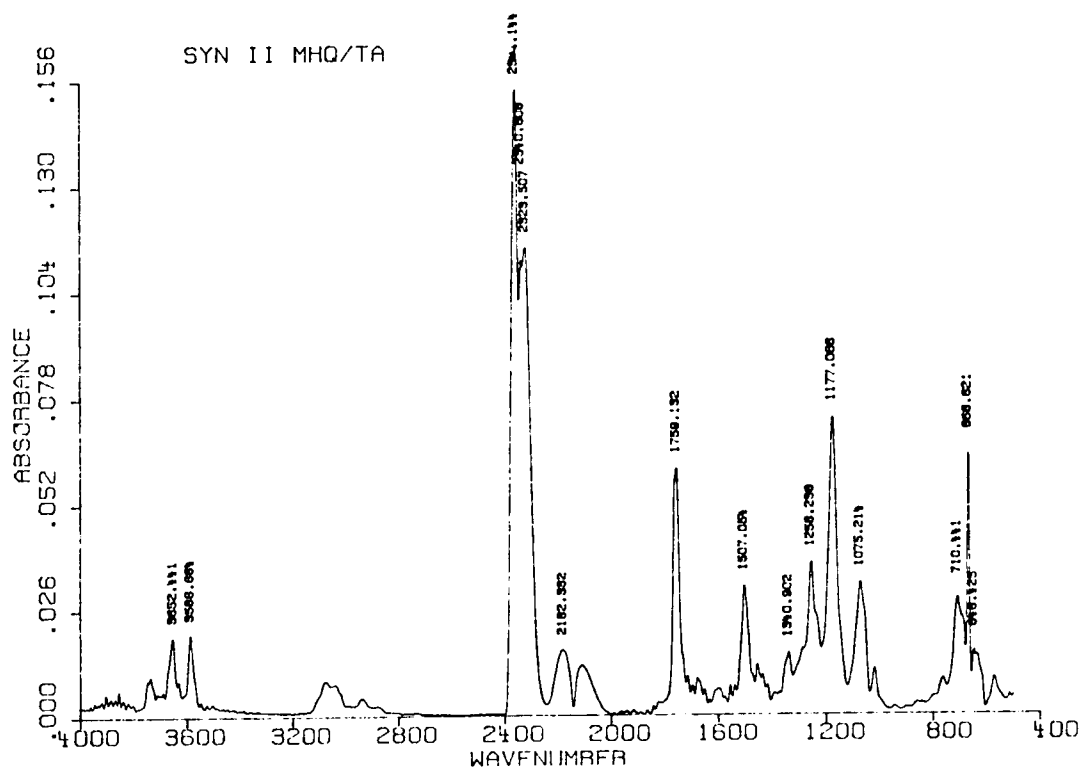
Figure 7. FTIR Spectrum of Hydroquinone Homopolymer Off-Gas

Figures 8 and 9 show a TGA and gaseous FTIRspectra, respectively, of a methylhydroquinone derived homopolymer. The TGA shows a smaller initial downslope than the hydroquinone polymer plot, indicating a lower quantity of low molecular weight material. The secondary downslope starts to stabilize at 534 C. An analysis of the FTIR off-gas spectra shows mainly benzoic acid, hydroquinone, and then carbon monoxide, in that order, with associated carbon dioxide. This implies that the primary initial decomposition mechanism is chain depolymerization starting from the ends of the molecule inwards for this homopolymer.

47

Figure 8. Thermal Analysis of Methylhydroquinone Homopolymer

Figure 9. FTIR Spectrum of Methylhydroquinone Homopolymer Off-Gas

48

Figures 10 and 11 depict a TGA and off-gas FTIRspectra, respectively, of a phenylhydroquinone derived homopolymer. The TGA shows an even smaller initial downslope, indicating the lowest amounts of low molecular weight material. An analysis of the FTIR decomposition spectra shows predominantly benzoic acid and carbon monoxide, in that order with associated carbon dioxide . This implies that initially, side-chain scission occurs, follow by chain depolymerization.

Sample: SYN IV PHQ/TA   TGA   File: C: TGARUSEK.005
Size: 7.6890 mg   Operator: PAUL JONES
Method: POLYMERS   Run Date: 5-Aug-93 08: 59
Comment: RATE 10°C/MIN, GN2 ATMOSPHERE 50 ML/MIN
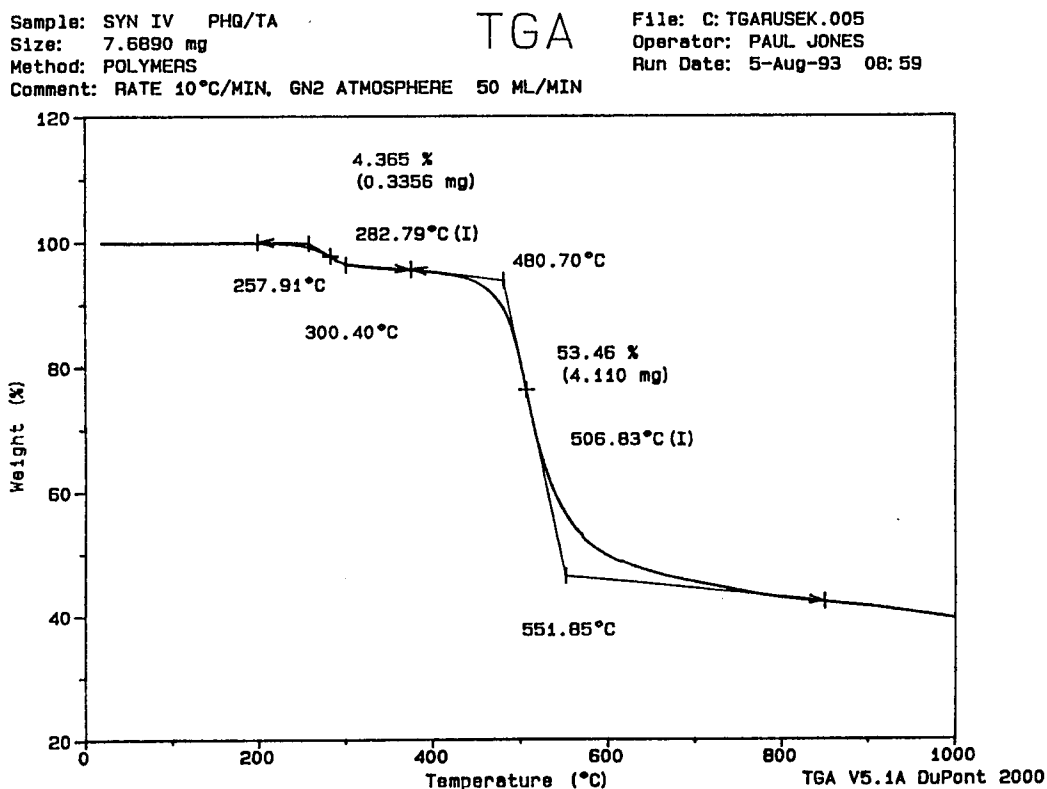
Figure 10. Thermal Analysis of Phenylhydroquinone Homopolymer

49
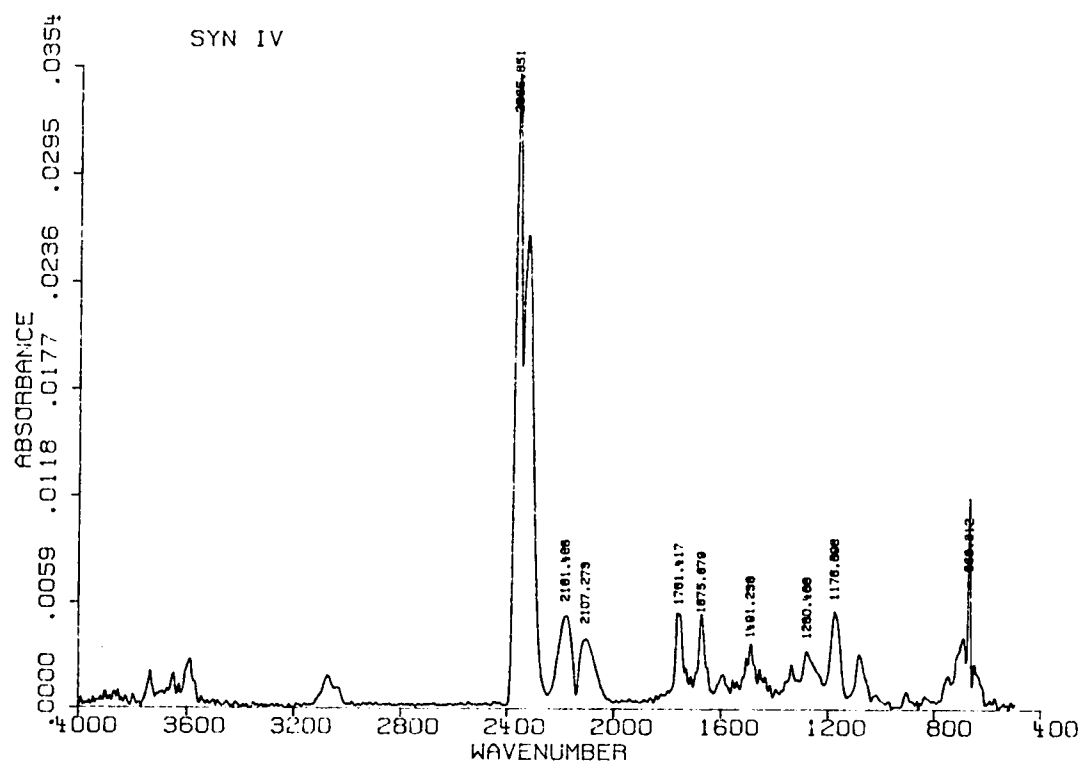
Figure 11. FTIR Spectrum of Phenylhydroquinone Homopolymer Off-Gas

Figures 12, 13 and 14 show TGA plots of homopolymers derived from styrylhydroquinone, t-butylhydroquinone and chlorohydroquinone. These plots are included to show that low molecular weight fractions are still evident to varying degree as seen by the initial weight loss plateaus. All of the data derived from the TGA results are shown as Table 1.
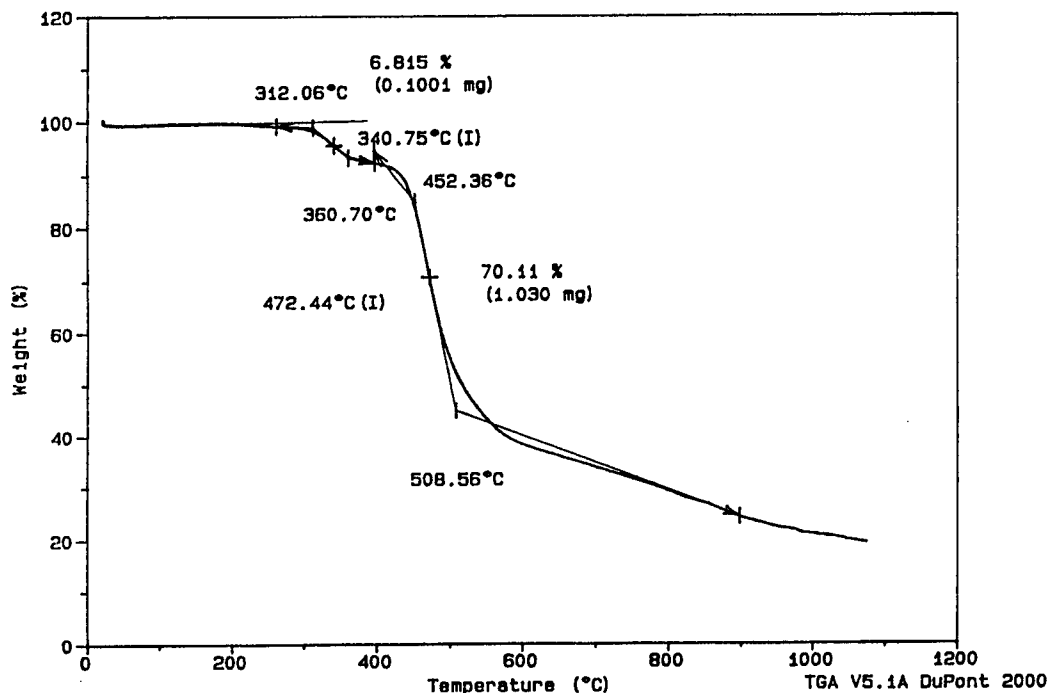
Figure 12. Thermal Analysis of Styrylhydroquinone Homopolymer
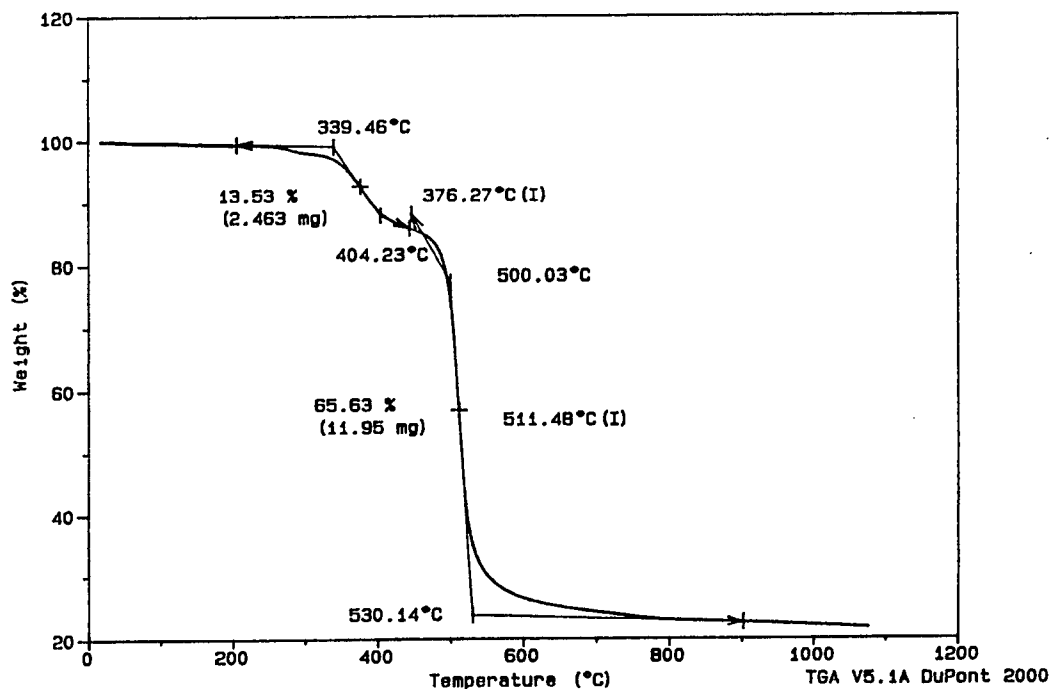
Figure 13. Thermal Analysis of t-Butylhydroquinone Homopolymer

51

Sample: SYN V   CHQ/TA   ·
Size: 7.9440 mg
Method: POLYMERS
Comment: RATE 10°C/MIN, GN2 ATMOSPHERE 50 ML/MIN

TGA

File: C: TGARUSEK.006
Operator: PAUL JONES
Run Date: 5-Aug-93 11: 42

269.76°C

294.82°C (I)

15.61 %
(1.240 mg)

330.88°C

520.31°C

529.66°C (I)

55.04 %
(4.373 mg)

553.77°C

TGA V5.1A DuPont 2000
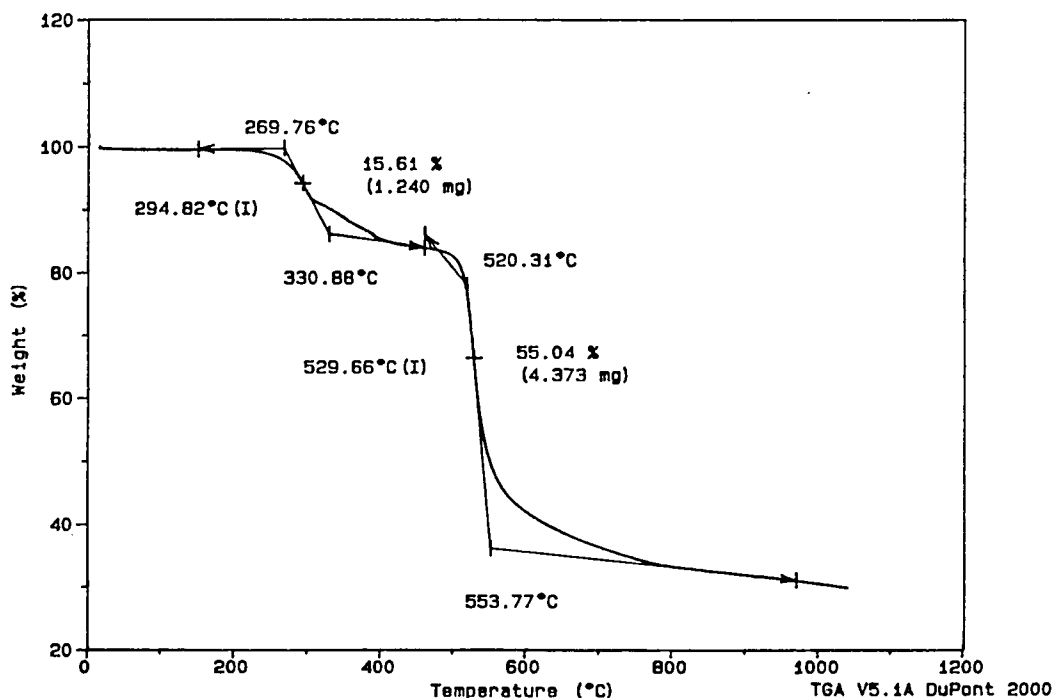
Figure 14. Thermal Analysis of Chlorohydroquinone Homopolymer

SPECIES	MW	OWL, C	MIL, C	IWL, %	MSL, C	SWL, %
HQ	1	322	359	38.7	559	41.4
CHQ	35	270	295	15.6	530	55.0
MHQ	37	365	406	8.1	512	61.2
tBHQ	57	339	376	13.5	512	65.6
PHQ	77	258	283	4.4	507	53.5
BHQ	80	276	302	6.3	510	62.6
SHQ/PHQ	91	269	290	4.4	474	51.4
SHQ	105	312	341	6.8	472	70.1

Table 1. Summary of Salient Thermal Analysis Data for Thermotropic Polyesters

The molecular weights listed are those of the pendant groups on the hydroquinone monomer used to make the polyester. It is seen that the MSL, or temperature at maximum true decomposition rate of the polymer, correlates inversely with the molecular weight of the pendant group. This is to be expected since more compact molecules should decompose at a higher temperature, all else being equal. The IWL, or weight loss of the polymer at the first plateau correlates

inversely with the molecular weight of the pendant group. This seems intuitive, since the reactivity of a species generally increases with decreasing molecular size; low molecular size monomer will react and cap easier forming more low molecular weight polymer.

CONCLUSIONS AND FORWARD PLANS

It has been the intent of this paper to show that thermotropic liquid crystal polyesters can be conveniently prepared by a solution polymerization. Further, thermal analysis coupled with FTIR is a powerful tool to study the bulk behavior of these liquid crystalline materials. This work has led to the following conclusions.

Novel thermotropic liquid crystal polymers can be produced based on substituted hydroquinone monomers.

Polymer physico-chemical annealing can be identified by TGA.

TGA can be used to qualitatively assess monomer reactivity.

FTIR shows decomposition initiated by either chain depolymerization or side-chain scission.

Decomposition temperatures correlate inversely with pendant molecular weights.

Generated low molecular weight fractions correlate inversely with pendant molecular weights.

Work over the next year will focus on varying reaction conditions to minimize low molecular weight contaminants. The polymer synthesis outlined in this paper will be scaled-up to the kilogram range. The entire series of substituted hydroquinone homopolymers will be characterized by TGA/FTIR as well as x-ray diffraction, both in the annealed and as-polymerized states.

REFERENCES

1 Rusek, J.J., "Proceedings of the First Annual Advanced Polymer Components Symposium," PL-TR-92-3018, Edwards Air Force Base, Ca, July 1992

2 Rusek, J.J., Chaffee, K.P., and Silver, D.S., "Property Transformation of Thermotropic Liquid Crystal Polymers," 1992 JANNAF Propulsion Meeting, Indianapolis, In, February 1992

3 Chaffee, K.P., "EXAFS of Halogenated Liquid Crystal Polymers," In Print, Edwards Air Force Base, Ca

DETERMINATION OF THE NUMBER AVERAGE MOLECULAR WEIGHT OF AROMATIC THERMOTROPIC LIQUID CRYSTALLINE POLYESTERS BY DRIFT SPECTROSCOPY

Key Words: FTIR, Liquid Crystalline Polyester

Debbie B. Saebø and Philip B. Oldham*

Department of Chemistry
Mississippi State University
Mississippi State, Mississippi 39762

ABSTRACT

Determination of the number average molecular weight of a series of liquid crystalline polyesters by diffuse reflectance infrared Fourier transform (DRIFT) spectroscopy are reported. End-group analysis is used to estimate chain persistance length by relating the respective acid and ester carbonyl bands in the infrared spectrum. This unconventional method of molecular weight determination is required due to extreme solubility restraints which practically eliminate the use of more conventional methods such as gel permeation chromatography or light scattering.

INTRODUCTION

Recently, considerable interest has been expressed in fully aromatic thermotropic liquid crystalline polyesters because they have attractive properties as engineering plastics or high strength fibers. Characteristic properties of this group of polyesters are high tensile strength, high thermal stability, and high crystal to nematic transition temperatures.

Another characteristic property of these polyesters is an extremely low solubility in most typical organic solvents. Of course, this is an attractive characteristic for structural applications where chemical stability is required. However, this also means that these polyesters have little or no solubility in typical solvents (such as tetrahydrofuran) used in traditional molecular weight determinations. Therefore, an alternative technique is reported to investigate the molecular size of these polyesters. In this technique, diffuse reflectance infrared spectra are acquired of the solid-state samples. Resolution enhancement is performed on each spectral data set using Fourier self-deconvolution and linear curve fitting.[1] The vibrational bands representing the ester carbonyl (repeat units) and acid carbonyl (endgroup) bonds are assigned using spectra from simple model compounds. A number average molecular weight can then be assigned to each of the polyesters based on the relative band areas associated with the appropriate vibrational modes.

EXPERIMENTAL

Polyester samples were synthesized at the Phillips Laboratories, Edwards Air Force Base, California, and were used as received. The polyesters were synthesized by reacting a solution of 25 weight percent terephthaloyl chloride in methylene chloride with a 25 weight percent solution of a substituted hydroquinone in methylene chloride using pyridine as an acid scavenger. The purity of all of the starting materials was 99.9% + polymer grade. These were also specially distilled prior to solution preparation. The substiuent groups on the hydroquinone were methyl, chloro, phenyl and phenylethyl. The commercial polyester, GRANLAR, is a copolyester of the phenyl and phenylethyl substitued hydroquinone terephthalate. Powdered KBr was obtained from Spectra-Tech, Inc. (Stamford, Connecticut) and oven dried prior to use. Spectra were acquired on a Bruker IFS-25 FTIR equipped with a Spectra-Tech Baseline DRIFT accessory and a mercury cadmium telluride (MCT) detector. Each polyester sample was prepared in powdered KBr to an approximate ratio of 0.30%. Spectral data files were subsequently transferred _via_ J-CAMP format to LAB CALC (Galactic Industries Corporation, Salem, New Hampshire) for deconvolution and linear curve fitting.

DATA ANALYSIS

The methods of Fourier self deconvolution and linear curve fitting were used to extract the molecular weight information for each polyester from their respective infrared

spectra. Fourier self-deconvolution is a method used to computationally resolve overlapping bands which are unresolved due to the instrument response function. Deconvolution narrows the lines in the spectrum but does not increase the intrinsic instrument resolution. Deconvolution involves use of a special high pass Fast Fourier Transform (FFT) filter which synthetically narrows the effective trace bandwidth features. Thus, the principal bands comprising a more complex band with overlapping features can be identified.[2] This research utilized the method of digital self-deconvolution carried out in Fourier transform space.[3-8]

The carbonyl band region for each spectra is displayed and deconvolved using LAB CALC. A best guess estimate for the exponential filter constant (g) is
first selected. Then the bessel apodization filter is selected. The bessel apodization filter is an exponential filter of the form exp^{2pgx} where g is the deconvolution filter constant specified and x is the array whose normilized range is from x = 0 to 1. At this point, the trace feature which is to be deconvolved is defined. The deconvoluted spectrum is then used instead of the original spectral data for linear curve fitting because the deconvoluted spectrum gives peaks which are more resolved than the original spectral peaks. This procedure is also performed using LAB CALC. The number of bands and their positions are taken from the second derivative spectrum and/or the deconvoluted spectrum for each polyester. The curve fitting routine automatically calculates the best fit of

Gaussian, Lorentizian, of Log normal bands (selectable) which make up a complex set of overlapping peaks. The evaluation of the results is based on obtaining a small chi-squared value for a given data set. The smaller the chi-squared value, the better the fit to the curve. Several passes are performed to minimize the chi-squared value until performing additional passes does not change the chi-squared value, at this point the best fit has been accomplished for this deconvoluted spectrum. These spectral bands were all curvefit using a Lorentizian line shape with the exception of GRANLAR, where the Gaussian line shape provided the best fit. The curve fitting routine also yields information concerning peak height and area.

RESULTS AND DISCUSSION

The liquid crystlline polyesters studied were poly(3-methyl-1,4-phenylene terephthalate), poly(3-chloro-1,4-phenylene terephthalate), poly(3-phenyl-1,4-phenylene terephthalate), poly(3-phenylethyl-1,4-phenylene terephthlate) and GRANLAR [poly(3-phenyl-1,4-phenylene terephthalate-co-3-phenylethyl-1,4-phenylene terephthalate)]. A DRIFT spectrum was also acquired for terephthalic acid which was subtracted from each of the polyesters using the subtraction routine of LAB CALC. The terephthalic acid spectrum was subtracted from each of the infrared spectra of the polyesters to remove any residual terephthalic acid typically found in the sample from the synthetic process. The spectrum of terephthalic acid was also used to define the

carbonyl region for an acid. A diffuse reflectance spectrum of mono-methyl terephthalate was acquired to define the carbonyl region for an ester. The region of the infrared spectrum which was deconvolved and curvefit was 1765 cm^{-1} to 1685 cm^{-1}. This region was selected because it corresponds to the carbonyl band region for both the acid and ester carbonyl bands.

Figure 1 shows the deconvolved infrared spectrum of poly(3-methyl-1,4-phenylene terephthalate) in the carbonyl region along with the curvefit peaks. The bessel apodization (g) value was 1.031 for this deconvolution. The g value for each spectrum is determined by increasing the value for g until the highest point of the peaks begin to flatten then the g value is reduced slightly to obtain a sharp peak. Each component peak was obtained from a Lorentizian band fit and required two hundred passes in order to obtain an overall chi-square value of 0.535. A total of nine peaks were found, where the peak areas for peaks two through six were summed to account for the ester carbonyl vibrational band and the peak areas for peaks seven through nine were summed to account for the acid carbonyl vibrational band. These combinations of peaks were selected to account for the acid carbonyl band by the process of overlapping the carbonyl region of the infrared spectrum for terephthalic acid with the infrared spectrum of each polyester. Likewise, to determine which peaks should be combined to represent the ester carbonyl, the carbonyl region of the infrared of monomethyl terephthalate was overlapped with the

same region for each polyester. It was assumed for each polyester infrared spectrum that the extinction coefficients for the ester carbonyl and acid carbonyl bands were approximately the same. The ester carbonyl band area was ratioed to the acid carbonyl band area to find that there was 6.3 ester carbonyls present in the po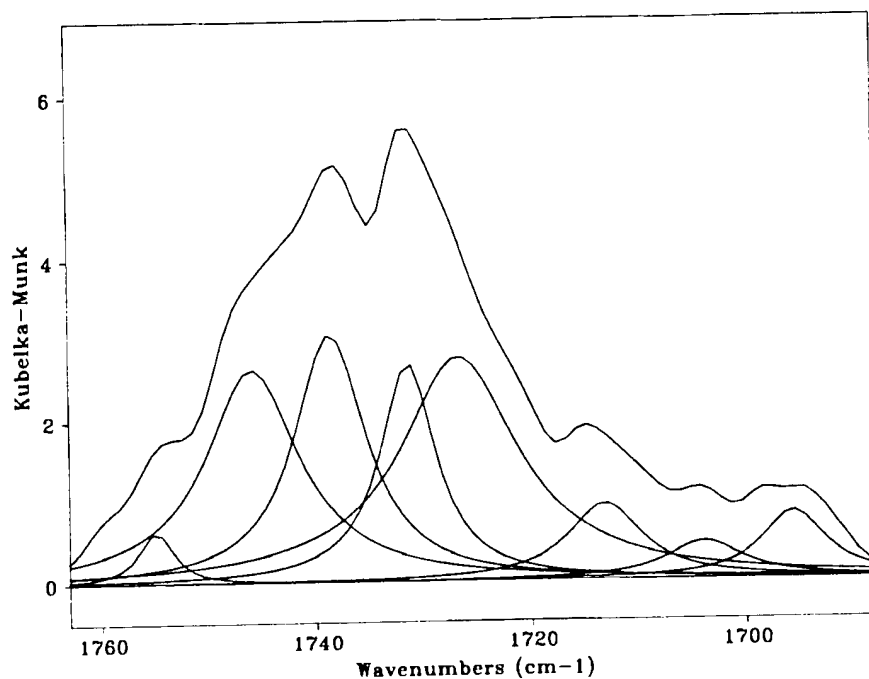lyester for each acid carbonyl. This gave an estimated number average molecular weight of approximately 1621 g/mol for poly(3-methyl-1,4-phenylene terephthalate) as shown in Table 1.

Figure 2 shows the deconvolved infrared spectrum of poly(3-chloro-1,4-phenylene terephthalate) in the carbonyl region along with the curvefit peaks. The bessel apodization (g) value was 1.054 for this deconvolution. Each peak was obtained from a Lorentizian band fit and required two hundred passes in order to obtain an overall chi-squared value of 0.637. A total of ten peaks were found, where the peak areas for peaks two through six were summed to account for the est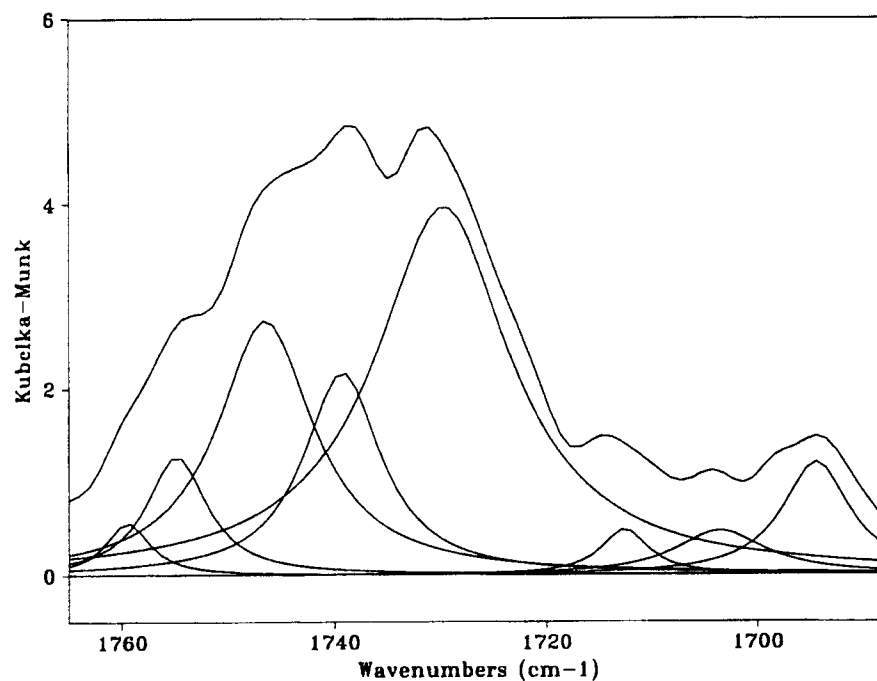er carbonyl vibrational band and peak areas for peaks seven through ten were summed to account for the acid carbonyl vibrational band. The ester carbonyl band area was ratioed to the acid carbonyl band area to find that there was 5.0 ester

carbonyls present in the polyester for each acid carbonyl. This

Figure 1. Curvefit of carbonyl bands for poly(3-methyl-1,4-phenylene terephthalate).
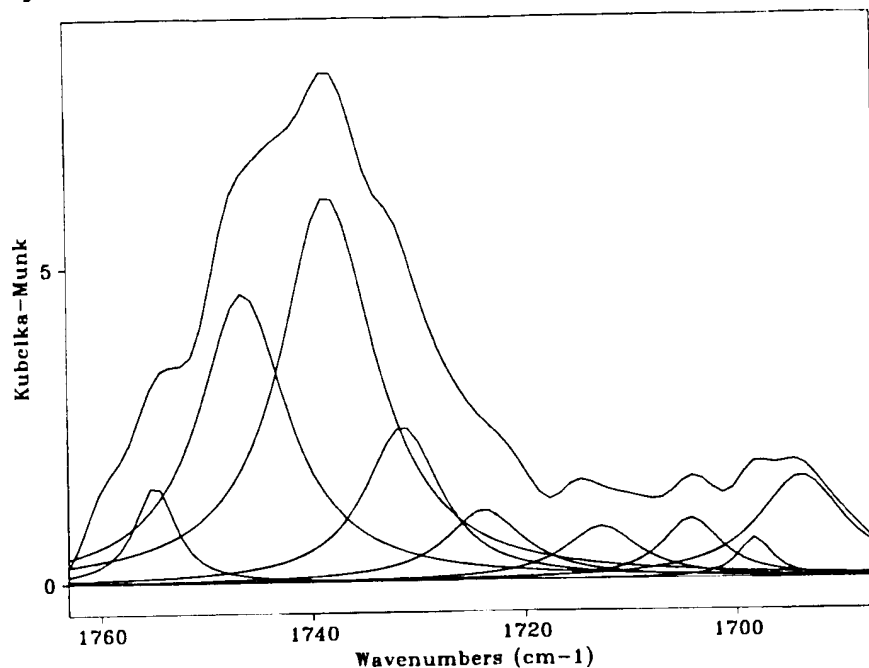
Figure 2. Curvefit of the carbonyl bands for poly(3-chloro-1,4-phenylene terephthalate).

gave an estimated number average molecular weight of approximately 1250 g/mol for poly(3-chloro-1,4-phenylene terephthalate) as shown in Table 1.

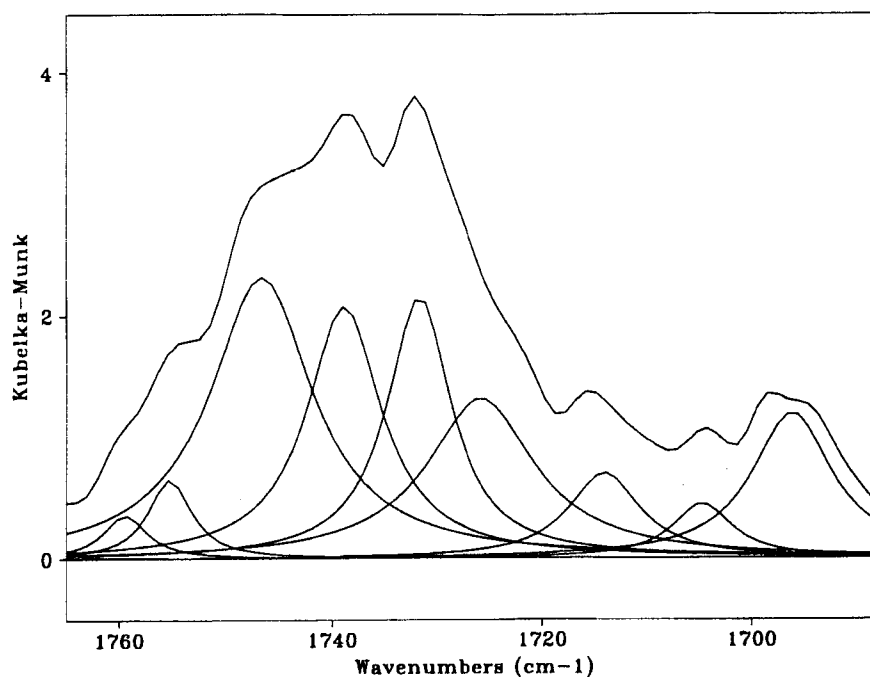Figure 3 shows the carbonyl region of deconvolved infrared spectrum of poly(3-phenyl-1,4-phenylene terephthalate) along with the curvefit peaks. The bessel apodization (g) value was 0.607 for this deconvolution. Each resolved peak was obtained from a Lorentizian band fit and required two hundred passes in order to obtain an overall chi-squared value of 0.967. A total of nine peaks were found where the peak areas for peaks one through six were summed to account for the ester carbonyl vibrational band and peak

Figure 3. Curvefit of the carbonyl bands for poly(3-phenyl-1,4-phenylene terephthalate).

areas for peaks seven through nine were summed to account for the acid carbonyl vibrational band. The ester carbonyl band area was ratioed to the acid carbonyl band area to find that there was 7.5 ester carbonyls present in the polyester for each acid carbonyl. This gave an estimated number average molecular weight of approximately 2391 g/mol for poly(3-phenyl-1,4-phenylene terephthalate) as shown in Table 1.

Figure 4 shows the deconvolved infrared spectrum of poly(3-phenylethyl-1,4-phenylene terephthalate) in the carbonyl region along with the curvefit peaks. The bessel apodization (g) value was 0.826 for this deconvolution. Each peak was obtained from a Lorentizian band fit and required two hundred passes in order to obtain an overall chi-squared value of 0.497. A total of nine peaks were found, where the peak areas for peaks one through six were summed to account for the ester carbonyl vibrational band and peak areas for peaks seven through nine were summed to account for the acid carbonyl vibrational band. The ester carbonyl band area was ratioed to the acid carbonyl band area to find that there was 4.3 ester carbonyls present in the polyester for each acid carbonyl. This gave an estimated number average molecular weight approximately 1501 g/mol for poly(3-phenylethyl-1,4-phenylene terephthalate) as shown in Table I.

Figure 5 shows the deconvolved infrared spectrum of poly(3-phenyl-1,4-phenylene terephthalate-co-3-phenylethyl-

Figure 4. Curvefit of the carbonyl bands of poly(3-phenylethyl-1,4-phenylene terephthalate).

1,4-phenylene terephthalate) in the carbonyl region along with the curvefit peaks. The bessel apodization (g) value was 1.049 for this deconvolution. Each peak was obtained from a Gaussian band fit and required two hundred passes in order to obtain an overall chi-squared value of 0.781. A total of five peaks were found where the peak areas for peaks two and three were summed to account for the ester carbonyl vibrational band and peak areas for peaks four and five were summed to account for the acid carbonyl vibrational band. The ester carbonyl band area was ratioed to the acid carbonyl band area to find that there was 6.5 ester carbonyls present in the

65

polyester for each acid carbonyl. This gave an estimated number average molecular weight of approximately 4296 g/mol for poly(3-phenyl-1,4-phenylene terephthalate-co-3-phenylethyl-1,4-phenylene terephthalate) as shown in Table II.
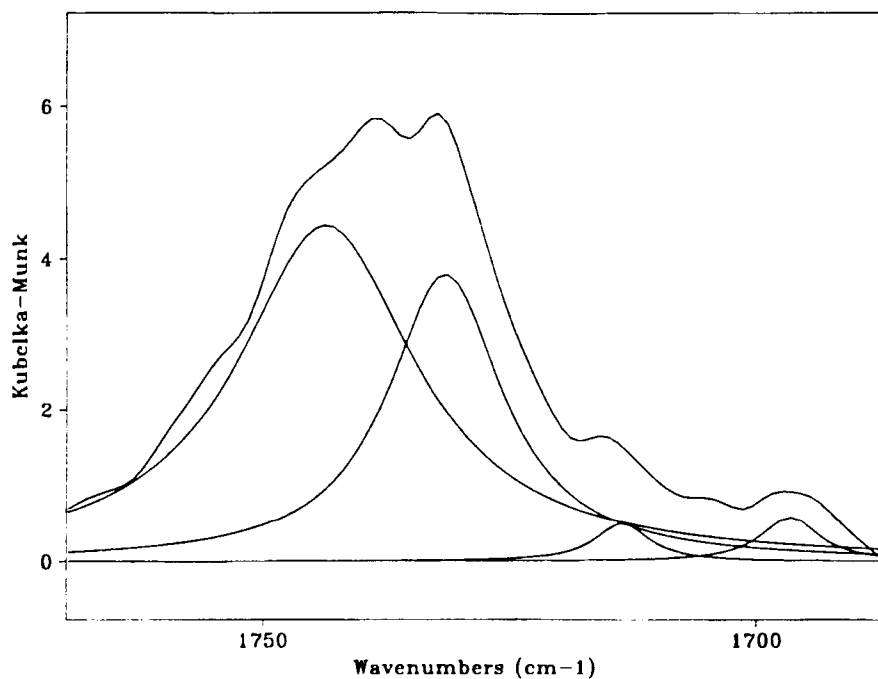
Figure 5. Curvefit of the carbonyl band for the poly(3-phenyl-1,4-phenylene terephthalate-co-3-phenylethyl-1,4-phenylene terephthalate)

Table I

Estimated Number Average Molecular Weight For Liquid Crystalline Polyesters
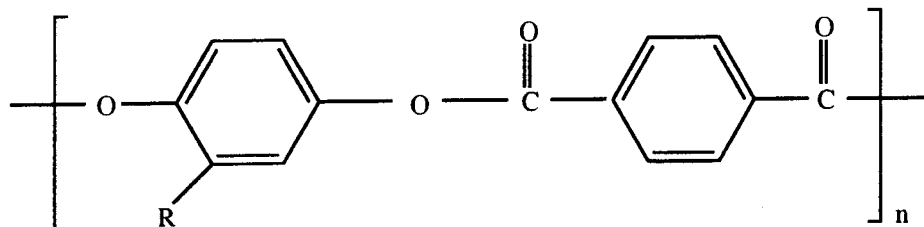
Substituent Group R	Estimated Number of Monomers	Molecular Weight (Est)
Methyl-	6	1544 g/mol
Chloro-	5	1250 g/mol
Phenyl-	7	2232 g/mol
Phenylethyl-	4	1396 g/mol

Table II

Estimated Number Average Molecular Weight For Liquid Crystalline Polyesters
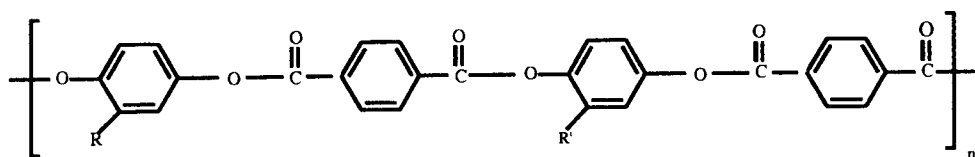
Substituent Group R	Estimated Number of Monomers	Molecular Weight (Est)
R = Phenyl-		
R' = Phenylethyl-	6.5	4296 g/mol

CONCLUSIONS

The DRIFT method of analyzing insoluble polyesters for their molecular weight has been extremely useful. We were able to determine an estimated number average molecular weight for each of the polyesters using end group analysis of the carbonyl region in the FTIR spectrum. These data resulted in the following molecular weights for each of the following esters: 1544 g/mol for poly(3-methyl-1,4-phenylene terephthalate) with 6 repeat units, 1250 g/mol for poly(3-chloro-1,4-phenylene terephthalate) with 5 repeat units, 2232 g/mol for poly(3-phenyl-1,4-phenylene terephthalate) with 7 repeat units, 1396 g/mol for poly(3-phenylethyl-1,4-phenylene terephthalate) with 4 repeat units, 4296 g/mol for poly(3-phenyl-1,4-phenylene terephthalate-co-3-phenylethyl-1,4-phenylene tere-phthalate) with 6.5 repeat units.

REFERENCES

1. Fabian, H.; Naumann, D.; Misselwitz, R.; Ristau, O.; Gerlach, D.; Welfle, H. *Biochemistry* **1992**, 31 (28), 6532.

2. "Trends in Analytical Chemistry", P. R. Griffiths and G. Pariente, Vol. 5, 8 (1986).

3. Jansson, P. A.; Hunt, R. H.; Plyter, E. K. *J. Opt. Soc. Am.* **1970**, *60*, 596.

4. Willson, P. D.; Hanratty, J. R.; Edwards, T. H. *Symposium on Molecular Spectroscopy*, Columbus, OH, **1972**.

5. Willson, P. D. Michigan State University, Ph.D. Dissertation, 1973.

6. Halsey, G.; Blass, W. E. *Appl. Opt.* **1977**, *16*, 286.

7. Pliva, J.; Pine, A. S.; Willson, P. D. *Appl. Spectrosc.* **1980**, *19*, 1833.

8. Kauppinen, J. K.; Moffatt, D. J.; Mantsch, H. H.; Cameron, D. G. *Appl. Spectrosc.* **1981**,*35(3)*, 271.

NMR STUDIES OF AROMATIC LIQUID CRYSTALLINE POLYESTERS

BY

Debbie B. Saebø, Philip B. Oldham and Rickey P. Hicks*

MISSISSIPPI STATE UNIVERSITY

DEPARTMENT OF CHEMISTRY

INTRODUCTION

One-dimensional and two-dimensional nuclear magnetic resonance (NMR) studies were performed to determine the feasibility of studying the conformational differences between a homologous series of polyesters. The aromatic copolyesters of terephthalic acid and substituted hydroquinones (Figure 1) all exist as liquid crystals where their transitions from the crystal to nematic phase occurs around 300°C. At room-temperature they are solids with remarkable physical properties. These properties make them attractive engineering plastics or high strength fibers. Characteristic properties of this group of polyesters are high tensile strength, high thermal stability, and high crystal to nematic transition temperatures. The materials can be injection molded and due to their physical properties and light weights the United States Air Force has considered using these materials in engine parts and rocket nossels.[1] The polymers are also easy to synthesize through a reaction between the appropriate hydroquinone derivative and the acid chloride of terephthalic acid in aqueous solution. When the polymers are produced this way the number of repeat units is small. All experimental studies[2,3] indicate that the number of repeat units in these polymers is between 4 and 7, - a remarkably low number considering their physical properties.

Nuclear magnetic resonance (NMR) is a very popular technique for structural elucidation of organic compounds. NMR can give information on the chemical shift and coupling constants of various compounds. Examination of a multiplet pattern in a one-

71

Figure 1. The structure of the aromatic liquid crystalline copolyesters.

B ring   A ring
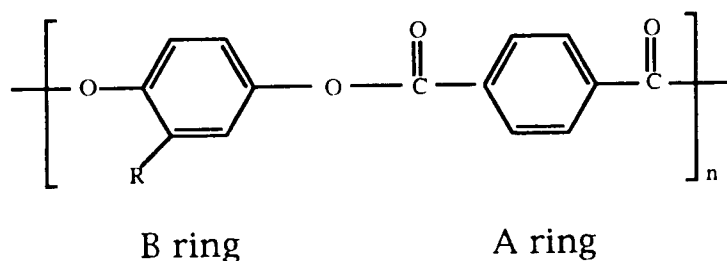
R substituent	Abbreviated Name
Methyl-	MHQ
Chloro-	CHQ
Phenyl-	PHQ
Phenylethyl-	PEHQ

B ring   A ring   B ring   A ring
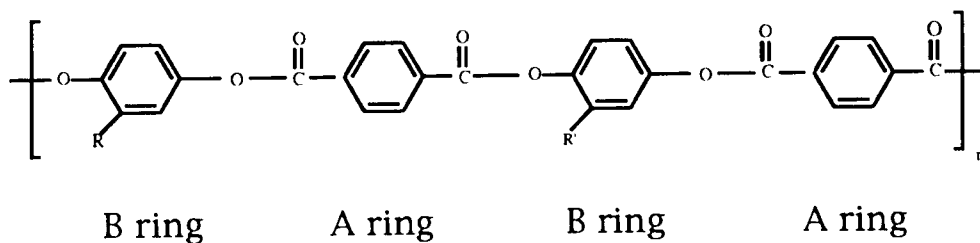
(R and phenyl of R' = C ring)

R Substituent	Abbreviated Name
R = Phenyl-	
R' = Phenylethyl-	GRANLAR

dimensional proton spectra can often yield information for the determination of how many protons are in closely proximity to another proton. Coupling occurs in very perdictable circumstances; for protons, two and three bond couplings are usually in the range 2-20 Hertz, however, longer range couplings are usually very small. Coupling gives pairing information between nuclei whereas chemical shifts only gives a crude indication of the environment of individual nuclei.[1]

Many NMR investigations require the use of two-dimensional experiments to obtain complete information about a particular compound. The information obtained from proton spectra lead to the need for additional information which could be obtained from several different two-dimensional experiments. A systematic evaluation of the structure of these polyesters was performed using one-dimensional and two-dimensional NMR experiments. The two-dimensional experiments used were the HOHAHA (Homonuclear Hartman-Hahn Spectroscopy), NOESY (Nuclear Overhauser Spectroscopy), HMQC (Heteronuclear Multiple-Quantum Coherence), and HMBC (Heteronuclear Multiple-Bond Coherence). Each of these two-dimensional experiments will be explained briefly.

The HOHAHA experiment gives information about the connectivities between neighboring protons in the molecule. This experiment involves J-coupling information.[4,5] The main application of the HOHAHA experiment is to separate and assign individual spin systems less than the sequential assignment of proton resonances.

The NOESY experiment gives information about the long range dipolar coupling between nuclei. This dipolar coupling information provided indirectly from the nOe is related to internuclear distances and molecular motion.[4] Two-dimensional Nuclear Overhauser Enhancement (NOESY)[6] and Rotating frame Overhauser Enhancement (ROESY)[7,8] spectra delineate through space or dipolar spin-spin conductivity. Two protons that are dipolar coupled (share a relaxation pathway) to each other will yield a cross peak. The intensity or volume integral of this cross peak is related by $1/r^{-6}$ to the inter-proton distance between the two protons.[6] The measurement of NOE buildup rates provides a means to measure inter-proton distances. The NOESY experiment is commonly used to measure these buildup rates.[7] Several potential problems exist, if one is not careful, in the use of this NOE data.[7] NOEs may be relayed from one proton to another; these relayed signals will yield erroneous information. The existence of relayed NOEs may be determined by using spin-lock ROE spectroscopy, (CAMELSPIN[8] or ROESY). In ROESY spectra, cross peaks due to direct NOEs are always opposite in sign relative to the diagonal peaks and relayed ROEs yield cross peaks that are in phase with the diagonal.[7] The second potential problem for conventional nuclear Overhauser effect (NOE) measurements for small molecules, such as small polymers, is that NOEs often fail for such molecules, irrespective of the inter-nuclear distances involved, simply because the tumbling rate or correlation time for these molecules is close to that at which the maximum

possible homonuclear NOE passes through zero.[7] Spin lock NOEs or ROEs are always positive and increase with slower molecular tumbling [9] with the result that molecules of intermediate size can show substantial transverse NOE enhancement in the ROESY experiment and little or no enhancement in the NOESY experiment. ROEs obtained from ROESY experiments can be useful for conformational studies of small molecules, such as small polymers or peptides.[9,10]

These polyesters were investigated using NMR to determine the structural features of each of the polyesters. The one-dimensional proton NMR spectra of the individual polyesters proved to point out very interesting differences between the polyesters depending on which substituent was on the polyester being investigated.

EXPERIMENTAL SECTION

Each of the following polyesters were synthesized at the Phillips Laboratory, and used as received. The polyesters studied are poly(3-methyl-1,4-phenylene terephthalate), poly(3-chloro-1,4-phenylene terephthalate), poly(3-phenyl-1,4-phenylene tereph-thalate), poly(3-phenylethyl-1,4-phenylene terephthalate) and poly(3-phenyl-1,4-phenylene terephthalate)-co-(3-phenylethyl-1,4-phen-ylene terephthalate). The solvents used were a mixture of deuterated trifluoroacetic acid and deuerated chloroform. These solvents were mixed in a 1:3 ratio of deuerated trifluoroacetic acid to

deuerated chloroform for dissolving each polymer.

These experiments were all performed on a Bruker AMX300 NMR. The NMR experiment for each polyester was performed at 325 K in order to sharpen the lines in the spectrum.

RESULTS AND DISCUSSION

Each of the polyesters were first investigated using ^{1}H NMR. The one-dimensional ^{1}H spectrum of each of the polyesters revealed a very interesting and characteristic differences among the conformational structures for each polyester. The ^{1}H NMR spectrum (Figure 2) for poly(3-methyl-1,4-phenylene terephthalate), labelled MHQ, revealed that the ring protons for the terephthaloyl portion of the polyester (called the A ring protons) are all degenerate; meaning they have the same chemical shift. This indicates that the MHQ polyester is likely in a random coil conformation. The ^{1}H NMR spectrum (Figure 3) for poly(3-chloro-1,4-phenylene terephthalate), labelled CHQ, shows a similar spectrum to that of MHQ in the aromatic proton region. The ^{1}H spectrum (Figure 4) for poly(3-phenyl-1,4-phenylene tereph-thalate)-co-(3-phenylethyl-1,4-phenylene terephthalate), labelled GRANLAR, shows two peaks for the A ring protons. Since there is more than one chemical environment for the A ring protons (labelled in Figure 1), then there is more of a conformational effect occurring. The ^{1}H NMR spectrum (Figure 5) for poly(3-phenylethyl-1,4-phenylene terephthalate), labelled PEHQ, shows even more splitting of the A ring protons as

Figure 2. The ^{1}H NMR spectrum for poly(3-methyl-1,4-phenylene terephthalate).
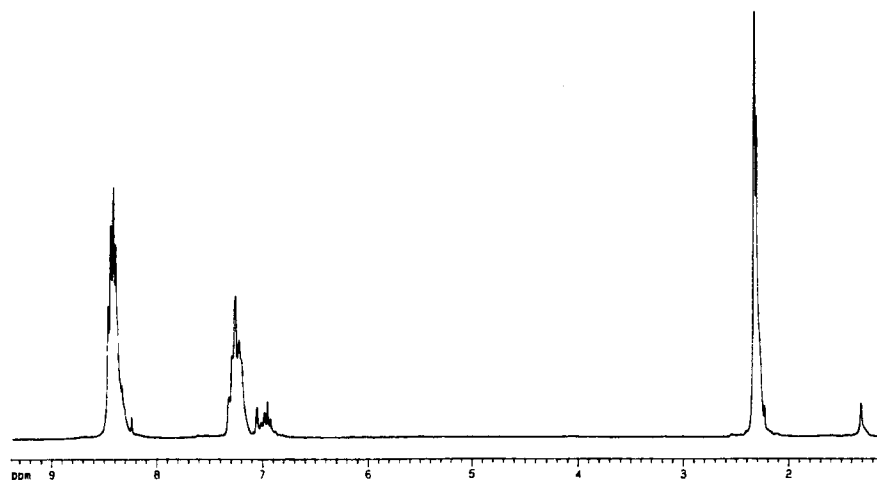
Figure 3. The ^{1}H spectrum for poly(3-chloro-1,4-phenylene terephthalate).
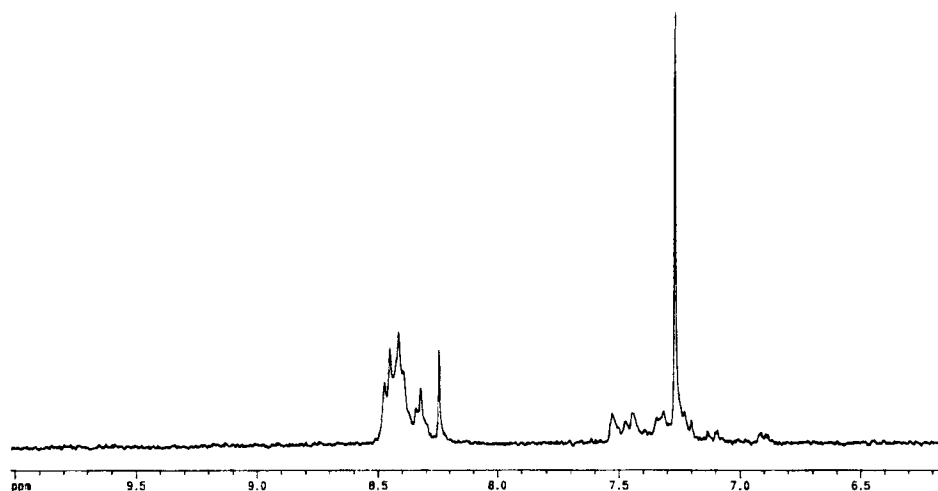
Figure 4. The ^{1}H spectrum for poly(3-phenyl-1,4-phenylene tereph-thalate)-co-(3-phenylethyl-1,4-phenylene terephthalate).
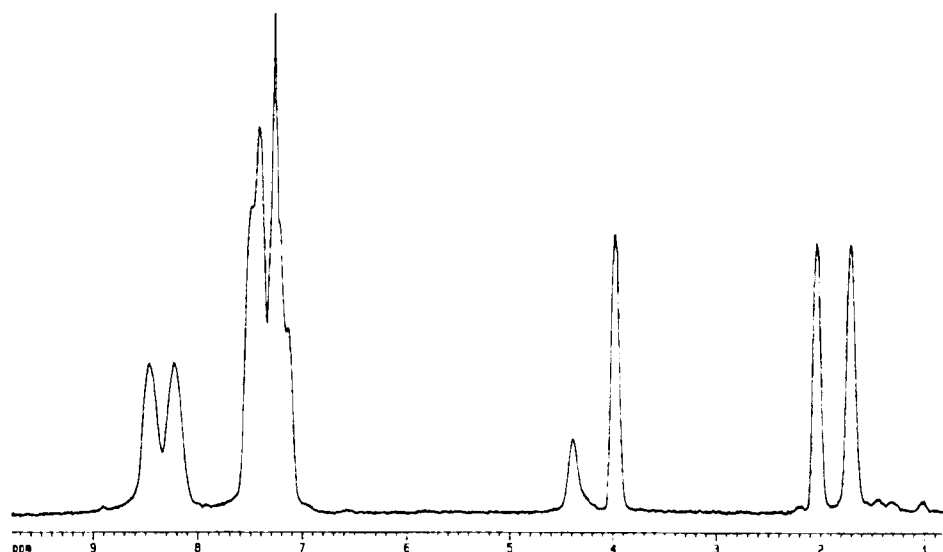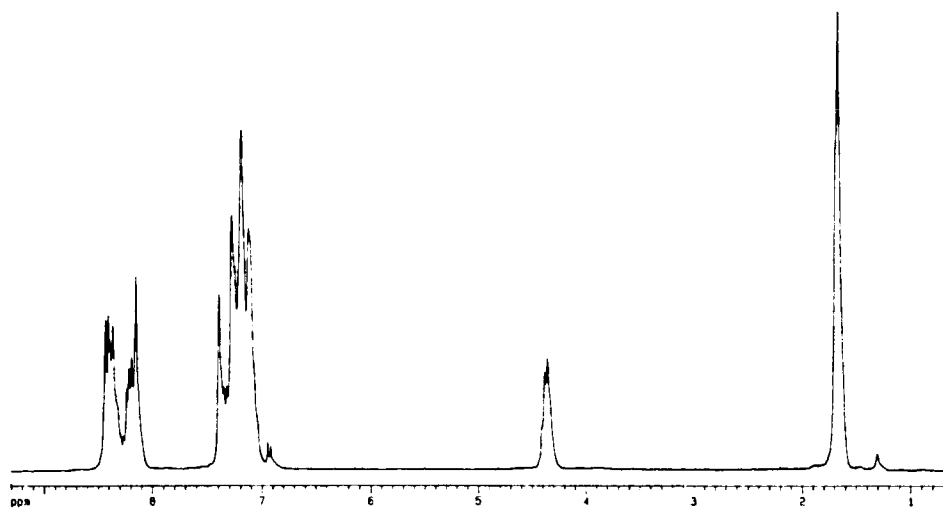

Figure 5. The ^{1}H NMR spectrum (Figure 5) for poly(3-phenylethyl-1,4-phenylene terephthalate).

compared to the A ring protons for GRANLAR. This splitting indicates that this polyester has some fixed conformation as compared to the MHQ polyester. In the ^{1}H NMR spectrum (Figure 6) for poly(3-phenyl-1,4-phenylene terephthalate), labelled PHQ, the A ring protons show a pronounced splitting which gives information

Figure 6. In the ^{1}H NMR spectrum for poly(3-phenyl-1,4-phenylene terephthalate).
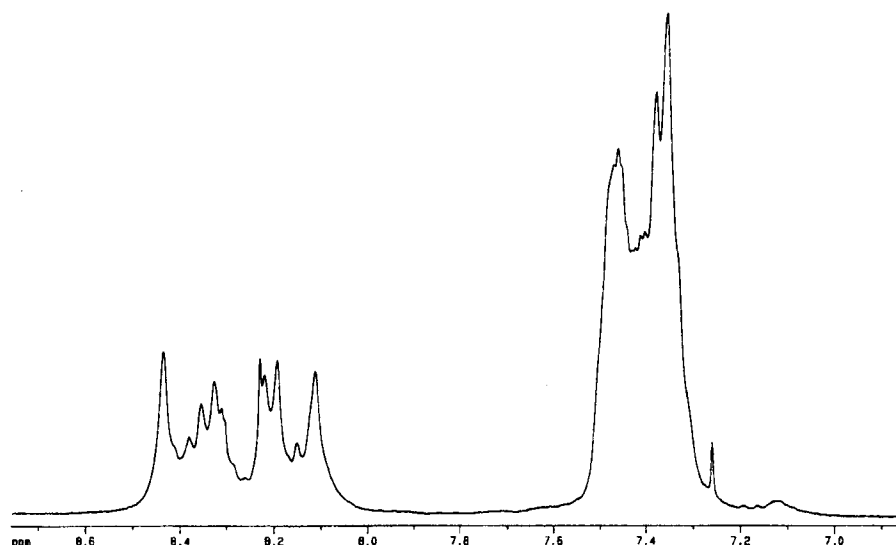
about conformational effects of these A ring protons. There are different microenvironments for the A ring protons. Thus the PHQ looks to be more ordered than the other polyesters. However, two-dimensional NMR experiments are required to verify these possible conformations. While looking for structural features, the different splitting pattern of the A ring protons shown in the one-dimensional proton spectra lead to an investigation of the three-dimensional structure of the polyesters using two-dimensional experiments.

The HOHAHA experiment was used to investigate the differences between the ordered and nonordered polyesters by evaluating the aromatic region of the spectra. Figure 7 shows the HOHAHA for poly(3-phenylethyl-1,4-phenylene terephthalate). The connectivities between the two methylene groups are shown in the aliphatic region of the spectrum (1.5 ppm and 4.5 ppm). No connectivities are observed between the protons on the two phenyl rings. The only connectivities observed are between two of the A ring protons (protons on the phenyl ring of the terephthaloyl portion of the polyester) to the other two A ring protons (Figure 8).

Figure 7. The HOHAHA for poly(3-phenylethyl-1,4-phenylene terephthalate)
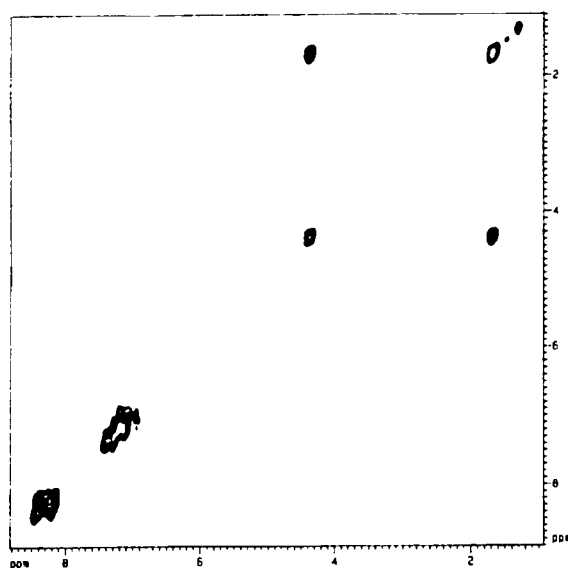
The HOHAHA experiment (Figure 9) for poly(3-phenyl-1,4-phenylene terephthalate) showed no connectivities between the A ring protons (protons on the phenyl ring of the terephthaloyl protion of the polyester) and the B ring protons (protons on the phenyl ring of the hydroquinone portion of the polyester). However, Figure 10 shows the three sets of A ring protons which are found in the HOHAHA data. Therefore the structural features of poly(3-phenyl-1,4-phenylene terephthalate) yields three environments for these A ring protons. These data reveal that this particular polyester has an ordered structure as compared to the other polyesters because no strucutural feature similar to this is observed for any of the other polyesters. The proton NMR spectrum of a random coil polymer should exhibit characteristics of random chemical shifts. Rapidly averaging conformations will lead to rapidly averaging chemical shifts which will result in sharp degenerate lines as seen in Figure 2. Increasing discreet local conformational features of the polymers will remove these degenericies and will result increase number of resonance lines and broadening of the observed lines as seen in Figure 6 for example. Two dimensional homonuclear Hartmann Hahn spectroscopy experiments were used to analyze the complex coupling observed in the polymers with a high degree of secondary structure. The two sets of proton pairs on the A ring do not show connectivities to the phenyl substituent group. The B ring protons (labelled in Figure 1) also do not show connectivities to the protons on this phenyl substituent. However, the NOESY of this polyester (Figure 11) does show connectivities between the A ring protons and B ring

81

Figure 8. The HOHAHA for poly(3-phenylethyl-1,4-phenylene tere-phthalate) showing the aromatic proton connectivites.
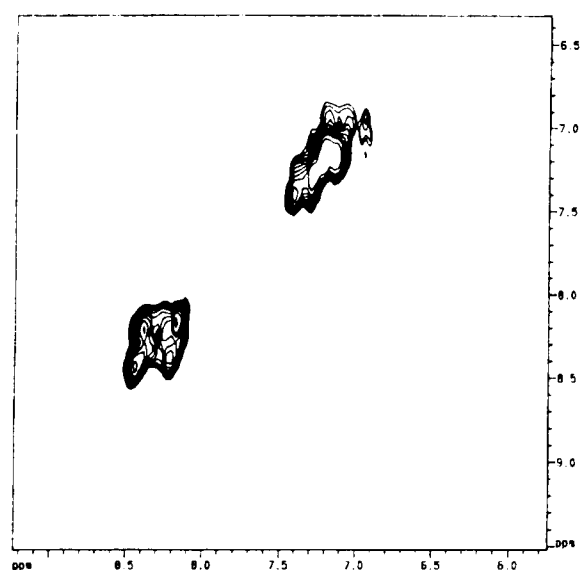

Figure 9. The HOHAHA spectrum for poly(3-phenyl-1,4-phenylene terephthalate).
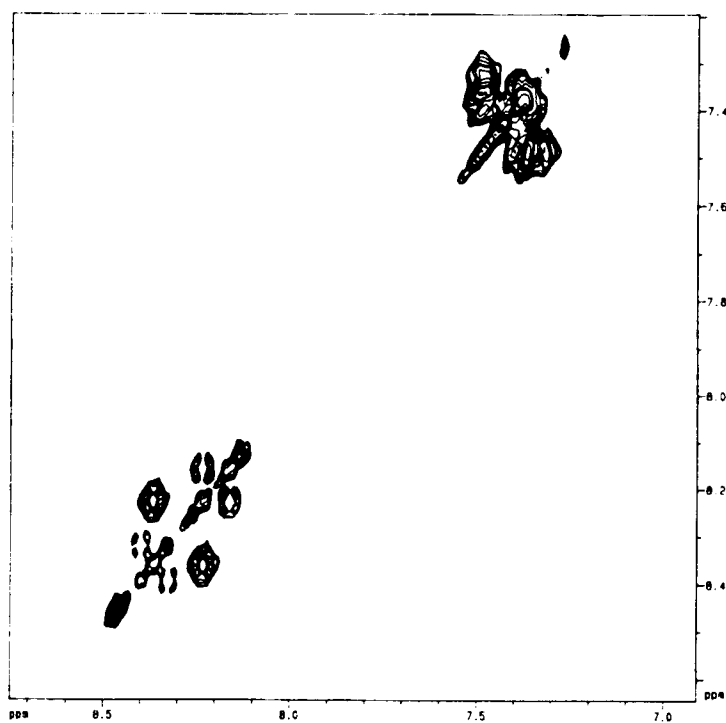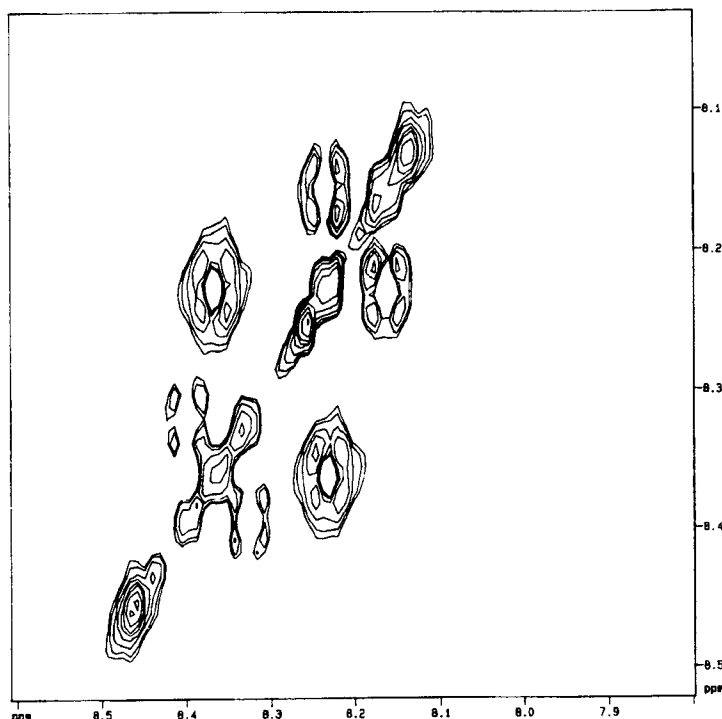
Figure 10. The HOHAHA spectrum for poly(3-phenyl-1,4-phenylene terephthalate).

protons and between the A ring protons with the protons of the phenyl substituent.

The HOHAHA for poly(3-phenyl-1,4-phenylene)-co-(3-phenyl-ethyl-1,4-phenylene terephthalate) (Figure 12(a)) shows two separate environments for the methylene groups. In this case, two connectivites are observed instead of having one from one methylene group to the other methylene group. The A ring protons are observed to have only one environment (Figure 12 (b)). The NOESY (Figure 13) of this polyester shows the connectivities between the B ring protons and the protons on the phenylethyl substituent to the methylene protons.

Figure 11. The NOESY spectrum for poly(3-phenyl-1,4-phenylene terephthalate).
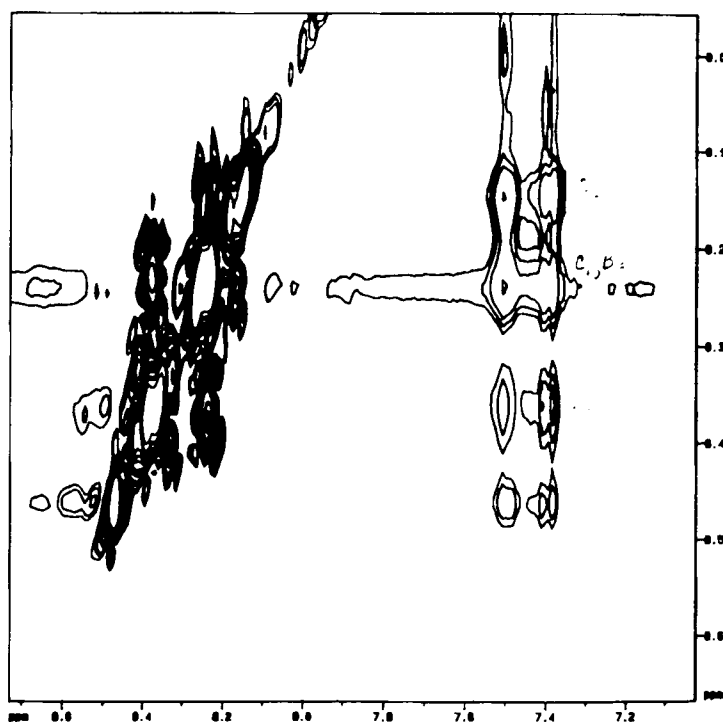
A T1 relaxation experiment was performed on poly(3-phenyl-1,4-phenylene terephthalate) to further investigate the hypothesis of different environments for the aromatic protons. Table 1 shows the T1 values for the aromatic protons and these data does indeed support the one-dimensional ^{1}H data and the two-dimensional HOHAHA and NOESY data. The T1 data shows that all of the chemical shifts have different T1 values which means they all have different relaxation times and therefore must have different chemical environments.

Figure 12. The HOHAHA for poly(3-phenyl-1,4-phenylene)-co-(3-phenyl-ethyl-1,4-phenylene terephthalate).
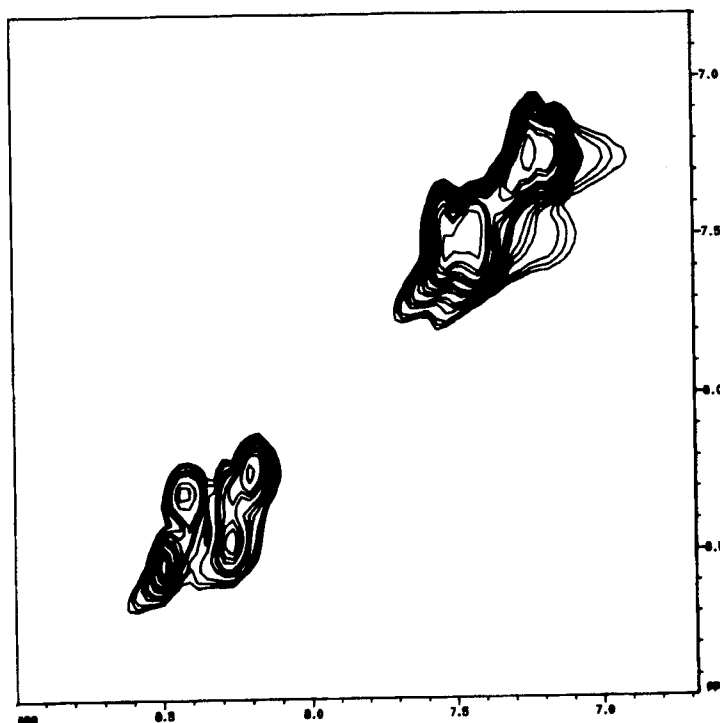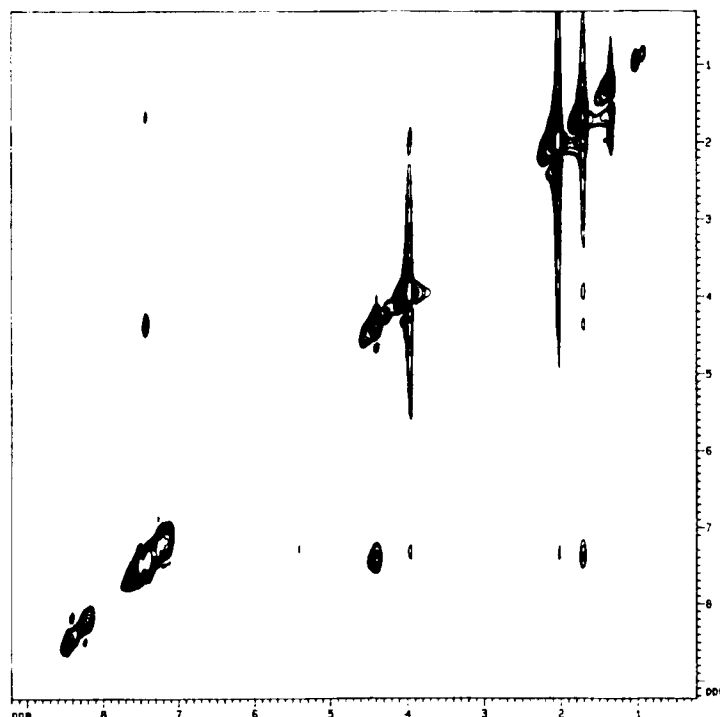
(a)
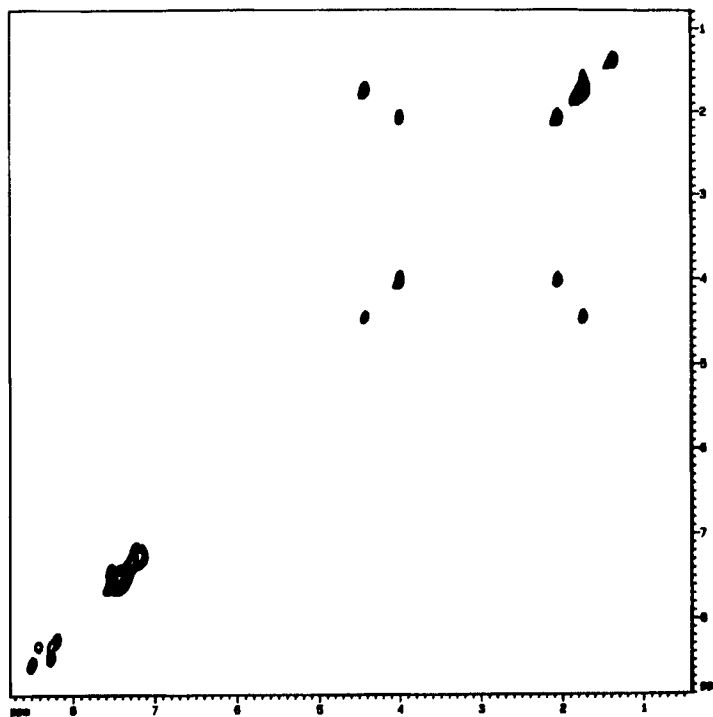
(b)

Figure 13. The NOESY for poly(3-phenyl-1,4-phenylene)-co-(3-phenyl-ethyl-1,4-phenylene terephthalate).

CONCLUDING REMARKS

These NMR studies reveal that the particular polyesters in question have different structural features depending upon the substituent that is placed on the phenylene group of the hydroquinone protion of the molecule. The poly(3-methyl-1,4-phenylene terephthalate), MHQ, and poly(3-chloro-1,4-phenylene terephthalate), CHQ, have the least ordered conformations. The poly(3-phenyl-1,4-phenylene terephthalate)-co-(3-phenylethyl-1,4-phenylene terephthalate), GRANLAR, is more ordered than MHQ or CHQ, since two environments are shown for the phenylethyl ring

Table 1.
List of chemical shifts and T1 relaxation data for the aromatic
protons for poly(3-phenyl-1,4-phenylene terephthalate).

T1 RELAXATION DATA

CHEMICAL SHIFT δ (ppm)	T1 (seconds)
8.39	2.16
8.36	2.74
8.33	3.03
8.24	3.10
8.23	2.89
8.16	2.09
7.47	2.01
7.46	2.09
7.45	2.52
7.43	2.38
7.42	2.38
7.41	2.45
7.38	1.95
7.35	2.05

protons. The poly(3-phenylethyl-1,4-phenylene terephthalate), PEHQ, shows more order than GRANLAR. Poly(3-phenyl-1,4-phenylene tereph-thalate) is the most ordered of the five polyesters as shown by the three environments for its A ring protons.

ACKNOWLEDGEMENT

REFERENCES

1. Advanced Polymer Component Symposium, Butler University 1992.

2. D. B. Saebø and P. B. Oldham, Department of Chemistry, Mississippi State University, unpublished IR, fluorescence, and NMR studies.

3. S. Lieb, Butler University, private communication.

4. Derome, A. E. "Modern NMR Techniques for Chemistry Research" Pergamon Press, New York, 1987.

5. Eich, G. ;Bodenhausen, G.; Ernst,R.R. " Coherence Transfer by Isotropic Mixing: Application to Proton Correlation Spectroscopy" *J. Am. Chem. Soc.* **1982**, 104, 3731.

6. States, D.J.; Haberkorn, R.A.; Rubin,D.J. " A Two-Dimensional Nuclear Overhauser Experiment with Pure Absorption Phase in Four Quadrants" *J. Magn. Reson.*, **1982**, 48, 286-292.

7. Bax, A.; Davis, D.G. " Practical Aspects of Two-Dimensional Transverse NOE Spectroscopy" *J. Magn. Reson.*, **1985**,63, 207-213 .

8. Bothern-By, A.A.; Stephens, R. L.; Lee, J." Structure Determination of a Tetrasacahride: Transient Nuclear Overhauser Effect in the Rotating Frame" *J. Am. Chem. Soc.* **1984**,106, 811-813.

9. Kessler, H.: Gehrke, M.; Griesinger, C. "Two-Dimensional NMR Spectroscopy: Background and Overview of the Experiments" *Angew. Chem. Int. Ed. Engl.* , **1988**, 27, 490-536.

10. Bull, T. E. "ROESY Relaxation Theory" *J. Magn. Reson.* **1988**, 80, 470-481.

The Structure and Conformation of 4-Hydroxyphenyl Terephthalate: A Model Compound for a Liquid Crystalline Polyester.

Debbie B. Saebø, Philip B. Oldham, and Svein Saebø[*]

Department of Chemistry

Mississippi State University

Mississippi State, Mississippi 39762

USA

[*] Corresponding author

ABSTRACT

A theoretical analysis using ab initio calculations of the possible conformations of 4-hydroxyphenyl terephthalate which represents the repeat unit for poly(p-phenylene terephthalate) is reported. The study includes complete geometry optimizations and calculation of vibrational frequencies at the SCF/STO-3G level of 10 distinct stationary points on the molecular potential surface. The calculations show that both the terephthalic and the hydroquinone fragments of the system prefer planar conformations. For the entire molecule the low energy form is a twisted conformation where the hydroquinone part is twisted by about 65 degrees relative to the terephthalic part of the molecule. The barrier to internal rotation around the ester bond is about 2 kcal/mole.

INTRODUCTION

The aromatic copolyesters of terephthalic acid and substituted hydroquinones (Figure 1) all exist as liquid crystals where their transitions from the crystal to nematic phase occurs around 300 °C. At room-temperature they are solids with remarkable physical properties. These properties make them attractive engineering plastics or high strength fibers. Characteristic properties of this group of polyesters are high tensile strength, high thermal stability, and high crystal to nematic transition temperatures. The materials can be injection molded and due to their physical properties and light weights the United States Air force has considered using these materials in engine parts and rocket nossels [1]. The polymers are also easy to synthesize through a reaction between the appropriate hydroquinone derivative and the acid chloride of terephthalic acid in aqueous solution. When the polymers are produced this way the number of repeat units is small. All experimental studies [2,3] indicate that the number of repeat units in these polymers is between 4 and 7, - a remarkably low number considering their physical properties. Besides the ongoing investigations carried out with support from the US Air Force, no experimental study of 4-hydroxyphenyl terephthalate (HPT) or poly(p-phenylene terephthalate) have been reported. A molecular dynamics simulation of long chains of poly(p-phenylene terephthalate) [4] is to our knowledge the only theoretical study that has been reported in the literature.

Clearly, the conformation relative to the ester bonds is important for the shape and ultimately the physical properties of the polymers. We have therefore carried out *ab initio* studies of the repeat unit of the simplest of these polyesters, 4-hydroxyphenyl terephthalate. It has been suggested that the fluctuations of the torsional angle about the ester bond should be treated as an intrinsic property that determines the stiffness or the flexibility of a polymer chain [4]. The goal of the present study was to determine the

geometries and relative energies of all conformers as well as the barriers to inter conversion between conformers.

COMPUTATIONAL DETAILS

All geometries were completely optimized at the SCF/STO-3G [5] level using the *ab initio* gradient program TX90 written by Pulay and coworkers [6]. A large number of stationary points were detected, and in order to characterize the stationary points as minima, saddle points or higher order saddle points, vibrational frequencies were calculated with the same basis set for all optimized structures. For the calculations of vibrational frequencies the Gaussian-90 program [7] was used. As a final check that all local minima were detected we carried out geometry optimizations starting at each saddle point distorted slightly in both positive and negative directions along the internal coordinate with the negative force constant.

For molecules of this size (29 atoms and 81 internal degrees of freedom) an efficient set of internal coordinates is required to reach convergence in a reasonable number of force relaxation steps. A recipe for constructing efficient internal coordinates was reported by Pulay et al [8] more than a decade ago. However, these coordinates have not been widely used mainly because their construction was relatively tedious. Recently, the construction of these internal coordinates has been made automatic as part of the TX90 program [6], and geometry optimization of molecules 30 atoms or more can now be routinely carried out, and if the DIIS procedure is used [9], the geometries normally converge in about 10 steps.

Most of the calculations were carried out of Mississippi State University's two SUN 490 systems, and the Department of Chemistry's IRIS Crimson Computer. The vibrational frequency calculations were performed on the Cray-XMP 2-16 at Mississippi

Center for Supercomputing Research. On the SUN-490 optimization of one structure required roughly 50 hours of CPU-time.

RESULTS AND DISCUSSION

As expected the potential surface for 4-hydroxyphenyl terephthalate (HPT) has a large number of stationary points. Many of these forms are only distinguished by the orientation of the hydroxyl groups on the hydroquinone end of the molecule and the acid group on the terephthaloyl end of the system. The small energy differences between these forms are probably of no significance for the shape of the polymer, however, we report here a complete description of the potential surface.

A large number of geometry optimizations from many different start geometries were performed. Based on these calculations we can conclude that the terephthalic acid fragment of the molecule is rather rigid and a planar conformation was always preferred for this part of the molecule. The terminal acid and hydroxyl groups always prefer conformations co-planar with the adjacent phenyl rings. Internal rotation around the (phenyl)C-O ester bond takes place relatively unhindered, and the conformation relative to this bond is also essential for the shape of the polymer of HPT. The presentation of the results below will therefore focus on the conformation relative to the ester bond.

In order to describe all local minima in terms of the (phenyl)C-O dihedral angle, two distinct potential surfaces, distinguished by the orientation of the terminal acid group, are required. As mentioned the terephthoyl part of the molecule remains planar in all conformations and all forms of the system is oriented with the ester carbonyl pointing up. We can describe the various forms of this system by two distinct potential surfaces, one for the "up" form, HPT(u), and one for the "down" form, HPT(d), with the hydroxyl group of the terminal acid group pointing up and down, respectively. Furthermore, the torsional angle with respect to the C-O ester bond is defined as zero when the system is

planar and the hydroxyl group of the hydroquinone end is pointing up. Thus, for the HPT(u) surface the τ=0 form is labeled HPT(uu) (Figure 4), where the first u refers to the hydroquinone hydroxyl being up and the second to the acid hydroxyl group being up. After rotation by 180 degrees another planar form labeled HPT(du) (Figure 8) is obtained. In an analogous manner the HPT(ud) (Figure 9)and HPT(dd) (Figure 13) correspond to τ=0 and τ=180 degrees, respectively.

Table 1 and Table 2 show the total energies and relative energies for different torsional angles for the HPT(u), and HPT(d) surface, respectively. Plots of the energy surfaces for internal rotation around the ester bond are shown in Figure 3 (for HPT(u)) and Figure 4 (for HPT(d)). This study includes full geometry optimization of 10 distinct forms of the molecule 4 minima and 6 transition states. The optimized bond lengths and bond angles are shown on Figure 4- Figure 13. The calculated vibrational frequencies are not included in this communication. These were calculated for the purpose of characterization of the stationary points, and with the computational level used (SCF/STO-3G) accurate prediction of vibrational frequencies are not expected.

Considering the HPT(u) potential surface, the planar form HPT(uu) with τ=0 is the transition state for the interconversion between two equivalent minima, labeled HPT(uum) with τ=±65°. The other planar form, HPT(du), with τ=180° is the transition state for the interconversion between an other set of equivalent minima, labeled HPT(dum) with torsional angles τ=113°and 243 (180 ± 66), respectively. Finally, the two distinct minima, HPT(uum) and HPT(dum), are separated by a perpendicular transition state, labeled HPT(90u). This form lies only a tenth of a kcal above the minima which have virtually equal energies about 2 kcal/mol below the two planar transition states. The HPT(d) potential surface(Figure 4) is virtually identical to the HPT(u) surface (Figure 3) thus the realtioships between the stationary points for this surface should be evident from the discussion above.

No attempts were made to locate the transition state(s) connecting the HPT(u) and HPT(d) surfaces. For a given torsional angle τ, the two surfaces are related through a rotation by 180 degrees of the terminal acid group. For terephthalic acid the barrier to internal rotation of one of the terminal acid groups is 3.2 kcal/mole as calculated at the SCF/STO-3G level of theory.

The only significant geometry changes of 4-Hydroxyphenyl Terephthalate upon internal rotation around the ester bond are the bond lengths and angles of the ester linkage and its immediate surroundings. The shortening of the two C-O single bonds observed when the molecule is forced to have planar geometries can be explained by increased cojugation. The angular distortions for the planar conformations are even more noticable. The O=C-O angle is 2-3 degrees larger, the (carbonyl)C-O-C(phenyl) angle about 5 degrees larger and one of the C(phenyl)-C(phenyl)-O angle almost 6 degrees larger in the planar conformation compared to any of the twisted minima. This is a manifestation of the repulsion between the cartbonyl oxygen and the phenyl hydrogen in the ortho position of the neighboring hydroquinone-ring.

Even though conjugation would favour the planar forms this molecule prefers a twisted conformation to avoid the steric repulsion between the carbonyl oxygen lone pairs and a hydrogen on the hydroquinone ring (see f. example Figure 5). In spite of the relatively large distortions of the angles the O..H nonbonded distance is only about 2.1A in the planar forms.

CONCLUDING REMARKS

A conformational analysis of 4-Hydroxyphenyl Terephthalate has been carried out using ab initio calculations at the HF/STO-3G level of theory. The molecule prefers a conformations where the hydroquinone ring is twisted relative to the rigid terephthalic

acid part of the molecule. In the most stable form the torsional angle is about 66 degrees, however, all conformations with torsional angles in the range 90 ± 25 degrees have virtually the same energy. One of the goals of the present study was to elucidate the structure of poly(p-phenylene terephthalate) and related polymers. Our theoretical study suggests that the secondary structure of the polymer is a form where the hydroquinone ring and the terephthalic acid fragement in each repeat unit are near perpendicular. This is consistent with a helical tertiary structure of strand of the polymer, however, more random shapes can not be excluded.

REFERENCES

1   Advanced Polymer Component Symposium, Butler University 1992.

2   D. B. Saebø and P. B. Oldham, Department of Chemistry, Mississippi State University, unpublished IR, fluorescence, and NMR studies

3   S. Lieb, Butler University, private communication

4   M. Depner and B. L. Schurmann, Polymer 33 (1992), 398

5   STO-3G basis

6   TX90

7   Gaussian 90

8   P. Pulay, Pang, Boggs in JACS ~1982

9   P Pulay DIIS

Table 1. Total Energies (in Hartrees) and Relative Energies (in kcal/mole) for the HPT(u) Potential Surface (see text).

Label[a]	τ[b]	Total Energy	ΔE[c]	Type[d]
uu	0	-898.668502	1.95	TS
uum	65.0	-898.671610	0.0	M
90u	92.1	-898.671423	0.12	TS
dum	113.4	-898.671583	0.0	M
du	180.0	-898.668243	2.11	TS

[a]See text for explanation. [b](phenyl)C-(phenyl)C-O-C dihedral angle. [c]Relative to the low energy form (uum). [d]Classification of the stationary point based one vibrational analysis, M- minimum, TS- transition state.

Table 2. Total energies (in Hartrees) and relative energies (in kcal/mole) for the HPT(d) potential surface (see text).

Label[a]	τ[b]	Total Energy	ΔE[c]	Type[d]
ud	0	-898.668495	1.95	TS
udm	65.5	-898.671601	0.0	M
90d	92.1	-898.671419	0.11	TS
ddm	113.5	-898.671569	0.02	M
dd	180.0	-898.668222	2.12	TS

[a]See text for explanation. [b](phenyl)C-(phenyl)C-O-C dihedral angle. [c]Relative to the low energy form (uum). [d]Classification of the stationary point based one vibrational analysis, M- minimum, TS- transition state.

Figure 1. The structure of the aromatic liquid crystalline copolyesters.

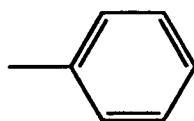$$R \quad = \quad \text{—H}$$

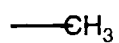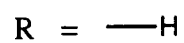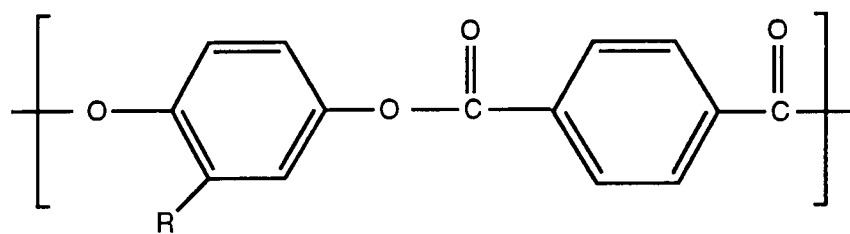—CH$_3$

—Cl

—⬡

—CH$_2$CH$_2$—⬡
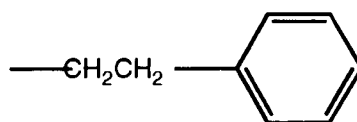
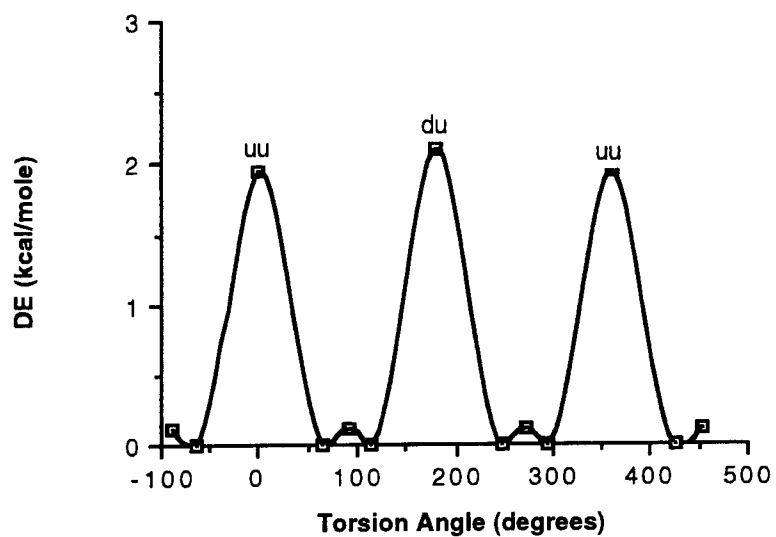Figure 2.   4-Hydroxyphenyl Terephthalate HPT(u) Potential Surface.

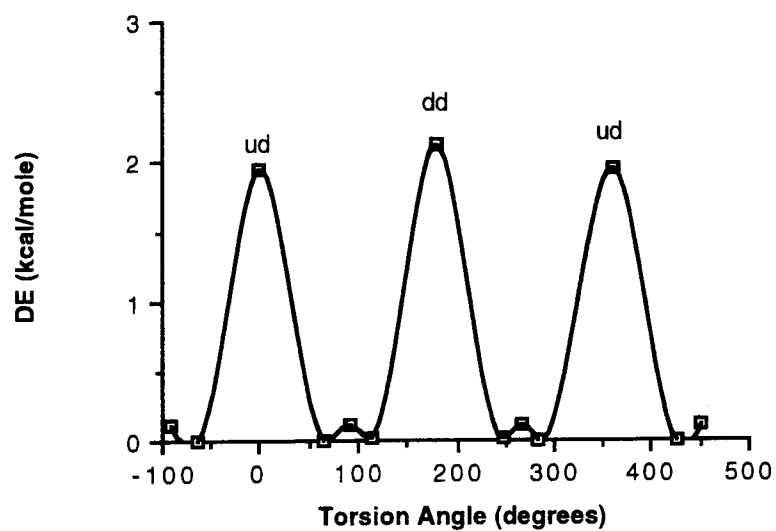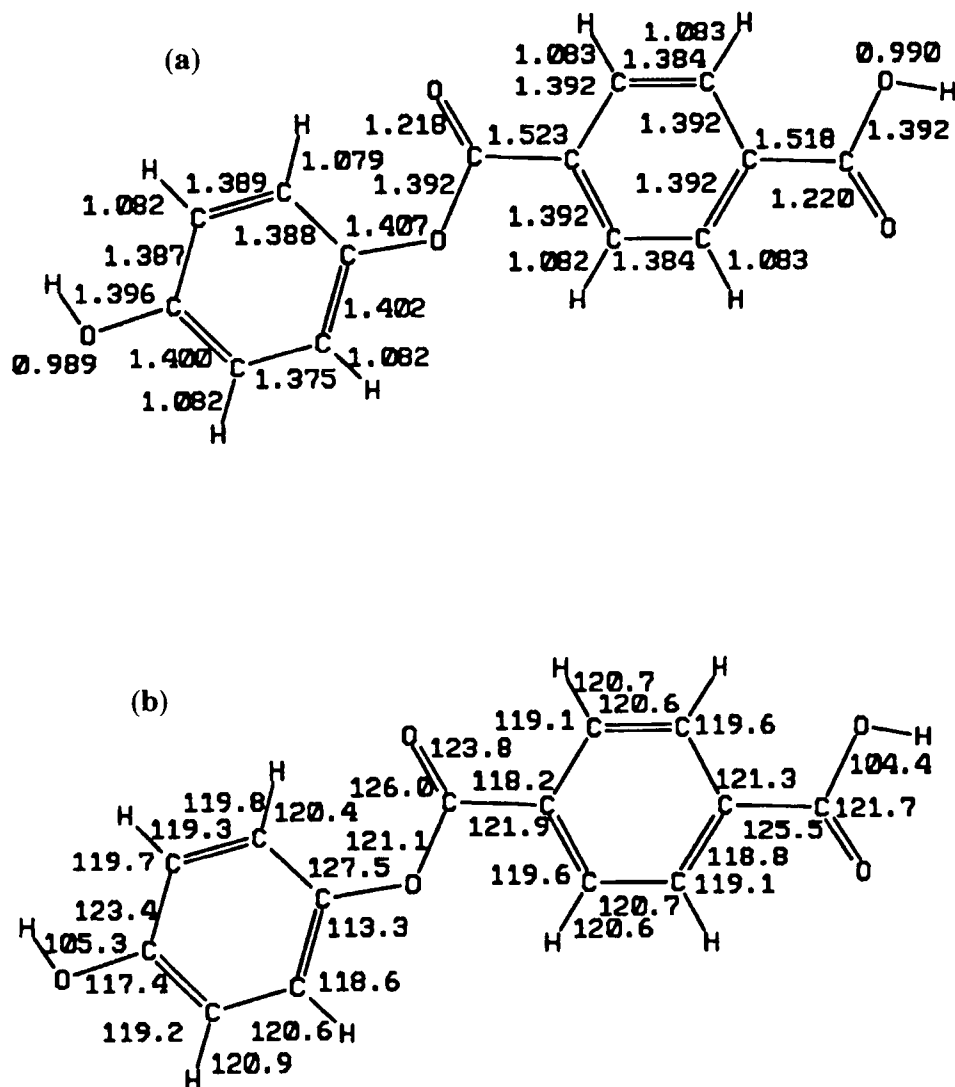Figure 3.   4-Hydroxyphenyl Terephthalate HPT(d) Potential Surface.

Figure 4. Optimized Geometry for the Planar uu-form (see text) of 4-Hydroxyphenyl Terephthalate. (a) Bond Lengths in Angstroms. (b) Angles in Degrees. The uu-form is a Transition State on the Molecular Potential Surface. The Torsion Angle $\tau = 0$ (see text).
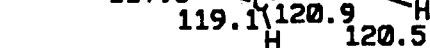
Figure 5. Optimized Geometry for the uum-Form (see text) of 4-Hydroxyphenyl Terephthalate. (a) Bond Lengths in Angstroms. (b) Angles in degrees. The uum-Form is the Global Minimum on the Molecular Potential Surface. The Torsion Angle τ= 65° (see text).

Figure 6. Optimized geometry for the 90u-Form (see text) of 4-Hydroxyphenyl Terephthalate. (a) Bond length in Angstroms. (b) Angles in degrees. The 90u-Form is a Transition State on the Molecular Potential Surface. The Torsion Angle $\tau=90^\circ$ (see text).
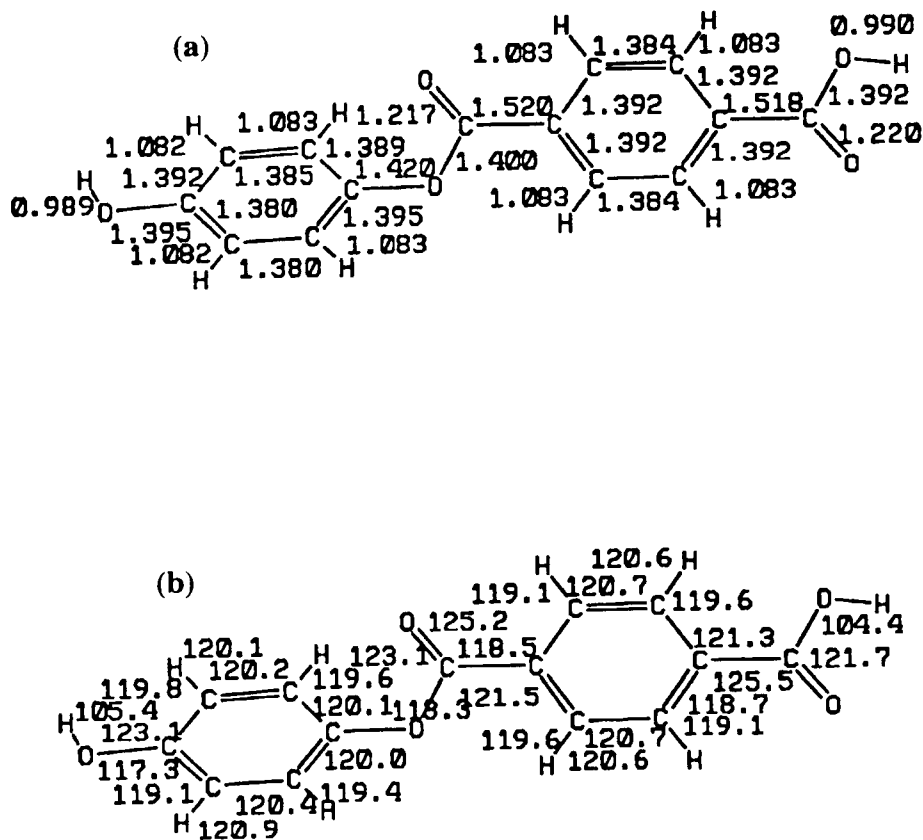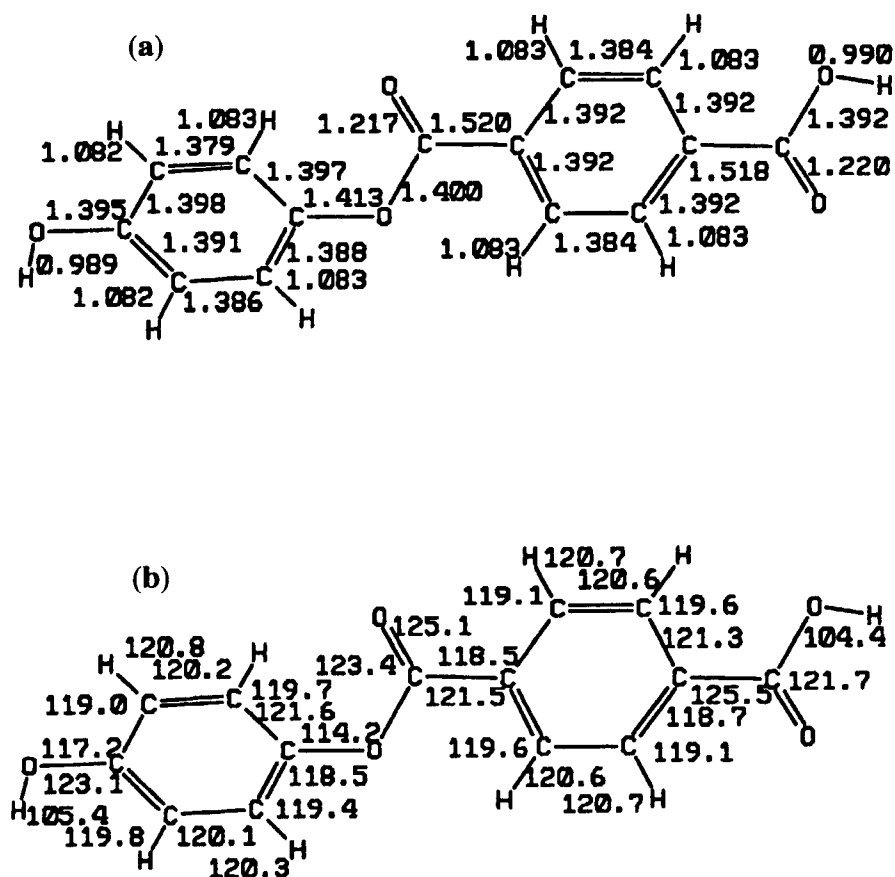
(a)

(b)

Figure 7. Optimized geometry for the dum-Form (see text) of 4-Hydroxyphenyl Terephthalate. (a) Bond length in Angstroms. (b) Angles in degrees. The dum-Form is a Local Minimum on the Molecular Potential Surface. The Torsion Angle τ=113.4° (see text).

Figure 8. Optimized Geometry for the du-Form (see text) of 4-Hydroxyphenyl Terephthalate. (a) Bond Lengths in Angstroms. (b) Angles in Degrees. The du-Form is a Transition State on the Molecular Potential Surface. The Torsion Angle $\tau=180^\circ$ (see text).
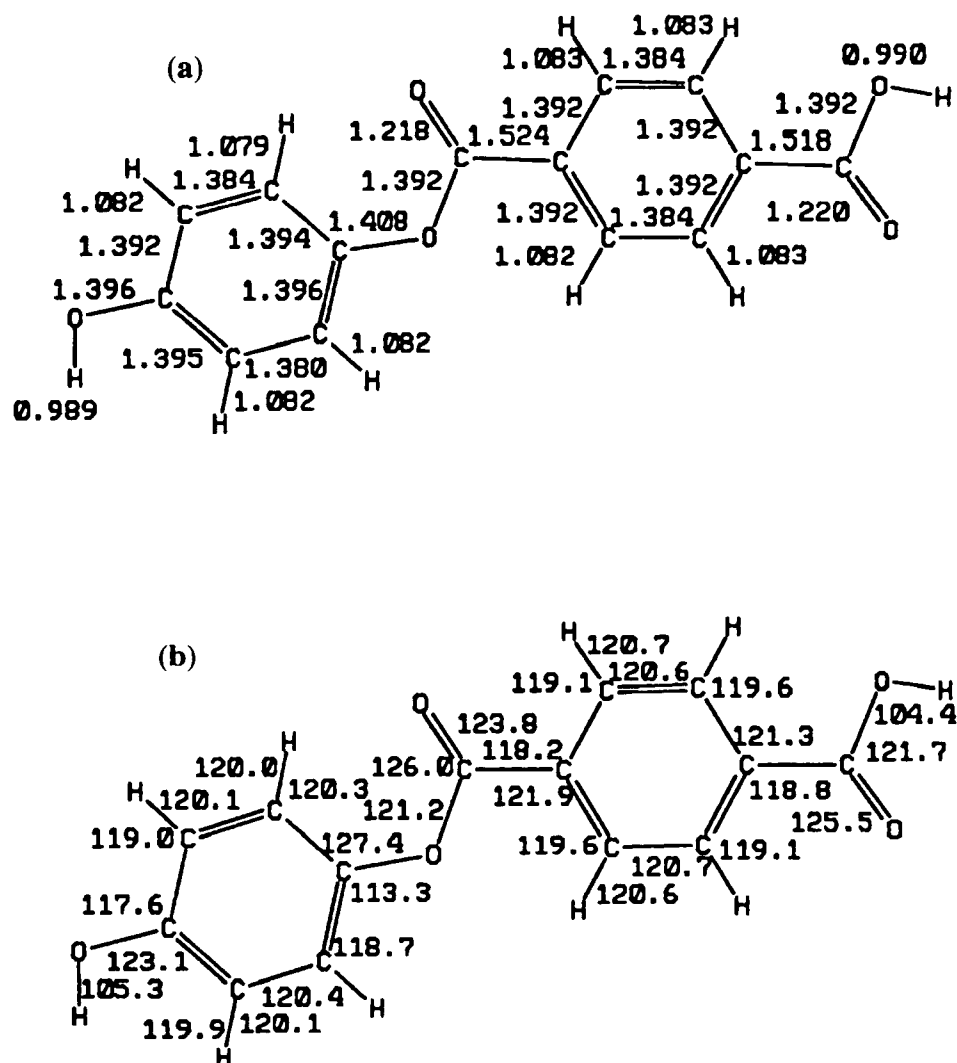
Figure 9. Optimized Geometry for the ud-Form (see text) of 4-Hydroxyphenyl Terephthalate. (a) Bond Lengths in Angstroms. (b) Angles in Degrees. The ud-Form is a Transition State on the Molecular Potential Surface. The Torsion Angle τ=0° (see text).
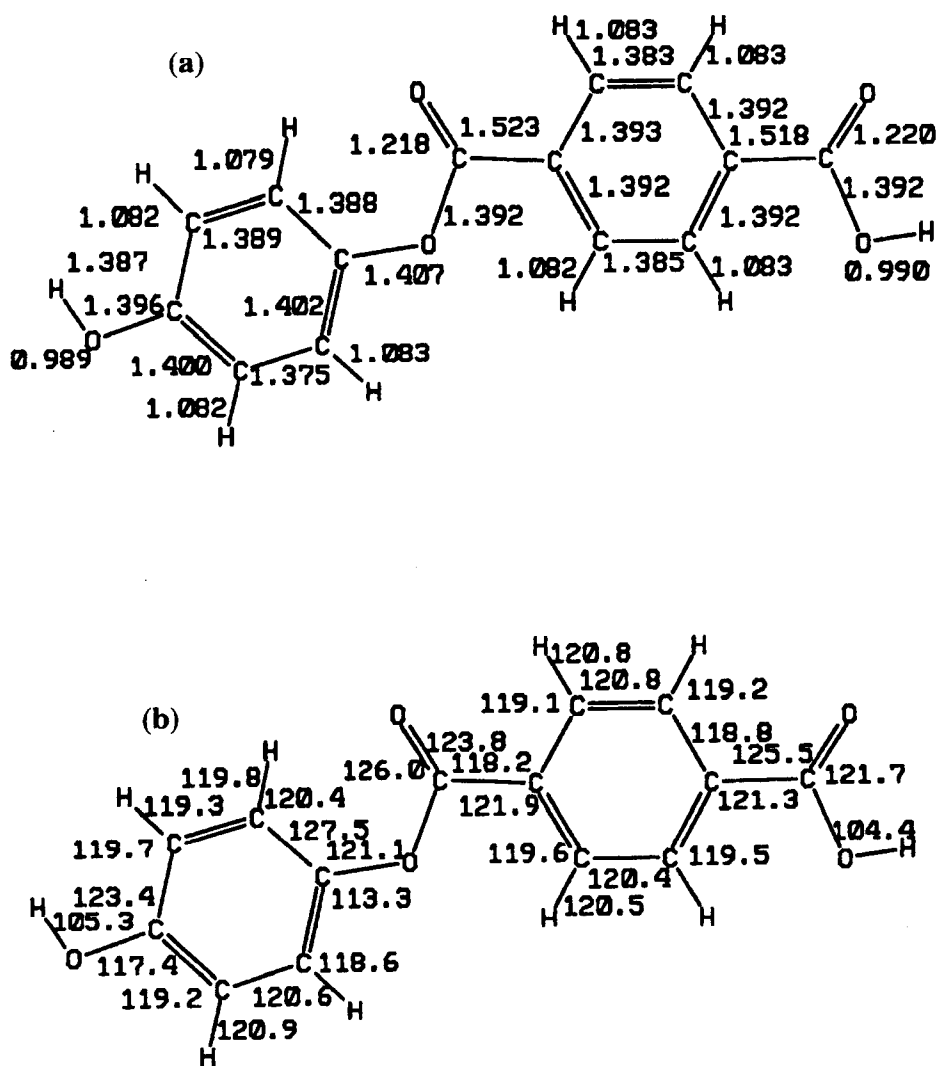
Figure 10. Optimized Geometry for the udm-Form (see text) of 4-Hydroxyphenyl Terephthalate. (a) Bond length in Angstroms. (b) Angles in Degrees. The udm-Form is a Local Minimum on the Molecular Potential Surface. The torsion angle $\tau=65.5^{\circ}$ (see text).
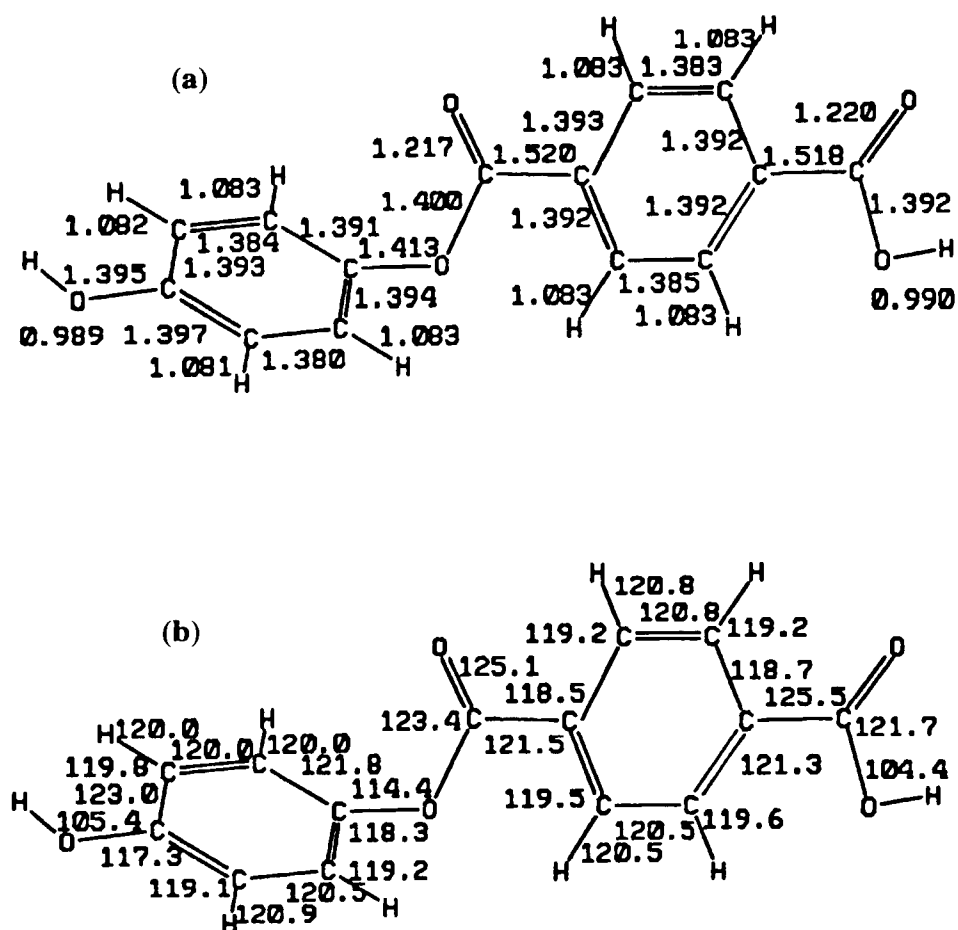
Figure 11. Optimized Geometry for the 90d-Form (see text) of 4-Hydroxyphenyl Terephthalate. (a) Bond lengths in Angstroms. (b) Angles in Degrees. The 90d-Form is a Transition State on the Molecular Potential Surface. The Torsion Angle τ=90° (see text).

Figure 12. Optimized Geometry for the ddm-Form (see text) of 4-Hydroxyphenyl Terephthalate. (a) Bond lengths in Angstroms. (b) Angles in Degrees. The ddm-Form is a Local Minimum on the Molecular Potential Surface. The Torsion Angle τ=113.5° (see text).
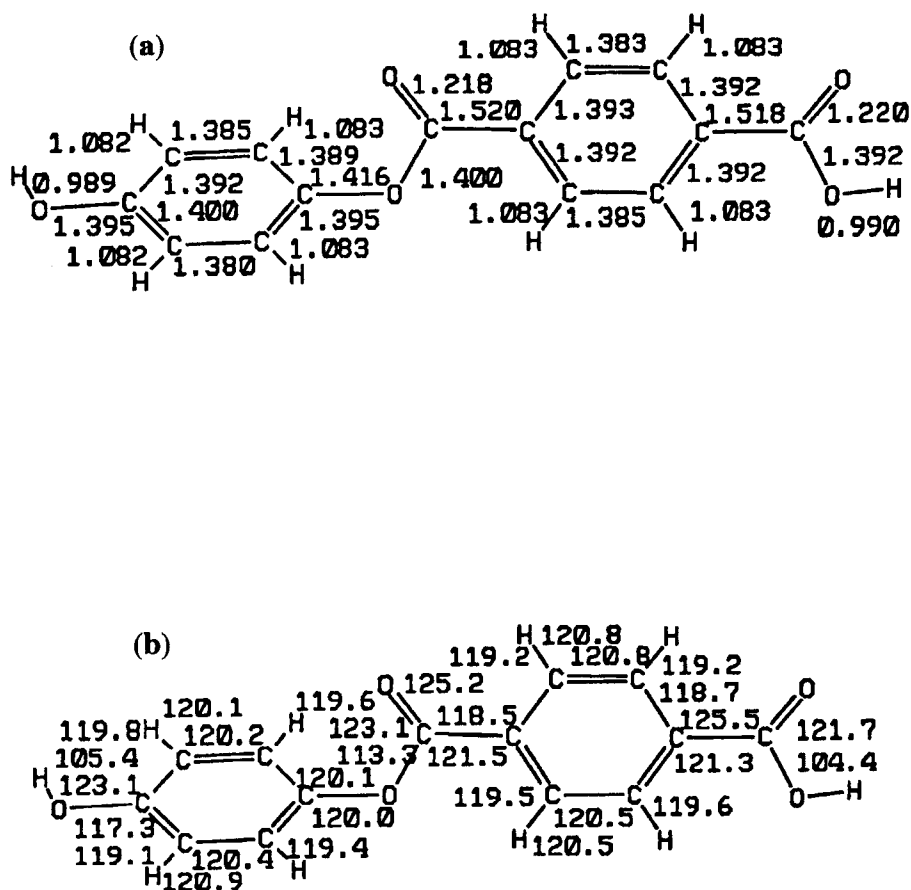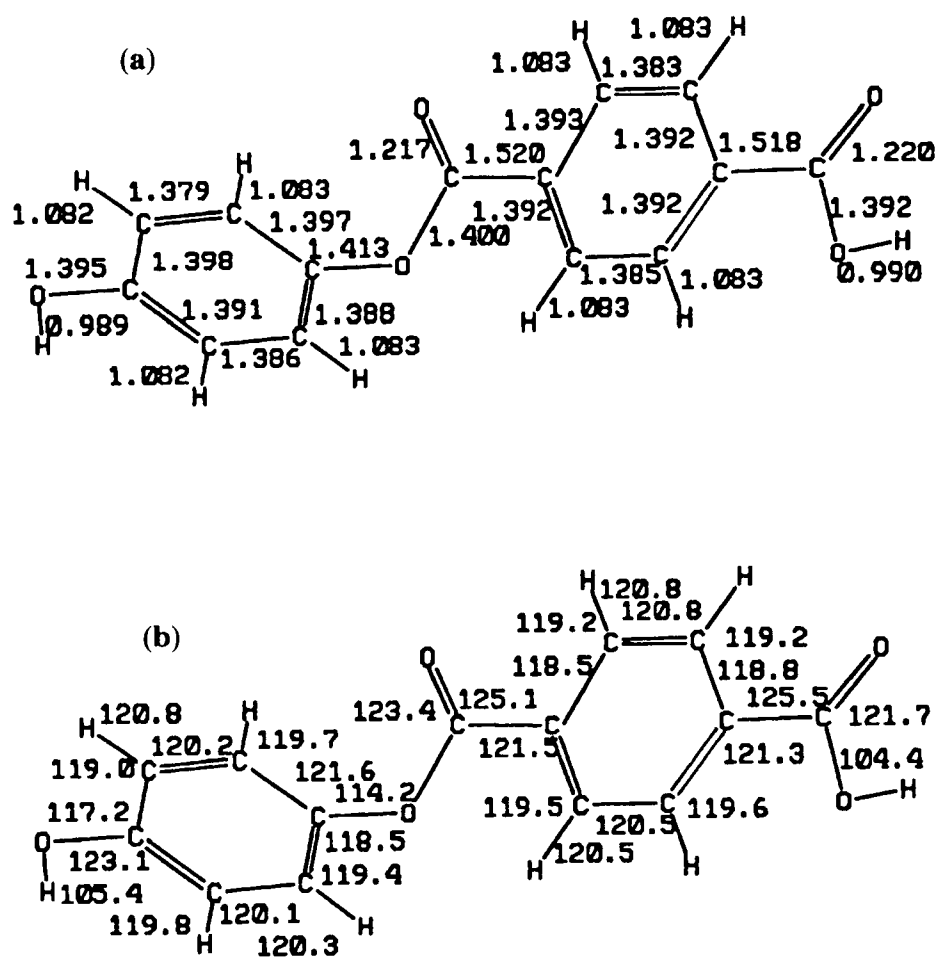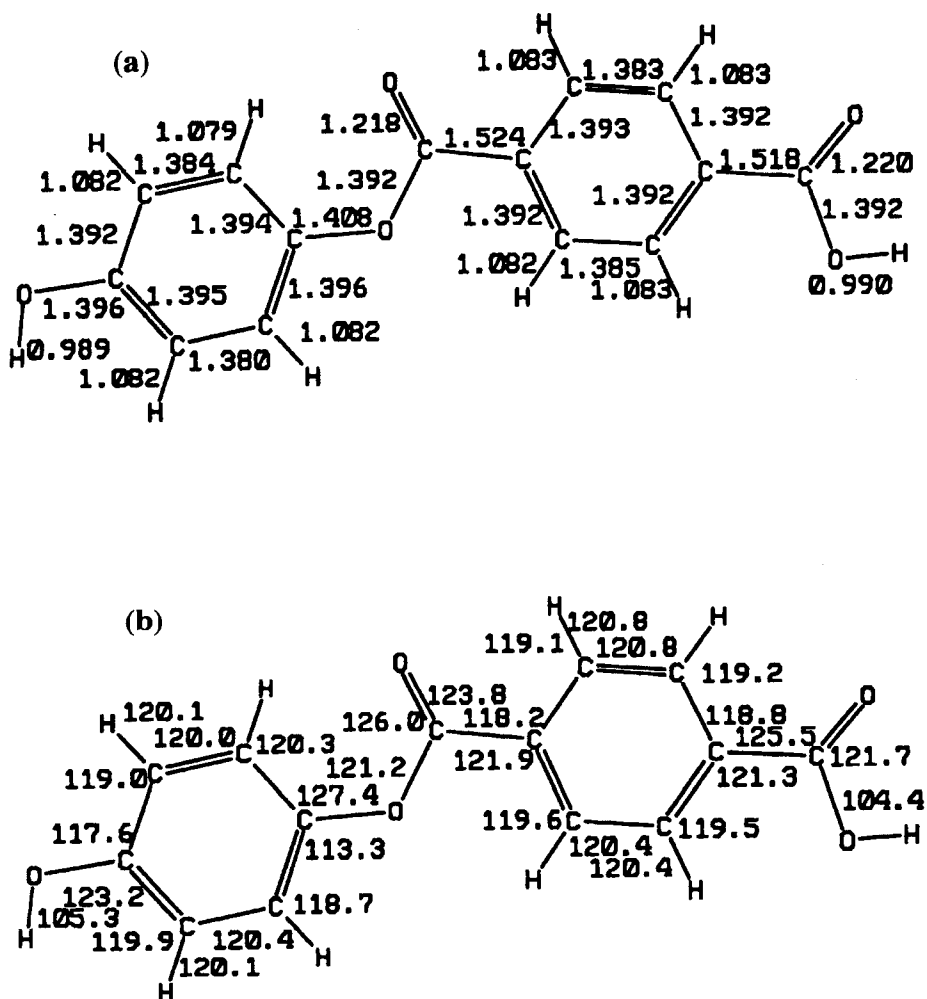
Figure 13. Optimized Geometry for the dd-Form (see text) of 4-Hydroxyphenyl Terephthalate. (a) Bond Lengths in Angstroms. (b) Angles in Degrees. The dd-Form is a Transition State on the Molecular Potential Surface. The Torsion Angle $\tau=180^\circ$ (see text).

Thermotropic Polymers; Theory and Experiment

Dr. Shannon G. Lieb
Butler University
Indianapolis, IN 46208

Abstract

The approach of this research group which has included seven undergraduates in the past two years has been an effort to integrate theory and experiment for the mutual benefit of both. The specific objective in this project has been to characterize the "annealing" of some polyesters formed by the condensation of terphthaloyl chloride with a monosubstituted hydroquinone. The annealing phenomenon manifests itself as a thermosetting plastic which has a rather high decomposition temperature and forms a "skin" which is quite resistant to chemical attack. The annealed polyester with the most stability is displayed by the phenethyl substituent on the hydroquinone. This particular piece of information is quite suggestive of a phase change accompanied by a reorganization of the phenethyl groups into a favorable interlocking arrangement with neighboring chains. As has already been established by X-ray diffraction studies of solid benzene, the most favorable energetic arrangement for benzene is a T-shaped structure (i.e., a configuration in which the plane of one ring is orthogonal to the plane of neighboring ones). This has also been demonstrated in dimer formation found in molecular jets. The nature of this stability is most definitely associated with electrostatic attractions. Whether this is ascribed to partial charge redistribution or electrostatic multipole interactions between benzenes is not as important as the assessment of the magnitude of many cross-linking interactions of this type between polymer chains. Offsetting this energetic stability is the decrease in entropy accompanying this order/disorder transition. The complete analysis of this problem lies in the computation of the Free Energy of this process.

This project has taken on several directions in order to characterize this problem. There are ongoing projects in synthesis, kinetic modeling, Fourier Transform Infrared (FTIR) spectroscopy and molecular dynamics calculations. These are all pursued with the purpose of developing a complete picture of this problem. The synthesis projects were initially aimed at producing enough polymer to spectroscopically characterize the polymer's average length. The current method of producing the polyester requires dry box procedures and the combining of two subunits to form the polymer. This introduces three problems: (1) the difficulty in maintaining a dry enough environment so as to avoid contamination with unreactive terphthalic acid, (2) the difficulty in precisely controlling stoichiometry so as to have one end of the polymer as an acid functional group and the other an alcohol functional group and (3) the complete lack of stereo regularity in the pendant side groups (i.e., only atactic polymers can be generated with the current synthesis route). There are preliminary steps at synthesis of a "true" monomer unit which will allow the synthesis of a polymer which will be

stereo regular (isotatic) with one end of the polymer always being an acid functional group and possibly the process can be carried out without regard to moisture. The FTIR studies have proven to be quite useful in the determination of the average (number average) length of the polymer, but the prerequisite to accurate analysis is to be certain of the number of ester carbonyls relative to the number of acid carbonyls. Under the current method of synthesis either there should be stoichiometric amounts of the alcohol and acid or an excess of acid to assure that the average number of terminating acid functional groups is either one or two. The infrared bands of the ester and acid carbonyls are distinguishable in the solid infrared spectra of these compounds (either KBr pellets or diffuse reflectance). The different bands have been assigned and band fitted to allow the relative amounts of acid to ester carbonyl concentrations to be determined. A correction for the differences in the relative intensities of these bands has been investigated as well. In addition to the average length of the polymer, one can infer the polymer length distribution function by introducing reasonably simplifying assumptions in the kinetics of polymer formation and solving the coupled differential equations using standard methods that are easily programmed on a Macintosh (with suitable FORTRAN compiler). One particularly simplifying discovery resulting from the FTIR work was that the average polymer is about 15 units long (an oligomer). With this spectroscopic piece of evidence and a development of a "complete" model for the kinetics of this polymerization, one can deduce the polymer length distribution function. All of these inputs combined with an accurate description of the oligomer in terms of the intermolecular potentials, the most stable conformations, radius of gyration, etc. are needed to generate a molecular mechanics description of the annealing phenomenon. The programs CHARMm and CERIUS are being employed currently to build a model of the molecular state which is large enough to infer bulk property behavior. Since the electrostatics of this interaction are believed to be most important in discerning the feasibility of the "interlocking chains" hypothesis, a theoretical development of a scheme which will allow a reasonable estimate of the energetics of this interaction is underway.

Introduction

The problem of characterizing polymer behavior of bulk properties as inferred from molecular level interactions requires an enormous distillation of information. The opposite approach of inferring the molecular level interactions from bulk properties of polymers is fraught with as many difficulties. It is apparent that molecular problems of this size require both approaches to build a bridge of understanding that links the observable (bulk) properties to the molecular properties. Polymer systems go well beyond the *ab initio* Quantum Mechanical computational approach to solution. That is not to say that *ab initio* calculations are not needed in the basis of the search for such links, but in the final analysis one must somehow envision and compute the properties of a large ensemble of atoms; i.e., a cluster of polymer

chains whose collective interactions mimic essential characteristics of the bulk properties observed for this particular chemical system. In the past 15 years much work has been accomplished in this area for biopolymers. In part, this is due to the acceptance and support received by computational chemists in the pharmaceutical industry. Funding has been sufficient to support this work, as well as, the rapidly advancing development of bigger and faster computers. The graphics workstation provides a powerful interface between supercomputers and the researcher, as well as, a powerful stand-alone tool in its own right. The graphics themselves provide an essential, alternative method of displaying the results of an equilibrium or dynamic calculation.

The calculations that can be performed on these large molecular systems are referred to as molecular mechanics. Molecular mechanics differs from quantum mechanics in that the intra and intermolecular potentials are treated in a Newtonian mechanics fashion. The potentials are quantum mechanical in origin, but no quantization of energy states are introduced. In order to create an equilibrium state, one must minimize the forces which are parameterized by bonding and non-bonding types of interactions. The dynamic simulations are created through integration of Newton's equations of motion. Essential to the program of molecular mechanics calculations are good estimates of the intra and intermolecular force field parameters. This is another point at which *ab initio* or semiempirical calculations provide useful input. The parameters are determined from model molecular systems and assumed to be transferable to other similar molecular systems. This approach is not novel, but rather an obvious extension of molecular model kits that have been popularized since the time of the construction of DNA by Watson and Crick using their own carefully constructed molecular models.

Even though molecular modeling (mechanics) is greatly enhanced by the use of a computer, the problems to which this technique is applied are enormous in terms of the number of possible equilibrium states and possible channels for dynamic state evolution. This requires a large investment of physical insight into a problem to help limit the possibilities of molecular interactions which are the essential ones in describing the bulk property observables. Along this line, there have been three other branches of investigation to bring together as much of the experimental information that can augment the theoretical development of this problem. Those experimental branches are: (1) synthesis, (2) Fourier Transform InfraRed (FTIR) spectroscopy and (3) kinetics simulations of polymer formation. These areas will be discussed and connected to the theoretical work
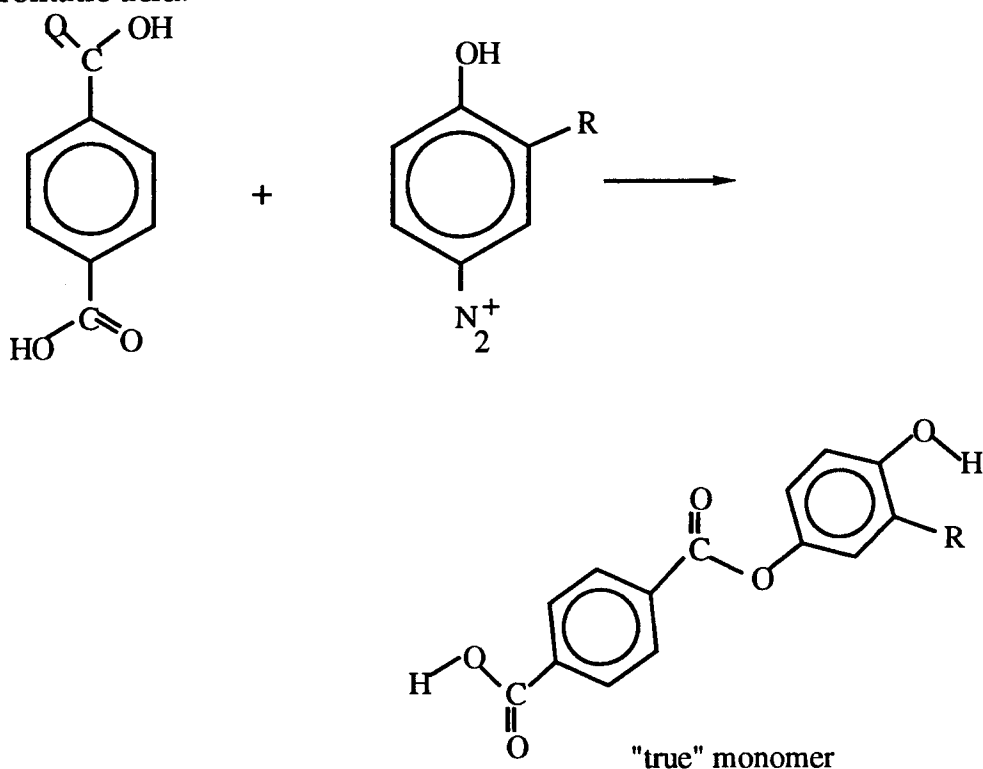
Synthesis

The synthesis of these compounds is indicated on the next page as a reaction between terphthoyl chloride and a monosubstituted hydroquinone. If the reaction is carried out with stoichiometric amounts of each of the reagents, the product will have two different terminal functional groups on the average. The location of the side chain on the hydroquinone will randomly vary along the backbone (an atactic stereochemistry). Several of

these polymers have been synthesized in which the R group is H, CH₃, t-butyl and chloro. During the course of this synthesis, several options have been
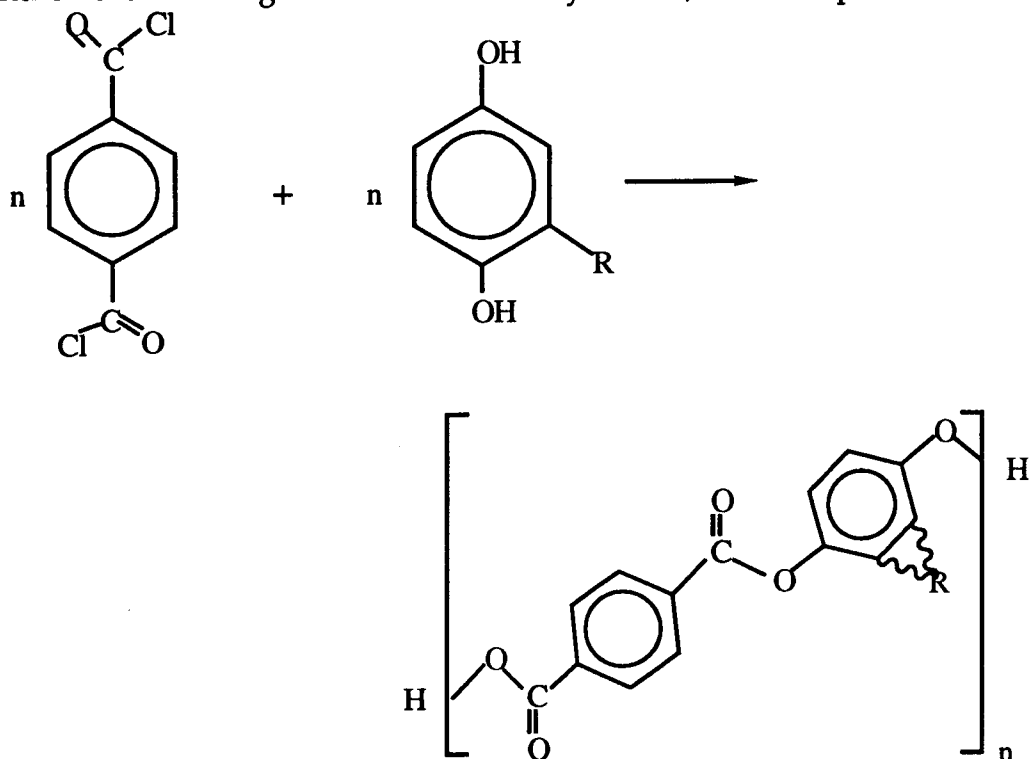

discussed. This synthesis needs to be carried out in a moisture free atmosphere so that the acid chloride does not revert to the unreactive aromatic acid.

"true" monomer

Although this can be accomplished with a bit of care, an alternate synthesis in which moisture would not be a factor has been considered. One method of generating the acid chloride in situ is the addition of thionyl chloride and a catalytic (10%) amount of dimethylformamide. This alternate method allows more flexibility in the synthesis of the "true" monomer. Since the aromatic acid group is relatively unreactive, it is protected until the step of polymerization. On the preceding page is a proposed synthesis of the true monomer. An acid plus the diazonium salt react to form the ester linkage. The advantage of this approach is two fold: (1) the reagents do not require special handling and are readily available and (2) the R-group can be made stereoregular (in this case isotactic). Stereoregular polymers are more crystalline and thereby have properties which are advantageous for particular applications.

If one is not wed to the notion that the bridging group of the monomer needs to be an ester, then several alternate synthetic pathways are suggested. One of these is the use of a diazo bridge which is relatively simple to make. Another advantage to the diazo compounds is that they are richly colored.
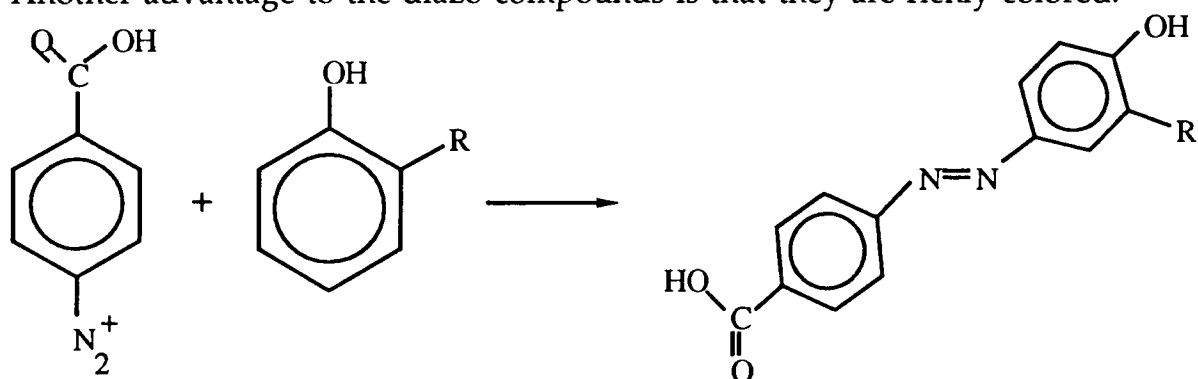
The synthesis of this type was accomplished. The material was a deep red and had a melting temperature above 200°C, but tended to decompose. A problem that arose was the insolubility of this compound in most solvents except acetone and aqueous acid solutions. In those solvents the compound was sparingly soluble. The limited solubility poses problems for polymerization of this monomer. As an alternative, a synthesis of the true monomer with a carbonyl bridging group is currently under investigation. The advantage sought here is the close similarity to the ester bridge and expected increased solubility in inert solvents such as chloroform or methylene chloride.
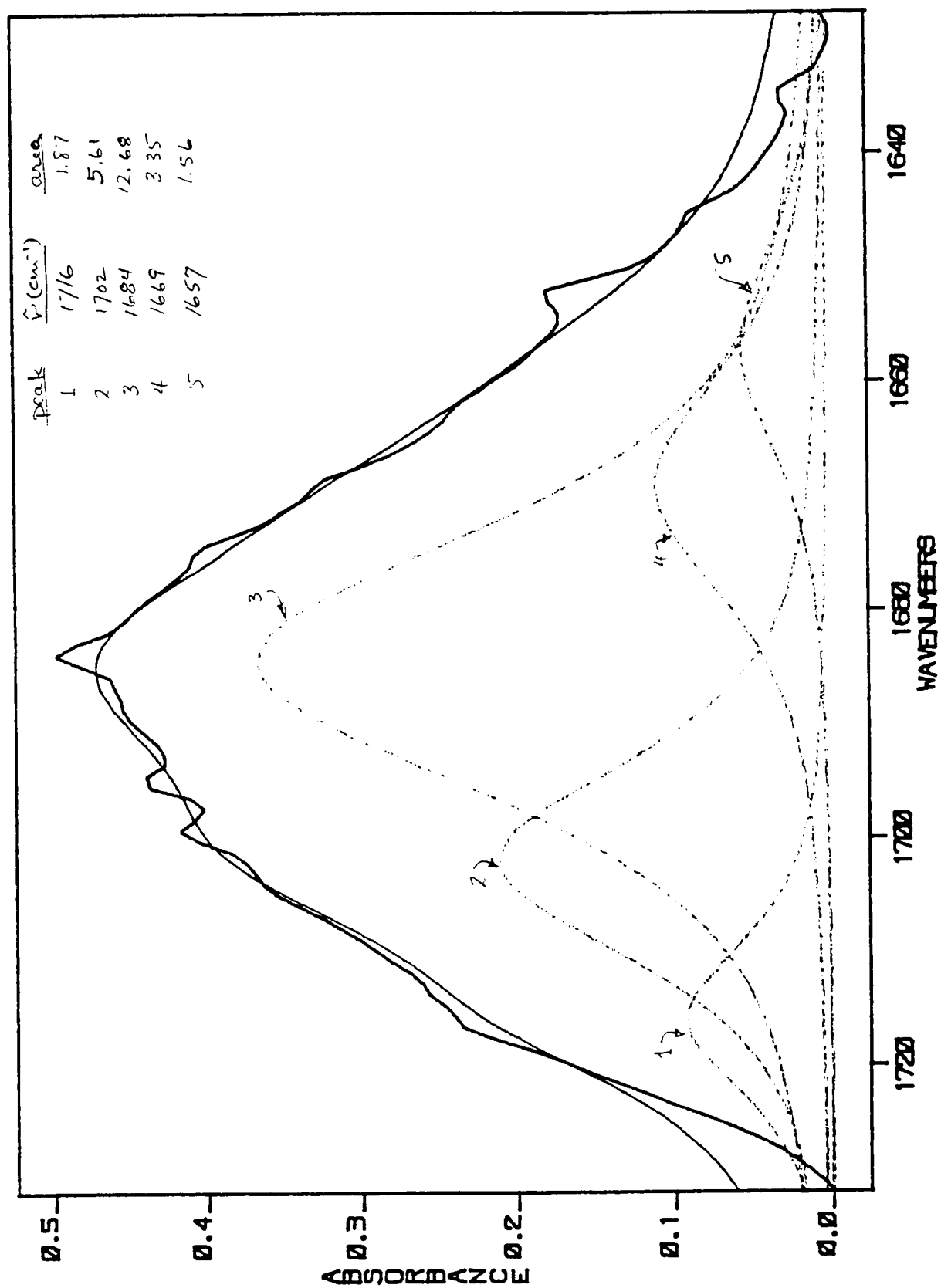
Spectroscopy

The spectroscopic analysis of the ester and acid carbonyl peaks in the polyesters can lead to the determination of the average degree of polymerization. To date only Granlar has been carefully studied using diffuse reflectance accessory in a Fourier Transform Infrared (FTIR) spectrometer. In order to assign infrared bands to the ester vs. acid carbonyl peaks, the prototypical molecules - benzoic acid and phenyl benzoate - were studied independently and then as a mixture. The independent spectra were produced to determine what Gaussian bands were essential to reproducing
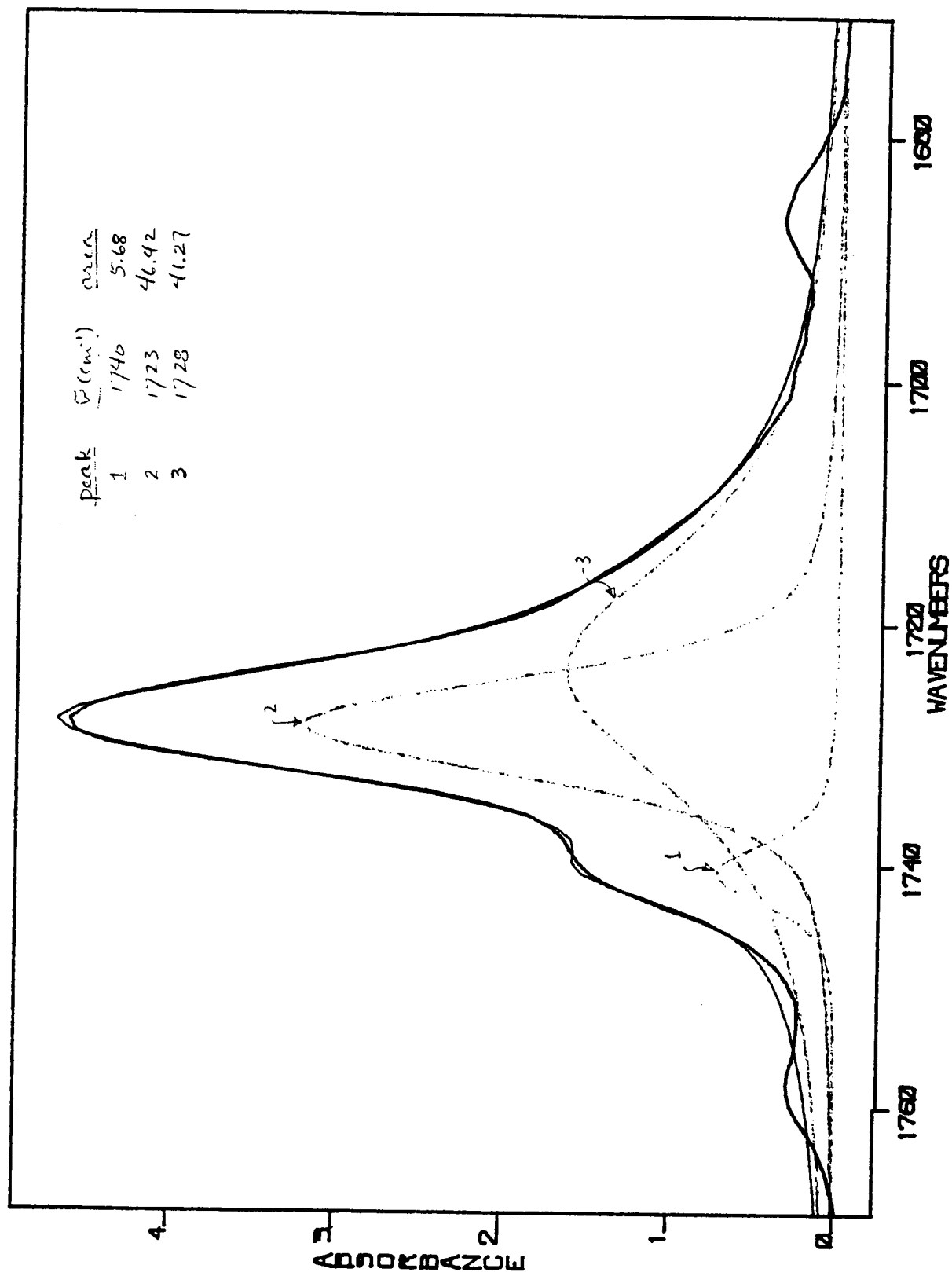
116

the carbonyl band shape for the acid and ester peaks. The pure benzoic acid peak is rather rough even after averaging for an extended period of time. The first attempt at fitting the spectrum is shown on the next page. There were five Gaussian bands placed under the experimental peak. The software with the instrumentation varies the Gaussian peak height, width and position to minimize the difference between the computed spectral envelope and the experimental peak. The smooth line running through the rather jagged line is the sum of the Gaussian peaks. The peak positions and areas are noted on the figure. The only two peaks of significance turn out to be the one at 1702 cm^{-1} and 1684 cm^{-1}. These peaks are in agreement with other solid infrared solid benzoic acid studies[1], which quote these positions as 1688 cm^{-1} and 1710 cm^{-1}. The latter peak is small but notable at room temperature. The phenyl benzoate experimental peak is fit with three peaks in the example shown and could just as well have been fit with the peaks labeled 1 and 2 on the figure. Eliminating peak 3 causes peak 2 to increase in size to pick up most of the area captured by peak 3. A stoichiometric (1:1) mixture of benzoic acid and phenyl benzoate were prepared several times to try to experimentally determine the relative intensities of the two different carbonyls. These different attempts lead to estimates of the ratio of the acid carbonyl intensity to ester carbonyl intensity from 1.5:1 to 4:1. The problem is clearly one of getting a homogeneous mixture of the benzoic acid with phenyl benzoate. To circumvent this problem, the absolute intensities were computed along with the harmonic frequencies of formic acid and methyl formate. The ab initio package, CADPAC, has this feature built into the functions it performs. The result of this calculation indicated that the acid to ester ratio was 1.3:1. This result was not sensitive to the basis set used as was the harmonic frequency calculation.

With the peak position and relative intensities in hand, the problem attacked was the determination of the average degree of polymerization. Granlar was the compound studied thus far. That spectrum is the third page of spectra and is labeled USAF Polymer Bandfit. The area under the curve is directly proportional to the number of absorbing species. The acid peak is located right near 1700 cm^{-1} and the ester peaks are located at 1736 and 1751 cm^{-1}. It is interesting to note that the ester band is somewhat mis-shapened indicating the presence of two bands. In the spectrum, one can see the overall band contour as a lighter line and the Gaussian bands that are used to reproduce that envelope are darker lines below the overall envelope. In this particular fit the ratio of the band areas is about 12.3:1 for the ester to acid area ratios. If one end cap of the polymer is an acid functional group and the other a hydroxy group, the degree of polymerization will be 2n-1:1 (where n = the average degree of polymerization). Based on that analysis the average degree of polymerization is 6.6 monomer units. This is a rather short average oligomer, but there are two effects that must be accounted for before any
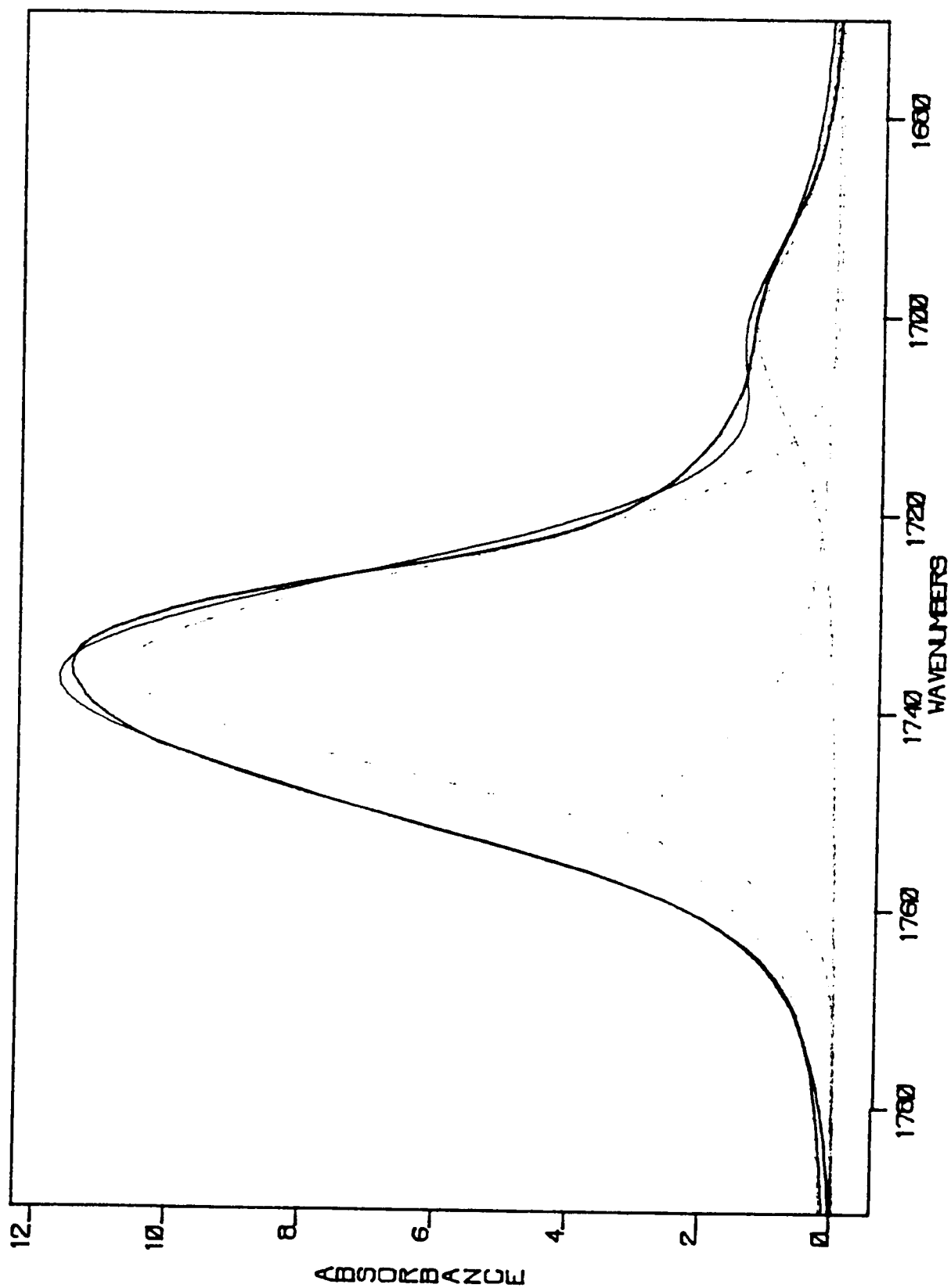
[1]S. Hayashi, M. Oobatake, R. Nakamura and K. Machida, "Interpretation for the anomaly of the C=O stretching band in benzoic acid crystal", J. Chem. Phys. 94, 4446 (1991).

| peak	$\hat{\nu}$ (cm^{-1})	area
1	1716	1.87
2	1702	5.61
3	1684	12.68
4	1669	3.35
5	1657	1.56

WAVENUMBERS

ABSORBANCE

— Benzoic Acid (ν_3) BandFit —

| Peak	$\bar{\nu}\,(cm^{-1})$	area
1	1746	5.68
2	1723	46.42
3	1728	41.27

— Vinyl Benzoate (#3) Curvefit.

definitive conclusion can be drawn. First, there was an excess of terphthaloyl chloride, which produces the limiting case of the two end groups being acid terminal groups. The limiting case produces 2n ester carbonyls to 2 acid carbonyls which is to say the ratio of ester to acid area ratio would be exactly equal to the average degree of polymerization. In this case that would be 12.3. Second, the intensities of the two absorbing species is not the same. Accounting for the 1.3:1 acid to ester intensity ratio, gives an average degree of polymerization of 16.

The appearance of two peaks under the ester band leads to interesting speculation. If one looks at hydrogen bonding studies, there is a distinct shift in the "bound" partner H-X stretch relative to the "free" partner in the H-X$\cdots$H-X. The hydrogen bond is denoted by the three dots connecting the middle X and H. The "bound" partner is the one to the right of the three dots and the "free" is to the left. There is electron density removed from between the H-X of the bound partner which weakens that bond and shifts the stretching frequency roughly 100 cm^{-1}. The free partner is not significantly altered by the interaction and absorbs in the same position as the pure monomer H-X stretch. If one projects this model onto the dipole-dipole interaction that can go on between pairs of carbonyls between two different chains, one would expect that the shift of the bound carbonyl stretching frequency to be much less than the bound hydrogen bond stretching frequency because of the weaker interaction found between carbonyls relative to hydrogen bonding. The displacement of the two peaks by 20 cm^{-1} for the two different carbonyl peaks is expected. The pictorialization of this interaction is below.

$$\begin{array}{ccc} \backslash & & \backslash \\ \delta+ \text{ C=O } \delta- \cdots> & \delta+ \text{ C=O } \delta- \\ / & & / \end{array}$$
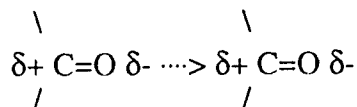
Kinetics

A kinetic modeling of a polymerization process can uncover various pieces of information that will make an understanding of the distribution of polymer lengths clearer. In order to model the polymer distribution for a condensation reaction, an oversimplified kinetic system was devised. The assumptions in the kinetic equations are: (1) stoichiometric amounts of the two units used to create the true monomer are used, (2) the rate constants for dimer, trimer, etc. are all the same, (3) only the monomer reacts with other species (e.g., dimer does not react with dimer or higher polymer lengths) and (4) the formation of the longest chain which is soluble truncates the kinetic expressions (e.g., if the trimer is the insoluble polymer, then the rate expressions will only contain terms which involve reaction of monomer and dimer species). In order to test out the numerical differentiation scheme employed (fourth order Runge Kutta), the trimer was assumed to be insoluble in solution. This leads to the following sets of equations:

$$x_1 + x_1 \xrightarrow{k} x_2$$

$$x_2 + x_1 \xrightarrow{k} x_3$$
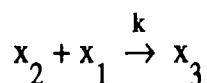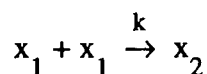
where x_1, x_2 and x_3 represent monomer, dimer and trimer, respectively. The "k" above the reaction arrow is the rate constant which is assumed equal for all steps. When these equations are translated into kinetic rate expressions the following equations result.

$$\frac{dx_1}{dt} = -2kx_1^2 - kx_1 x_2$$

$$\frac{dx_2}{dt} = kx_1^2 - kx_1 x_2$$

$$\frac{dx_3}{dt} = kx_1 x_2$$

In order to reduce these equations to dimensionless quantities, the following definitions will be used.

$$p_i \equiv \frac{n_i x_i}{x_1^o} \quad \text{and} \quad \tau \equiv kx_1^o t$$

The terms in the above equation are the initial concentration of the monomer (all other species are assumed to have zero concentration at time zero), x_1^o, the reduced (dimensionless) time, τ, and coefficient, n_i, of the i-th species x_i which satisfies the following equation:

$$x_1 + 2x_2 + 3x_3 = x_1^o$$

This equation is simply a conservation of mass expression. Using the conservation of mass expression and the definition of p_i, one can readily verify that the sum of the p_i's is one (just as a sum of probabilities). With these definitions the above differential equations are transformed to the following expressions.

$$\frac{dp_1}{d\tau} = -2p_1^2 - \frac{1}{2}p_1 p_2$$

$$\frac{dp_2}{d\tau} = 2p_1^2 - p_1 p_2$$

$$\frac{dp_3}{d\tau} = \frac{3}{2}p_1 p_2$$

As is evident from the above equations, p_1 is a monotonically decaying function, whereas, at the maximum value for p_2 (i.e., set the second equation equal to zero) $p_2 = 2\ p_1$. Using standard techniques in differential equations the maximum value of p_2 is found to be:

122

$$p_2^{max} = \frac{2}{\sqrt{3}} \exp\left(-\frac{\pi}{2\sqrt{3}}\right)$$

which numerically is approximately 0.466238. The numerical solution to these equations yields the same value for p_2^{max} at $\tau = 1.3000$. This simple set of three equations allows a comparison of an analytic solution to the numerical solution. The extension of this to a system of equations which admits of a larger polymer which is soluble is now investigated. One fact became evident very quickly. Once polymer systems of maximum length got beyond six units, the analysis of the systems did not vary. One useful measure that can be extracted from the numerical solutions of the p_i's with respect to time, τ, is the average degree of polymerization, DP. The definition of DP[2] is usually given as:

$$DP = \frac{1}{1 - \phi}$$

where $\phi = (N_0 - N)/N_0$, N_0 is the number of monomer units at time = 0, and N = the number of all molecules at time t. Experimentally this definition of DP is quite convenient, but with the data generated numerically, this definition is tedious to program, especially when the obvious definition follows from the use of the probabilities, p_i, that have been defined. The definition of the number average degree of polymerization, DP, using the probabilities is:

$$DP = \sum_{i=1}^{M} n_i p_i$$

where M is the maximum number of monomer units in the system of equations, and n_i is consistent with its definition used in the conservation of mass expression above. Both definitions of DP give an average degree of polymerization of 2.999 for large values of τ; hence, the use of the same symbol for both definitions. This second definition based on the theoretical development of the kinetic expressions provides a simple computation of a useful experimental value, DP.

The first approximation to be dropped from the kinetics model is that only the monomer can react with other species. This obviously leads to the result that the average degree of polymerization is 3 at infinite time in the above analysis independent of the number of monomer units in the maximum length chain. By elimination of this one restraint, the equations for the maximum chain length of an octamer (for example) become (note that the time derivative of a function is now represented by a dot above the function):

$$\dot{p}_1 = -2p_1^2 - \frac{1}{2}p_1 p_2 - \frac{1}{3}p_1 p_3 - \frac{1}{4}p_1 p_4 - \cdots - \frac{1}{7}p_1 p_7$$

$$\dot{p}_2 = 2p_1^2 - p_1 p_2 - p_2^2 - \frac{1}{3}p_2 p_3 - \cdots - \frac{1}{6}p_2 p_6$$

[2]Koenig, Jack L., Spectroscopy of Polymers, ACS Professional Reference Book, American Chemical Society Publications, Washington DC (1992).

Model 2: Octamer
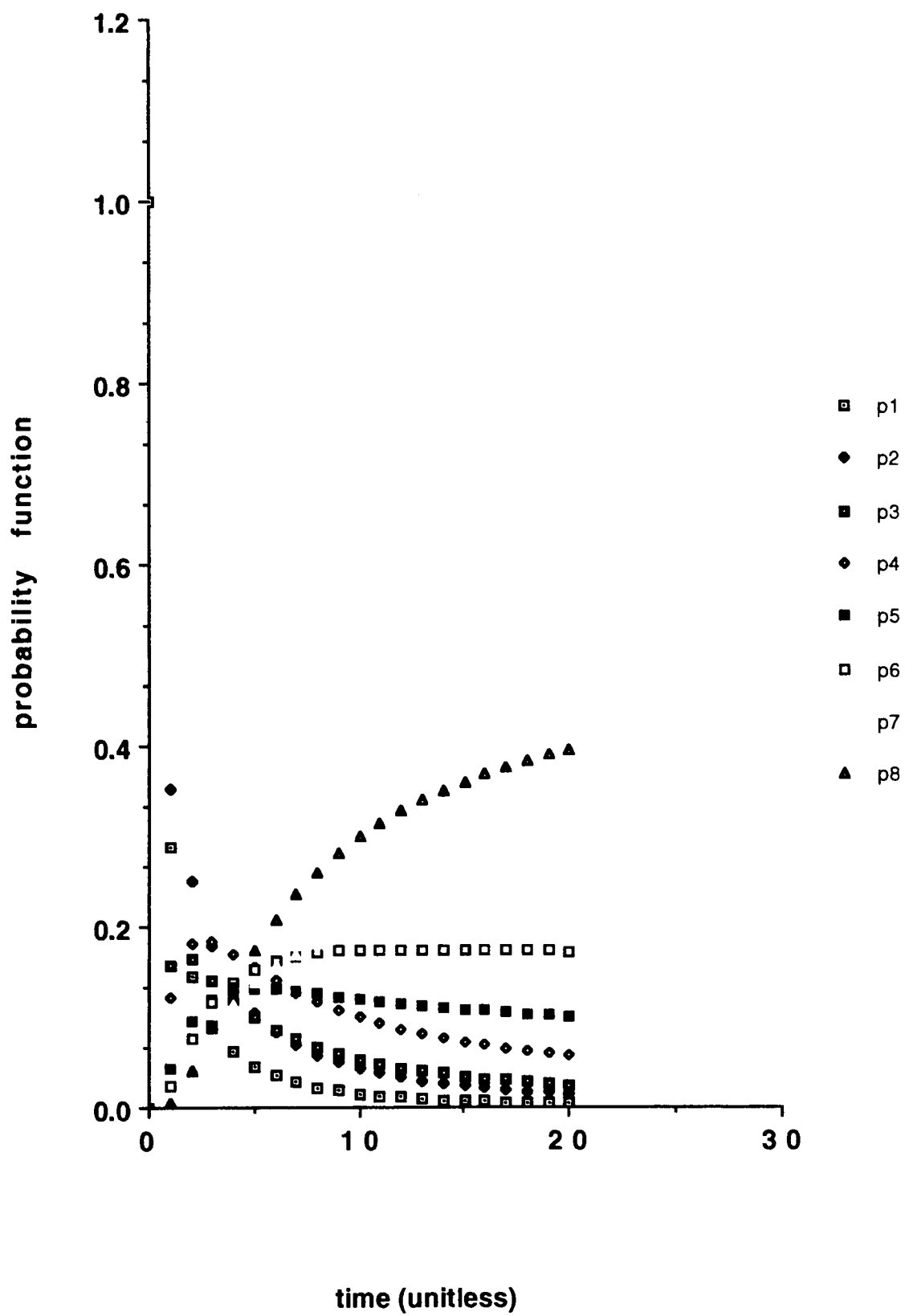
$$\dot{P}_3 = \frac{3}{2}P_1P_2 - P_1P_3 - \frac{1}{2}P_2P_3 - \frac{2}{3}P_3^2 - \frac{1}{4}P_3P_4 - \frac{1}{5}P_3P_5$$

$$\dot{P}_4 = \frac{4}{3}P_1P_3 + P_2^2 - P_1P_4 - \frac{1}{2}P_2P_4 - \frac{1}{3}P_3P_4 - \frac{2}{4}P_4^2$$

$$\dot{P}_5 = \frac{5}{4}P_1P_4 + \frac{5}{6}P_2P_3 - P_1P_5 - \frac{1}{2}P_2P_5 - \frac{1}{3}P_3P_5$$

$$\dot{P}_6 = \frac{6}{5}P_1P_5 + \frac{6}{8}P_2P_4 + \frac{6}{9}P_3^2 - P_1P_6 - \frac{1}{2}P_2P_6$$

$$\dot{P}_7 = \frac{7}{6}P_1P_6 + \frac{7}{10}P_2P_5 + \frac{7}{12}P_3P_4 - P_1P_7$$

$$\dot{P}_8 = \frac{8}{7}P_1P_7 + \frac{8}{12}P_2P_6 + \frac{8}{15}P_3P_5 + \frac{8}{16}P_4^2$$

From the above set of equations, one can readily see that the equations become more complicated, but possess a rather simple pattern which makes programming a simple general algorithm associated with the assumptions in this second model quite easy. A graph of the eight probability functions as a function of unitless (dimensionless) time up through the value of 20 is plotted. An analysis of the DP for the second model for the octomer gives a value of 6.660 as the number average degree of polymerization at $\tau = 20$. At $\tau = 40$, the curves are leveling off and yield a DP of 6.962. Similar results are obtained for longer chains in that the DP is relatively close to the maximum length of the chain for long time analysis. Clearly this model has the requisite flexibility to mimic the experimental DP with τ and the maximum chain length as the parameters that are left to be determined.

Clearly there are two steps which remain to be studied in this problem. First, the changing of the restraint that the maximum length chain based on solubility cuts off the highest value of the polymer length. For instance, in the above equations there should be terms which include the formation of the polymer represented by the term p_{14}. Since there are p_7 terms which correspond to polymers of seven monomer lengths, it is reasonable to expect that two of these could react to form a polymer of length 14. Therefor, even though an octomer may be the first insoluble polymer, there should be greater length polymer chains as a result of joining of shorter chains that yield a polymer larger than an octomer. This leads to another restraint relaxation; that of different values of k (rate constant) for different terms in the rate expression. Currently, the thinking is that the rate constant is proportional to the diffusion of the polymers to one another. The diffusion is in turn proportional to the "surface area" of the polymer. The rate constant would then be equal to the rate constant for the reaction of two monomers divided by the geometric mean of the two reacting polymer surface areas.

Theoretical

Up to this point, there has been an introduction of three areas of research that are connected to elucidating different chemical aspects of polyester formation. There are theoretical developments that underlie and unite these investigations. Those aspects are discussed here. As mentioned in the introduction, the aspiration (and success) of the Newtonian approach

to describing the equilibrium and dynamic states of a large molecular system has been explored in biopolymer areas of research. The obvious extension to "synthetic" polymers is being explored here. This type of problem requires that the essential interactions are transferable from small prototype systems that are well characterized and that there is sufficient experimental input to verify various aspects of the theoretical conclusions. In this chemical system there is sufficient rigidity of the backbone to insure that liquid crystalline behavior should result. In fact, some work that has already been done[3] in which a copolymer of terphthalic acid, ethylene glycol and varying amounts of parahydroxybenzoic acid were mixed together. As the mole fraction of parahydroxybenzoic acid (PABA) increases the melt viscosity (at 275°C) increases up to ~.30 mole fraction. The increase in viscosity is attributed to the increased rigidity imparted by PABA. Beyond the 0.30 mole fraction of PABA, the melt became more opaque (while the viscosity decreased) which is attributed to the onset of thermotropic liquid crystalline morphology. The decrease in viscosity is an alignment of mesophases (small regions of liquid crystallinity) in the direction of the flow of the melt. This alignment reduces the frictional flow. The inference from this copolymer experiment is that the polyester formed from terphthaloyl chloride and hydroquinone (TAHQ) would be a thermotropic liquid crystal as has been observed. A question arises as to the degree of liquid crystallinity of TAHQ from the synthesis of the polymer at low temperatures and the degree of liquid crystallinity that is obtained by forming a melt. What is the difference between the "skin" formed at the surface of a molded polyester and the bulk portion of the polyester? Morphological questions such as these can be answered by describing the molecular level mechanisms of liquid crystal formation. The observation that the phenethyl side chain substituent "anneals better" than other polyesters with aliphatic side chains suggests that a possible mechanism for annealing lies in the enhanced number of inter-chain benzene-benzene interactions. In order to model this interaction, one must get a sense of the strength of the benzene-benzene interactions (enthalpy considerations) and the cost of going from the disordered to ordered state of the annealed material (entropy considerations).

It is proposed that there is a phase transition which is brought on by a "strong" interaction between the hydroquinone substituent and neighboring backbone benzenes and/or phenethyl groups. In the crystal structure of benzene the molecules are stacked such that the neighboring benzenes are orthogonal to the plane of a reference benzene. This is attributed to the electron-rich pi-orbital electrons interacting with the neighboring protons. The figures on the next page depict the interactions and the computed charges

---

[3]W.J. Jackson Jr. and H.F. Kuhfuss, J. Polym. Sci., Polym. Chem. Ed., 14, 2043 (1976).

of the essential hydrogen-carbon interactions. .
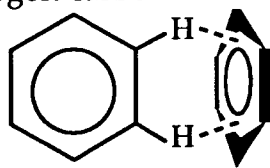
Two benzene rings in their favored orientation in the crystal

In order to understand the phase transition proposed here, one must dissect the problem into its components and estimate the relative energetic contributions to the whole of this problem. As indicated in the figure above, the strength of the benzene-benzene inter-action must be estimated. The implication is that the primary contribution to this interaction is electrostatic. Using a charge equilibration calculation, the following behavior is observed.

(a) (b)
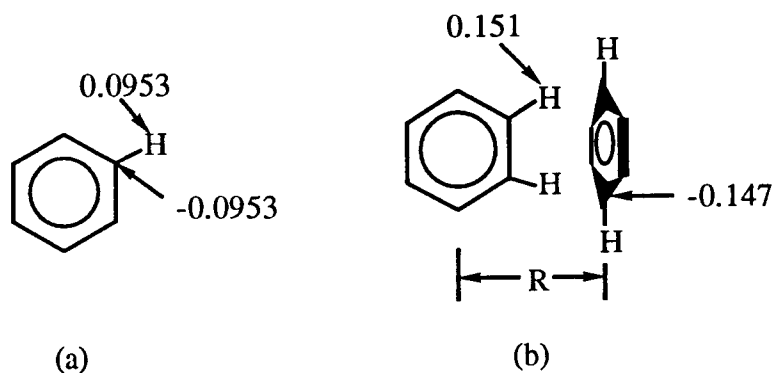
(a) The electrostatic charges of carbon and hydrogen on "free" benzene.
(b) The change of the charges of those atoms which are most affected by the inter-action presented. The value of $R = 3.8$ Angstroms. The other atoms symetrically displaced do not have their charge shown. The other atoms do have the absolute value of their charge increased but not more than 20%.

A more detailed comparison between the estimated electrostatic charges based on the work of D.E. Williams[4] and that computed using the charge equilibration method of A.K. Rappe and W. Goddard III[5] is summarized below in tabular form. The first part of this table indicates the hydrogen-hydrogen, carbon-hydrogen and carbon-carbon non-bonded interaction parameter values based on the exp-6-1 potential. The charges on the carbons and hydrogens were set equal in magnitude but opposite in sign in order to maintain electroneutrality of each molecule. The interpretation of the numbers associated with different center to center displacements for the T-shaped dimers is rather straight forward when one realizes that the benzene which is shown as coming in and out of the plane only has two distinct carbons (and attached hydrogens) because of symmetry. The horizontal

[4]D.E. Williams, Acta Cryst., A36, 715 (1980).

[5]W.A. Goddard III and A.K. Rappe, "Charge Equilibration for Molecular Dynamic Simulations", J. Chem. Phys. 98, 3358-63 (1991).

benzene has the four numbers to the left side with the negative charges associated with carbon atoms and the positive numbers associated with the hydrogens. The larger negative number corresponds to the carbon which has a hydrogen from the benzene in the plane of the paper (vertical benzene) pointing at it. The vertical benzene has three sets of carbon-hydrogen pairs with the most positive value corresponding to the hydrogen which is pointing at a horizontal carbon atom. For example, at 3.8 Angstroms the -1.465 charge is the horizontal carbon atom charge with a hydrogen atom pointing at it. The value of 0.1511 is the hydrogen atom charge of the vertical ring hydrogen which is pointing at the benzene ring below it.

Charge density study of benzene and benzene dimer

Non-bonded potential "exp-6-1" [D.E. Williams, <u>Acta Cryst</u> <u>A36</u>, 715-23 (1980)]
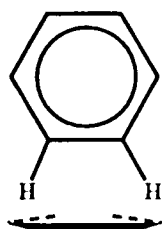
$$V_{jk} = B \exp(-C\, r_{jk}) - A\, r_{jk}^{-6} + q_j\, q_k\, r_{jk}^{-1}$$

parameters (kJ/mole, A°, e)

	H···H	H···C	C···C
A	136.	573.	2414.
B	11677.	65485.	367250.
C	3.74	3.67	3.60

center to center for dimer = 4.69 A°

q(H) = 0.153   q(C) = -0.153

charge equilbration

benzene monomer   q(H) = 0.0953   q(C) = -0.0953

3.8 A°	0.0933				0.0925		
separation	-0.1465				-0.1062		
of centers		-0.1057	0.1038	0.1511	-0.0802	-0.0965	0.0965
4.2 A°	0.0942				0.0934		
separation	-0.1292				-0.1070		
of centers		-0.1010	0.0995	0.1333	-0.0814	-0.0963	0.0962
4.6 A°	0.0933				0.0936		
separation	-0.1131				-0.1022		
of centers		-0.1004	0.0980	0.1294	-0.0955	-0.0963	0.0956

5.0 A°
separation
of centers

0.0938			0.0942		
-0.1062			-0.0956		
	-0.1004	0.0972	0.1164 -0.0902		-0.0956 0.0953

3.8 A°
separation
of centers

0.1065			0.0923		
-0.0962			-0.1047		
	-0.1311	0.0977	0.1515 -0.0825		-0.0962 0.0962

4.2 A°
separation
of centers

0.1010			0.0935		
-0.0953			-0.1094		
	-0.1179	0.0959	0.1314 -0.0769		-0.0968 0.0965

4.6 A°
separation
of centers

0.0988			0.0936		
-0.0953			-0.1022		
	-0.1091	0.0951	0.1292 -0.0953		-0.0963 0.0956

5.0 A°
separation
of centers

0.0979			0.0942		
-0.0979			-0.1014		
	-0.1043	0.0950	0.1159 -0.0898		-0.0956 0.0954

There are two apparent discrepancies between the description of this calculation of the charges of the atoms and the electrostatics of Williams. One is that the charge is dependent on the internuclear separations of the two rings and the other is that the size of the charge of the two closest hydrogens of one ring and carbons on the other ring are not very close to Williams fixed charge until the rings are 3.8 Angstroms apart. In terms of the electrostatics, the two hydrogens and two carbons of closest contact dominate the electrostatic energy. Currently under investigation is the dependence of the charge of the dominate hydrogen-carbon interactions as a function of intermolecular separation and re-evaluation of the exp-6 potential energy parameters to give reasonable agreement between experiment and theory.

In addition to studying the energetics of the electrostatics of the interchain interactions, the charge equilibration calculation can also be used to estimate the relative infrared intensities of the ester versus acid carbonyls. The prototypical molecules used in this case for calculation of the change in dipole moment with respect to the carbonyl stretch were the same as used in the FTIR spectroscopic investigation - phenylbenzoate and benzoic acid. The equilibrium geometry of each of these structures was determined using a Macintosh software package "Alchemy" from TRIPOS. The carbonyl oxygen of the ester and acid was varied 0.01 Angstroms from the equilibrium position and the molecular dipole was calculated for all six of these carbonyl bond lengths. Three of these bond lengths belong to phenylbenzoate and the

graphical display of the results of the variation of molecular dipole versus the relative displacement of the carbonyl oxygen is shown below.

Phenylbenzoate relative intensity determination

$y = 1.4008 + 1.5580x - 9.9540e\text{-}2x^\wedge 2$
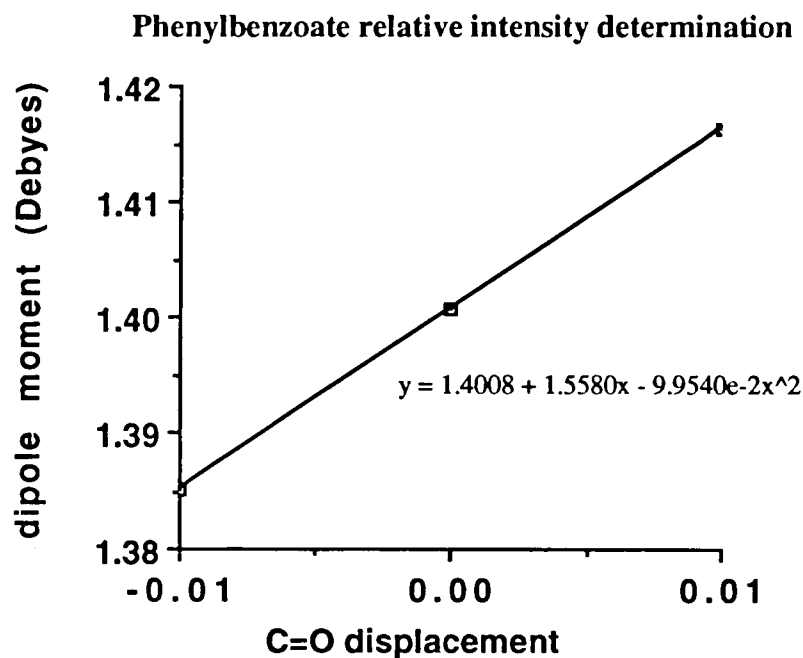
The first derivative of the dipole moment with respect to the coordinate change is the same as the linear coefficient to a least squares regression of a polynomial fit to the data. In this case the first derivative of the dipole moment with respect to the coordinate displacement for phenylbenzoate is 1.5580 Debyes/Angstrom and for benzoic acid this is 1.6500 Debyes/Angstrom. The infrared line intensity is proportional to the square of the derivative of the dipole moment. This leads to the relative ratio of benzoic acid to phenylbenzoate infrared line intensities of 1.12 or in other words the acid carbonyl is about 10% more intense than the ester carbonyl at the same concentration. This estimate of the relative intensities indicates that the average chain length is 14 monomer units in contrast to the earlier estimate of 16 monomer units.

In addition to the electrostatic calculations, molecular mechanics calculations are needed to complete the macroscopic property predictions. As an example, the creation of a 15 monomer chain length has been created and the application of "Boltzmann Jump" has been applied to obtain a random sampling of many conformations that the polymer chain can assume. This sampling is in the spirit of Monte Carlo techniques in which one can get an estimate of a property if sufficient, random sampling is applied to the system under study. Obviously, in a case like this the number of conformations far exceeds human patience and computer storage. The torsional angles of the backbone are given random bumps to create other conformations which are then energy minimized. The conformational energies are Boltzmann

130
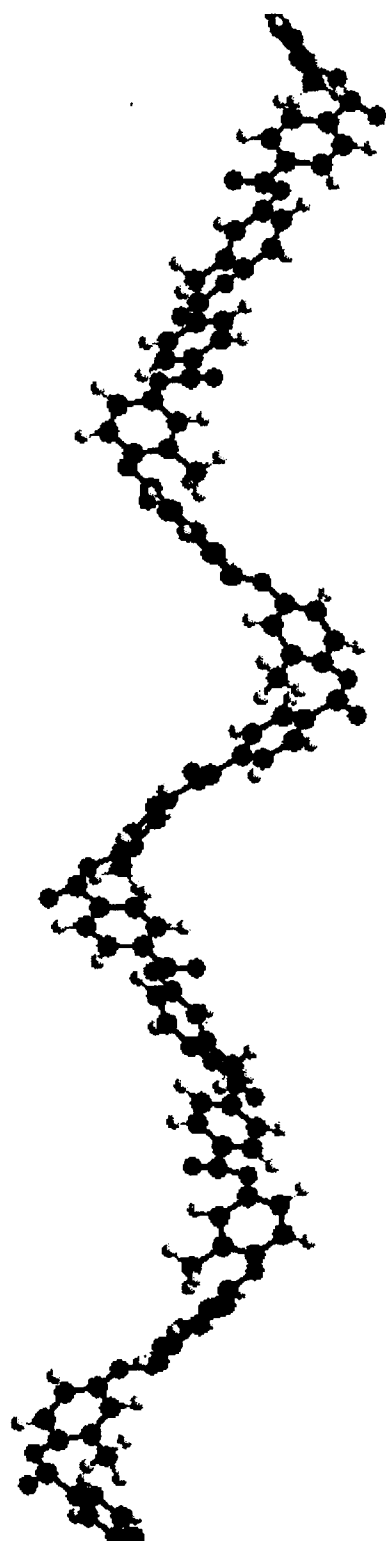
15PCH3
Model 1
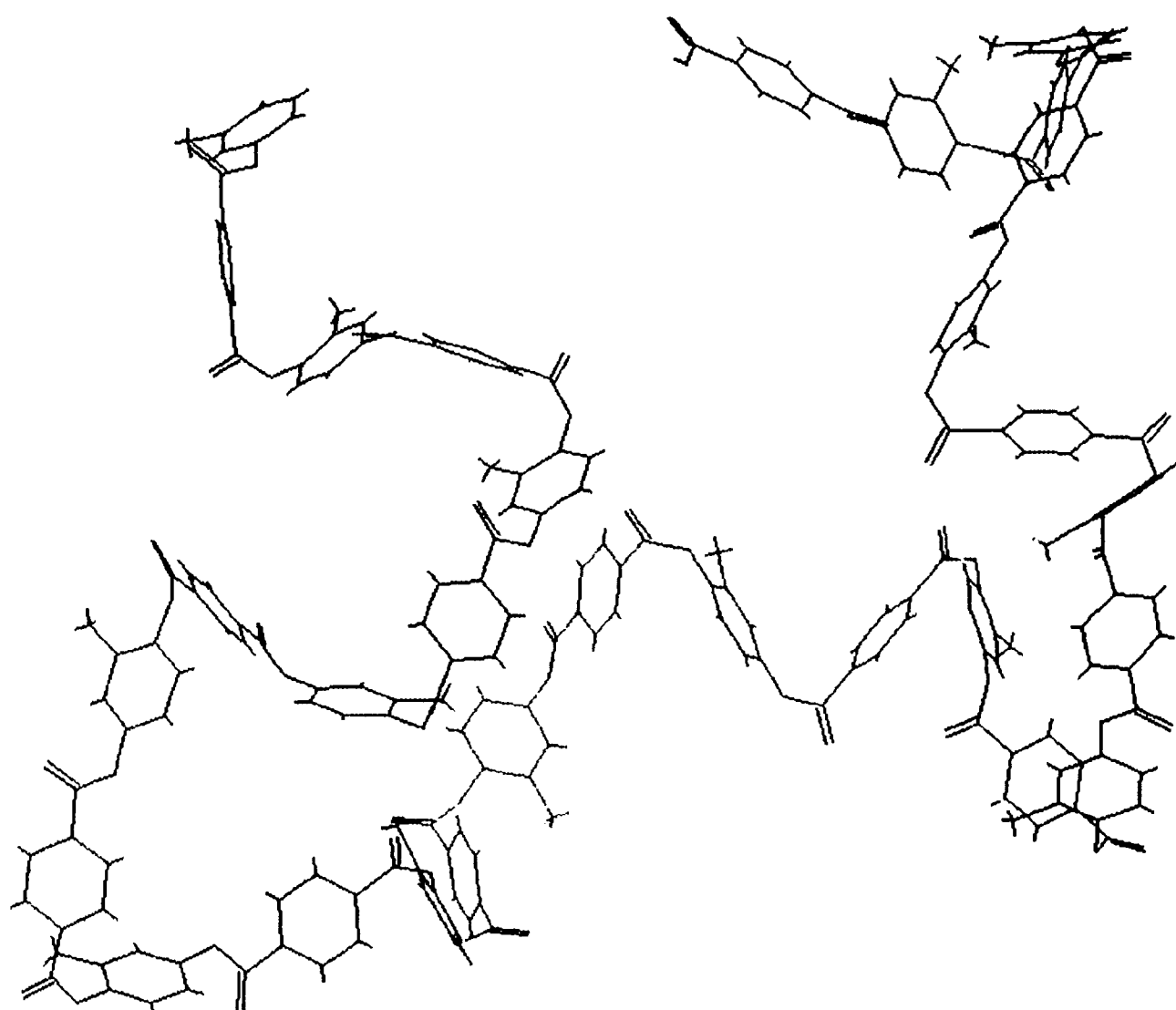
131

weighted in computing the average property that is sought. When the polyester was first created the conformation that was obtained after minimization is shown on the next page. The structure is a familiar helical coil. A study of the torsional energies reveal that a left or right hand twist of the torsions about the ester linkage are the lowest in energy. If one applies a uniform twist to the entire polymer, the resultant structure is the highly symmetric helix. The usual techniques of energy minimization will not move the conformation into any other shape because of the torsional energy barriers that drive the algorithms back to the starting conformation. The Boltzmann Jump method imparts significant and random "kinks" to the torsional angles of the polymer backbone so that regions of lower energy can be explored. A Boltzmann Jump of 100 conformations was explored and the lowest energy conformation of those leads to a structure which is much more randomized in its structure than the starting helix. Many conformations were found to be lower in energy than the helical structure and they also were of a more random coil. There are regions in the backbone which preserve the helical structure, but there is a secondary structure which is more "ball-like" than the "stick-like" helix. From this weighted average of structures the average end-to-end distance and radius of gyration of the polymer are computed. One important use of this information is to weight the rate constants in the kinetic study above. The rate of diffusion of the polymers toward one another affects the relative rate constant associated with two monomers forming a dimer to the rate constant associated with a trimer reacting with a tetramer to form a heptamer. The diffusion would in turn be related to the "surface area" of the reacting species. An estimate of the surface area of a particular polymer chain length could be estimated from the surface of a sphere generated by the radius of gyration of the polymer. The more stick-like the polymer, the larger the radius of gyration and the larger the surface area. Conversely, the more ball-like the polymer the smaller the surface area and the more quickly the polymer will diffuse. The rate constant of the trimer with the tetramer would have a rate constant equal to the monomer with monomer rate constant divided by a number proportional to the geometric mean of the radii of gyration. In both (stick and ball-like conformations) cases, the longer the chain the less probable the reactive end of the chain will encounter another correctly oriented polymer. This effect would have to be incorporated as well.

Conclusions

The interconnectedness of these various topics of research manifest themselves in several ways. In regards to the kinetic studies, once a "realistic" set of kinetic equations is developed with the help of surface area estimates of the different polymer lengths, a polymer distribution of molecular weights can be described once the average molecular weight is obtained via FTIR spectroscopy. A handle on the molecular weight distribution is important in physical property predictions. The spectroscopic evaluation of the "number" average molecular weight of a polymer in turn

133

depends on a knowledge of the relative line intensities of the ester and acid carbonyls. Although there are experimental ways of determining these values there are theoretical methods as well. The synthesis of alternate and/or homologous polymers helps establish the strength of the predictiveness of the molecular mechanics approach to the "phase transition" hypothesis used to account for the annealing of these polyesters. The heavier weighting of the more randomly coiled polymer is consistent with the hypothesis that the phase transition from disorder to order is an operative mechanism in the annealing of these polymers. As the temperature of the system is raised the less energetically favored "stick-like" polymers become more probable. At the same time, the interchain interactions such as the side phenyl rings sticking to neighboring chains becomes more probable. If sufficient energy is gained by the chain to chain interactions, the liquid crystalline behavior is frozen into the structure. That is, the more interchain interactions the more straight and aligned the polymer backbones become relative to one another.

A STUDY OF THERMOTROPIC LIQUID CRYSTAL POLYMERS

David M. Elliott

Arkansas Tech University

ABSTRACT

Researchers at the Phillips Laboratory at Edwards Air Force Base have been instrumental in both the development and the characterization of thermotropic liquid crystal polymers (LCPs). The mechanical and chemical properties of parts made by injection molding some of these materials are known to dramatically improve upon thermal annealing. In order to realize the full potential of annealed LCPs, a firm understanding of the molecular and crystalline structure, morphology, texture, and the dynamics and mechanism of formation of the annealed state must be obtained.

Very little of known about the crystalline structure of injection molded LCPs and how that structure varies or changes with direction of flow into the mold and other mold processing variables or with thermal annealing of molded parts. The principal objective of this work was to assess the feasibility of using neutron diffraction as a tool to investigate the crystalline properties of these parts. Concurrent with work towards this objective, a number of other techniques of investigation were utilized to provide further information about the crystalline and mechanical properties. These other techniques included x-ray diffraction, tensile testing, hardness testing, and scanning electron microscopy of fracture surfaces.

It was found that the neutron diffraction technique is capable of establishing that these materials do have a crystalline structure and of measuring some of the crystalline properties but it is not capable of determining the crystalline structure itself. X-ray diffraction was found to be better, faster and less expensive for these measurements.

Injection molded parts made form five commercial LCPs were studied. It was found that both crystalline and mechanical properties were dramatically influenced by annealing in argon at 260 deg. C.

INTRODUCTION

The development of advanced new materials possessing very high specific strength and specific modulus is critically important to the Air Force mission in both the exploration of interplanetary space and the development of higher performance and lower cost missile systems. Composite materials with superior mechanical properties have been made from high-strength fibers and graphite. Parts and structures made from these composite materials are, however, relatively costly because of the complexity of the manufacturing process. The high-strength fibers used in these composite materials are often prepared from stiff-chain aromatic polymers. These polymers are called stiff-chain polymers because the molecules tend to be quite elongated in solution or in the melt. These elongated molecules have a propensity to form a definite crystalline organization in the liquid state (either solution or melt) and consequently they are referred to as liquid-crystal polymers (LCPs). In addition to their use in high-strength fibers, LCPs can be injection or blow molded inexpensively into complex shapes. The liquid crystalline order persists and is often enhanced as the LCPs are carried into the solid state during the molding process. Solid materials molded from LCPs are, however, inhomogeneous and highly anisotropic. They can be thought of as molecular composites.

The mechanical properties of solid LCPs depend importantly on the processing as well as on the material itself. Flow, either in the spinning of fibers or in the molding of parts, can result in an increase in the crystalline order and this in turn can result in significant enhancements of both strength and modulus. Temperature is also an important processing variable. The relationships between molecular conformation and crystalline order and mechanical and chemical properties are not well known yet understanding these relationships is vital to developing these molecular composites to their full potential.
Recognizing this, researchers at the Phillips Laboratory are pursuing a program of both theoretical and experimental studies to characterize the molecular structure, dynamics, and mechanism of formation of the annealed state in selected linear LCPs. In addition, a number of Air Force installations are cooperating in a related program to fabricate injection molded parts from commercial LCPs, to measure the mechanical properties of these injection molded LCPs, and to use the parts in demonstration applications including solid rocket motors.

A process known as physico-chemical annealing is of particular interest in the design of parts made from LCPs. In this process, the material is

136

heated to a temperature below the melting point and held there for a period of time. When the material is cooled·it sometimes happens that the mechanical properties, particularly the modulus and the ultimate strength, are significantly improved, the resistance to solvents is improved and the material no longer melts; it decomposes instead.

This annealing process is commonly utilized in making high-strength LCP fibers and the details of the process and its effects on physical and chemical properties are relatively well known in this field. The annealing process appears to work best when the long chain molecules of the material are highly oriented prior to annealing as they are in spun or drawn fibers.

Fundamental to all of these programs is the ability to determine and reliably measure the important crystalline properties and those mechanical properties essential for design purposes. Because of the highly anisotropic nature of injection molded LCP parts, it is necessary to determine these properties as functions of both orientation and position within the part. Because there is strong evidence that thermal annealing affects a number of these properties, it is desirable to measure the effect of annealing on each important property individually. The measurement of these properties requires a wide variety of the modern techniques of material science. It is unusual for all of the necessary equipment and investigative skills to exist in a single laboratory. As a consequence, cooperative efforts between a number of different organizations are usually required. The current program involves a number of Air Force installations and laboratories, other government facilities, both U.S. and foreign, universities, and industrial organizations. The work reported here is a joint effort involving the United States Air Force Phillips Laboratory, Arkansas Tech University, and the Australian Nuclear Science & Technology Organisation, ANSTO. The experimental work was carried out at the ANSTO facilities at Lucas Heights in Australia.

The principal objective of this work was to assess the feasibility of using neutron diffraction as a tool to investigate the crystalline properties of injection molded parts made from commercially available liquid crystal polymers. Because of the work was carried out at ANSTO where on site there is available a wide variety of world class experimental facilities and competent and genuinely helpful people, a number of other techniques were used to obtain additional data which added significantly to the knowledge base and suggested fruitful areas for further work. These other techniques included x-ray diffraction, tensile testing, hardness testing, and scanning electron microscopy of fracture surfaces.

MATERIALS

The materials available for this work consisted of injection molded parts made from five commercially available liquid crystal polymers. These were: POLYMER A, VECTRA A950, VECTRA B950T, HX 4000, and SRT 500. Very small quantities of parts were available at the time the project was carried out and this limited the number of experiments which could be performed. The physical form of the parts is given in the following table.

Sample Number	Designation	Form
1	POLYMER A	Sheet
2	VECTRA A950	Dogbones
3	VECTRA B950T	Sheet
4	HX 4000	Sheet & Dogbones
5	SRT 500	Small Pieces

Notes:
1.   Sheets were ridged with the thick part being 4.8mm and the thin part being 3.1mm. The sheets were approximately 10cm by 10cm.

2.   The dogbones were all 3.1mm thick.

Table 1.   Sample materials injection molded from commercial liquid crystal polymers

EXPERIMENTAL METHODS

Neutron Diffraction

The neutron diffraction measurements were made using the High Resolution Powder Diffractometer (HRPD) located at beam hole 4H2 on the High Flux Australian Reactor (HIFAR). HIFAR is a 10 megawatt DIDO class research reactor. The reactor is heavy water moderated and light water cooled. It uses 60 percent enriched uranium and produces a peak thermal neutron flux of 14×10^{12} neutrons/cm^2/sec.

HRPD is conventional in design but is carefully optimized for high resolution diffraction experiments. Both diffractometer operation and data collection are computerized. Figure 1. shows the basic geometry of a neutron diffraction experiment. Figure 2. is a diagram of the VANESSA powder diffractometer in Britain which is similar in design to HRPD.
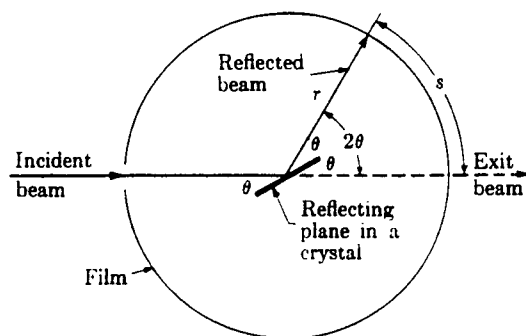

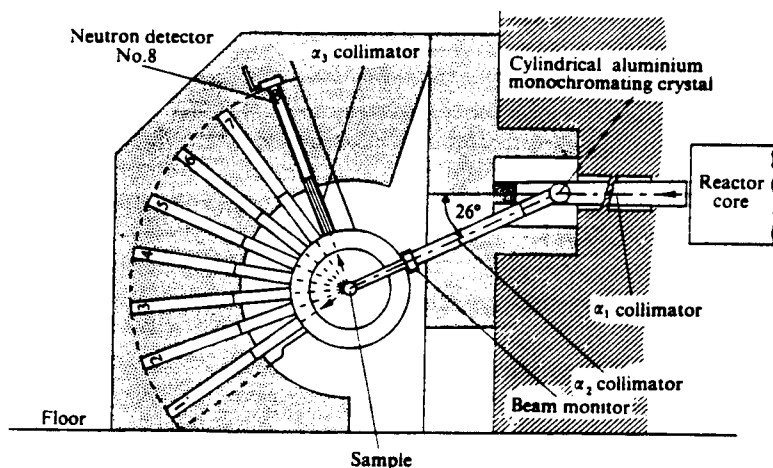Figure 1. Basic geometry of a neutron diffraction experiment[1]

Figure 2. Diagram of the VANESSA powder diffractometer[2]

Like VANESSA, HRPD uses eight detectors spaced six degrees apart. These
detectors rotate as a unit about the vertical axis through the sample. The
sample itself can rotate during the experiment if the investigator so chooses.
A monitor counter is placed in the beam at the point where it emerges from the
concrete shield. This counter is used to assure uniform exposures. The
important parameters of HRPD are given in Table 2.

Beam Hole	4H2
Monochromator	Ge (hhl)
Take Off Angle	120 degrees
Beam Size	20mm X 50mm
Flux at Sample	5×10^4 n/cm^2/sec
Available Wavelengths	1.377, 1.493, 1.893 Angstroms
Temperature Range	14K to 2000K

Table 2. HRPD parameters

All of the measurements reported in this work utilized a wavelength of 1.893
Angstroms and a two-theta step size of 0.05 or 0.1 degrees.

The results of a neutron diffraction experiment are usually presented in
the form of a plot of intensity or counts vs the diffraction angle (2θ). For
most samples of crystalline material, the plot looks like Figure 3. Note the
presence of numerous well defined and relatively sharp peaks. In the case of
liquid crystal polymers, however, the plot typically looks like Figure 4. In
these plots there is typically only one peak that is well enough resolved to
permit quantitative measurement. Sometimes there was evidence of one or two
smaller peaks but these were not resolvable. The reason for this behavior is
that the LCPs contain a high percentage of hydrogen. Hydrogen bound in
crystals has a large incoherent scattering cross section. The effect of a
high concentration of nuclei with a high incoherent scattering cross section
is to smear the neutrons scattered from such nuclei rather uniformly over the
total range of diffraction angles. The result is a very high background
against which it is difficult to detect diffraction peaks. It should be
mentioned that this problem could be significantly reduced by replacing the

normal hydrogen with deuterium. This is however, chemically difficult and
extremely expensive.
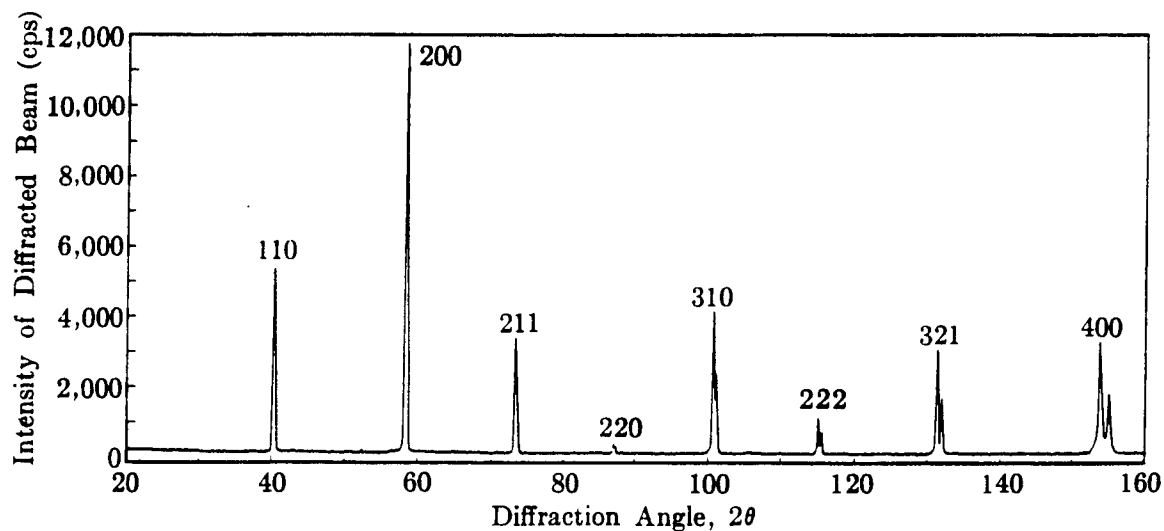

Figure 3.   Typical neutron diffraction pattern for an inorganic crystalline
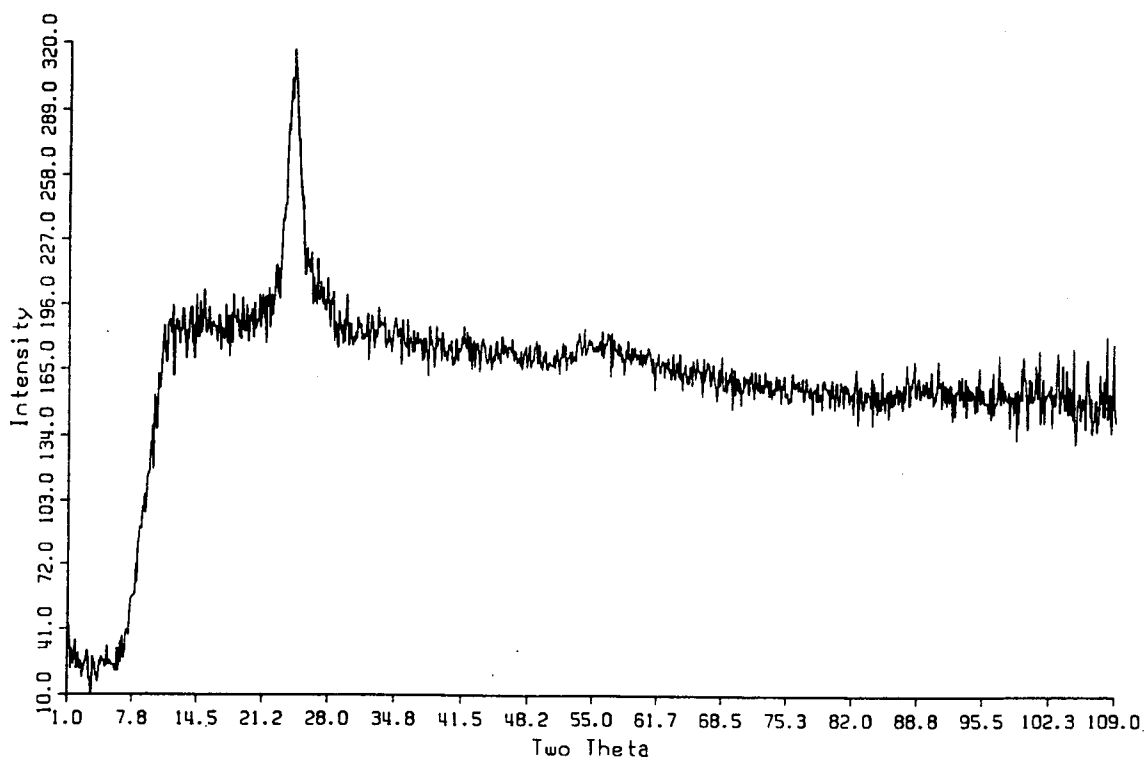   material

Figure 4.   Typical neutron diffraction spectrum for a liquid
             crystal polymer

Given that there is only one peak to work with in these LCP diffraction patterns, one naturally asks: What useful information can be extracted from these data? The answer is a lot. First of all, the very presence of a peak indicates that the material is at least partially crystalline as opposed to wholly amorphous. Theory suggests that neutron diffraction peaks should be gaussian. A least squares fit to a gaussian riding on a linearly decreasing background was performed for each peak. The results of the fitting process yielded numerical values for the peak height, the peak width at half-maximum, and the location of the peak in 2θ. A relative area was calculated as the product of the peak height and the width at half-maximum. The location of the peak is related to the spacing of the reflecting planes in the crystal, the d spacing, through Bragg's law.

$$n\lambda = 2d\sin\theta$$

Changes in d spacing strongly suggest a change in the crystalline structure. The area of the peak is proportional to the intensity of neutrons scattered through 2θ which is in turn proportional to the square of the concentration of crystals with the proper orientation to satisfy Bragg's law. (Intensity is also proportional to the square of the structure factor which is a function of the positions of the atoms within the crystal.) The width of the peak is a measure of the degree of alignment of the set of individual crystals; the narrower the peak, the better the alignment. So even though there is only one peak (which precludes the determination of the exact crystal structure), the quantification of its parameters provides a great deal of interesting and useful information.

X-ray Diffraction

The basic idea of x-ray diffraction is very similar to neutron diffraction. In both experiments, a beam of radiation is made to impinge on a sample and the intensity of the scattered radiation is measured as a function of the scattering angle. Figure 5 shows a schematic diagram of an x-ray diffractometer. A fundamental difference between the two experiments is that the x-rays interact with the orbital electrons in the sample while the neutrons interact with the sample nuclei. Bragg's law, however, applies in both cases. One result of this difference is that x-rays are strongly absorbed by the sample while neutrons are not. X-rays can, therefore, see only the sample surface and those atoms close to it. This can be an advantage or a disadvantage depending on what is wanted from the experiment. For polymers and other hydrogenous materials, x-ray diffraction does not suffer

142

from the problem of incoherent scattering from the bound hydrogen. The
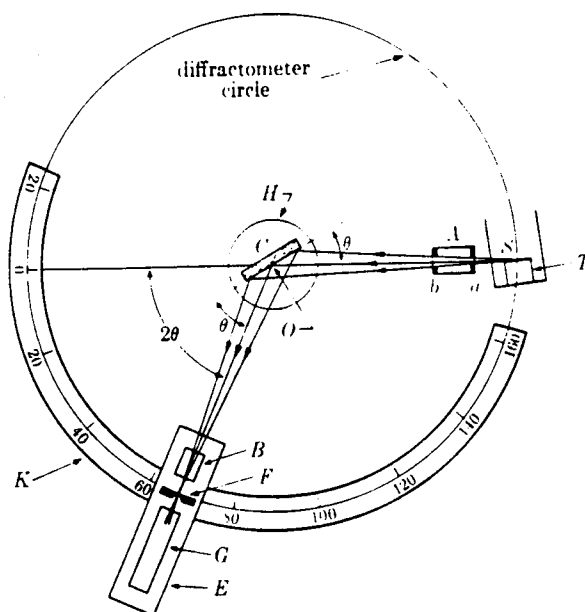spectra are, therefore, much better resolved.

Figure 5. X-ray Diffractometer (schematic)

While the basic idea of x-ray and neutron diffraction is similar, in
practice the two methods are very different. Neutron diffraction requires an
intense source of neutrons, usually a nuclear reactor or a particle
accelerator. Both types of neutron source are very large and very expensive
to build and operate. The neutron diffractometers are usually custom built at
the site where they will be used. X-ray diffractometers, on the other hand,
are commercially available from a number of sources and cost only a few
hundred thousand dollars. The source of the x-rays is part of the
diffractometer package. Figure 6 shows a typical x-ray diffraction pattern
obtained from a liquid crystal polymer.

The x-ray diffractometer used in this work was a Siemens model D-500. The
wavelength was 1.789 Angstroms and the diffraction angle step size was 0.05
degrees.

Tensile Testing

Several of the mechanical properties of interest from a design standpoint
can be measured utilizing standard tensile testing methods. For the current
work, injection molded dogbone samples were subjected to tensile testing. The
samples were 15 to 20cm in overall length and 3.1mm thick. The width of the gage
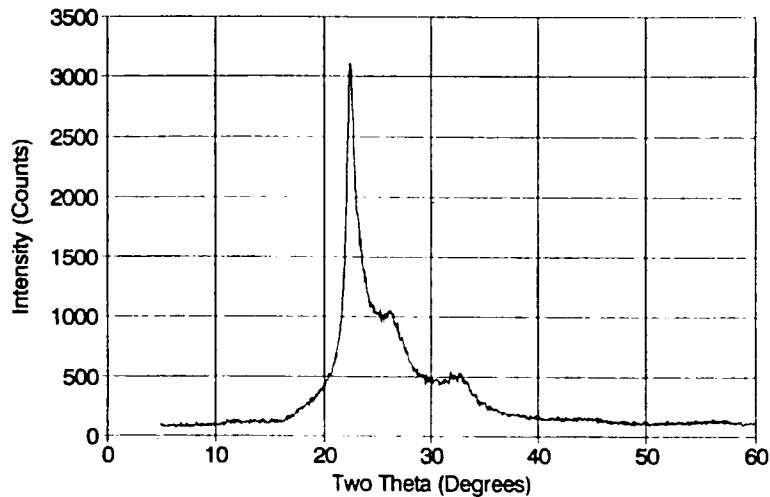
Figure 6.   Typical x-ray diffraction pattern for a liquid crystal
polymer

area was about 13.8mm.   The testing machine was an Instron Model 8561 with a
100KN load.   The extensometer was an Instron Model 045 with a 50mm gage length.
The test environment was air at room temperature of 22 degrees C.   All of the
samples were tested in displacement control at a cross head rate of 0.01mm/sec.
The following mechanical properties were measured: Elastic modulus, ultimate
tensile strength, elongation at break, and reduction of area.   It must be
recognized that injection molded liquid crystal polymers are inhomogeneous and
highly anisotropic.   The tensile testing done in this work was restricted to
uniaxial along the direction of flow into the mold.

Hardness Testing

Given the inhomogeneous and anisotropic nature of injection molded LCP
parts, the interpretation of the results of standard hardness testing methods is
difficult at best.   All of these methods measure the extent to which a pointed
probe penetrates the sample surface when pushed with a standard force.   The
Vickers method was chosen for this work because it uses an indentor in the form
of a square pyramid with an apical angle of 136 degrees and because it uses much
lighter loads.   The other methods use spherical or conical indentors.   The
impression is measured by means of a medium-power compound microscope.   In the

144

normal test, both dimensions of the diamond shaped indentation are measured and an average value is used. The Vickers hardness number is found from the relation

$$V = P/0.539d^2$$

where P is the imposed load in Kg and d is the diagonal of the indention in mm. The anisotropy of the samples is evident from the different values of d parallel to and perpendicular to the direction of flow into the mold. Vickers hardness numbers are reported parallel to the flow direction, perpendicular to it, and as an average of these two values.

Scanning Electron Microscopy of Fracture Surfaces

Scanning electron microscopy is preferred over optical microscopy for the examination of fracture surfaces because it has much better resolution and depth of field. These characteristics are very beneficial in revealing the topographical features of fracture surfaces. In scanning electron microscopy, the image is formed by reflected electron beams. It is necessary for the surface being examined to be electrically conductive. To provide this surface conductivity, the LCP fracture surfaces were coated with a thin layer of carbon by a sputtering process. The instrument used was a JEOL Model JXA-840 Scanning Microanalyzer. Photomicrographs were taken of the dogbone fracture surfaces of VECTRA A950 and HX 4000 both untreated and annealed for 16 hours at 260 deg. C.

RESULTS

Neutron Diffraction Studies of Orientation

The size of the peak obtained by neutron diffraction of injection molded LCP samples was found to be very dependent upon the orientation of the sample in the diffractometer. The peak was found to larger in all cases when the sample was oriented in the diffractometer such that the direction the material flowed into the mold was aligned with the vertical axis of the diffractometer. In the results which follow, this direction is referred to as "vertical". The horizontal direction is, of course, rotated 90 degrees. Figures 7 and 8 show the spectra at both orientations and the difference between them for VECTRA B950T and HX 4000 respectively. The samples were 50mm X 50mm squares cut from injection molded sheets. The direction of flow into the mold was determined visually from the appearance of the surface of the sheets.
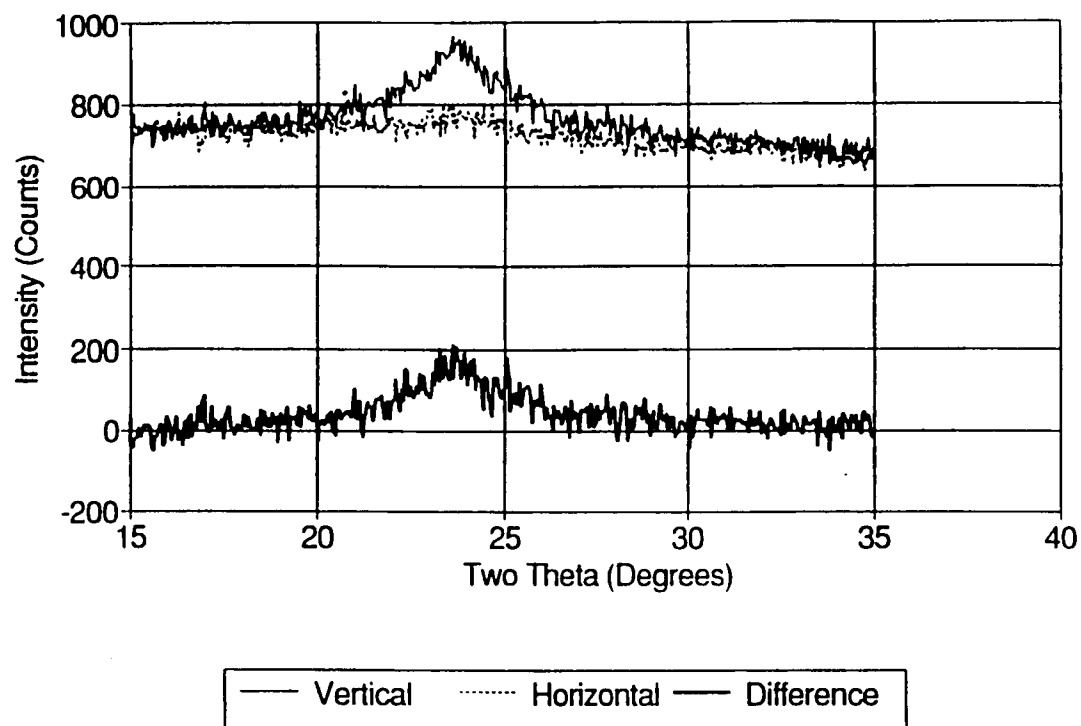
145

Figure 7.   Neutron Diffraction Spectra as a Function of Orientation for VECTRA B950T
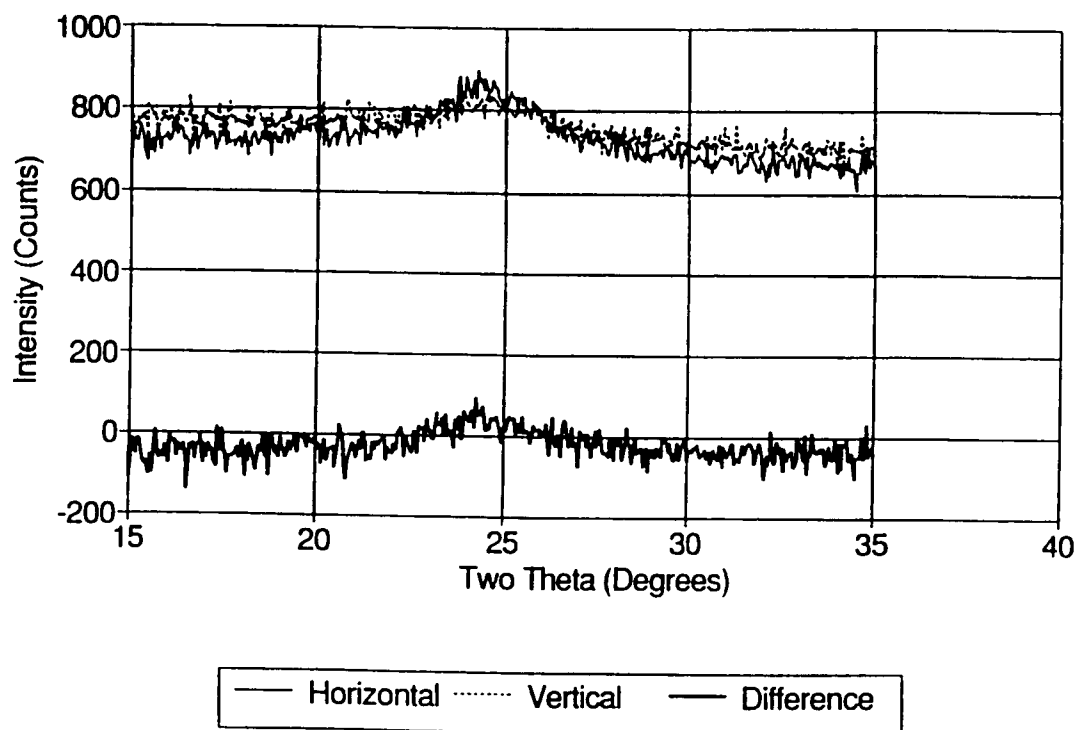

Figure 8.   Neutron Diffraction Spectra as a Function of Orientation for HX 4000

146

Even though the peak is larger in the vertical direction for all materials tested, the extent to which it is larger varies considerably from one material to the next.

Neutron Diffraction Studies of Annealing Versus Orientation

Figures 9 through 11 show the measured neutron diffraction peak parameters individually for the two different orientations both for untreated LCPs and for LCPs which have been annealed for 16 hours in argon at 260 de. C. The legend "UV" means an untreated sample oriented in the vertical direction while "AH" means an annealed one oriented in the horizontal direction. The ordinates give the actual values calculated from the peak fits. The units of height are counts, width is in 2θ with units of degrees, area is the product of peak height and width, and d is in Angstroms calculated from Bragg's law. With the results presented in this way, it is easy to see the effects of orientation and annealing individually or combined.

Figures 12 through 14 show the same information as the previous figures but in a different format. Here the percent increase in the individual parameters after annealing is shown for both the vertical and horizontal directions.

Neutron Diffraction Studies of Annealing of Powders

When the molten LCP flows into the mold, the shear field tends to align the molecules in the direction of flow. In an attempt to remove this preferred alignment and obtain a diffraction pattern for randomly oriented crystals, a powder was made from two of the sheet samples by belt sanding the edges and collecting the dust. This was done for POLYMER A and for SRT 500. Half of the resultant powder for each material was annealed at 260 deg. C for 16 hours under argon and the other half was left untreated. The powder samples were put into vanadium sample cans. These sample cans were rotated about their vertical axis while being exposed to the neutron beam. The resultant spectra are shown in Figures 15 and 16. The background areas far removed from the peaks do not lie on top of each other either because the sample weights were (POLYMER A) different or the irradiation time was different(SRT 500). What is of most interest in both cases is that the peak does grow significantly with annealing.
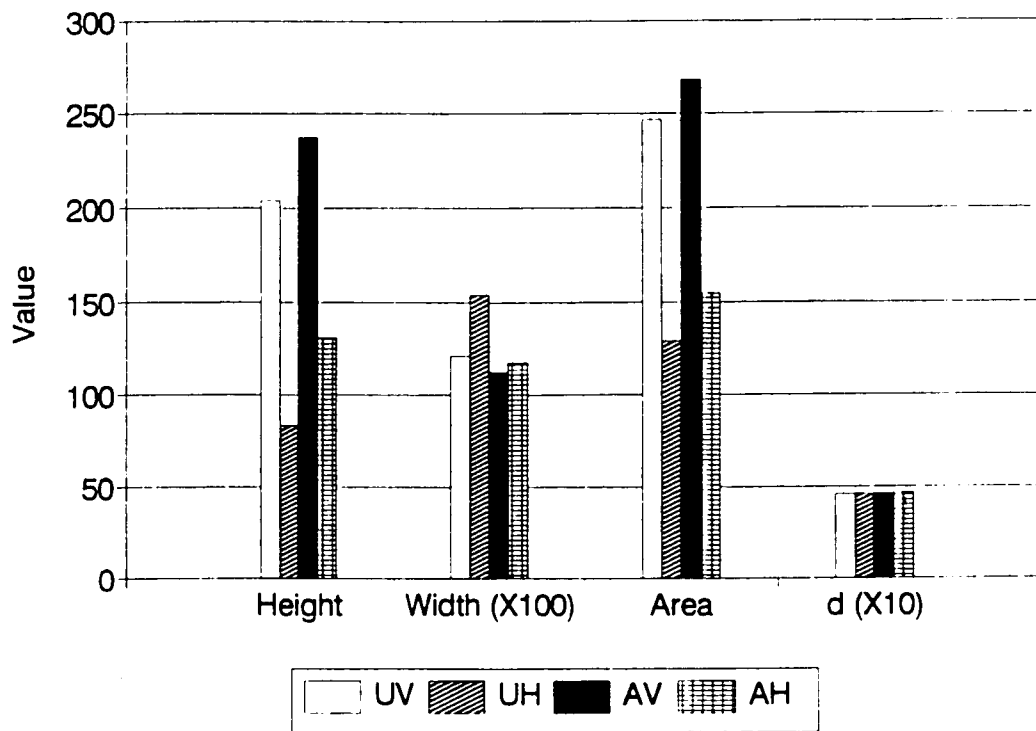
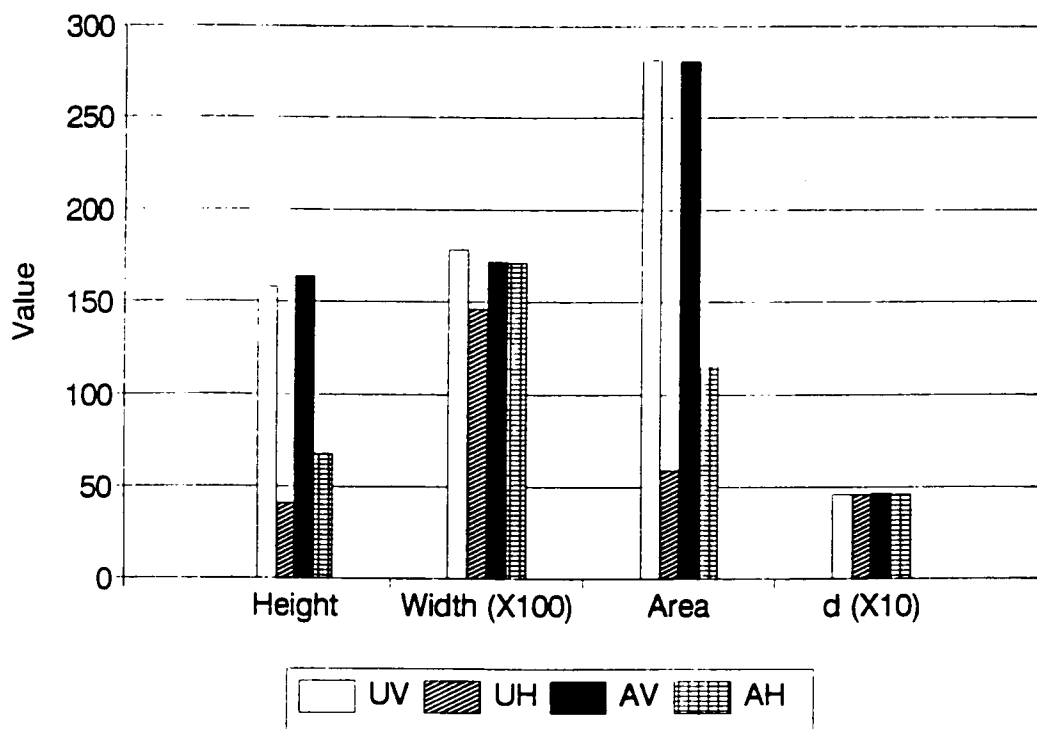Figure 9. Peak parameters for POLYMER A

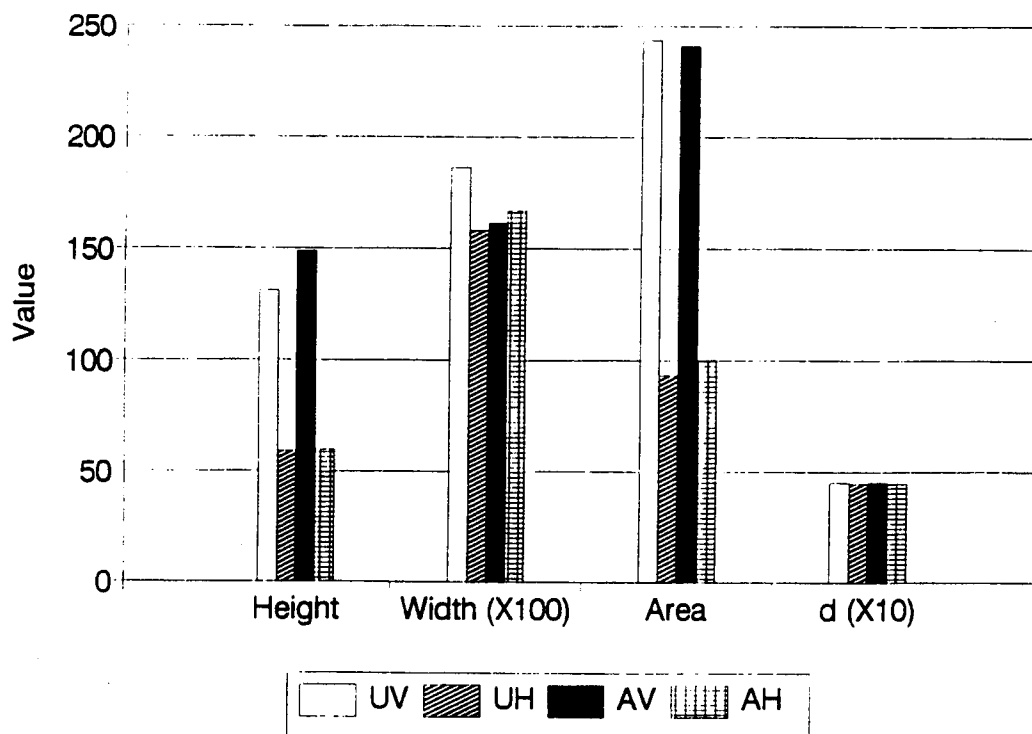Figure 10. Peak parameters for VECTRA B950T

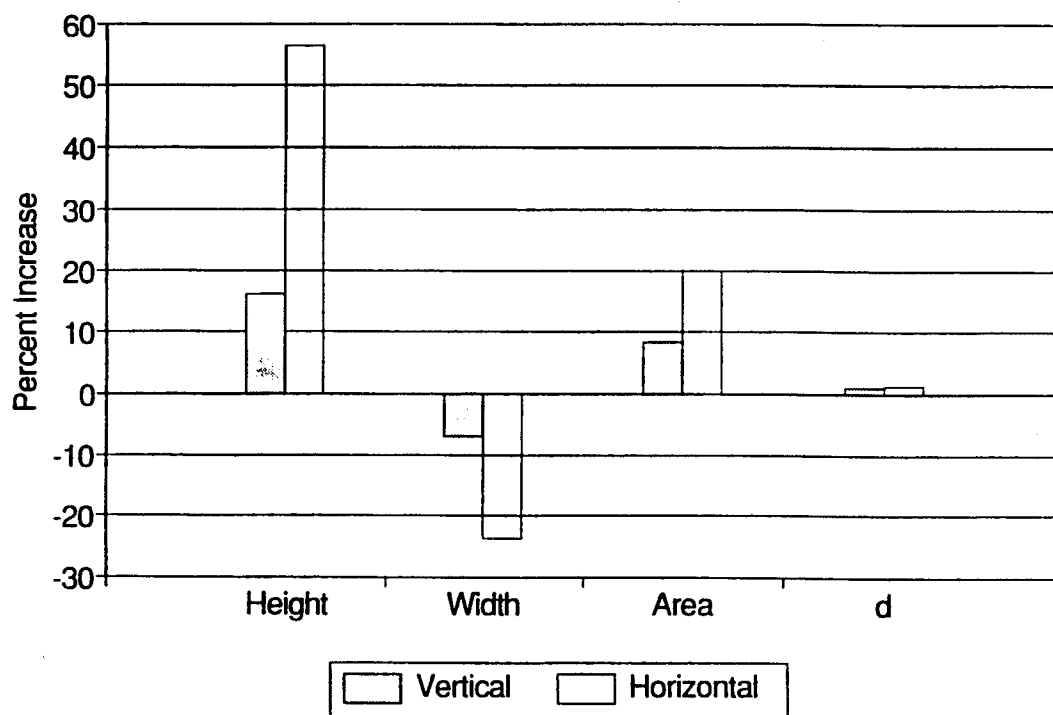Figure 11.   Peak parameters for HX 4000

Figure 12   Percent change in peak parameters for POLYMER A
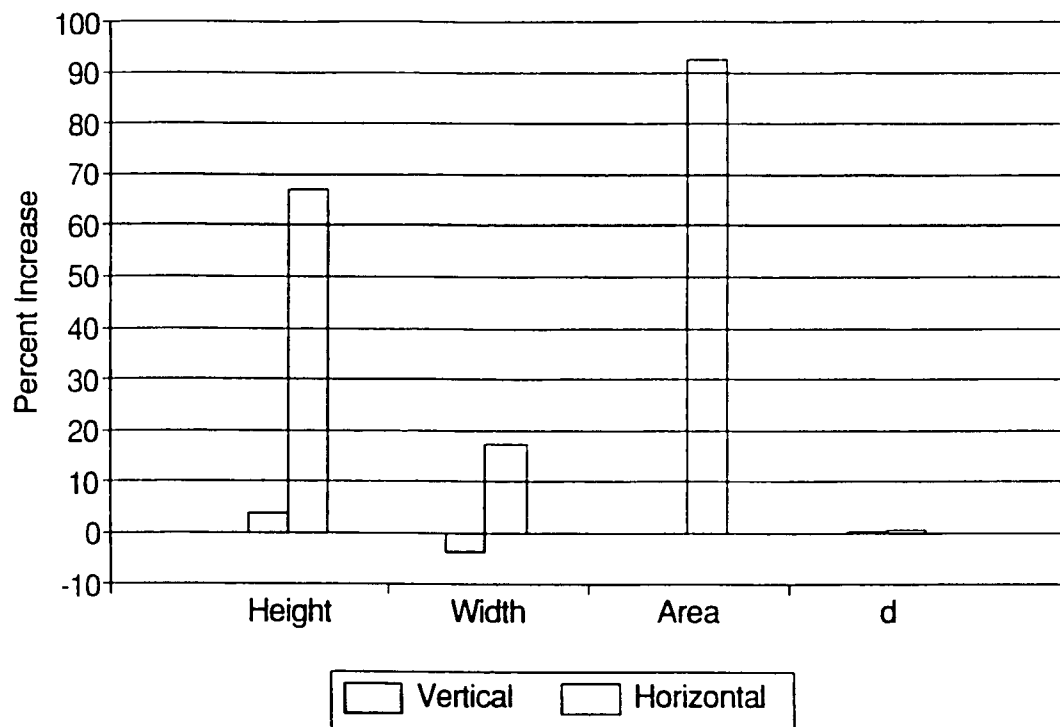
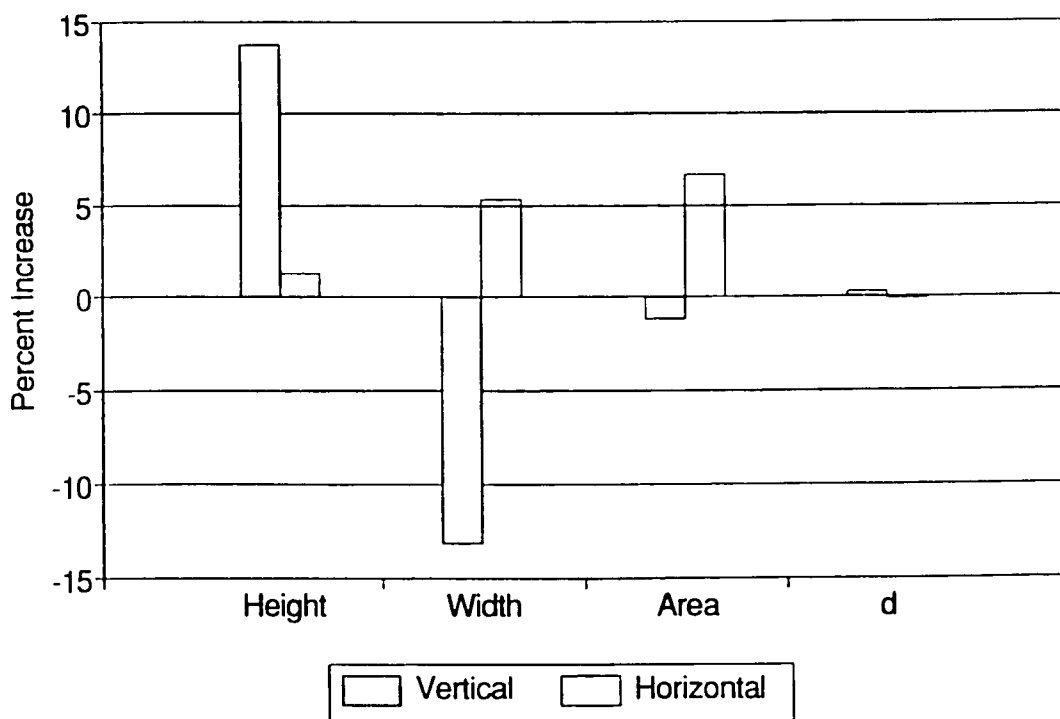Figure 13. Percent change in peak parameters for VECTRA B950T

Figure 14. Percent change in peak parameters for HX 4000

Neutron Diffraction Investigation of the Effect of Gamma Rays

It was suggested by some that gamma rays might have an effect similar to thermal annealing. A sample of SRT 500 powder was exposed to 500 KGray of Co-60 gamma rays. Spectra of the exposed and unexposed powders are shown in Figure 17. There was no difference in the spectra (the difference curve is flat), suggesting that the gamma rays had no effect on the crystalline structure of SRT 500.

X-Ray Diffraction

X-ray diffraction spectra were taken of both skin and core for POLYMER A and for HX 4000. This was done both for untreated and annealed samples. Because the x-rays do not penetrate deeply, the spectra of the skin region were taken of small pieces of sheet directly. To obtain surfaces of core material, the skin was milled off to a depth of about 0.3mm to expose the core. These spectra are shown in Figures 18 through 21.

These spectra are clearly more detailed than those produced by neutron diffraction. Changes with annealing in both the skin and core regions are evident. These spectra have not yet been quantified by peak fitting techniques. Fitting a spectrum with several peaks is significantly more difficult than fitting a single peak. Figure 19 shows that annealing causes the main peak to shrink in the core region of POLYMER A. This result is inconsistent with all of the other x-ray and neutron diffraction data and is therefore suspect. It is possible that the data sets were reversed inadvertently.

Tensile Testing

Table 3 presents the results of the tensile testing on the injection molded commercial LCPs. The HX 4000N polymers were supplied in July, 1993 by Hill Air Force Base. They were from a different batch than the other HX 4000 samples. The suffix "(A16)" means annealed for sixteen hours while "(A32)" means annealed for 32 hours.

Hardness Testing

Table 4. gives the results of Vickers hardness testing of two injection molded commercial liquid crystal polymers. The difference between the Vickers Hardness Numbers (VHN) in the vertical and horizontal directions is a clear indication of the anisotropy of the samples.
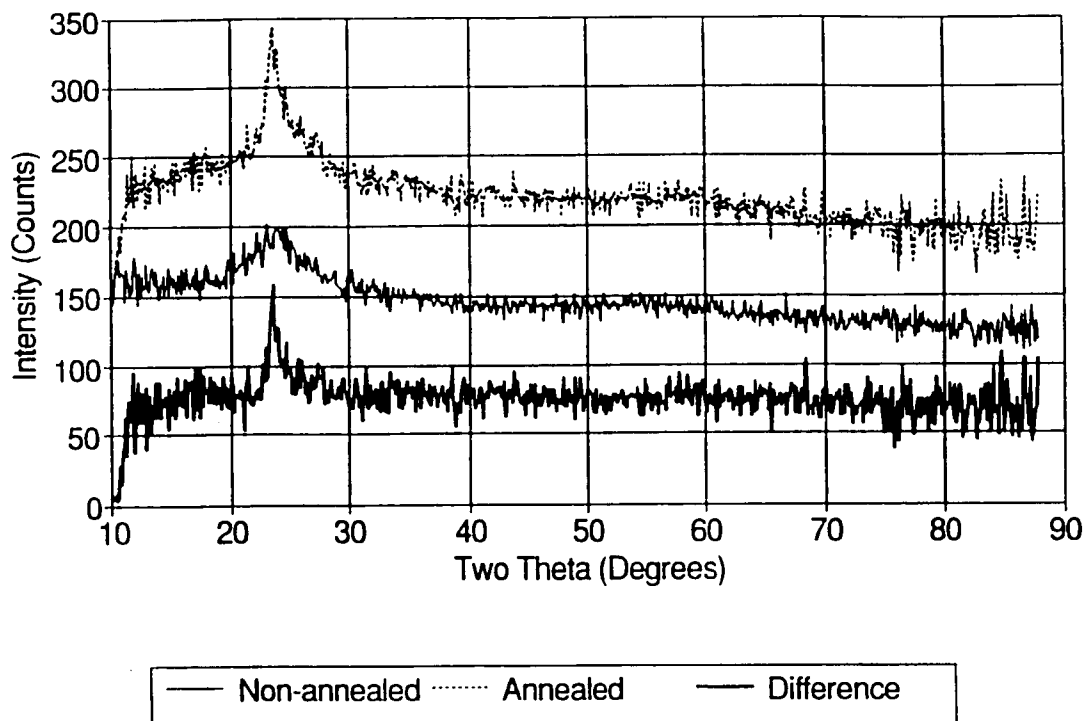
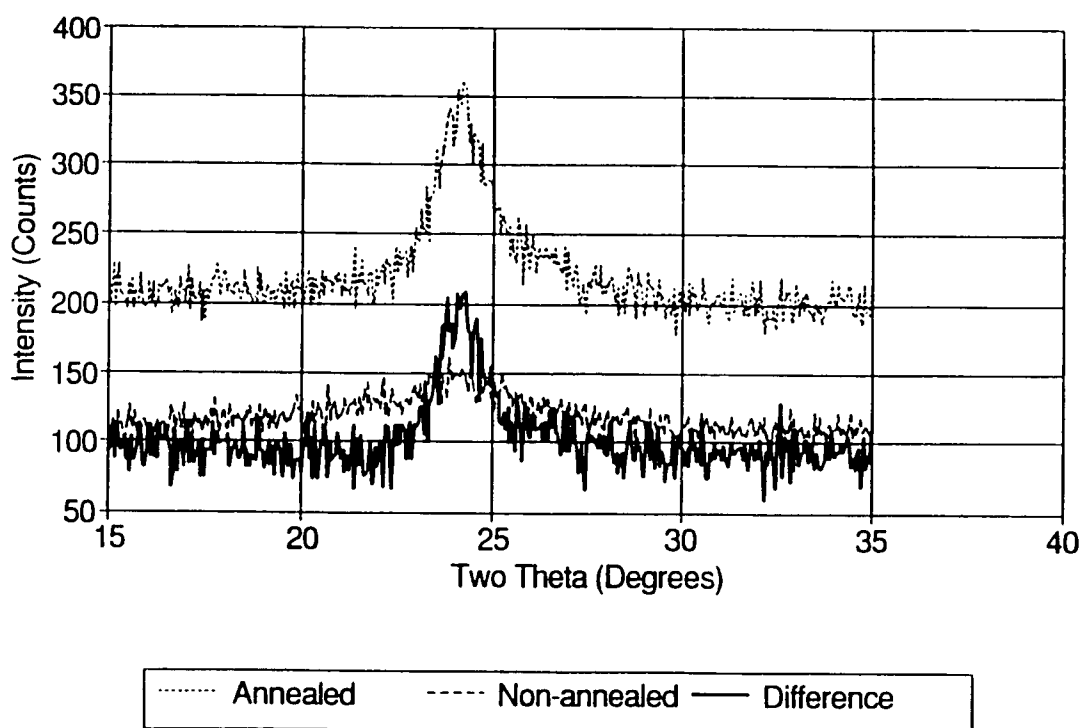Figure 15 Powder spectra for POLYMER A

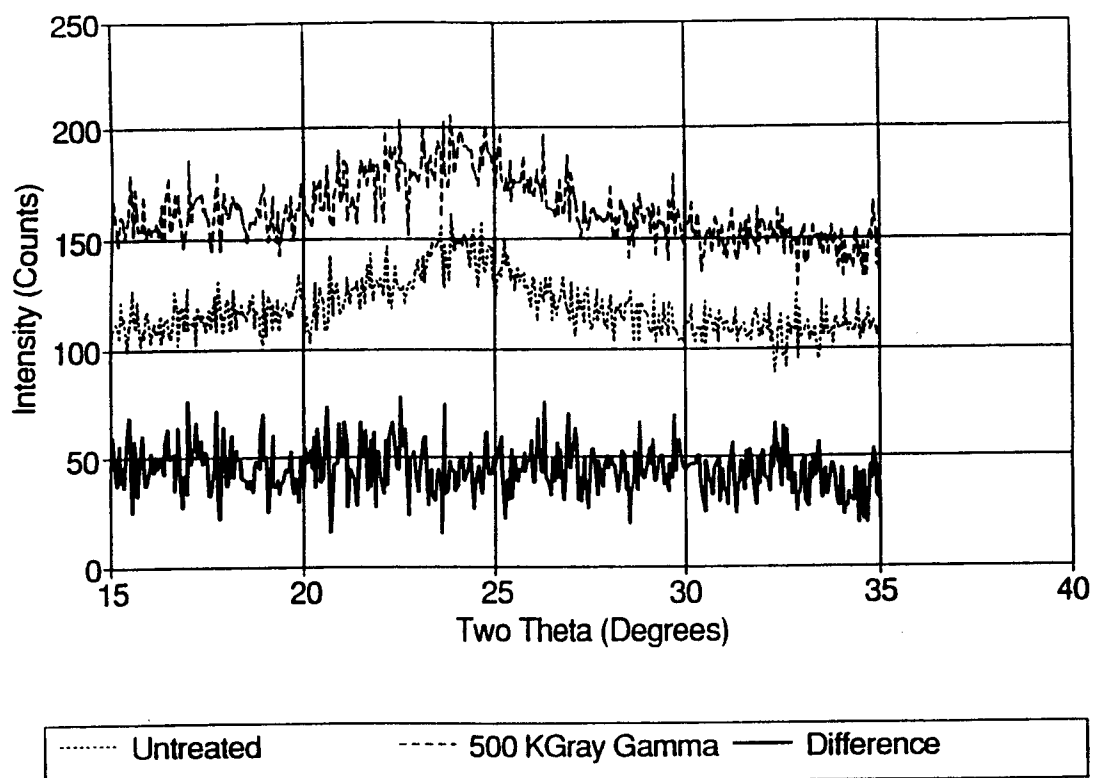Figure 16. Powder Spectra for SRT 500

Figure 17. Spectra for SRT 500 powder untreated and exposed to
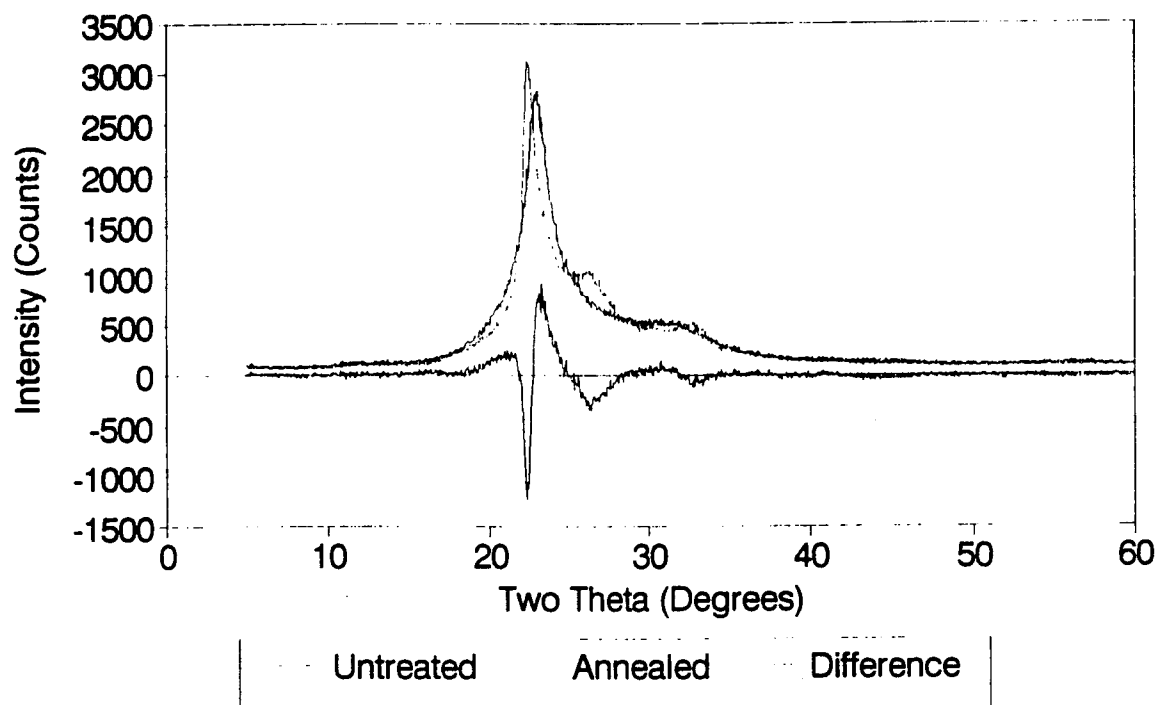500 KGray of Co-60 gamma rays

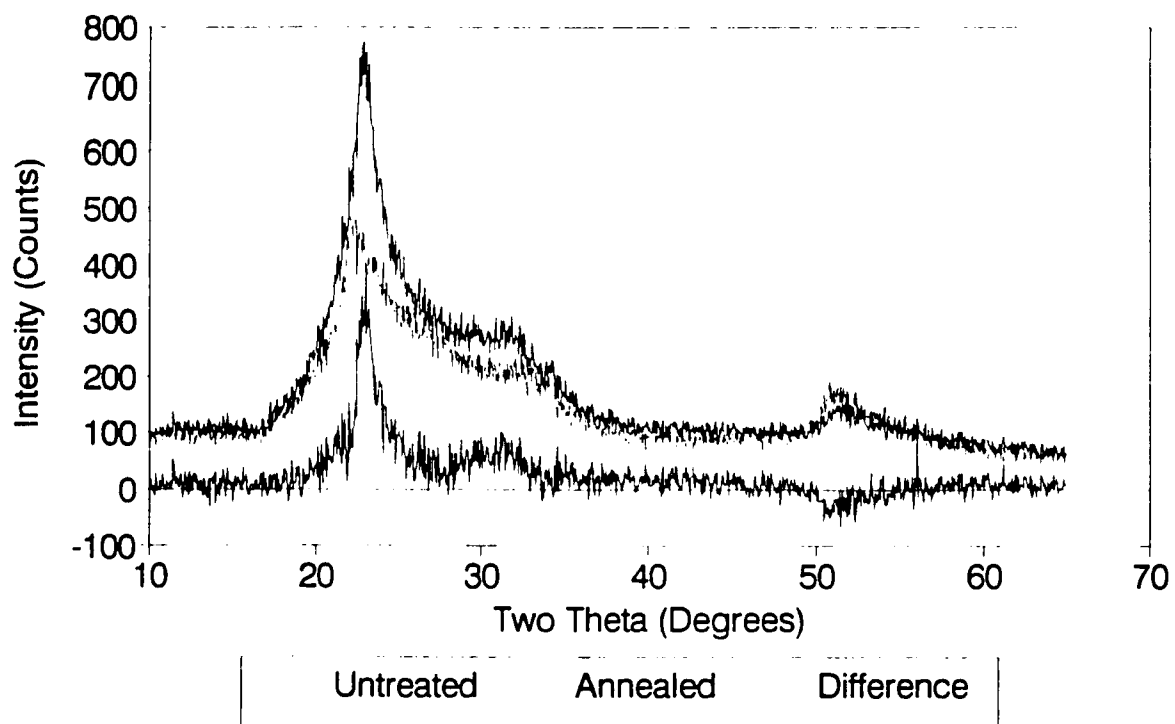Figure 18. X-ray diffraction spectra for POLYMER A skin

153

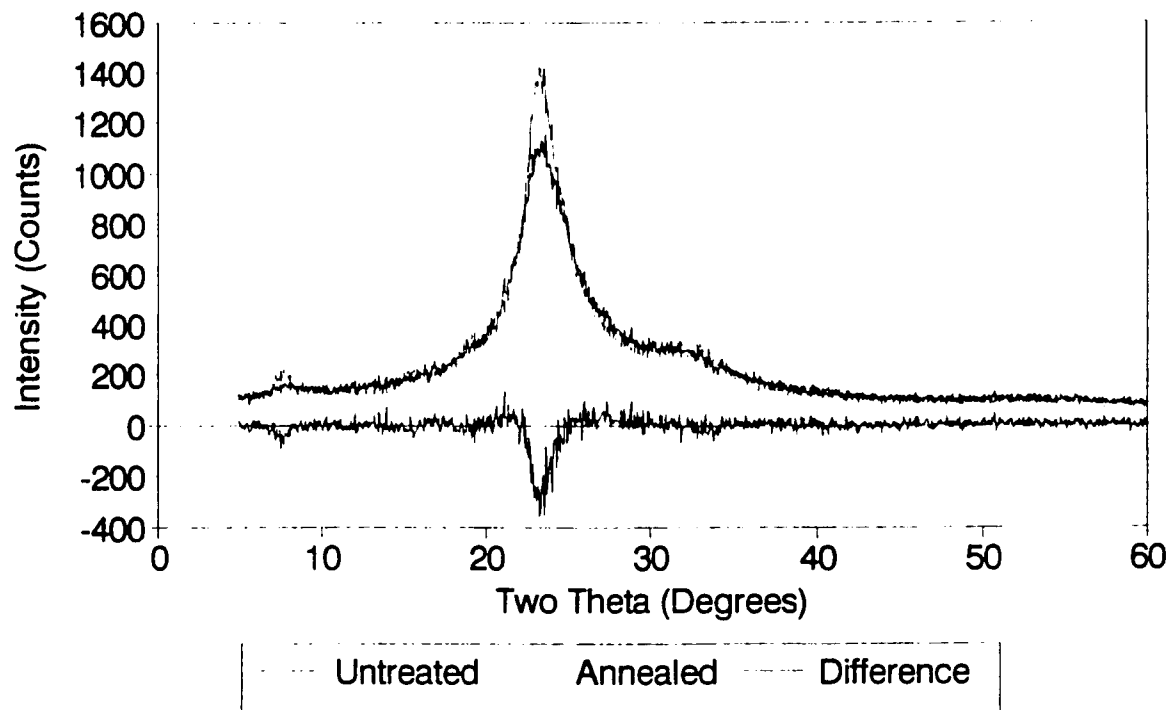Figure 19. X-ray diffraction spectra for POLYMER A core
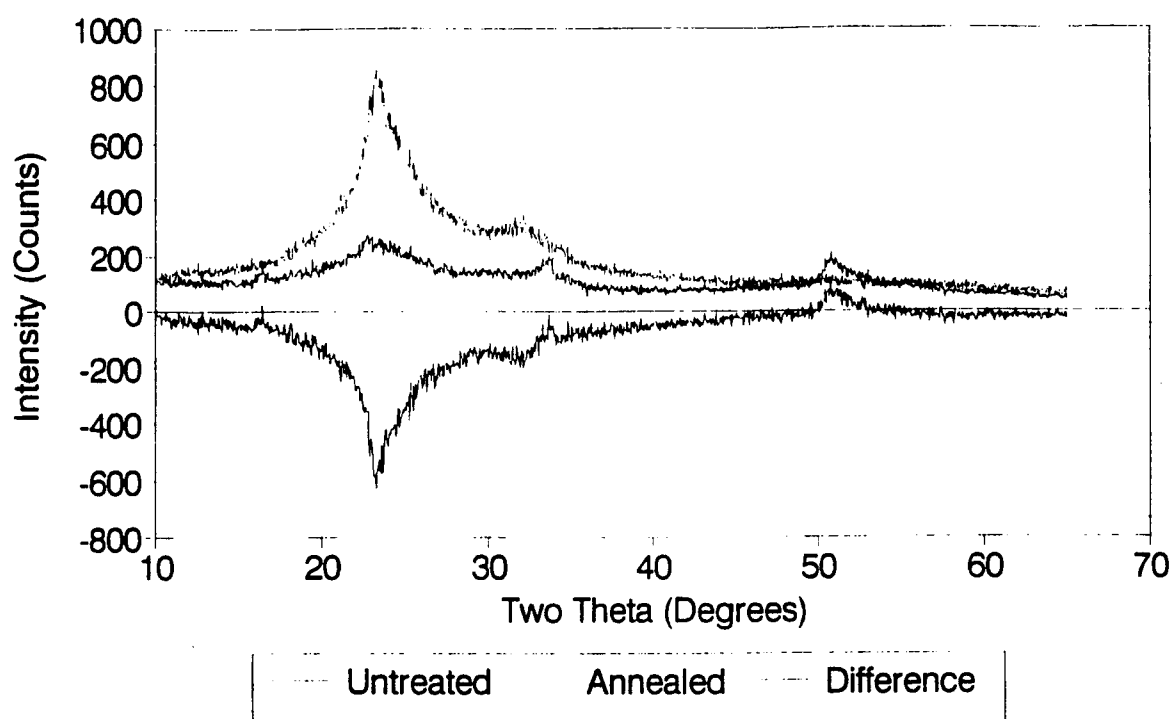

Figure 20. X-ray diffraction spectra for HX 4000 skin

154

Figure 21. X-ray diffraction spectra for HX 4000 core

Material	E (GPa)	UTS (MPa)	Elong. (%)	ROA (%)
VECTRA A950	5.71	97.0	2.64	0.29
VECTRA A950 (A16)	6.25	97.8	1.78	-1.24
HX 4000	11.95	94.4	1.69	-2.16
HX 4000 (A16)	14.01	75.4	2.07	-3.04
HX 4000N	11.56	95.5	0.30	
HX 4000 (A16)	16.56	95.5	0.30	
HX 4000N (A32)	12.15	86.7	0.35	

Table 3. Effect of annealing on the mechanical properties of injection molded LCPs.

HX 4000		
Sample	**d**	**VHN**
4 Vertical	258	27.87
4 Horizontal	318	18.35
4A Vertical	269	25.64
4A Horizontal	302	20.34

Percent increase after annealing:
    Vertical   -8.0%
    Horizontal 10.8%		

VECTRA A950		
Sample	**d**	**VHN**
2 Vertical	344	15.68
2 Horizontal	410	11.04
2A Vertical	274	24.71
2A Horizontal	328	17.25

Percent increase after annealing:
    Vertical   57.6%
    Horizontal 56.2%		

Table 4.   Hardness testing results ("A" means annealed for 16 hours at 260
deg. C in argon.)

Scanning Electron Microscopy of Fracture Surfaces

Visual examination of the surfaces of injection molded LCP parts
suggests that the mechanical properties might be anisotropic because the
direction of flow of the material into the mold is obvious in most cases.
Observation of cut surfaces reveals the highly inhomogeneous character of
these parts. There are obviously distinct skin and core regions. The
anisotropic and inhomogeneous character of these materials is dramatically
confirmed when the fracture surfaces of parts failed in tension are observed
under high magnification in a scanning electron microscope. In addition,
there is clearly a major effect of annealing on the macroscopic structure.

The annealing was done before the samples were failed. Figure 22 shows the fracture surface of untreated VECTRA A950 and Figure 23 shows the fracture surface of annealed VECTRA A950. The magnification for both Figures 22 and 23 was 4000. Figure 24 shows the fracture surface of untreated HX 4000 and Figure 25 shows the fracture surface of annealed HX 4000. As with the VECTRA A950, the magnification in both cases for HX 4000 was 4000.

The most startling observation for the untreated fracture surfaces of both materials is their highly fibrous nature. The fibers do not look like random fibers embedded in an amorphous matrix. Instead they appear very distinct and individualized. There is little or no evidence amorphous material or matrix in either case. The appearance of the fracture surfaces for these materials after thermal annealing is noticeably different than the appearance of the untreated surfaces. In the case of VECTRA A950, the fibers in the annealed sample appear to have been softened and some of them appear to be bonded together. There are regions where the fibers appear to have melted together to form a sheet like texture. In the case of HX 4000, this transformation from a fibrous to a sheet like texture appears to be essentially complete.

CONCLUSIONS

The principal objective of this work was to assess the feasibility of using neutron diffraction as a tool to investigate the crystalline properties of injection molded parts made from commercially available liquid crystal polymers. Neutron diffraction spectra were obtained from parts made from five different LCPs. Spectra were obtained both from solid parts and from powders obtained from solid parts. In all cases, only one peak was resolvable. Because there was only one peak, no characterization of the crystal structure itself was possible. The peak parameters of location in 2θ, height, width at half maximum, and area were easily quantifiable and these were found to vary with orientation of the solid sample and with thermal annealing in argon at 260 de. C for 16 hours. Because very little is known about the crystalline properties of these materials, particularly in the injection molded form, the temptation to try to draw conclusions about such properties from these results was very great. The results, unfortunately do not warrant drawing any such conclusions. They are based on very few (usually only one) data points. Therefore, these results must be considered interesting and certainly suggestive but not definitive.

It must also be recognized that neutron diffraction is a time consuming
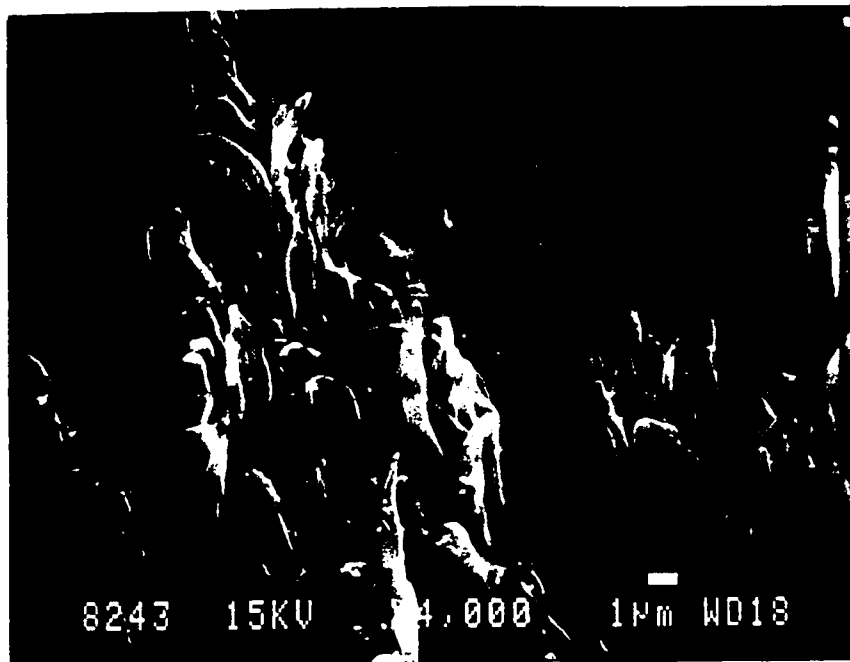
Figure 22   Fracture surface of untreated VECTRA A950
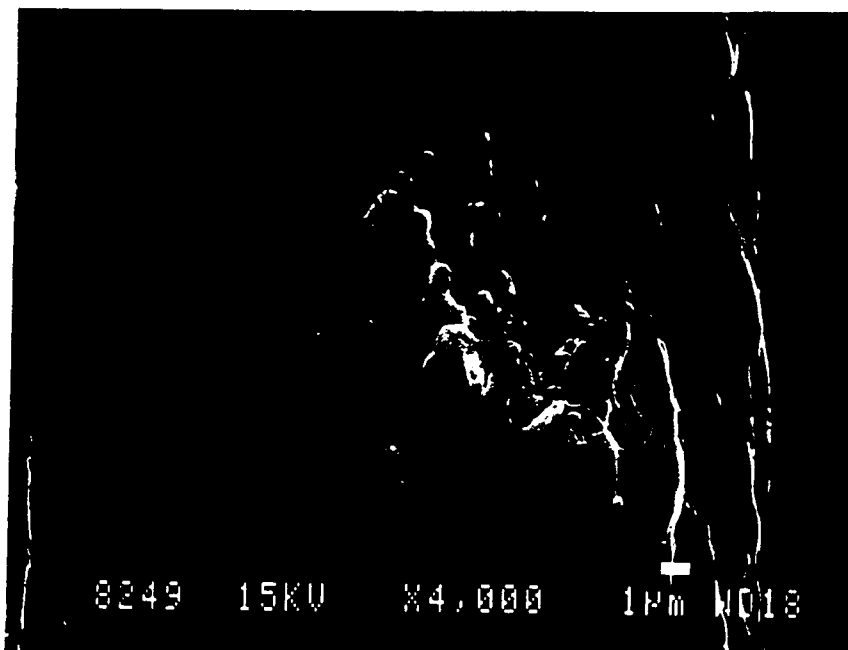

Figure 23   Fracture surface of annealed VECTRA A950

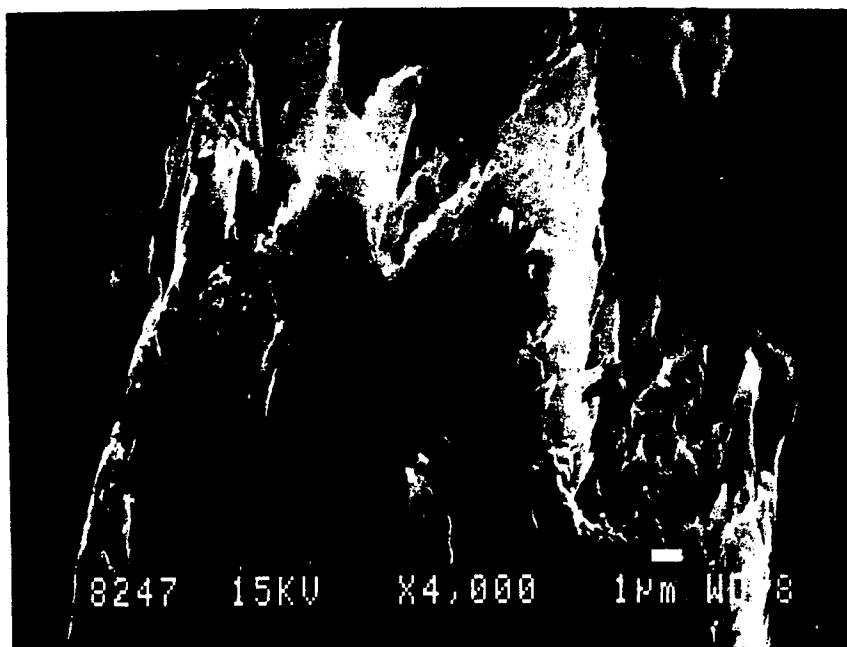Figure 24   Fracture surface of untreated HX 4000

Figure 25   Fracture surface of annealed HX 4000

and expensive experimental technique. It takes from five to ten hours of dedicated beam time to obtain a single full range spectrum. Beam time, if it had to be paid for, would be very expensive. It can be concluded, therefore, that neutron diffraction is capable of measuring some but not all of the crystalline properties of injection molded LCPs. At the same time it must be observed that X-ray diffraction appears to be capable of measuring these same parameters while providing significantly more detailed information about the crystalline structure.

In summary, the several specific conclusions about the crystalline and mechanical properties of injection molded parts made from commercial liquid crystal polymers can be drawn from this work. The more important of these are listed below.

- o   Neutron diffraction of injection molded LCPS using the HRPD at ANSTO is capable of resolving only a single peak.
- o   All five of the commercial LCPs tested showed a strong peak corresponding to a d spacing of 4.4 to 4.6 Angstroms. All of these materials are, therefore, at least partially crystalline.
- o   Changes in the peak parameters of position, height, width at half maximum, and area can be measured reliably and consistently.
- o   The peak parameters are clearly affected by sample orientation and by annealing at 260 deg. C for 16 hours.
- o   The measured d spacing corresponding to the single neutron diffraction peak increases by 1% to 1.5% on annealing for POLYMER A and VECTRA A950. The change is not measurable for the other samples.
- o   For POLYMER A, VECTRA B950T, and HX 4000, The area of the neutron diffraction peak is greater in the vertical orientation.
- o   For POLYMER A, VECTRA B950T, and HX 4000, the area of the neutron diffraction peak either stays essentially the same or grows with annealing. The peak growth is greater in the horizontal orientation.
- o   For HX 4000, annealing for 16 hours causes substantial growth in the area of the vertically oriented neutron diffraction peak. Annealing for 32 hours results in the peak area returning nearly to its unannealed value.
- o   For HX 4000, annealing for 16 hours causes a substantial increase in the elastic modulus (about 43%). Annealing for 32 hours results in the elastic modulus returning nearly to its unannealed value. This effect correlates well with the change in the area of

160

the vertically oriented neutron diffraction peak.

o   Irradiation with Co-60 gamma rays to 500 KGray causes no
    measurable effect on the neutron diffraction peak.

o   X-ray diffraction, being capable of resolving three or four peaks
    in injection molded commercial LCPs and being much cheaper and
    less time consuming than neutron diffraction is the preferred
    technique for investigating the crystalline properties of these
    materials.

o   The elastic modulus increases with annealing in argon at 260
    deg. C for 16 hours for VECTRA A950 and HX 4000. The increase for
    HX 4000 (17% to 43% depending on the sample batch) is greater than
    for VECTRA A950 (9%).

o   Hardness measurements for these materials are difficult to perform
    and interpret. The Vickers method is uniquely capable of
    detecting difference in hardness as a function of orientation.

o   The effect of annealing on hardness is very different for VECTRA
    A950 (56% increase) and HX 4000 (little effect).

o   Both the crystalline and the mechanical properties of parts made
    from injection molded LCPs are profoundly affected by processing
    variables during the molding process.

o   The fracture surfaces of HX 4000 and VECTRA A950 show an almost
    totally fibrous structure with little visible evidence of
    amorphous regions.

o   Annealing at 260 deg. C in argon for 16 hours profoundly affects
    the macroscopic structure of the fracture surfaces of HX 4000 and
    VECTRA A950. The texture changes from fibrous to sheet like, the
    effect being much more pronounced in HX 4000.

RECOMMENDATIONS

Further experimental investigations of the crystalline and mechanical
properties of injection molded liquid crystal polymers and how these
properties are affected by processing variables, both during and after molding
should be carried out. X-ray diffraction should be the primary technique for
future investigations of the crystalline properties.

Molecular modelling of these materials is critical to understanding
their behavior in the solid state. Theoretical studies should be pursued
vigorously.

161

Design and preparation of samples optimized for each particular experiment is crucial in future efforts. Careful control of process variables is essential. Thin shear sheet samples could be used for both x-ray and neutron diffraction experiments as well as future small angle neutron scattering and inelastic neutron scattering experiments. These later experiments should provide answers to fundamental questions on interchain interactions.

A serious effort should be undertaken to model the crystalline properties of these materials as they exist in injection molded parts. Modelling of the crystalline structure might begin with consideration of the structure of KEVLAR fibers as reported in the literature [4] and how that structure changes with thermal annealing. Thin shear sheet samples should be useful in this effort as well as in support of the molecular modelling. X-ray diffraction appears to be a particularly promising technique here. Studies of the effects of thermal annealing in thin shear sheets can be done in situ with x-ray diffraction and such studies are highly recommended.

ACKNOWLEDGEMENTS

REFERENCES

1. Elements of Physical Metallurgy, Third Edition, A.G. Guy and J.J. Hren, Addison-Wesly, Reading, MA, 1974
2. Neutron Diffraction, G.E. Bacon, Clarendon Press, Oxford, 1975
3. Elements of X-ray Diffraction, B.D. Cullity, Addison-Wesley, Reading, MA, 1956
4. Properties and Applications of Liquid-Crystalline Main-Chain Polymers, M.G. Dobb and J.E. McIntyre, Advances in Polymer Science 60/61, Springer-Verlag, Berlin, 1984

ION BEAM ANALYSIS TECHNIQUES APPLIED TO POLYMER SAMPLES

Christian A. Zorman and Richard W. Hoffman
Department of Physics
Case Western Reserve University
Cleveland, Ohio 44106

Rutherford backscattering spectroscopy (RBS), elastic recoil detection (ERD) and proton elastic scattering (PES) are a few of the ion beam analysis techniques that can be used to acquire composition and thickness information on thin solid films. RBS is used to determine the non-hydrogen atomic composition of a specimen and is well-suited for depth profiling high Z elements in a low Z matrix. PES provides the same information but is more sensitive to low Z elements than RBS. ERD is one of the few techniques that directly measures the depth profile of hydrogen or deuterium in a sample. Requiring only high vacuum conditions and a modest set of electronics, the only real obstacle to performing ion beam analysis is obtaining access to an MeV ion accelerator. Each of these techniques is routinely used in many areas of material science but has seen limited use on polymers.

This paper presents our experiences with MeV ion beam analysis probes on polymer samples. An overview of each technique will be presented as well as the advantages and disadvantages of each as they pertain to polymers. Special emphasis will be placed on methods of minimizing beam induced damage.

INTRODUCTION

Rooted in the study of low-energy atomic and nuclear physics of the mid 20th Century, MeV

ion scattering spectroscopy has found a very important niche in materials fabrication and analysis. By collecting important information such as scattering cross sections and stopping powers, the nuclear physics community laid the necessary groundwork for material scientists to develop powerful ion beam based techniques used to depth profile thin films. The transition of these techniques from nuclear physics to materials research occurred when high energy accelerators were produced. Abandoned by the nuclear physics community, low energy accelerators such as the 3 MeV van de Graaff electrostatic generator, were resurrected by the materials community. With minor modification, these accelerators provide ion beams which can be used to measure the atomic composition and thickness of samples to depths of several microns. Used widely in semiconductor and metallurgical fields, ion scattering has seen limited use in studying polymers.

The main component in an MeV ion scattering setup is, of course, the ion beam source. Commercial sources are available, but many researchers have recommissioned old Van de Graaff electrostatic generators for this purpose. Most of these machines were designed to produce helium and proton beams with energies between 1 to 4 MeV, suitable for most ion scattering spectroscopies. The rest of the required equipment is really quite simple, a scattering chamber capable of maintaining a vacuum of 10^{-6} torr, a few surface barrier detectors and the associated counting electronics, a multichannel analyzer and a PC. A detailed outline of an ion scattering setup has been described by many sources, most notably Chu, Mayer and Nicolet[1] and will not be described here.

RUTHERFORD BACKSCATTERING SPECTROSCOPY

Rutherford Backscattering Spectroscopy (RBS) is the most common of the MeV ion scattering spectroscopies. In RBS a beam of monoenergetic ions, $^4He^+$ for example, is directed at a sample, which is typically oriented perpendicular to the beam. A solid state surface barrier detector is placed at a large angle with respect to the incident beam and is calibrated to collect the backscattered He ions. This detector is energy sensitive and by means of a preamp, amplifier and MCA, the backscattered ions are displayed as the number of counts vs channel. Computer software then converts the data to counts vs energy by means of a known channel to energy conversion. From this data, a depth profile of the sample for every element except hydrogen can be obtained.

To obtain the composition of a sample, an understanding of the scattering processes is required. Determining the composition involves two key concepts, the collision process and the scattering cross sections of the target atoms. The backscattering process involves a simple binary elastic collision. From conservation of energy and momentum, the energy transferred from the projectile to the target can be calculated. Therefore a measurement of the energy of the backscattered helium yields the mass of the target atoms. Since each element has a unique mass, excluding isotopes, the elements contained in a compound target can be determined. To obtain the amount of each element in a sample, one must also know the scattering cross sections of its atomic components. Fortunately for this energy regime, these cross sections, known commonly as Rutherford cross sections, are well behaved, varying monotonically with energy and as the square of the atomic number of the target atoms. Since the scattering yield is proportional to the Rutherford cross section, the scattering yield from heavy elements is much greater than that from

light elements. Combining the collision information with the scattering cross sections enables the spectroscopist to determine the surface composition of the sample.

In order to obtain a depth profile of a sample, the energy loss of the beam as it traverses the sample must be known. As the beam penetrates the sample, it undergoes inelastic collisions with electrons, thus loosing energy. It undergoes similar losses after a backscattering collision in the sample. This energy loss can be converted to a depth scale if the stopping cross section of the target is known. For single element targets, these cross sections have been measured. It has been shown that for most multielemental samples, the stopping cross section of the sample is the weighted sum of the stopping cross sections of its components. Therefore, for most materials, RBS can be used for depth profiling. Due mainly to the mass dependence of the scattering cross sections, RBS is most effective in probing heavy elements in a light element matrix. Because the collision takes place between the projectile and target nuclei, RBS is not generally sensitive to chemical effects in the target. But because of this, RBS does not yield any direct information about the chemical state of the target.

PROTON ELASTIC SCATTERING

In many ways, proton elastic scattering (PES) is similar to RBS. Aside from the fact that the beam is comprised of protons, the main difference lies in the fact that the scattering cross section for light elements deviates from classical Rutherford scattering, usually by 1 to 2 orders of magnitude[2]. In select energy regions the cross section can also have resonance peaks, an

effect not found in typical RBS. Since the scattering yield is proportional to the scattering cross section, these deviations can be used as a tool to probe concentrations too small to detect with RBS. This is especially true for light elements in a heavy element matrix. In RBS the yield from the heavy element would dominate the spectrum, obscuring the yield from the light element. But for the same system studied using PES, the yield from the light element is enhanced by the non-Rutherford scattering cross section, thus lessening the impact of the heavy element. N. R. Parikh et. al. showed that PES is much more effective at profiling light elements like B, N, and O in a heavy element matrices like Ga, Ba and Si than RBS[3]. Unfortunately some of the cross sections are not well known, ie B at 1 to 3 MeV, so some care must be taken before formulating an experiment. Aside from its greater sensitivity to light elements, PES has other advantages over RBS. Since protons have a greater range in matter than helium, PES can profile much thicker films than RBS. Compared to helium ions at the same energy, protons generally do less thermal damage to a sample since the energy is dissipated over a longer range. Disadvantages of PES include a lower mass resolution and depth resolution than RBS.

ELASTIC RECOIL DETECTION

Due to the mass of the projectiles in RBS and PES, neither technique can be used to profile hydrogen in a sample. However, if an MeV helium beam strikes a sample at grazing incidence, typically 75 degrees to the sample normal, hydrogen in the near surface region will undergo elastic collisions with the helium ions and recoil from the sample in the forward direction. Helium, elastically scattered by heavier elements in the sample, will also recoil in the forward

direction. The recoiling particles can be detected by a surface barrier detector placed in the forward direction, typically 30 deg from the incident beam. In order to insure that only recoiled hydrogen is counted, a stopping foil is placed in front of the detector. Using the fact that at 2 MeV the range of hydrogen is eight times that of helium, the thickness of the stopping foil is adjusted to stop helium while only slightly attenuating hydrogen[4]. As with RBS and PES, if the cross section for the scattering event is known, then the amount of hydrogen in the sample can be determined. This spectroscopy is known by a number of names, most commonly elastic recoil detection (ERD). Until recently, the scattering cross section for this event was not well documented, leaving the experimenter to rely on hydrogenated standards to experimentally determine the cross section. But heightened interest ERD has led numerous groups to make accurate measurements of the cross section[5]. Because of the grazing angle of incidence, ERD does not have the range or depth resolution of RBS and PES. At 2 MeV, ERD can effectively profile hydrogen to a depth of 0.5 microns.

THE ION BEAM ANALYSIS FACILITY AT CWRU

The ion beam analysis facility at Case Western Reserve University is equipped with a model KN Van de Graaff capable of generating He and proton beams of 1 to 3 MeV, sufficient for all the techniques described above. For RBS and PES a detector is positioned at 170 deg with respect to the incoming beam. Beam currents are measured with a Faraday cup and range from 5 to 50 nA, depending on the durability of the sample. The detector subtends a solid angle of 1.25×10^{-3} steradians. A typical spectrum can be collected in 15 to 25 minutes. In the ERD

168

mode, a detector, placed 30 deg with respect to the incoming beam, subtends a solid angle of .1x10^{-3} steradians. Beam currents are generally kept between 10 and 20 nA. An RBS spectrum is collected simultaneously and this information is used to determine the total charge incident on the sample. For RBS and ERD, the RUMP program is used to analyze the data[6]. Due to the non-Rutherford cross sections, PES data is not currently analyzed using RUMP. Therefore, PES is used solely as a qualitative tool.

RBS, PES and ERD are best suited for conducting samples. These techniques can be used on insulators, but special precautions are usually taken to minimize decomposition of the sample. The simplest is to limit the current density and total charge on target. This can be done by defocussing and increasing the diameter of the incident beam. Some facilities can raster the incident beam, therefore minimizing the total charge on any particular part of the sample. One can simply move to different spots on the sample to accomplish the same result. This only works if the sample is uniform over the area being probed. Other researchers use a liquid nitrogen cooled sample holder to essentially "freeze" the atoms in place[7]. Since RBS, PES and ERD are not influenced by chemical effects in the sample, this technique seems to work. At CWRU we do not have such a sample holder, but have found that by minimizing exposure and defocussing the beam, decomposition of the polymer samples studied has been minimal.

EXAMPLES

To demonstrate the usefulness of RBS, PES and ERD in studying polymer and insulating

samples, this paper will present four examples. Ionic profiling of polypyrrole and bromine substitution in polythiophene were studied using RBS. The hydrogen content of a spin coated polystyrene thin film was determined by ERD. PES was used in a qualitative way to profile an amorphous diamondlike carbon film.

In the first example RBS was used to determine the ionic profile in polypyrrole films as a function of charge[8]. The polypyrrole films were deposited onto Grafoil (GTA grade - Union Carbide) substrates from deaerated, aqueous solutions of 0.05 M pyrrole in 0.1 M NaClO$_4$. A potential of 0.7 V SCE was used to deposit the films. After deposition, the films were cycled between -700 and +250 mV SCE at 20 mV/s and the cycle was stopped at either the upper or lower limit and held for 10 minutes to completely oxidize or reduce the films. At this point the films were either removed from the solution or the potential was stepped to the other limit until the desired quantity of charge had passed. Once out of solution, the films were analyzed for ionic content by RBS. Figure #1 shows a typical RBS spectrum for a polypyrrole film grown in NaClO$_4$ solution and oxidized at +250 mV for 10 minutes. The backscattered yield in channels 200 and below is that from the grafoil substrate, the rest being from the film. The edges indicated by N and C represent the yield from the polypyrrole, while the edges indicated with O and Cl represent the yield from the perchlorate ion. From this data, the ionic content of the polymer can be determined. Not only can the ionic content be determined, but also the relationship between deposition charge and film thickness. Figure 2 shows RBS spectra for five films deposited with varying deposition charges. The region shown encompasses only the Cl peak. The width of the peak, representing the energy loss of the incident helium ions as they

travel through the film, directly corresponds to the thickness of the film. As expected, the greater the deposition charge, the thicker the film. An analysis of the RBS data showed no deviation from the expected C:N ratio, suggesting that the polymer was not damaged.

RBS was also conducted on bromine substituted polythiophene thin films in order to determine the amount of Br substitution. The films were made by personnel at Wright Laboratory following a prescription outlined elsewhere[9]. The films analyzed by RBS where deposited onto Si substrates. Figure 3 shows a representative spectrum. The signals denoted by C, S, and Br are from the polymer film. It is clearly evident from the spectrum that the sulfur is uniformly distributed throughout the film. However the shape of the bromine signal near the high energy edge indicates that the region near the surface of the film is bromine deficient. This may be evidence of beam induced damage. Since bromine is substituted for hydrogen at the ends of the polymer chains, it is more likely to break from the polymer when hit by the ion beam than sulfur or carbon, which comprise the polymer backbone. But this Br deficiency may result from the deposition process and not beam damage. In any case, it is clear from the spectrum that RBS can be used to detect nonuniformities in polymer films.

As mentioned earlier, ERD requires hydrogenated calibration standards in order to check detector alignment and scattering cross section data. A common standard is hydrogen implanted silicon because it suffers minimal beam damage. Polymer films are not usually used as reference standards because of the possibility of extensive beam damage, but they can be used to check detector alignment. Figure 4 show an ERD spectrum from a 1000 angstrom thick

polystyrene film spin coated on a stainless steel substrate. Analysis of the data yielded a hydrogen content of about 50 atomic percent, very close to polystyrene. If care is taken, ERD can be used as a tool in determining the hydrogen content of polymer thin films.

The last example illustrates the difference between PES and RBS. Figure 5 shows an RBS spectrum collected from a diamondlike carbon film deposited on a Si substrate. Figure 6 shows the same film studied by PES. Two differences are obvious, the sharp peak associated with the carbon signal in the PES spectrum and the decrease in the silicon yield at lower energies in the PES spectrum. Both of these effects result from the proton non-Rutherford scattering cross section associated with carbon and silicon. By employing the carbon resonance at 1.735 MeV, dilute concentrations of carbon can be detected.

CONCLUSIONS

The four examples shown here illustrate just a few of the applications MeV ion scattering spectroscopy has in studying polymer systems. With each of technique, some care must be taken to insure minimal beam damage. RBS, the most common of the techniques, is best suited for heavy element detection in a light element matrix, while PES is better at detecting light elements. ERD is one of only a few thin film techniques that can be used to determine the hydrogen content of a material.

The authors would like to thank Dr K. P. Chaffee of the Phillips Laboratory, Edwards AFB

for teaching the fine art of operating a 30 year old Van de Graaff, Dr. J. S. Wainright of

CWRU's Chemical Engineering Department for depositing the polypyrrole films, Dr. G. A.

DeRose of Wright Laboratory, Wright Patterson AFL for providing the bromine substituted

polythiophene samples and Dr. J. S. Shiao of CRWU's Physics Department for depositing the

diamondlike carbon films.

REFERENCES

1. W. K. Chu, J. W. Mayer and M. A. Nicolet, "Backscattering Spectroscopy", (Academic Press, New York, 1977).

2. N. R. Parikh, Z. H. Zhang, M. L. Swanson, N. Yu and W. K. Chu, Mat. Res. Soc. Symp. Proc. Vol. **128**, pp 375-380 (1989).

3. N. R. Parikh, Z. H. Zhang, M. L. Swanson, N. Yu and W. K. Chu, Mat. Res. Soc. Symp. Proc. Vol. **128**, pp 375-380 (1989).

4. L. C. Feldman and J. W. Mayer, "Fundamentals of Surface and Thin Film Analysis", (North-Holland, New York, 1986) p. 63.

5. Y. Kido, S. Miyauchi, O. Takeda, Y. Nakayama, M. Sato and K. Kusao, Nucl. Instr. and Meth. **B9** 474-480 (1993).

6. L. R. Doolittle, Nucl. Instr. and Meth. **B9** 344 (1985).

7. R. Oganjanovic, C. Y. Hui and E. J. Kramer, Jour. of Mat. Sci. **25** 514-518 (1990).

8. Ph.D. dissertation, J. S. Wainright, Case Western Reserve University, 1992.

9. P. Haaland and J. Targrove, Appl. Phys. Lett. **61**, (1), 34-36, (1992).
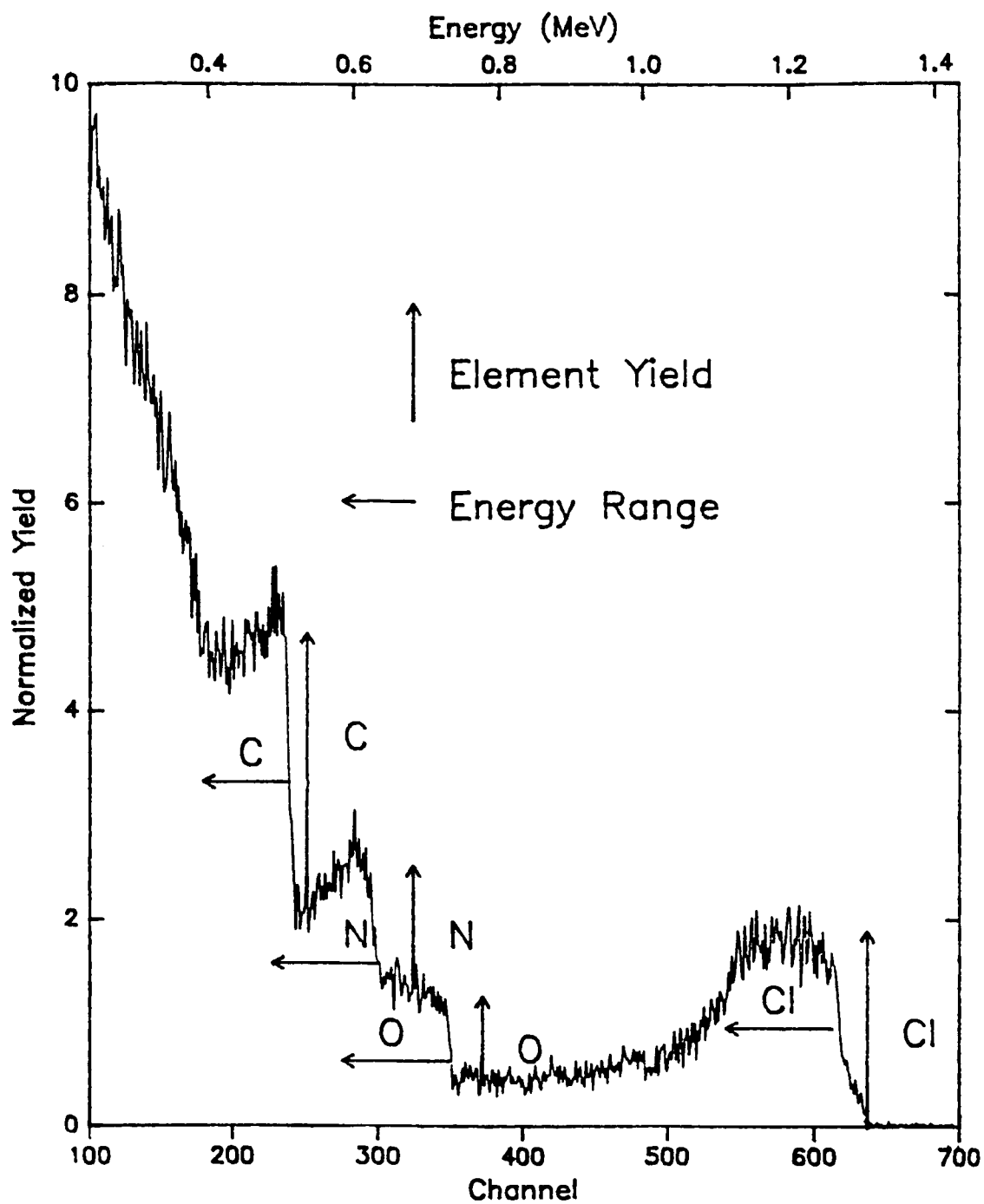
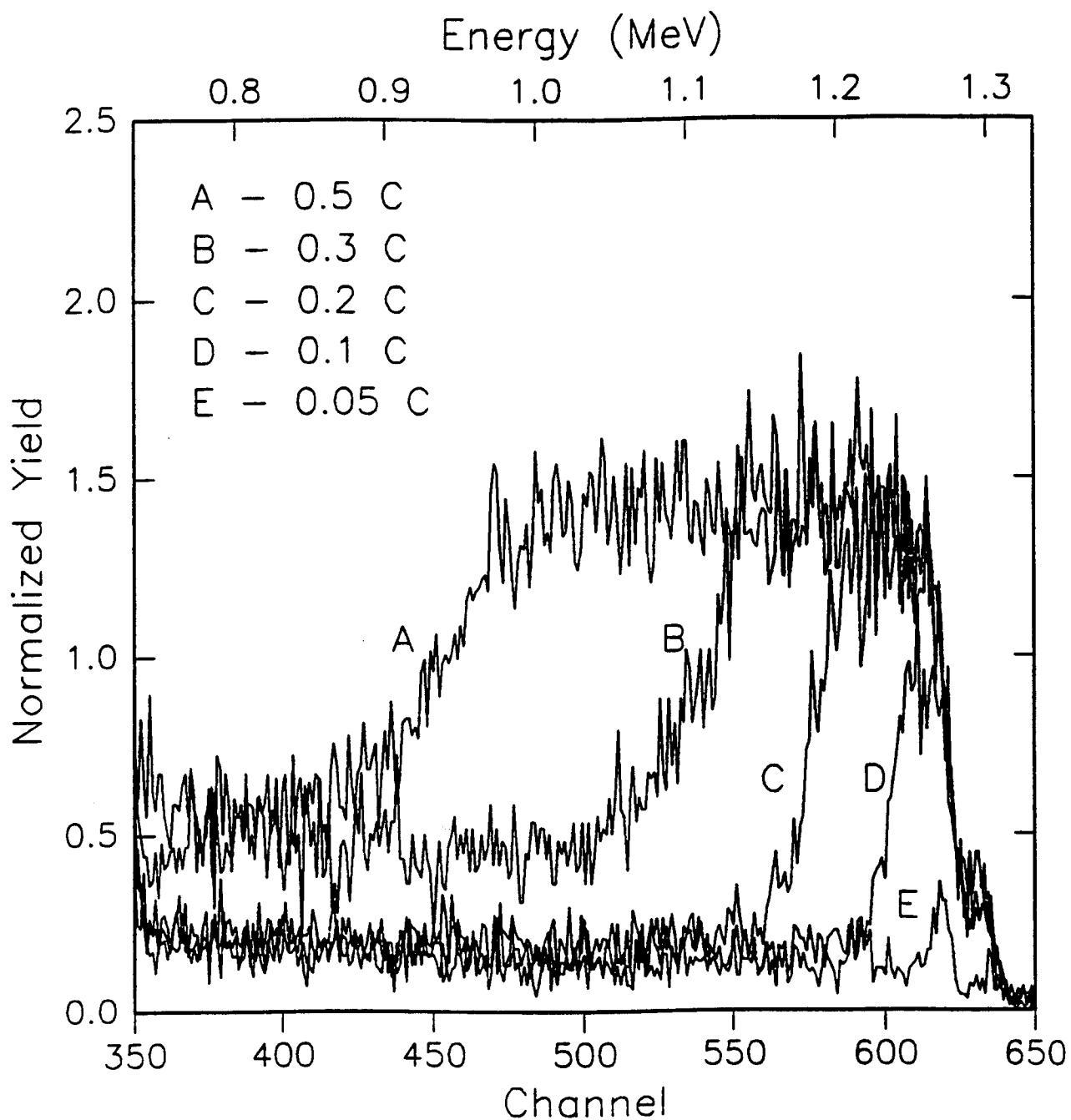FIGURE 1. RBS spectrum of a polypyrrole thin film grown in a NaClO₄ solution.

FIGURE 2. RBS spectrum a of polypyrrole thin film at the Cl edge showing the relationship between depostion charge and film thickness.
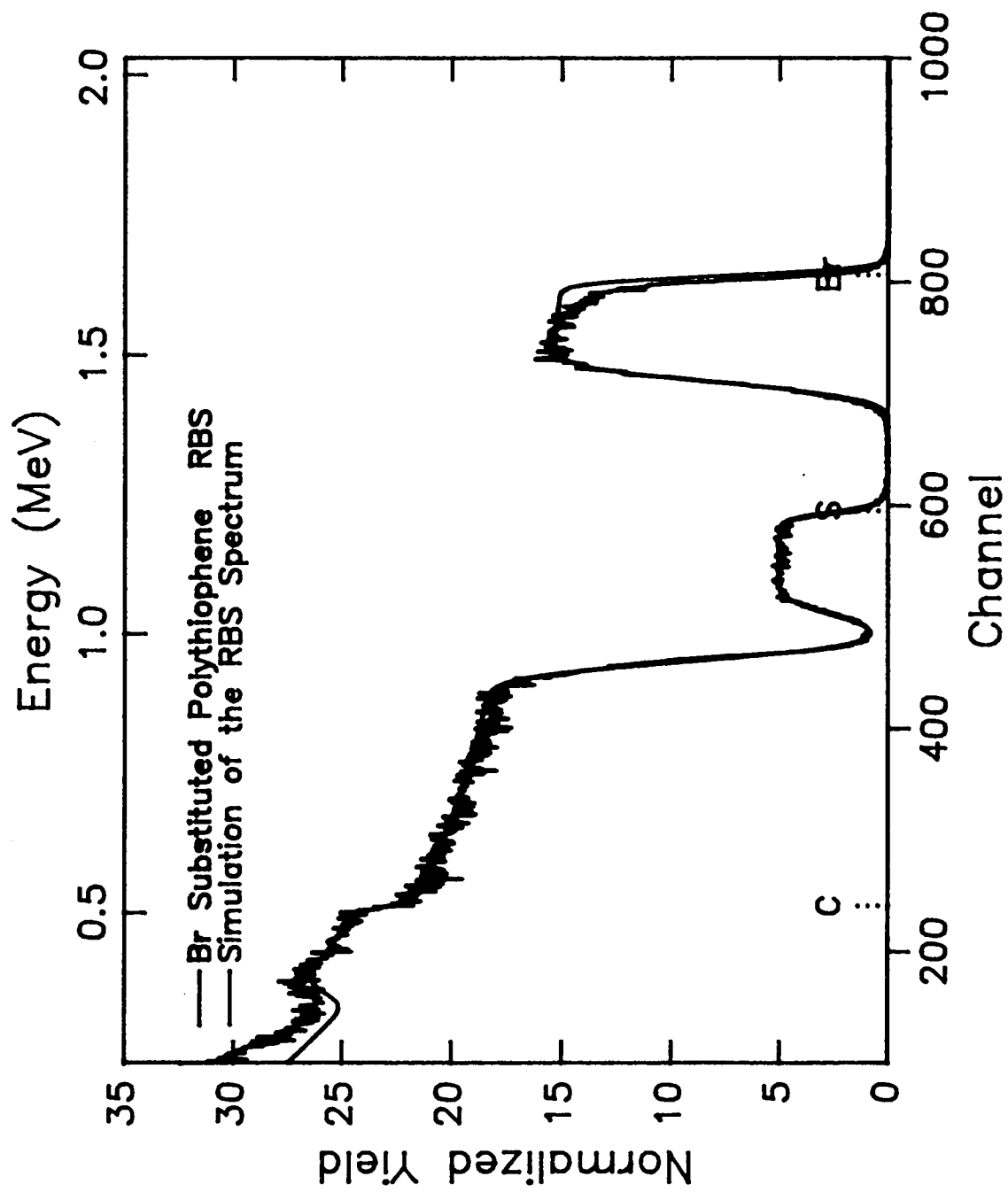
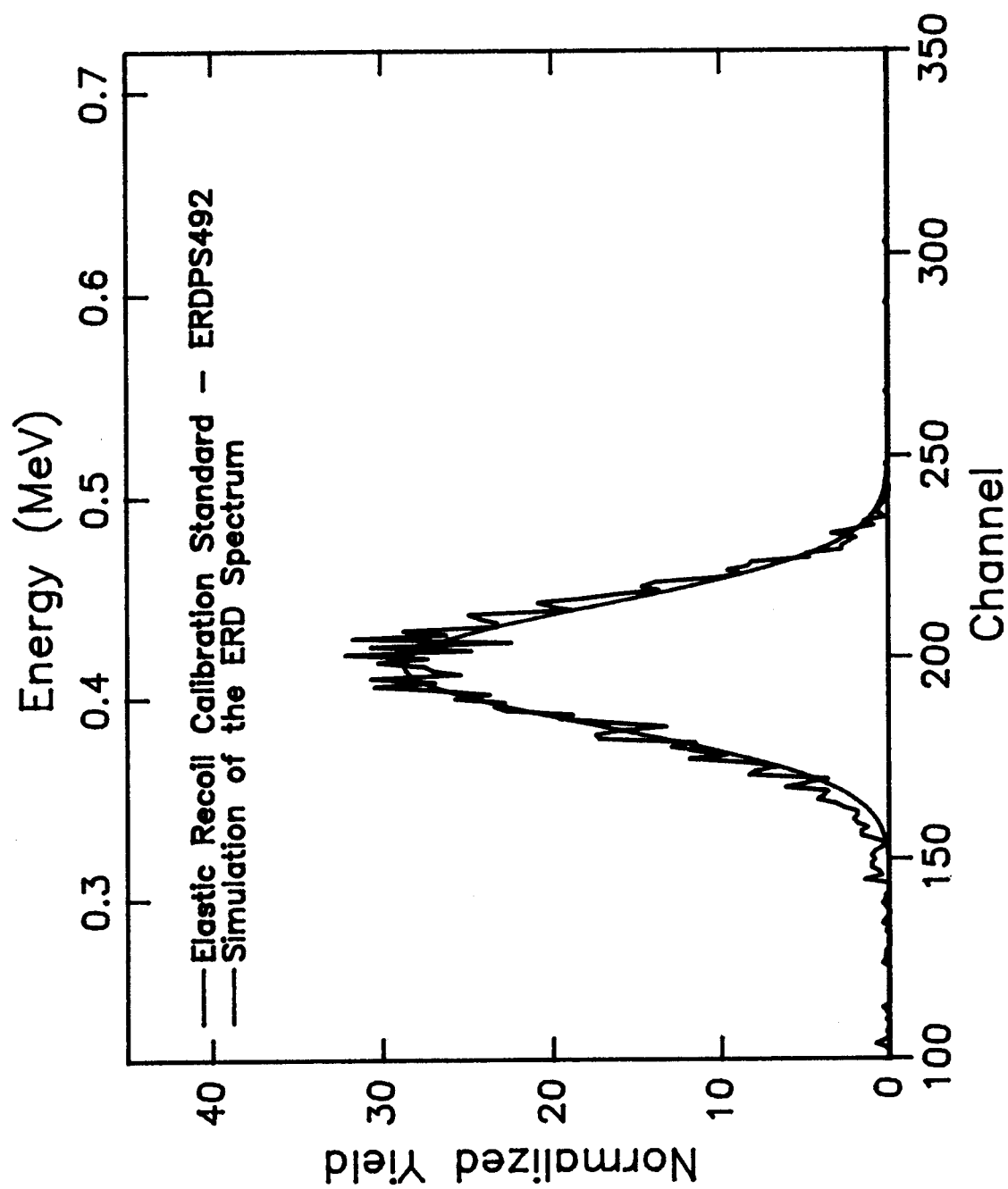FIGURE 3. RBS spectrum from a Br substituted polythiophene thin film.

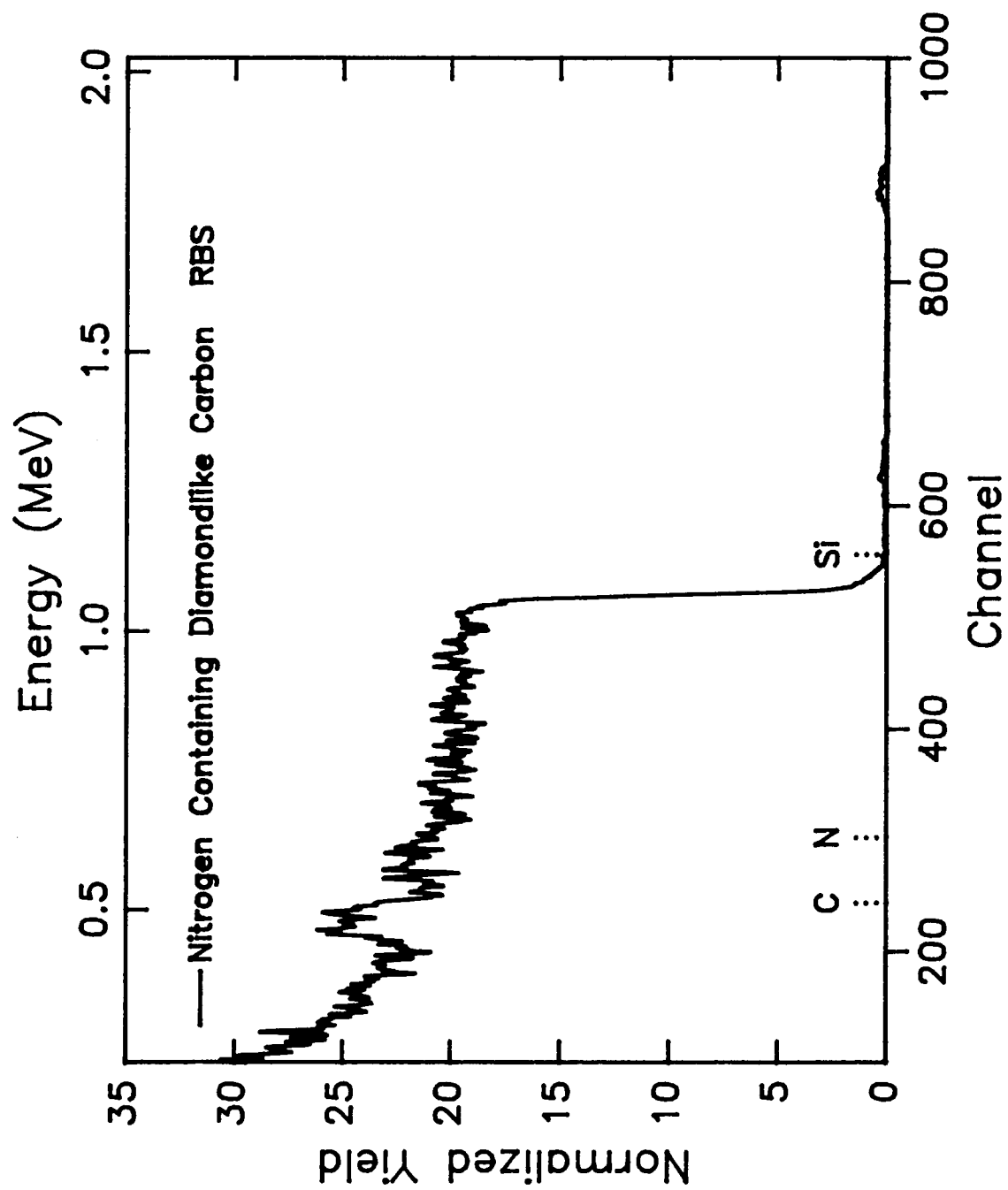FIGURE 4. ERD spectrum of a spin cast polystyrene thin film.

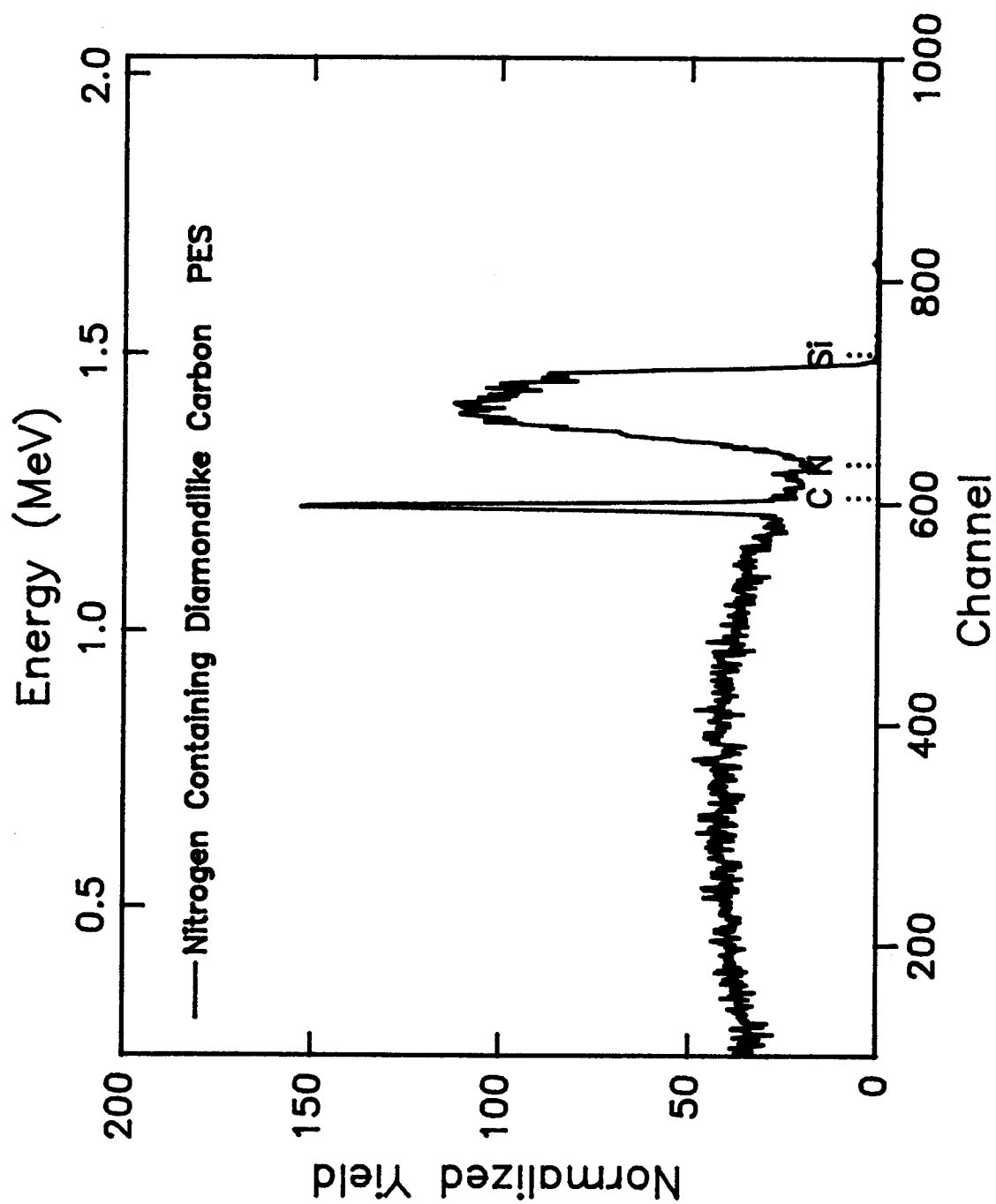FIGURE 5. RBS spectrum of a nitrogen containing diamondlike carbon thin film.

FIGURE 6. PES spectrum of a nitrogen containing diamondlike carbon thin film.

INDEX
AUTHORS